

# BRAIN AND DIABETES

EDITED BY: Hubert Preissl, Cristina García Cáceres and Rachel Nicole Lippert  
PUBLISHED IN: Frontiers in Endocrinology and Frontiers in Neuroscience





# frontiers

## Frontiers eBook Copyright Statement

The copyright in the text of individual articles in this eBook is the property of their respective authors or their respective institutions or funders. The copyright in graphics and images within each article may be subject to copyright of other parties. In both cases this is subject to a license granted to Frontiers.

The compilation of articles constituting this eBook is the property of Frontiers.

Each article within this eBook, and the eBook itself, are published under the most recent version of the Creative Commons CC-BY licence.

The version current at the date of publication of this eBook is CC-BY 4.0. If the CC-BY licence is updated, the licence granted by Frontiers is automatically updated to the new version.

When exercising any right under the CC-BY licence, Frontiers must be attributed as the original publisher of the article or eBook, as applicable.

Authors have the responsibility of ensuring that any graphics or other materials which are the property of others may be included in the CC-BY licence, but this should be checked before relying on the CC-BY licence to reproduce those materials. Any copyright notices relating to those materials must be complied with.

Copyright and source acknowledgement notices may not be removed and must be displayed in any copy, derivative work or partial copy which includes the elements in question.

All copyright, and all rights therein, are protected by national and international copyright laws. The above represents a summary only. For further information please read Frontiers' Conditions for Website Use and Copyright Statement, and the applicable CC-BY licence.

ISSN 1664-8714

ISBN 978-2-88976-501-0

DOI 10.3389/978-2-88976-501-0

## About Frontiers

Frontiers is more than just an open-access publisher of scholarly articles: it is a pioneering approach to the world of academia, radically improving the way scholarly research is managed. The grand vision of Frontiers is a world where all people have an equal opportunity to seek, share and generate knowledge. Frontiers provides immediate and permanent online open access to all its publications, but this alone is not enough to realize our grand goals.

## Frontiers Journal Series

The Frontiers Journal Series is a multi-tier and interdisciplinary set of open-access, online journals, promising a paradigm shift from the current review, selection and dissemination processes in academic publishing. All Frontiers journals are driven by researchers for researchers; therefore, they constitute a service to the scholarly community. At the same time, the Frontiers Journal Series operates on a revolutionary invention, the tiered publishing system, initially addressing specific communities of scholars, and gradually climbing up to broader public understanding, thus serving the interests of the lay society, too.

## Dedication to Quality

Each Frontiers article is a landmark of the highest quality, thanks to genuinely collaborative interactions between authors and review editors, who include some of the world's best academicians. Research must be certified by peers before entering a stream of knowledge that may eventually reach the public - and shape society; therefore, Frontiers only applies the most rigorous and unbiased reviews.

Frontiers revolutionizes research publishing by freely delivering the most outstanding research, evaluated with no bias from both the academic and social point of view. By applying the most advanced information technologies, Frontiers is catapulting scholarly publishing into a new generation.

## What are Frontiers Research Topics?

Frontiers Research Topics are very popular trademarks of the Frontiers Journals Series: they are collections of at least ten articles, all centered on a particular subject. With their unique mix of varied contributions from Original Research to Review Articles, Frontiers Research Topics unify the most influential researchers, the latest key findings and historical advances in a hot research area! Find out more on how to host your own Frontiers Research Topic or contribute to one as an author by contacting the Frontiers Editorial Office: [frontiersin.org/about/contacts](https://frontiersin.org/about/contacts)

# BRAIN AND DIABETES

Topic Editors:

**Hubert Preissl**, Institute of Diabetes Research and Metabolic Diseases, Helmholtz Center München, Helmholtz Association of German Research Centres (HZ), Germany

**Cristina García Cáceres**, Ludwig Maximilian University of Munich, Germany

**Rachel Nicole Lippert**, German Institute of Human Nutrition Potsdam-Rehbruecke (DIfE), Germany

**Citation:** Preissl, H., Cáceres, C. G., Lippert, R. N., eds. (2022). Brain and Diabetes. Lausanne: Frontiers Media SA. doi: 10.3389/978-2-88976-501-0

# Table of Contents

- 04    *Astrocyte Clocks and Glucose Homeostasis***  
Olga Barca-Mayo and Miguel López
- 20    *Brain-Body Control of Glucose Homeostasis—Insights From Model Organisms***  
Alastair J. MacDonald, Yu Hsuan Carol Yang, Ana Miguel Cruz, Craig Beall and Kate L. J. Ellacott
- 30    *Obesity and Dietary Added Sugar Interact to Affect Postprandial GLP-1 and Its Relationship to Striatal Responses to Food Cues and Feeding Behavior***  
Sabrina Jones, Shan Luo, Hilary M. Dorton, Alexandra G. Yunker, Brendan Angelo, Alexis Defendis, John R. Monterosso and Kathleen A. Page
- 39    *Vildagliptin Has a Neutral Association With Dementia Risk in Type 2 Diabetes Patients***  
Chin-Hsiao Tseng
- 48    *Altered White Matter Microstructures in Type 2 Diabetes Mellitus: A Coordinate-Based Meta-Analysis of Diffusion Tensor Imaging Studies***  
Cong Zhou, Jie Li, Man Dong, Liangliang Ping, Hao Lin, Yuxin Wang, Shuting Wang, Shuo Gao, Ge Yu, Yuqi Cheng and Xiufeng Xu
- 58    *Attenuated Induction of the Unfolded Protein Response in Adult Human Primary Astrocytes in Response to Recurrent Low Glucose***  
Paul G. Weightman Potter, Sam J. Washer, Aaron R. Jeffries, Janet E. Holley, Nick J. Gutowski, Emma L. Dempster and Craig Beall
- 65    *Microglial Lipid Biology in the Hypothalamic Regulation of Metabolic Homeostasis***  
Andrew Folick, Suneil K. Koliwad and Martin Valdearcos
- 80    *Activity-Based Anorexia Induces Browning of Adipose Tissue Independent of Hypothalamic AMPK***  
Angela Fraga, Eva Rial-Pensado, Rubén Nogueiras, Johan Fernø, Carlos Diéguez, Emilio Gutierrez and Miguel López
- 91    *Gray Matter Abnormalities in Type 1 and Type 2 Diabetes: A Dual Disorder ALE Quantification***  
Kevin K. K. Yu, Gladys L. Y. Cheing, Charlton Cheung, Georg S. Kranz and Alex Kwok-Kuen Cheung
- 102    *Retinal Neurovascular Impairment in Non-diabetic and Non-dialytic Chronic Kidney Disease Patients***  
Xiaomin Zeng, Yijun Hu, Yuanhan Chen, Zhanjie Lin, Yingying Liang, Baoyi Liu, Pingting Zhong, Yu Xiao, Cong Li, Guanrong Wu, Huiqian Kong, Zijing Du, Yun Ren, Ying Fang, Zhiming Ye, Xiaohong Yang and Honghua Yu
- 114    *Altered Cortisol Metabolism Increases Nocturnal Cortisol Bioavailability in Prepubertal Children With Type 1 Diabetes Mellitus***  
Julie Brossaud, Jean-Benoît Corcuff, Vanessa Vautier, Aude Bergeron, Aurelie Valade, Anne Lienhardt, Marie-Pierre Moisan and Pascal Barat



# Astrocyte Clocks and Glucose Homeostasis

Olga Barca-Mayo<sup>1\*</sup> and Miguel López<sup>2</sup>

<sup>1</sup> Circadian and Glial Biology Lab, Physiology Department, Molecular Medicine and Chronic Diseases Research Centre (CiMUS), University of Santiago de Compostela, Santiago de Compostela, Spain, <sup>2</sup> NeurObesity Lab, Physiology Department, Molecular Medicine and Chronic Diseases Research Centre (CiMUS), University of Santiago de Compostela, Santiago de Compostela, Spain

## OPEN ACCESS

### Edited by:

Cristina García Cáceres,  
Ludwig Maximilian University of  
Munich, Germany

### Reviewed by:

Alexandre Benani,  
Centre National de la Recherche  
Scientifique (CNRS), France  
Paulo Kofuji,  
University of Minnesota Twin Cities,  
United States

### \*Correspondence:

Olga Barca-Mayo  
olga.barca.mayo@usc.es

### Specialty section:

This article was submitted to  
Neuroendocrine Science,  
a section of the journal  
Frontiers in Endocrinology

**Received:** 31 January 2021

**Accepted:** 01 March 2021

**Published:** 18 March 2021

### Citation:

Barca-Mayo O and López M  
(2021) Astrocyte Clocks and  
Glucose Homeostasis.  
Front. Endocrinol. 12:662017.  
doi: 10.3389/fendo.2021.662017

The endogenous timekeeping system evolved to anticipate the time of the day through the 24 hours cycle of the Earth's rotation. In mammals, the circadian clock governs rhythmic physiological and behavioral processes, including the daily oscillation in glucose metabolism, food intake, energy expenditure, and whole-body insulin sensitivity. The results from a series of studies have demonstrated that environmental or genetic alterations of the circadian cycle in humans and rodents are strongly associated with metabolic diseases such as obesity and type 2 diabetes. Emerging evidence suggests that astrocyte clocks have a crucial role in regulating molecular, physiological, and behavioral circadian rhythms such as glucose metabolism and insulin sensitivity. Given the concurrent high prevalence of type 2 diabetes and circadian disruption, understanding the mechanisms underlying glucose homeostasis regulation by the circadian clock and its dysregulation may improve glycemic control. In this review, we summarize the current knowledge on the tight interconnection between the timekeeping system, glucose homeostasis, and insulin sensitivity. We focus specifically on the involvement of astrocyte clocks, at the organism, cellular, and molecular levels, in the regulation of glucose metabolism.

**Keywords:** astrocytes, circadian clock, metabolism, diabetes, glucose homeostasis

## FUNCTIONAL HIERARCHY OF THE TIMEKEEPING SYSTEM

The circadian (in Latin “circa”, around; “diem”, day) clock is an endogenous and self-sustaining oscillator that operates with a periodicity of 24 hours (h) to maintain proper rhythms of the vast majority of physiological and behavioral processes, including food intake, energy balance, sleep-wake cycles and many others (1). In mammals, the timekeeping system comprises a pacemaker located in the hypothalamic suprachiasmatic nucleus (SCN) (2, 3), as well as non-SCN brain and peripheral clocks and cell-autonomous oscillators within virtually every cell type of the body (4, 5). In the absence of any time cue from the environment, these clocks free run with a period close to 24 h. To compensate discrepancies between this intrinsic period and the environmental cycle, circadian clocks entrain to external Zeitgebers (ZT, in German “time giver”). The light entrains the SCN to local time which in turn, conveys the temporal information to other clocks in the brain and peripheral tissues *via* neuronal, hormonal, or behavioral activity rhythms, such as the

feeding-fasting and sleep-wake cycles, which serve as entrainment signals for extra-SCN clocks (6, 7) (**Figure 1**).

While a substantial amount of information is known about the neuroanatomy of the SCN, the mechanisms of light-affected entrainment and the transmission of time cues to other brain areas or peripheral clocks are not yet fully understood. Briefly, the SCN is a heterogeneous and complex bilateral nucleus (8, 9) comprising approximately 10,000 self-oscillating neurons on each side, in mice (10–12). Each part is divided into two functional subgroups, one in the ventrolateral region and the other in the dorsal SCN. The ventrolateral region or core receives direct photic inputs from the intrinsically photosensitive retinal ganglion cells (ipRGCs) (13–15). Activation of the retino hypothalamic tract by light increases the firing of vasoactive intestinal polypeptide (VIP)-expressing SCN cells and VIP release. VIP neurons set and phase-shift the circadian time by VIPergic and  $\gamma$ -aminobutyric acid (GABA)ergic signaling to arginine vasopressin (AVP)-expressing neurons within the

second subgroup of cells located in the dorsal SCN or shell (**Figure 1**). Ultimately, this results in the induction of the so-called clock genes *Period1* (*Per1*) and *Period2* (*Per2*) (16) and subsequent time-of-day dependent phase responses of the SCN, thereby enabling entrainment to the light-dark (LD) cycle.

If food availability is restricted to a particular time of day or night (often referred to as time-restricted feeding, TRF), animals exhibit increased activity in anticipation of feeding (termed food anticipatory activity, FAA). Moreover, in this paradigm, the peripheral clocks shift their phase to preserve alignment with mealtime. The effects of TRF on peripheral clocks and/or behavior persist even when the feeding is out of phase with the LD cycle, and, indeed, can be uncoupled from the SCN, which remains synchronized to the light (17–19). Remarkably, in the absence of a functional SCN, FAA is preserved and food intake becomes an effective ZT capable of coordinating circadian rhythms of behavior, peripheral clock gene expression, and clock outputs, such as hormone secretion (20, 21). Thereby,

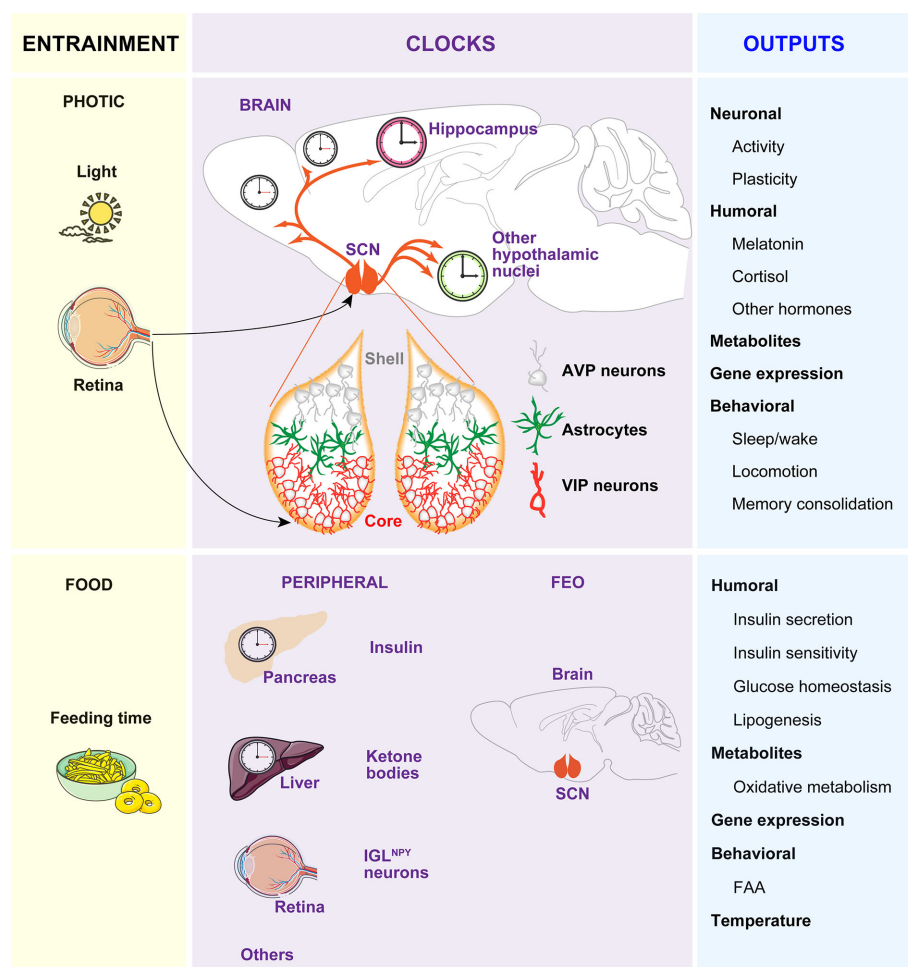


**FIGURE 1** | The circadian timing system. The timekeeping system is composed of two pacemakers (the SCN and the FEO), and peripheral clocks in other brain areas and peripheral tissues. Light inputs reaching the SCN via the retina and the retinohypothalamic tract, are the most important Zeitgeber for the SCN, which in turn synchronizes peripheral clocks through neural, endocrine, temperature, and behavioral signals. Feeding-related signals (INS and ketones bodies) generated by peripheral tissues and IGL<sup>NPY</sup> neurons entrain the FEO, which regulate the outputs such as FAA.

the entrainment to TRF has been proposed to be independent of the SCN and driven by a food-entrainable oscillator (FEO) of still unknown location. A recent study reported that innervation of ipRGC to neuropeptide Y (NPY)-expressing intergeniculate leaflet (IGL) neurons in early postnatal stages, allow the entrainment to TRF in adults. In this model, TRF inhibitory signals from IGL<sup>NPY</sup> neurons modulate the SCN activity, allowing the FEO signals to influence FAA (22).

As hypothalamic lesions and gene knockouts (KOs) targeting specific cell types in the hypothalamus, brainstem, or forebrain areas also impair FAA (23–29), it is reasonable to hypothesize that the FEO might be functionally distributed among brain areas that are competent to drive changes in behavior instead to be restricted to a particular brain region. In line with this idea, it was recently reported that the action of insulin (INS) and insulin-like growth factor-1 (IGF-1) triggered after feeding, on different brain regions, are necessary and sufficient for both the FAA and the phase-shift of body clocks (7). Remarkably, an elegant study showed that the signal that generates FAA might be synthesized in the liver. Specifically, it was shown that liver PER2 is required for hepatic-derived ketone bodies production which in turn signals the brain to induce FAA (30). In sum, the FEO may not be in a single tissue but it might be of systemic nature. In this context, the feeding-related signals, such as INS and ketones generated in peripheral tissues, entrain different brain regions competent to drive changes in behavior. Among these regions is included the SCN, which is tuned by innervation of ipRGCs to IGL during development to allow non-photoc entrainment to food (22) (**Figure 1**).

## ASTROCYTE CIRCADIAN CLOCKS

How the activity of a small number of SCN neurons is translated into rhythmic behaviors or physiology at the organism level? The human brain contains more than 100 billion cells, the majority being glial cells, coordinated by this endogenous clock to determine alertness waxes and wanes in a highly predictable manner over the course of a 24 h day (31). However, how this clock signaling is orchestrated within so many brain cells that lead to the cycle-to-cycle precision of circadian rhythmicity is unknown. Consequently, we face a lack of knowledge on the mechanisms by which circadian dysfunction affects a wide range of physiological processes such as metabolic imbalance, premature aging, and reduced longevity (32–38).

Astrocytes have long lived in the shadow of the neurons as they were thought to have mainly a structural role in the central nervous system. The recent findings showing the critical role of the astrocyte clock in the control of SCN function and circadian behavior (39–43) is a game-changing discovery that offers radically new research directions for therapy of brain diseases originated by environmental miss functioning of circadian rhythms or genetic factors affecting clock genes or outputs. This glial cell type is highly diverse in its morphological appearance, functional properties, and distribution among and within different brain regions (44, 45). However, they share three

anatomical features that are crucial to understand its functional contributions to the timekeeping system.

Firstly, the longstanding concept that astrocytic processes interdigitate to create a scaffold for the neuronal organization, has been challenged by several studies showing that, *in vivo*, astrocytes are organized in nonoverlapping domains, i.e., with little interaction between adjacent cells (46–48). Thus, one astrocyte can coordinate the activity of multiple sets of contiguous synapses, *via* regulation of neurotransmitters levels in the synaptic cleft, *via* control of the extracellular space, or by releasing chemical signals that actively modulate synaptic transmission, often referred to as gliotransmitters. Specifically, astrocytes play an essential role in the coupling of SCN neurons by controlling both glutamate and GABA levels (40, 42, 43, 49–51). Moreover, SCN astrocytes undergo rhythmic structural rearrangements (52), along with rhythms in GFAP expression (53), which allows differential day/night coverage of VIP neurons to facilitate entrainment to light (52, 54). Similarly, in response to metabolic cues, astrocytes undergo structural and morphological changes to influence the synaptic inputs within the hypothalamic melanocortin system, which might ultimately affect the feeding behavior (55–58). Astrocytes also regulate the extracellular space (59–62), enabling the exchange of solutes between the cerebrospinal fluid and the interstitial space, a system referred to as glymphatic clearance. As the diffusion of SCN output signals is sufficient for rhythmic behavior (63, 64), daily changes in the glymphatic system may underly the synchronization among different brain regions across the circadian cycle. On the other hand, in *Drosophila*, a glial-released factor was shown to be critical for normal rhythmicity by regulating a neurotransmitter, pigment dispersing factor, acting on a receptor similar to that for VIP in mammals (65–67). Similarly, in rodents, astrocytes release gliotransmitters, such as ATP, in a circadian manner (68), and arrhythmic astrocytes alter VIP expression *in vivo* (40). However, whether ATP release and/or astrocytic rhythmic metabolism impact the activity patterns of VIP neurons is still unknown.

Secondly, astrocytes form a syncytium, *via* gap junctions, that allow the propagation of small signaling molecules through the glial network (69). Pharmacological inhibition of gap junctions in SCN slices (70, 71) and mouse models with deletion of the neuronal connexin-36, impairs the circadian pattern of neuronal activity without affecting the long-term synchronization of clock gene expression (72) and with mild effect on behavioral rhythms (73). Similarly, studies in mouse models with deletion of astrocytic specific connexins indicate that the astrocytic coupling in the SCN is dispensable for circadian rhythm generation and light-entrainment (74). However, recently, a long-range function of astrocytes for the transmission of timing cues to distant neural populations was investigated *in vitro* with microfluidic devices that allowed compartmentalizing distinct neuronal populations connected through a network of astrocytes. In this paradigm, astrocytes were able to synchronize the clock of segregated cortical neuronal populations if intercellular communication between the glial network and/or calcium signaling were intact (75). Whether astrocytes are

involved in the spatial transmission of timing cues in other extra-SCN brain regions *in vivo* is still unknown.

Thirdly, the exchange of metabolites and hormones through the blood-brain barrier (BBB) relies on astrocytes and is dependent both on the sleep/wake state and in the circadian clock (59, 76–80). As hypothalamic astrocytes have a crucial role in sensing nutrients such as glucose and fatty acids (56, 81–83) and express receptors for leptin (84, 85), IGF-1 (86), thyroid hormone (87), INS (57), and glucocorticoids (GCs) (88, 89) among others, they could link or coordinate peripheral and central oscillators. For example, astrocytes, as well-known targets of GCs, might be sensitive to the negative feedback loop of the hypothalamus-pituitary-adrenal axis. It is widely accepted that GC signaling can reset peripheral clocks but not the central pacemaker because SCN neurons do not express the GC receptor (90). However, astrocytic feedback loops, *via* GC signaling, could explain the so far puzzling results showing that the *Per1*-Luc phases of SCN were affected significantly when adrenalectomized animals were treated with hydrocortisone (6).

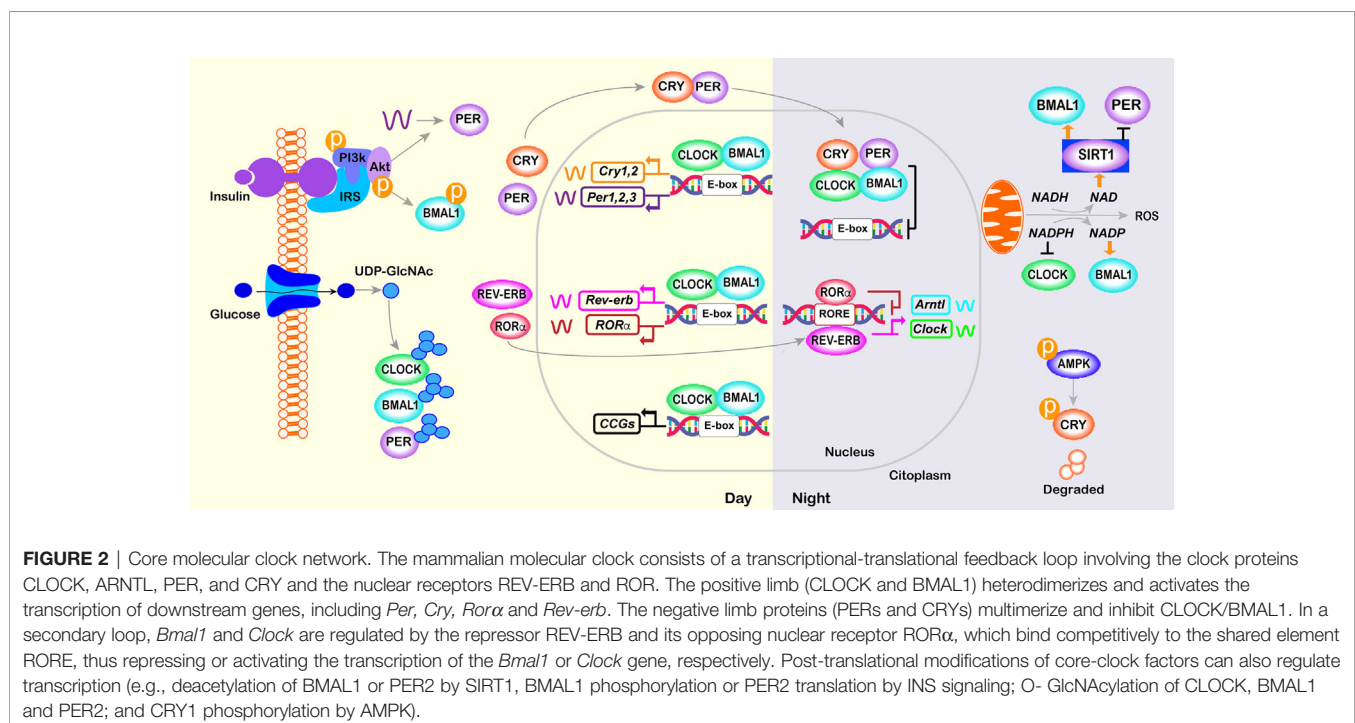
## MOLECULAR DYNAMICS OF THE CLOCK

The Nobel Prize in Physiology or Medicine in 2017 was awarded to three Chronobiologists who first cloned the *Drosophila Period* gene in 1984 (91, 92). This finding allowed us to understand how the timekeeping system anticipates the environmental changes related to the Earth's rotation in most, if not all, living organisms.

The molecular clock involves rhythmic and self-sustained transcriptional-translational feedback loops (TTFLs) of clock genes/proteins (Figure 2). The E-box specific transcription factors BMAL1 (Brain and muscle Arnt-like protein-1) and

CLOCK (Circadian locomotor output cycles kaput) are the positive limb of the TTFL, which heterodimerize to activate transcription of the repressors *Per1/2/3* and *Cryptochrome* genes (*Cry1/2*) (93, 94). The negative loop comprises PER/CRY heterocomplex that, upon accumulation, lead to the degradation of BMAL1/CLOCK dimers, thus inhibiting their own transcription (95). Hence, a new cycle of PER and CRY protein accumulation begins, generating rhythmic changes in the levels of the core clock transcripts and proteins that persist for approximately 24 h (96) (Figure 2). In a secondary feedback loop, the CLOCK- BMAL1 complex controls the rhythmic expression of the genes encoding the REV-ERB nuclear hormone receptors and ROR (97). In turn, REV-ERB and ROR compete for the same RORE elements within the *Clock* and *Bmal1* promoter, repressing or activating, respectively, *Clock* and *Bmal1* transcription (Figure 2).

Direct targets of CLOCK/BMAL1, referred to as clock-controlled genes (CCGs), include genes that are critically involved in rhythmic processes such as feeding behavior, sleep-wake cycle, and glucose homeostasis (34, 98) (Figure 2). In turn, metabolic state sensing pathways also alter the molecular clock in anticipation of the LD cycle. Specifically, during feeding, anabolic processes are triggered by the activation of the INS-AKT-mTOR pathway, whereas during fasting, AMP-activated protein kinase (AMPK) activation triggers catabolic processes and inhibits mTOR activity (99). BMAL1 phosphorylation and PER2 translation are regulated by the INS-AKT-mTOR pathway that is activated in the postprandial state (7, 100–102). Similarly, in peripheral tissues, AMPK1, which senses cellular ATP levels, modulate CRY1 phosphorylation and thus its rhythmic degradation (103). Additionally, high levels of glucose control the period length *via* O- GlcNAcylation of CLOCK, BMAL1, and



PER2 (104–106). The molecular clocks are also sensitive to the ratio of reduced to oxidized nicotinamide adenine dinucleotide (NAD) and flavin adenine dinucleotide (FAD), which are indirect sensors of cellular energy status. Oxidation of NAD is under control of the clock and, in turn, prevents the deacetylation and thus the transcriptional activity of CLOCK-BMAL1 complex by Sirtuin 1 (SIRT1) and poly-ADP-ribosylation mediated by poly(ADP-ribose) polymerase 1 (107–110) (**Figure 2**).

In summary, the circadian system ensures a temporal partitioning of catabolic and anabolic reactions synchronizing organism metabolism to the feeding-fasting cycle. However, as the connection of metabolism and the circadian clock works in both directions (111) is not surprising that animal models of genetic clock defects display metabolic alterations and that clock alterations can be found in metabolically challenged conditions (112).

## COORDINATION OF GLUCOSE HOMEOSTASIS BY CENTRAL AND PERIPHERAL CLOCKS

Glucose homeostasis is optimal when fasting-feeding and rest-activity cycles, hormonal rhythms, and central and peripheral clocks oscillate in synchrony with each other to ensure that the timing cues and tissue responsiveness are achieved at the right time. During the active phase, metabolic tissues such as the liver, muscle, and fat are very sensitive to INS to guarantee that glucose uptake is properly achieved after food intake. Conversely, these tissues are more resistant to the hormone during the fasting phase, to facilitate the endogenous glucose production and free fatty acid (FFA) secretion (113–115). In this section, we discuss the clocks in the tissues and organs involved in the control of glucose homeostasis and describe their role in the regulation of INS sensitivity and secretion.

The hypothalamus integrates glucose-sensing mechanisms with multiple effector pathways to precisely coordinate hepatic glucose production, muscle and fat glucose uptake, and endocrine pancreas function (**Figure 3**). Briefly, in the arcuate nucleus of the hypothalamus (ARC), orexigenic agouti-related peptide (AgRP)-producing neurons, and anorexigenic neurons releasing the pro-opiomelanocortin (POMC)-derived peptide,  $\alpha$ -melanocyte-stimulating hormone, together with the neurons expressing the melanocortin 4 receptor (MC4R), are essential for glucose sensing (117). AgRP neurons are glucose-inhibited cells whereas POMC neurons are glucose-excited (118). In general terms, competitive binding of  $\alpha$ -MSH and AgRP to MC4Rs defines the activation magnitude of downstream pathways and effectors. Furthermore, POMC and AgRP neurons project to numerous extrahypothalamic and hypothalamic regions, including the ventromedial nucleus (VMH) (119), which is crucial to initiate the glucose counter-regulatory response to hypoglycemia (120) (**Figure 3**). On the other hand, hypothalamic astrocytes respond to hyperglycemia

by retraction of the coverage around POMC neurons to modify meal patterns (56). Consistently, astrocytes sense INS and leptin to co-regulate behavioral responses and metabolic processes *via* the control of brain glucose uptake and the glial ensheathment of POMC neurons, respectively (57, 58). Moreover, deletion of leptin receptors in astrocytes reduces the physiological anorexigenic response to this hormone and enhances fasting or ghrelin-induced hyperphagia (58). Additionally, stimulation of astrocytes with ghrelin modify glutamate and glucose metabolism as well as glycogen storage by decreasing GLUT2, glutamine synthetase, and lactate dehydrogenase, and increasing glutamate uptake, glycogen phosphorylase, and lactate transporters, which might modulate the signals/nutrients reaching neighboring neurons (121). Finally, activated astrocytes release adenosine to inhibit AgRP neurons, thus suppressing the ghrelin-mediated increase of food intake (122, 123) (**Figure 3**).

As the SCN imposes the sleep-wake cycle and food intake occurs in the active period, the involvement of the pacemaker in controlling glucose homeostasis and systemic INS sensitivity is indirect (124). Indeed, BMAL1 deletion in SCN does not affect the body weight despite complete loss of rhythmic behavior (20). Moreover, the circadian locomotor activity but not the metabolic disturbances of *Bmal1*<sup>-/-</sup> mice were rescued by restoring BMAL1 expression in the SCN (125). Similarly, mice with astrocyte-specific deletion of BMAL1 show altered energy balance and glucose homeostasis despite their circadian locomotor activity is not lost (39–43). Thus, peripheral and/or extra-SCN hypothalamic clocks, but not the SCN, might have a crucial role in developing glucose intolerance and INS resistance. In line with this idea, BMAL1 ablation within SF1 neurons in the VMH is sufficient to alter energy expenditure (126). Additionally, AgRP-specific ablation of BMAL1 increases hepatic gluconeogenesis (127). However, currently, little is known about the specific physiological functions of extra SCN brain clocks. This knowledge could be highly valuable for biomedical understanding and future therapeutic advancement in the metabolic imbalance associated with circadian disruption.

Metabolic tissues involved in glucose homeostasis also have autonomous clocks that govern and adjust their daily metabolic function or outputs. For example, in the liver, with an essential role as a buffer for glucose variations arising from rhythmic food consumption, ablation of the local clock leads to hypoglycemia restricted to the fasting phase and exaggerated glucose clearance (128). Moreover, it was reported that while hepatic glycogenesis is controlled by CLOCK (129), gluconeogenesis in the fasted state, is under the regulation of the repressor CRY1 (130–133). On the other hand, efficient glucose uptake by the hepatocytes at the beginning of the active phase depends on the rhythmic expression of glucose transporters and glucagon receptor (134, 135). Another tissue with a key role in the control of glucose homeostasis is the skeletal muscle. This tissue is responsible for 70–80% of INS-stimulated glucose uptake in the postprandial state (136). Interestingly, INS sensibility in muscle is controlled both by light and the local clock (137–140). Specifically, it was shown that photic inputs entrain diurnal changes in clock gene

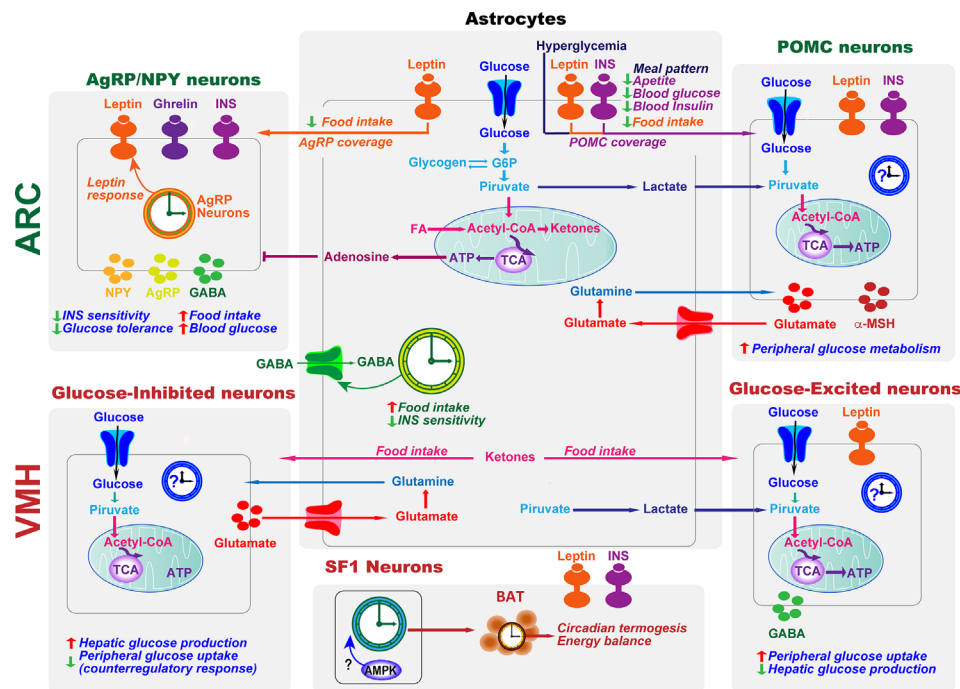


**FIGURE 3 |** Astrocytes and clocks modulate hypothalamic glucose-sensing mechanisms. The ability of POMC and NPY/AgRP neuronal populations in ARC to alter energy metabolism is due to their sensitivity to several circulating signals, including hormones, such as leptin and insulin (INS), and nutrients. Hypothalamic astrocytes provide neurons with structural support and nutrients. Moreover, hyperglycemia, INS, and leptin signaling in this glial cell type lead to changes in the astrocytic coverage of POMC and/or AgRP neurons to regulate glucose sensing. Glucose transported into astrocytes can be metabolized to lactate, which is released and taken up by neurons and metabolized into pyruvate to serve as a glycolytic substrate. Astrocytes can also modulate synaptic transmission by uptake of neurotransmitters from the synaptic cleft (glutamate and GABA) and by releasing gliotransmitters such as adenosine, which inhibits AgRP neurons. In the ARC, the astrocyte circadian clock might control food intake and glucose homeostasis by regulating the uptake of GABA. On the other hand, the clock in AgRP neurons is required for coordinating leptin response and glucose metabolism. VMH neurons include glucose-sensing cells, referred to as glucose-excited and glucose-inhibited neurons. The activation of glucose-excited neurons leads to decreased hepatic glucose production and increased peripheral glucose uptake. VMH glucose-inhibited neurons are activated in response to hypoglycemia. In recurrent hypoglycemia, high accumulation of lactate enhances the glucose-excited neuronal activity and consequent GABA release, inhibiting the counterregulatory response. A high-fat diet increases astrocyte ketone bodies production, which are exported to VMH neurons to ultimately control food intake. Subsets of VMH neurons also express SF1. These SF1 neurons contain a clock that modulates energy expenditure by regulating cyclic thermogenesis in brown adipose tissue (BAT). As hypothalamic AMPK modulates BAT thermogenesis (116), and has a crucial role in the molecular clock, it would be interesting to investigate its involvement in the control of rhythmic BAT thermogenesis by the SF1 neuronal clock. TCA, tricarboxylic acid cycle.

expression and INS sensitivity in muscle *via* SIRT1 in SF1 neurons (140). On the other hand, deletion of the autonomous clock in muscle is sufficient to cause local INS resistance (137). Glucose uptake is also dependent on rhythmic INS action in the white adipose tissue (WAT) (141). However, contrary to liver or skeletal muscle, ablation of the local clock in WAT do not impact glucose homeostasis and INS sensitivity (142), suggesting that lipid mobilization is mainly regulated by the hypothalamic actions of INS and leptin. Finally, brown adipose tissue (BAT), which relays in FFA and glucose supply to regulate thermogenesis, is highly flexible in terms of glucose uptake potential and can significantly contribute to whole-body glucose metabolism under some conditions. In this tissue, INS-stimulated glucose uptake is regulated by the VMH and AgRP neurons (143–145), as well as by the local clock (146, 147). Interestingly, mouse and human BAT express a red-light-sensitive protein, OPN3 (148), which increases glucose uptake upon red light stimulation. Recently, an elegant study demonstrated that animals reared without violet light show

increased responses to  $\beta$ -agonists, which in humans activate BAT, lower blood glucose levels, and increase and INS sensitivity. This effect was mediated by a violet light-sensing photoreceptor Opsin 5 (OPN5) in glutamatergic warm-sensing hypothalamic preoptic area neurons (149). Altogether, these studies open the possibility of modulating glucose homeostasis by manipulating environmental light.

Altogether this suggests that perturbed rhythms of the central and/or tissue clocks might lead to a mismatch between hepatic glucose production, muscle glucose uptake, and carbohydrate intake which could contribute to elevated levels of glucose and an imbalance between lipid storage in WAT and lipid oxidation in the brown adipose tissue. Furthermore, hyperglycemia in diabetes is traditionally attributed to reduced INS sensitivity in skeletal muscle and liver but also coupled to decreased INS secretion by the pancreas. Not only glucose homeostasis and INS sensitivity is under control of the local clocks in most of the above-mentioned metabolic tissues, but the pancreatic clock also controls rhythmic INS secretion (150, 151). Indeed, ablation of the pancreatic clock,

in mice, is sufficient to cause hypoinsulinemia and hyperglycemia (150, 152–154).

Interestingly, feeding-related hormones involved in the control of glucose homeostasis are timing cues for circadian behaviors. For example, leptin is involved in the regulation of sleep-wake cycles (155, 156); ghrelin, stimulate FAA in mice (157) and INS action, triggered after feeding, is a critical entrainment signal for the FEO (7). Thus, an intriguing unsolved question concerns how the neurocircuits involved in glucose homeostasis and the central or peripheral clocks crosstalk and coordinate appropriate metabolic and/or circadian responses.

## INTEGRATION OF GLUCOSE HOMEOSTASIS BY ASTROCYTE CLOCKS AND CELLULAR METABOLISM

As brain metabolic pathways are compartmentalized between astrocytes and neurons, the coordination of both cell types is needed to meet the high energy requirements of synaptic transmission and correct brain function (158). Thereby, it is not surprising that hypothalamic glucose sensing requires an intact metabolic coupling between astrocytes and neurons (159). Interestingly, a big percentage of components of cellular metabolic pathways are direct targets of the molecular clock (96, 111, 160). Together, this suggests that the close association between altered glucose homeostasis and circadian disruption may arise from a shared defect in the astrocyte-neuron metabolic coupling. In turn, this might impact the neurocircuitry governing energy and glucose homeostasis or alter metabolic adaptations to hypoglycemia in the diabetic brain. In this section, we discuss the current evidence that supports this hypothesis.

The major energy source for the brain is glucose, which is taken up by astrocytes and neurons *via* glucose transporters (GLUTs) (161–163). In the hypothalamus, the neuron-astrocyte glucose coupling expands beyond the accomplishment of energy requirements. For instance, astrocytes actively cooperate with hypothalamic neurons in detecting circulating glucose levels and in the generation of proper systemic metabolic responses (164). Not only astrocytic GLUT2 activity is involved in the regulation of systemic glucose homeostasis in rodents (165–167), but restoring astrocytic GLUT2 reestablish the counterregulatory response to low-glucose in GLUT2 deficient mice (165). Remarkably, rhythmic GLUTs expression (137, 168, 169) is impaired in the brain of experimental streptozotocin-induced diabetes rats (169). Moreover, 24 h oscillation in glucose levels may modulate the expression of clock genes and transcriptional outputs within hypothalamic neurons involved in glucose homeostasis (170). Whether astrocyte-neuron metabolism in hypothalamic glucose sensing and associated-systemic response in the normal or diabetic brain relies on the astrocyte molecular clock remains to be investigated. However, this idea is reinforced by the recent finding that deletion of *Bmal1* in astrocytes impairs INS sensitivity and glucose homeostasis (39).

Further, glucose can be stored as glycogen or metabolized in the glycolytic pathway to produce pyruvate, which is either transferred into mitochondria or converted to lactate. According to the “Astrocyte-to-Neuron Lactate Shuttle” (ANLS) hypothesis (171), lactate is primarily produced by astrocytes and transferred to neurons, where it is converted to pyruvate for aerobic energy production in mitochondria (Figure 3). Thereby, the production and the release of lactate by astrocytes is directly linked to neuronal activity, as showed in orexin neurons (172, 173). Consistent with the ANLS hypothesis, brain lactate levels increase during the awake state when neuronal firing rates are higher and vice versa, leading to a 24 h rhythm of lactate concentration (174, 175). In turn, astrocytic lactate release regulates the sleep-wake cycle (74) and entrain forebrain oscillators between states of alertness and tiredness by controlling the DNA binding of CLOCK/BMAL1 (176). Remarkably, during hypoglycemia in diabetes patients, brain lactate levels drop while its infusion increased brain lactate levels compared to healthy subjects (177–179). These findings suggest increased lactate use as a metabolic substrate, impaired astrocyte lactate release, or perturbed compensatory metabolic mechanisms in the diabetic brain. Whether these effects underlie a potential astrocytic dysrhythmia is currently unknown.

More than half of the energy used by neurons during fasting derives from ketones bodies (180) synthesized by astrocytes. The astrocytic switch from glucose to FFA utilization (181, 182) to produce ketones is particularly enhanced in the hypothalamus (181), where stimulate neuropeptides critically involved in glucose sensing and energy homeostasis (83, 182, 183) (Figure 3). On the other hand, recurrent exposure to low glucose, mimicking variations often seen in patients with diabetes, results in increased astrocytic ketogenesis (184–186), likely to preserve brain ATP production (187). In turn, increased astrocytic ketogenesis alters INS signaling and consequently glucose homeostasis (183). Despite it was shown that *Per2* controls the hepatic production of ketone bodies (30), whether hypothalamic ketogenesis is under the control of the astrocyte clock remains to be investigated. Similarly, whether arrhythmic astrocytes impair glucose homeostasis by contributing to the increased ketogenesis is unknown and could be crucial for therapeutic interventions involving the potentiation of the astrocyte clock.

On the other hand, glucose, as well as glutamine, can be metabolized to uridine diphosphate N-acetylglucosamine (UDP-GlcNAc) through the hexosamine biosynthetic pathway. The reversible enzymatic post-translational modification of proteins (on serine and threonine residues) with UDP-GlcNAc as glucose donor is termed O-GlcNAcylation. This process is conserved across species as occurs both in mouse brains and *Drosophila* neurons. While in conditions of glucose hypometabolism, brain levels of O-GlcNAc-modified proteins are reduced (188), hyperglycemia increases GlcNAcylation of proteins related to the INS pathway, thus contributing to INS resistance (189). Hyperinsulinemia is also associated with increased GlcNAcylation (189) of proteins involved in the pathology of diabetes, such as glycogen synthase, a major gatekeeper of

glucose metabolism (190, 191). On the other hand, O-GlcN Acylation serves as a metabolic sensor to control the circadian period length *via* modification, and thus changes in the transcriptional activity of CLOCK and PER2 (104). As neurons depend on astroglial glucose and glutamine, this suggests that O-GlcNAcylation of the neuronal clocks might be coupled to astrocyte metabolism. However, further studies are needed to verify this hypothesis.

The metabolic endpoint of glycolysis and the mitochondrial metabolism is ATP generation, which apart from being used to fuel biological reactions is released to the extracellular space (eATP) (eATP) (192). Remarkably, INS stimulates ATP release from astrocytes (193). In turn, eATP leads to rapid upregulation of glycolysis (194) and promotes glucose uptake into both neurons and astrocytes (195). eATP is also a signaling molecule that acts on purinergic, ionotropic P2X, and G-protein coupled P2Y receptors to regulate neuronal activity (196). In the hypothalamus, NPY and AgRP neurons express P2X2R (197), whereas SF-1 neurons are excited by ATP *via* the P2X4 receptor (198). eATP released by astrocytes can also be metabolized to adenosine. While activation of the A1 receptor by adenosine inhibits appetite-stimulating AgRP neurons (122) (**Figure 3**), in astrocytes modulate sleep homeostasis (46). Thus, the circadian release of astrocytic ATP (199) and the circadian activity of enzymes involved in adenosine synthesis (200) suggest a central role of the astrocyte clock in modulating both processes. On the other hand, decreased ATP production activates the AMPK pathway to impact the circadian clock *via* degradation of CRY1 (103). Further investigation will clarify whether astrocytic rhythmic ATP release entrains the neuronal clocks *via* circadian activation of AMPK to control energy homeostasis and circadian sleep-wake changes in the brain.

Glutamate, the major excitatory neurotransmitter in the adult CNS, is released from neurons and recycled by astrocytes to form glutamine (**Figure 3**), which is returned to neurons and used as a precursor for synthesizing glutamate and GABA (201). The uptake of glutamate by astrocytes, critical for neuronal activity (202), is metabolically expensive and requires an increase in glycolysis and lactate production (171). Remarkably, control of glutamate and GABA levels, coupled to astrocyte rhythms (40–43, 203), is necessary for the generation of molecular and behavioral rhythms and, is also critically involved in the modulation of hypothalamic neural circuits controlling glucose homeostasis (39, 204, 205). However, excessive demands on astrocytes, in response to a decrease in glucose levels, impair glutamate uptake (206), altering the glutamatergic signaling to delay the onset of the normal counterregulatory response to hypoglycemia (206). Conversely, intake of an obesogenic diet rapidly increases hypothalamic glutamatergic signaling (207) and the expression of astrocytic glutamate transporters (208). It is reasonable to hypothesize that chronic elevated glutamatergic signaling, associated with diet-induced obesity, increases the metabolic demands on astrocytes to prevent glutamate-induced excitotoxicity. This in turn negatively impacts their ability to support neuronal activity thus, contributing to hypothalamic synaptic dysfunction and the death of POMC neurons (55, 209, 210). Altogether, this suggests that the regulation of glutamate and GABA levels might be a key astrocyte circadian

function in normal physiology and likely involved in the alterations of the diabetic brain.

The enteric nervous system is gaining more attention in the last few years. While most of the research focused on the enteric neurons, less attention was directed towards the enteric glial cells (EGCs). Glucose enters the body *via* the gastrointestinal (GI) tract, and conversely, diabetes-induced GI dysfunction is related to increased apoptosis of EGC in the myenteric plexus (211). On the other hand, the gut clock synchronized by food intake (27, 212) regulates the expression of brush border disaccharidases and glucose absorption to the habitual feeding period (168). Moreover, Glucagon-like peptide-1 secretion by enteroendocrine L-cells, with an important role in regulating glucose homeostasis (213, 214), is under control of the clock (215). In the gut, also anatomical and metabolome patterns of the microbiota undergo rhythmic fluctuations, resulting in system-wide effects on host circadian transcriptional, epigenetic, and metabolite cycles (216). Interestingly, repeated jet lag in mice disturbs the intestinal microbiome leading to reduced glucose tolerance (216). Similarly, fecal transfer from jet-lagged humans into germ-free mice impaired glucose tolerance (216). These findings suggest that the microbiome clock has an important role in the development of INS resistance due to repeated phase shifts. Altogether, this indicates that the contribution of the gut clock, specifically in the enteric glia, to the control of glucose homeostasis warrants further work.

Altogether, this data indicates that further investigations about the role of the astrocyte clock in maintaining the cycle-to-cycle precision of cellular metabolism and neural rhythmic behavior could be crucial to counteract the systemic metabolic abnormalities associated with circadian disruption.

## CIRCADIAN DISRUPTION AND DIABETES

In this section, we review the current evidence about the contribution of genetic or environmental factors (such as exposure to artificial light-dark cycles, disturbed sleep, shift work, and jet lag) that impact the timekeeping system to the development of insulin resistance and type 2 diabetes.

In humans, mutations in several clock genes are strongly associated with obesity, INS resistance, and type 2 diabetes. Specifically, it was reported associations between single nucleotide polymorphisms in *ARNT* and T2DM (217), specific haplotypes of *CLOCK* and obesity (218, 219), and between polymorphisms in *CRY2* and elevated fasting glucose (220, 221). In line with the human clock gene mutation studies, rodent models with genetic deletions of core-clock genes (in either a whole-body or a tissue-specific manner) showed INS resistance, obesity, and type 2 diabetes (32, 125, 142, 222, 223). Remarkably, deletion of *Bmal1* in astrocytes in mice is sufficient to phenocopy the obesity, INS resistance, and glucose intolerance of *Bmal1*<sup>-/-</sup> constitutive KO mice (39), suggesting that robust astrocyte circadian rhythms could preserve whole-body homeostasis and metabolic health.

The central pacemaker anticipates and synchronizes the daily function of peripheral tissues according to the entrainment by natural changes in light. With the advent of affordable artificial

lighting and the 24/7 lifestyle of our society, humans began to experience increased exposure to artificial lights and irregular light schedules. These environmental changes lead to a desynchronization between the internal clock and the external ZT, a phenomenon referred to as circadian misalignment. Remarkably, human and animal studies have linked obesity and type 2 diabetes with increased light exposure during naturally dark hours (224–230). In turn, exposure to bright morning light increases fasting and postprandial glucose levels in patients with type 2 diabetes (230). Despite its relevance for health, the molecular and cellular mechanisms of normal and pathological phototransduction in the SCN are unclear. For instance, VIP rhythm, with a key role in synchronizing SCN neurons to each other and with the LD cycle (231, 232), is driven by the LD cycle and not by the circadian clock (233). Thereby, the mechanism by which deletion of *Bmal1* in astrocytes constantly elevates VIP levels (40) remains unknown. Indeed, constant illumination increases VIP levels lengthening the circadian period and resulting in two or more peaks in daily activity (234), a circadian locomotor pattern that resembles that of mice with arrhythmic astrocytes (40). Consistently, studies in *Drosophila* showed that glial-specific genetic manipulations lead to circadian arrhythmicity due to alterations on a clock neuron peptide transmitter (pigment dispersing factor) that acts on a receptor similar to that for VIP in mammals (65, 66). These studies suggest that the astrocyte clock might facilitate the entrainment to light and therefore, to the light-induced phase shifts in physiology and behavior. Further investigations on the mechanism underlying circadian entrainment to light are critical for understanding why aberrant light exposure, disrupts circadian physiology leading to diabetes and INS resistance.

Evidence from epidemiological and experimental studies indicate that sleep restriction or disturbance, increases the risk of obesity and type 2 diabetes (235–239) likely due to increased food intake (237, 238), altered sympathovagal balance (240, 241), and increased circulating levels of catecholamines (242) or cortisol (241, 242). Interestingly, astrocytes modulate mammalian sleep homeostasis by controlling adenosine A1 receptors (243). The circadian release of the astrocytic transmitter ATP (199) as well as the circadian activity of enzymes involved in the synthesis of adenosine in areas of the brain related to sleep (200) suggests a central role of astrocytes in modulating circadian sleep-wake changes in the brain. Further studies will be needed to understand the importance of astrocyte clocks in the relationship between circadian sleep disorders and diabetes.

Whereas light is the dominant timing cue for the SCN, the time of meals represents the main ZT for peripheral clocks. Therefore is not surprising that extended/erratic eating patterns, such as in shift workers or subjects under experimental circadian misalignment, showed decreased glucose tolerance and insulin sensitivity (244–250). Indeed, a short-term circadian misalignment protocol of 8 days in humans is sufficient to cause higher blood glucose and insulin levels (249). It is reasonable to hypothesize that disturbance of nutrient fluxes or the misalignment of central and peripheral clock rhythms might contribute to the pathophysiology of insulin resistance at the tissue level. For instance, a mismatch between

hepatic glucose production, muscle glucose uptake, and carbohydrate intake could contribute to elevated glucose levels, while an imbalance between lipid storage in WAT, lipid oxidation in BAT, and hepatic lipid production might contribute to ectopic lipid accumulation. However, to improve or prevent the metabolic alterations caused by circadian misalignment we need to further understand the mechanisms involved in the entrainment of both central and peripheral circadian clocks. Remarkably, as astrocytes are at the interface between vessels and neurons, they are in a privileged position to act as metabolic sensors of systemic cues that entrain the peripheral clocks, such as GCs, INS, or IGF1 (7, 40, 203). Further studies will clarify whether those metabolic cues might play a crucial role in communicating time-of-feeding to the astrocyte molecular clock linking the periphery and the CNS clocks.

## CONCLUSION

A large body of evidence from human or animal studies demonstrated the circadian regulation of glucose homeostasis and INS sensitivity. However, the exact mechanisms involved in the metabolic derangements resulting from circadian disruption are not fully understood. Emerging groundbreaking findings, showing that astrocytes are pivotal for the circadian regulation of behavior and whole-body energy and glucose homeostasis, could provide a new cellular target to tune physiological responses operating on different timescales according to metabolic status. A key question that remains to be investigated is how the astrocyte clock is entrained to lead to the cycle-to-cycle precision of circadian rhythmicity in the SCN and/or in extra SCN clocks. Therefore, we face a lack of knowledge on the mechanisms by which astrocyte circadian dysfunction affects such a wide range of physiological processes. Understanding these mechanisms will be a challenge for years to come but a crucial aspect in designing better therapies, such as clock agonists, for diabetes. With this knowledge, the use of chronotherapies or temporally directed therapeutics to improve human metabolic health will be a matter of time.

## AUTHOR CONTRIBUTION

All authors contributed to the article and approved the submitted version. OB-M conceptualized and wrote the manuscript and made the figures. OB-M and ML discussed and edited the manuscript and the figures.

## ACKNOWLEDGEMENTS

OB-M is supported with a Ramón y Cajal award (RYC2018-026293-I.) from the Ministerio de Ciencia, Innovación y Universidades of Spain; by Spanish Agencia Estatal de Investigación (PID2019-109556RB-I00) and the Xunta de Galicia-Consellería de Cultura, Educación e Ordenación Universitaria (ED431F 2020/009).

## REFERENCES

- Hastings MH, Maywood ES, Reddy AB. Two decades of circadian time. *J Neuroendocrinol* (2008) 20:812–9. doi: 10.1111/j.1365-2826.2008.01715.x
- Moore RY, Eichler VB. Loss of a circadian adrenal corticosterone rhythm following suprachiasmatic lesions in the rat. *Brain Res* (1972) 42:201–6. doi: 10.1016/0006-8993(72)90054-6
- Stephan FK, Zucker I. Circadian rhythms in drinking behavior and locomotor activity of rats are eliminated by hypothalamic lesions. *Proc Natl Acad Sci U S A* (1972) 69:1583–6. doi: 10.1073/pnas.69.6.1583
- Nagoshi E, Saini C, Bauer C, Laroche T, Naef F, Schibler U. Circadian Gene Expression in Individual Fibroblasts Cell-Autonomous and Self-Sustained Oscillators Pass Time to Daughter Cells. *Cell* (2004) 119:693–705. doi: 10.1016/s0092-8674(04)01054-2
- Welsh DK, Yoo SH, Liu AC, Takahashi JS, Kay SA. Bioluminescence imaging of individual fibroblasts reveals persistent, independently phased circadian rhythms of clock gene expression. *Curr Biol* (2004) 14:2289–95. doi: 10.1016/j.cub.2004.11.057
- Pezük P, Mohawk JA, Wang LA, Menaker M. Glucocorticoids as entraining signals for peripheral circadian oscillators. *Endocrinology* (2012) 153:4775–83. doi: 10.1210/en.2012-1486
- Crosby P, Hamnett R, Putker M, Hoyle NP, Reed M, Karam CJ, et al. Insulin/IGF-1 Drives PERIOD Synthesis to Entrain Circadian Rhythms with Feeding Time. *Cell* (2019) 177:896–909.e20. doi: 10.1016/j.cell.2019.02.017
- Yan L, Karatsoreos I, LeSauter J, Welsh DK, Kay S, Foley D, et al. Exploring spatiotemporal organization of SCN circuits. *Cold Spring Harbor Symp Quantitative Biol* (2007) 72:527–41. doi: 10.1101/sqb.2007.72.037
- Wen S, Ma D, Zhao M, Xie L, Wu Q, Gou L, et al. Spatiotemporal single-cell analysis of gene expression in the mouse suprachiasmatic nucleus. *Nat Neurosci* (2020) 23:456–67. doi: 10.1038/s41593-020-0586-x
- Silver R, Schwartz WJ. The suprachiasmatic nucleus is a functionally heterogeneous timekeeping organ. *Methods Enzymol* (2005) 393:451–65. doi: 10.1016/S0076-6879(05)93022-X
- Welsh DK, Logothetis DE, Meister M, Reppert SM. Individual neurons dissociated from rat suprachiasmatic nucleus express independently phased circadian firing rhythms. *Neuron* (1995) 14:697–706. doi: 10.1016/0896-6273(95)90214-7
- Honma S, Nakamura W, Shirakawa T, Honma KI. Diversity in the circadian periods of single neurons of the rat suprachiasmatic nucleus depends on nuclear structure and intrinsic period. *Neurosci Lett* (2004) 358:173–6. doi: 10.1016/j.neulet.2004.01.022
- Gooley JJ, Lu J, Chou TC, Scammell TE, Saper CB. Melanopsin in cells of origin of the retinohypothalamic tract. *Nat Neurosci* (2001) 4:1165. doi: 10.1038/nn768
- Hattar S, Kumar M, Park A, Tong P, Tung J, Yau KW, et al. Central projections of melanopsin-expressing retinal ganglion cells in the mouse. *J Comp Neurol* (2006) 497:326–49. doi: 10.1002/cne.20970
- Güler AD, Ecker JL, Lall GS, Haq S, Altimus CM, Liao HW, et al. Melanopsin cells are the principal conduits for rod-cone input to non-image-forming vision. *Nature* (2008) 453:102–5. doi: 10.1038/nature06829
- Bae K, Jin X, Maywood ES, Hastings MH, Reppert SM, Weaver DR. Differential Functions of mPer1, mPer2, and mPer3 in the SCN Circadian Clock at The negative feedback loop involves the dynamic reg. *Neuron* (2001) 30:525–36. doi: 10.1016/S0896-6273(01)00302-6
- Damiola F, Le Minli N, Preitner N, Kornmann B, Fleury-Olela F, Schibler U. Restricted feeding uncouples circadian oscillators in peripheral tissues from the central pacemaker in the suprachiasmatic nucleus. *Genes Dev* (2000) 14:2950–61. doi: 10.1101/gad.183500
- Stokkan KA, Yamazaki S, Tei H, Sakaki Y, Menaker M. Entrainment of the circadian clock in the liver by feeding. *Sci* (80- ) (2001) 291:490–3. doi: 10.1126/science.291.5503.490
- Hara R, Wan K, Wakamatsu H, Aida R, Moriya T, Akiyama M, et al. Restricted feeding entrains liver clock without participation of the suprachiasmatic nucleus. *Genes to Cells* (2001) 6:269–78. doi: 10.1046/j.1365-2443.2001.00419.x
- Izumo M, Pejchal M, Schook AC, Lange RP, Walisser JA, Sato TR, et al. Differential effects of light and feeding on circadian organization of peripheral clocks in a forebrain Bmal1 mutant. *Elife* (2014) 3:e04617. doi: 10.7554/eLife.04617
- Sheward WJ, Maywood ES, French KL, Horn JM, Hastings MH, Seck JR, et al. Entrainment to feeding but not to light: Circadian phenotype of VPAC 2 receptor-null mice. *J Neurosci* (2007) 27:4351–8. doi: 10.1523/JNEUROSCI.4843-06.2007
- Fernandez DC, Komal R, Langel J, Ma J, Duy PQ, Penzo MA, et al. Retinal innervation tunes circuits that drive nonphotic entrainment to food. *Nature* (2020) 581:194–8. doi: 10.1038/s41586-020-2204-1
- Davidson AJ. Lesion studies targeting food-anticipatory activity. *Eur J Neurosci* (2009) 30:1658–64. doi: 10.1111/j.1460-9568.2009.06961.x
- Mistlberger RE. Neurobiology of food anticipatory circadian rhythms. *Physiol Behav* (2011) 104:535–45. doi: 10.1016/j.physbeh.2011.04.015
- Challet E, Mendoza J, Dardente H, Pévet P. Neurogenetics of food anticipation. *Eur J Neurosci* (2009) 30:1676–87. doi: 10.1111/j.1460-9568.2009.06962.x
- Butler AA, Girardet C, Mavrikaki M, Trevaskis JL, Macarthur H, Marks DL, et al. A life without hunger: The Ups (and downs) to modulating melanocortin-3 receptor signaling. *Front Neurosci* (2017) 11:128. doi: 10.3389/fnins.2017.00128
- Davidson AJ, Capparelli SLT, Stephan FK. Feeding-entrained circadian rhythms are attenuated by lesions of the parabrachial region in rats. *Am J Physiol - Regul Integr Comp Physiol* (2000) 278:R1296–304. doi: 10.1152/ajpregu.2000.278.5.r1296
- Mendoza J, Pévet P, Felder-Schmittbuhl MP, Bailly Y, Challet E. The cerebellum harbors a circadian oscillator involved in food anticipation. *J Neurosci* (2010) 30:1894–904. doi: 10.1523/JNEUROSCI.5855-09.2010
- Gallardo CM, Hsu CT, Gunapala KM, Parfyonov M, Chang CH, Mistlberger RE, et al. Behavioral and neural correlates of acute and scheduled hunger in C57BL/6 mice. *PloS One* (2014) 9:e95990. doi: 10.1371/journal.pone.0095990
- Chavan R, Feillet C, Costa SSF, Delorme JE, Okabe T, Ripperger JA, et al. Liver-derived ketone bodies are necessary for food anticipation. *Nat Commun* (2016) 7:10580. doi: 10.1038/ncomms10580
- Dunlap JC. Molecular bases for circadian clocks. *Cell* (1999) 96:271–90. doi: 10.1016/S0092-8674(00)80566-8
- Shi SQ, Ansari TS, McGuinness OP, Wasserman DH, Johnson CH. Circadian disruption leads to insulin resistance and obesity. *Curr Biol* (2013) 23:372–81. doi: 10.1016/j.cub.2013.01.048
- Stenvers DJ, Scheer FAJL, Schrauwen P, la Fleur SE, Kalsbeek A. Circadian clocks and insulin resistance. *Nat Rev Endocrinol* (2019) 15:75–89. doi: 10.1038/s41574-018-0122-1
- Marcheva B, Ramsey KM, Affinati A, Bass J. Clock genes and metabolic disease. *J Appl Physiol* (2009) 107:1638–46. doi: 10.1152/japplphysiol.00698.2009
- Bedrosian TA, Fonken LK, Nelson RJ. Endocrine Effects of Circadian Disruption. *Annu Rev Physiol* (2016) 78:109–31. doi: 10.1146/annurev-physiol-021115-105102
- Terzibasi-Tozzini E, Martinez-Nicolas A, Lucas-Sánchez A. The clock is ticking. Ageing of the circadian system: From physiology to cell cycle. *Semin Cell Dev Biol* (2017) 70:164–76. doi: 10.1016/j.semcdb.2017.06.011
- Uddin MS, Tewari D, Mamun AA, Kabir MT, Niaz K, Wahed MII, et al. Circadian and sleep dysfunction in Alzheimer's disease. *Ageing Res Rev* (2020) 60:101046. doi: 10.1016/j.arr.2020.101046
- Goh VHH, Tong TTY, Lee LKH. Sleep/wake cycle and circadian disturbances in shift work: Strategies for their management - A review. *Ann Acad Med Singapore* (2000) 29:90–6.
- Barca-Mayo O, Boender AJ, Armirotti A, De Pietri Tonelli D. Deletion of astrocytic BMAL1 results in metabolic imbalance and shorter lifespan in mice. *Glia* (2020) 68:1131–47. doi: 10.1002/glia.23764
- Barca-Mayo O, Pons-Espinal M, Follert P, Armirotti A, Berdondini L, De Pietri Tonelli D. Astrocyte deletion of Bmal1 alters daily locomotor activity and cognitive functions via GABA signalling. *Nat Commun* (2017) 8:14336. doi: 10.1038/ncomms14336
- Tso CF, Simon T, Greenlaw AC, Puri T, Mieda M, Herzog ED. Astrocytes Regulate Daily Rhythms in the Suprachiasmatic Nucleus and Behavior. *Curr Biol* (2017) 27:1055–61. doi: 10.1016/j.cub.2017.02.037
- Brancaccio M, Patton AP, Chesham JE, Maywood ES, Hastings MH. Astrocytes Control Circadian Timekeeping in the Suprachiasmatic Nucleus via Glutamatergic Signaling. *Neuron* (2017) 93:1420–1435.e5. doi: 10.1016/j.neuron.2017.02.030

43. Brancaccio M, Edwards MD, Patton AP, Smyllie NJ, Chesham JE, Maywood ES, et al. Cell-autonomous clock of astrocytes drives circadian behavior in mammals. *Sci (80- )* (2019) 363:187–92. doi: 10.1126/science.aat4104
44. Ben Haim L, Rowitch DH. Functional diversity of astrocytes in neural circuit regulation. *Nat Rev Neurosci* (2016) 18:31–41. doi: 10.1038/nrn.2016.159
45. Zhang Y, Barres BA. Astrocyte heterogeneity: An underappreciated topic in neurobiology. *Curr Opin Neurobiol* (2010) 20:588–94. doi: 10.1016/j.conb.2010.06.005
46. Halassa MM, Fellin T, Haydon PG. The tripartite synapse: roles for gliotransmission in health and disease. *Trends Mol Med* (2007) 3:54–63. doi: 10.1016/j.molmed.2006.12.005
47. Haber M, Zhou L, Murai KK. Cooperative astrocyte and dendritic spine dynamics at hippocampal excitatory synapses. *J Neurosci* (2006) 26:8881–91. doi: 10.1523/JNEUROSCI.1302-06.2006
48. Bushong EA, Martone ME, Jones YZ, Ellisman MH. Protoplasmic astrocytes in CA1 stratum radiatum occupy separate anatomical domains. *J Neurosci* (2002) 22:183–92. doi: 10.1523/jneurosci.22-01-00183.2002
49. Spanagel R, Pendyala G, Abarca C, Zghoul T, Sanchis-Segura C, Magnone MC, et al. The clock gene *Per2* influences the glutamatergic system and modulates alcohol consumption. *Nat Med* (2005) 11:35–42. doi: 10.1038/nm1163
50. Beaulé C, Swannstrom A, Leone MJ, Herzog ED. Circadian modulation of gene expression, but not glutamate uptake, in mouse and rat cortical astrocytes. *PloS One* (2009) 4:e7476. doi: 10.1371/journal.pone.0007476
51. Blanco ME, Mayo OB, Bandiera T, Tonelli DDP, Armirotti A. LC–MS/MS analysis of twelve neurotransmitters and amino acids in mouse cerebrospinal fluid. *J Neurosci Methods* (2020) 341:108760. doi: 10.1016/j.jneumeth.2020.108760
52. Becquet D, Girardet C, Guillaumond F, François-Bellan AM, Bosler O. Ultrastructural plasticity in the rat suprachiasmatic nucleus. Possible involvement in clock entrainment. *Glia* (2008) 56:294–305. doi: 10.1002/glia.20613
53. Monique L, Servière J. Circadian fluctuations in GFAP distribution in the syrian hamster suprachiasmatic nucleus. *Neuroreport* (1993) 4:1243–6. doi: 10.1097/00001756-199309000-00008
54. Girardet C, Blanchard MP, Ferracci G, Lévêque C, Moreno M, François-Bellan AM, et al. Daily changes in synaptic innervation of VIP neurons in the rat suprachiasmatic nucleus: Contribution of glutamatergic afferents. *Eur J Neurosci* (2010) 31:359–70. doi: 10.1111/j.1460-9568.2009.07071.x
55. Horvath TL, Sarman B, García-Cáceres C, Enriori PJ, Sotonyi P, Shanabrough M, et al. Synaptic input organization of the melanocortin system predicts diet-induced hypothalamic reactive gliosis and obesity. *Proc Natl Acad Sci USA* (2010) 107:14875–80. doi: 10.1073/pnas.1004282107
56. Nuzzaci D, Cansell C, Liénard F, Nédélec E, Ben Fradj S, Castel J, et al. Postprandial Hyperglycemia Stimulates Neuroglial Plasticity in Hypothalamic POMC Neurons after a Balanced Meal. *Cell Rep* (2020) 30:3067–3078.e5. doi: 10.1016/j.celrep.2020.02.029
57. García-Cáceres C, Quarta C, Varela L, Gao Y, Gruber T, Legutko B, et al. Astrocytic Insulin Signaling Couples Brain Glucose Uptake with Nutrient Availability. *Cell* (2016) 166:867–80. doi: 10.1016/j.cell.2016.07.028
58. Kim JG, Suyama S, Koch M, Jin S, Argente-Arizon P, Argente J, et al. Leptin signaling in astrocytes regulates hypothalamic neuronal circuits and feeding. *Nat Neurosci* (2014) 17:908–10. doi: 10.1038/nn.3725
59. Mendelsohn AR, Larrick JW. Sleep Facilitates Clearance of Metabolites from the Brain: Glymphatic Function in Aging and Neurodegenerative Diseases. *Rejuvenation Res* (2013) 16:518–23. doi: 10.1089/rej.2013.1530
60. Taoka T, Jost G, Frenzel T, Naganawa S, Pietsch H. Impact of the Glymphatic System on the Kinetic and Distribution of Gadodiamide in the Rat Brain: Observations by Dynamic MRI and Effect of Circadian Rhythm on Tissue Gadolinium Concentrations. *Invest Radiol* (2018) 53:529–34. doi: 10.1097/RLI.0000000000000473
61. Iliff JJ, Wang M, Liao Y, Plogg BA, Peng W, Gundersen GA, et al. A paravascular pathway facilitates CSF flow through the brain parenchyma and the clearance of interstitial solutes, including amyloid  $\beta$ . *Sci Transl Med* (2012) 4:147ra111. doi: 10.1126/scitranslmed.3003748
62. Murlidharan G, Crowther A, Reardon RA, Song J, Asokan A. Glymphatic fluid transport controls paravascular clearance of AAV vectors from the brain. *JCI Insight* (2016) 1:e88034. doi: 10.1172/jci.insight.88034
63. LeSauter J, Silver R. Output signals of the SCN. *Chronobiol Int* (1998) 15:535–50. doi: 10.3109/07420529808998706
64. Maywood ES, Chesham JE, O'Brien JA, Hastings MH. A diversity of paracrine signals sustains molecular circadian cycling in suprachiasmatic nucleus circuits. *Proc Natl Acad Sci USA* (2011) 108:14306–11. doi: 10.1073/pnas.1101767108
65. Ng FS, Tangredi MM, Jackson FR. Glial cells physiologically modulate clock neurons and circadian behavior in a calcium-dependent manner. *Curr Biol* (2011) 21:625–34. doi: 10.1016/j.cub.2011.03.027
66. Suh J, Jackson FR. Drosophila Ebony Activity Is Required in Glia for the Circadian Regulation of Locomotor Activity. *Neuron* (2007) 55:435–47. doi: 10.1016/j.neuron.2007.06.038
67. Jackson FR. Glial cell modulation of circadian rhythms. *Glia* (2011) 59:1341–50. doi: 10.1002/glia.21097
68. Womac AD, Burkeen JF, Neuendorff N, Earnest DJ, Zoran MJ. Circadian rhythms of extracellular ATP accumulation in suprachiasmatic nucleus cells and cultured astrocytes. *Eur J Neurosci* (2009) 30:869–76. doi: 10.1111/j.1460-9568.2009.06874.x
69. Cornell-Bell AH, Finkbeiner SM, Cooper MS, Smith SJ. Glutamate induces calcium waves in cultured astrocytes: Long-range glial signaling. *Sci (80- )* (1990) 247:470–3. doi: 10.1126/science.1967852
70. Shinohara K, Funabashi T, Mitushima D, Kimura F. Effects of gap junction blocker on vasopressin and vasoactive intestinal polypeptide rhythms in the rat suprachiasmatic nucleus in vitro. *Neurosci Res* (2000) 38:43–7. doi: 10.1016/S0168-0102(00)00141-3
71. Wang MH, Chen N, Wang JH. The coupling features of electrical synapses modulate neuronal synchrony in hypothalamic superchiasmatic nucleus. *Brain Res* (2014) 1550:9–17. doi: 10.1016/j.brainres.2014.01.007
72. Diemer T, Landgraf D, Noguchi T, Pan H, Moreno JL, Welsh DK. Cellular circadian oscillators in the suprachiasmatic nucleus remain coupled in the absence of connexin-36. *Neuroscience* (2017) 357:1–11. doi: 10.1016/j.neuroscience.2017.05.037
73. Long MA, Jutras MJ, Connors BW, Burwell RD. Electrical synapses coordinate activity in the suprachiasmatic nucleus. *Nat Neurosci* (2005) 8:61–6. doi: 10.1038/nn1361
74. Clasadonte J, Scemes E, Wang Z, Boison D, Haydon PG. Connexin 43-Mediated Astroglial Metabolic Networks Contribute to the Regulation of the Sleep-Wake Cycle. *Neuron* (2017) 95:1365–1380.e5. doi: 10.1016/j.neuron.2017.08.022
75. Giantomasi M, Malerba M, Barca-Mayo O, Miele E, De Pietri Tonelli D, Berdondini L. A microfluidic device to study molecular clocks synchronization among neuronal populations, in: *41st Annual International Conference of the IEEE Engineering in Medicine*. (2019) IEEE. doi: 10.1109/EMBC.2019.8856999
76. Cirrito JR, Deane R, Fagan AM, Spinner ML, Parsadanian M, Finn MB, et al. P-glycoprotein deficiency at the blood-brain barrier increases amyloid- $\beta$  deposition in an Alzheimer disease mouse model. *J Clin Invest* (2005) 115:3285–90. doi: 10.1172/JCI25247
77. Abbott NJ, Rönnbäck L, Hansson E. Astrocyte-endothelial interactions at the blood-brain barrier. *Nat Rev Neurosci* (2006) 7:41–53. doi: 10.1038/nrn1824
78. Xie L, Kang H, Xu Q, Chen MJ, Liao Y, Thiyagarajan M, et al. Sleep drives metabolite clearance from the adult brain. *Sci (80- )* (2013) 342:373–7. doi: 10.1126/science.1241224
79. Nakazato R, Kawabe K, Yamada D, Ikeno S, Mieda M, Shimba S, et al. Disruption of Bmal1 impairs blood-brain barrier integrity via pericyte dysfunction. *J Neurosci* (2017) 37:10052–62. doi: 10.1523/JNEUROSCI.3639-16.2017
80. Zhang SL, Yue Z, Arnold DM, Artushin G, Sehgal A. A Circadian Clock in the Blood-Brain Barrier Regulates Xenobiotic Efflux. *Cell* (2018) 173:130–139.e10. doi: 10.1016/j.cell.2018.02.017
81. Guillod-Maximin E, Lorisignol A, Alquier T, Pénicaud L. Acute intracarotid glucose injection towards the brain induces specific c-fos activation in hypothalamic nuclei: Involvement of astrocytes in cerebral glucose-sensing in rats. *J Neuroendocrinol* (2004) 16:464–71. doi: 10.1111/j.1365-2826.2004.01185.x
82. Gao Y, Layritz C, Legutko B, Eichmann TO, Laperrousaz E, Moullé VS, et al. Disruption of lipid uptake in astroglia exacerbates diet-induced obesity. *Diabetes* (2017) 66:2555–63. doi: 10.2337/db16-1278

83. Le Foll C, Levin BE. Fatty acid-induced astrocyte ketone production and the control of food intake. *Am J Physiol - Regul Integr Comp Physiol* (2016) 310: R1186–92. doi: 10.1152/ajpregu.00113.2016
84. Diano S, Kalra SP, Horvath TL. Leptin receptor immunoreactivity is associated with the Golgi apparatus of hypothalamic neurones and glial cells. *J Neuroendocrinol* (1998) 10:647–50. doi: 10.1046/j.1365-2826.1998.00261.x
85. Cheunsuang O, Morris R. Astrocytes in the arcuate nucleus and median eminence that take up a fluorescent dye from the circulation express leptin receptors and neuropeptide Y Y1 receptors. *Glia* (2005) 52:228–33. doi: 10.1002/glia.20239
86. Cardona-Gómez GP, DonCarlos L, García-Segura LM. Insulin-like growth factor I receptors and estrogen receptors colocalize in female rat brain. *Neuroscience* (2000) 99:751–60. doi: 10.1016/S0306-4522(00)00228-1
87. Dezonne RS, Lima FRS, Trentin AG, Gomes FC. Thyroid Hormone and Astroglia: Endocrine Control of the Neural Environment. *J Neuroendocrinol* (2015) 27:435–45. doi: 10.1111/jne.12283
88. O'Banion MK, Young DA, Bohn MC. Corticosterone-responsive mRNAs in primary rat astrocytes. *Mol Brain Res* (1994) 22:57–68. doi: 10.1016/0169-328X(94)90032-9
89. Carter BS, Meng F, Thompson RC. Glucocorticoid treatment of astrocytes results in temporally dynamic transcriptome regulation and astrocyte-enriched mRNA changes in vitro. *Physiol Genomics* (2012) 44:1188–200. doi: 10.1152/physiolgenomics.00097.2012
90. Rosenfeld P, Van Eekelen JAM, Levine S, De Kloet ER. Ontogeny of the Type 2 glucocorticoid receptor in discrete rat brain regions: an immunocytochemical study. *Dev Brain Res* (1988) 470:119–27. doi: 10.1016/0165-3806(88)90207-6
91. Zehring WA, Wheeler DA, Reddy P, Konopka RJ, Kyriacou CP, Rosbash M, et al. P-element transformation with period locus DNA restores rhythmicity to mutant, arrhythmic *Drosophila melanogaster*. *Cell* (1984) 39:369–76. doi: 10.1016/0092-8674(84)90015-1
92. Bargiello TA, Jackson FR, Young MW. Restoration of circadian behavioural rhythms by gene transfer in *Drosophila*. *Nature* (1984) 312:752–4. doi: 10.1038/312752a0
93. Van Der Horst GTJ, Muijtjens M, Kobayashi K, Takano R, Kanno SI, Takao M, et al. Mammalian Cry1 and Cry2 are essential for maintenance of circadian rhythms. *Nature* (1999) 398:627–30. doi: 10.1038/19323
94. Zheng B, Albrecht U, Kaasik K, Sage M, Lu W, Vaishnav S, et al. Nonredundant roles of the mPer1 and mPer2 genes in the mammalian circadian clock. *Cell* (2001) 105:683–94. doi: 10.1016/S0092-8674(01)00380-4
95. Kume K, Zylka MJ, Sriram S, Shearman LP, Weaver DR, Jin X, et al. mCRY1 and mCRY2 are essential components of the negative limb of the circadian clock feedback loop. *Cell* (1999) 98:193–205. doi: 10.1016/S0092-8674(00)81014-4
96. Cox KH, Takahashi JS. Circadian clock genes and the transcriptional architecture of the clock mechanism. *J Mol Endocrinol* (2019) 63:R93–R102. doi: 10.1530/JME-19-0153
97. Preitner N, Damiola F, Lopez-Molina L, Zakany J, Duboule D, Albrecht U, et al. The orphan nuclear receptor REV-ERB $\alpha$  controls circadian transcription within the positive limb of the mammalian circadian oscillator. *Cell* (2002) 110:251–60. doi: 10.1016/S0092-8674(02)00825-5
98. Richards J, Gumz ML. Advances in understanding the peripheral circadian clocks. *FASEB J* (2012) 26:3602–13. doi: 10.1096/fj.12-203554
99. Inoki K, Kim J, Guan KL. AMPK and mTOR in cellular energy homeostasis and drug targets. *Annu Rev Pharmacol Toxicol* (2012) 52:381–400. doi: 10.1146/annurev-pharmtox-010611-134537
100. Robles MS, Humphrey SJ, Mann M. Phosphorylation Is a Central Mechanism for Circadian Control of Metabolism and Physiology. *Cell Metab* (2017) 25:118–27. doi: 10.1016/j.cmet.2016.10.004
101. Dang F, Sun X, Ma X, Wu R, Zhang D, Chen Y, et al. Insulin post-transcriptionally modulates Bmal1 protein to affect the hepatic circadian clock. *Nat Commun* (2016) 7:12696. doi: 10.1038/ncomms12696
102. Luciano AK, Zhou W, Santana JM, Kyriakides C, Velazquez H, Sessa WC. CLOCK phosphorylation by AKT regulates its nuclear accumulation and circadian gene expression in peripheral tissues. *J Biol Chem* (2018) 293:9126–36. doi: 10.1074/jbc.RA117.000773
103. Lamia KA, Sachdeva UM, Di Tacchio L, Williams EC, Alvarez JG, Egan DF, et al. AMPK regulates the circadian clock by cryptochrome phosphorylation and degradation. *Sci* (80-) (2009) 326:437–40. doi: 10.1126/science.1172156
104. Kaasik K, Kivimäe S, Allen JJ, Chalkley RJ, Huang Y, Baer K, et al. Glucose sensor O-GlcNAcylation coordinates with phosphorylation to regulate circadian clock. *Cell Metab* (2013) 17:291–302. doi: 10.1016/j.cmet.2012.12.017
105. Li MD, Ruan HB, Hughes ME, Lee JS, Singh JP, Jones SP, et al. O-GlcNAc signaling entrains the circadian clock by inhibiting BMAL1/CLOCK ubiquitination. *Cell Metab* (2013) 17:303–10. doi: 10.1016/j.cmet.2012.12.015
106. Ma YT, Luo H, Guan WJ, Zhang H, Chen C, Wang Z, et al. O-GlcNAcylation of BMAL1 regulates circadian rhythms in NIH3T3 fibroblasts. *Biochem Biophys Res Commun* (2013) 431:382–7. doi: 10.1016/j.bbrc.2013.01.043
107. Nakahata Y, Kaluzova M, Grimaldi B, Sahar S, Hirayama J, Chen D, et al. The NAD<sup>+</sup>-Dependent Deacetylase SIRT1 Modulates CLOCK-Mediated Chromatin Remodeling and Circadian Control. *Cell* (2008) 134:329–40. doi: 10.1016/j.cell.2008.07.002
108. Asher G, Gatfield D, Stratmann M, Reinke H, Dibner C, Kreppel F, et al. SIRT1 Regulates Circadian Clock Gene Expression through PER2 Deacetylation. *Cell* (2008) 134:317–28. doi: 10.1016/j.cell.2008.06.050
109. Foteinou PT, Venkataraman A, Francey LJ, Anafi RC, Hogenesch JB, Doyle FJ. Computational and experimental insights into the circadian effects of SIRT1. *Proc Natl Acad Sci USA* (2018) 115:11643–8. doi: 10.1073/pnas.1803410115
110. Asher G, Reinke H, Altmeyer M, Gutierrez-Arcelus M, Hottiger MO, Schibler U. Poly(ADP-Ribose) Polymerase 1 Participates in the Phase Entrainment of Circadian Clocks to Feeding. *Cell* (2010) 142:943–53. doi: 10.1016/j.cell.2010.08.016
111. Takahashi JS. Transcriptional architecture of the mammalian circadian clock. *Nat Rev Genet* (2017) 18:164–79. doi: 10.1038/nrg.2016.150
112. Eckel-Mahan K, Sassone-Corsi P. Metabolism and the circadian clock converge. *Physiol Rev* (2013) 93:107–35. doi: 10.1152/physrev.00016.2012
113. Sutton EF, Beyl R, Early KS, Cefalu WT, Ravussin E, Peterson CM. Early Time-Restricted Feeding Improves Insulin Sensitivity, Blood Pressure, and Oxidative Stress Even without Weight Loss in Men with Prediabetes. *Cell Metab* (2018) 27:1212–1221.e3. doi: 10.1016/j.cmet.2018.04.010
114. Carroll KF, Nestel PJ. Diurnal variation in glucose tolerance and in insulin secretion in man. *Diabetes* (1973) 22:333–48. doi: 10.2337/diab.22.5.333
115. Gibson T, Jarrett RJ. Diurnal Variation in Insulin Sensitivity. *Lancet* (1972) 2:947–8. doi: 10.1016/S0140-6736(72)92472-5
116. López M, Tena-Sempere M. Estradiol effects on hypothalamic AMPK and BAT thermogenesis: A gateway for obesity treatment? *Pharmacol Ther* (2017) 178:109–22. doi: 10.1016/j.pharmthera.2017.03.014
117. Timper K, Brüning JC. Hypothalamic circuits regulating appetite and energy homeostasis: Pathways to obesity. *DMM Dis Model Mech* (2017) 10:679–89. doi: 10.1242/dmm.026609
118. Routh VH, Hao L, Santiago AM, Sheng Z, Zhou C. Hypothalamic glucose sensing: Making ends meet. *Front Syst Neurosci* (2014) 8:236. doi: 10.3389/fnsys.2014.00236
119. Wang D, He X, Zhao Z, Feng Q, Lin R, Sun Y, et al. Whole-brain mapping of the direct inputs and axonal projections of POMC and AgRP neurons. *Front Neuroanat* (2015) 9:40. doi: 10.3389/fnana.2015.00040
120. Shimazu T, Fukuda A, Ban T. Reciprocal influences of the ventromedial and lateral hypothalamic nuclei on blood glucose level and liver glycogen content [38]. *Nature* (1966) 210:1178–9. doi: 10.1038/2101178a0
121. Fuente-Martín E, García-Cáceres C, Argente-Arizón P, Díaz F, Granado M, Freire-Regatillo A, et al. Ghrelin Regulates Glucose and Glutamate Transporters in Hypothalamic Astrocytes. *Sci Rep* (2016) 6:23673. doi: 10.1038/srep23673
122. Yang L, Qi Y, Yang Y. Astrocytes Control Food Intake by Inhibiting AGRP Neuron Activity via Adenosine A1 Receptors. *Cell Rep* (2015) 11:798–807. doi: 10.1016/j.celrep.2015.04.002
123. Sweeney P, Qi Y, Xu Z, Yang Y. Activation of hypothalamic astrocytes suppresses feeding without altering emotional states. *Glia* (2016) 64:2263–73. doi: 10.1002/glia.23073
124. Bass J, Takahashi JS. Circadian integration of metabolism and energetics. *Sci* (80-) (2010) 330:1349–54. doi: 10.1126/science.1195027

125. McDermarmon EL, Patel KN, Ko CH, Walisser JA, Schook AC, Chong JL, et al. Dissecting the functions of the mammalian clock protein BMAL1 by tissue-specific rescue in mice. *Sci (80- )* (2006) 314:1304–8. doi: 10.1126/science.1132430
126. Orozco-Solis R, Aguilar-Arnal L, Murakami M, Peruquetti R, Ramadori G, Coppari R, et al. The circadian clock in the ventromedial hypothalamus controls cyclic energy expenditure. *Cell Metab* (2016) 23:467–78. doi: 10.1016/j.cmet.2016.02.003
127. Cedernaes J, Huang W, Ramsey KM, Waldeck N, Cheng L, Marcheva B, et al. Transcriptional Basis for Rhythmic Control of Hunger and Metabolism within the AgRP Neuron. *Cell Metab* (2019) 29:1078–1091.e5. doi: 10.1016/j.cmet.2019.01.023
128. Lamia KA, Storch KF, Weitz CJ. Physiological significance of a peripheral tissue circadian clock. *Proc Natl Acad Sci USA* (2008) 105:15172–7. doi: 10.1073/pnas.0806717105
129. Doi R, Oishi K, Ishida N. CLOCK regulates circadian rhythms of hepatic glycogen synthesis through transcriptional activation of Gys2. *J Biol Chem* (2010) 285:22114–21. doi: 10.1074/jbc.M110.110361
130. Zhang EE, Liu Y, Dentin R, Pongsawakul PY, Liu AC, Hirota T, et al. Cryptochrome mediates circadian regulation of cAMP signaling and hepatic gluconeogenesis. *Nat Med* (2010) 16:1152–6. doi: 10.1038/nm.2214
131. Lamia KA, Papp SJ, Yu RT, Barish GD, Uhlenhaut NH, Jonker JW, et al. Cryptochromes mediate rhythmic repression of the glucocorticoid receptor. *Nature* (2011) 480:552–6. doi: 10.1038/nature10700
132. Toledo M, Batista-Gonzalez A, Merheb E, Aoun ML, Tarabra E, Feng D, et al. Autophagy Regulates the Liver Clock and Glucose Metabolism by Degrading CRY1. *Cell Metab* (2018) 28:268–81.e4. doi: 10.1016/j.cmet.2018.05.023
133. Vollmers C, Gill S, DiTacchio L, Pulivarthy SR, Le HD, Panda S. Time of feeding and the intrinsic circadian clock drive rhythms in hepatic gene expression. *Proc Natl Acad Sci USA* (2009) 106:21453–8. doi: 10.1073/pnas.0909591106
134. Storch KF, Lipan O, Leykin I, Viswanathan N, Davis FC, Wong WH, et al. Extensive and divergent circadian gene expression in liver and heart. *Nature* (2002) 417:78–83. doi: 10.1038/nature744
135. Panda S, Antoch MP, Miller BH, Su AI, Schook AB, Straume M, et al. Coordinated transcription of key pathways in the mouse by the circadian clock. *Cell* (2002) 109:307–20. doi: 10.1016/S0092-8674(02)00722-5
136. DeFronzo RA, Tripathy D. Skeletal muscle insulin resistance is the primary defect in type 2 diabetes. *Diabetes Care* (2009) Suppl 2:S157–63. doi: 10.2337/dc09-s302
137. Dyar KA, Ciciliot S, Wright LE, Biensø RS, Tagliazucchi GM, Patel VR, et al. Muscle insulin sensitivity and glucose metabolism are controlled by the intrinsic muscle clock. *Mol Metab* (2014) 3:29–41. doi: 10.1016/j.molmet.2013.10.005
138. Perrin L, Loizides-Mangold U, Chanon S, Gobet C, Hulo N, Isenegger L, et al. Transcriptomic analyses reveal rhythmic and CLOCK-driven pathways in human skeletal muscle. *Elife* (2018) 7:e34114. doi: 10.7554/eLife.34114
139. Hong S, Zhou W, Fang B, Lu W, Loro E, Damle M, et al. Dissociation of muscle insulin sensitivity from exercise endurance in mice by HDAC3 depletion. *Nat Med* (2017) 23:223–34. doi: 10.1038/nm.4245
140. Aras E, Ramadori G, Kinouchi K, Liu Y, Ioris RM, Brenachot X, et al. Light Entrained Diurnal Changes in Insulin Sensitivity of Skeletal Muscle via Ventromedial Hypothalamic Neurons. *Cell Rep* (2019) 27:2385–98.e3. doi: 10.1016/j.celrep.2019.04.093
141. Carrasco-Benso MP, Rivero-Gutierrez B, Lopez-Minguez J, Anzola A, Diez-Noguera A, Madrid JA, et al. Human adipose tissue expresses intrinsic circadian rhythm in insulin sensitivity. *FASEB J* (2016) 30:3117–23. doi: 10.1096/fj.201600269RR
142. Paschos GK, Ibrahim S, Song WL, Kunieda T, Grant G, Reyes TM, et al. Obesity in mice with adipocyte-specific deletion of clock component Arntl. *Nat Med* (2012) 18:1768–77. doi: 10.1038/nm.2979
143. Minokoshi Y, Haque MS, Shimazu T. Microinjection of leptin into the ventromedial hypothalamus increases glucose uptake in peripheral tissues in rats. *Diabetes* (1999) 48:2287–7. doi: 10.2337/diabetes.48.2.287
144. Morgan DA, McDaniel LN, Yin T, Khan M, Jiang J, Acevedo MR, et al. Regulation of glucose tolerance and sympathetic activity by MC4R signaling in the lateral hypothalamus. *Diabetes* (2015) 64:1976–87. doi: 10.2337/db14-1257
145. Coutinho EA, Okamoto S, Ishikawa AW, Yokota S, Wada N, Hirabayashi T, et al. Activation of SF1 neurons in the ventromedial hypothalamus by DREADD technology increases insulin sensitivity in peripheral tissues. *Diabetes* (2017) 66:2372–86. doi: 10.2337/db16-1344
146. Van Der Veen DR, Shao J, Chapman S, Leevy WM, Duffield GE. A diurnal rhythm in glucose uptake in brown adipose tissue revealed by in vivo PET-FDG imaging. *Obesity* (2012) 20:1527–9. doi: 10.1038/oby.2012.78
147. van den Berg R, Kooijman S, Noordam R, Ramkisoensing A, Abreu-Vieira G, Tambyrajah LL, et al. A Diurnal Rhythm in Brown Adipose Tissue Causes Rapid Clearance and Combustion of Plasma Lipids at Wakening. *Cell Rep* (2018) 22:3521–33. doi: 10.1016/j.celrep.2018.03.004
148. Nayak G, Zhang KX, Vemmaraju S, Odaka Y, Buhr ED, Holt-Jones A, et al. Adaptive Thermogenesis in Mice Is Enhanced by Opsin 3-Dependent Adipocyte Light Sensing. *Cell Rep* (2020) 30:672–86.e8. doi: 10.1016/j.celrep.2019.12.043
149. Zhang KX, D'Souza S, Upton BA, Kernodde S, Vemmaraju S, Nayak G, et al. Violet-light suppression of thermogenesis by opsin 5 hypothalamic neurons. *Nature* (2020) 585:420–5. doi: 10.1038/s41586-020-2683-0
150. Perelis M, Marcheva B, Ramsey KM, Schipma MJ, Hutchison AL, Taguchi A, et al. Pancreatic  $\beta$  cell enhancers regulate rhythmic transcription of genes controlling insulin secretion. *Sci (80- )* (2015) 350:aac4250. doi: 10.1126/science.aac4250
151. Peschke E, Peschke D. Evidence for a circadian rhythm of insulin release from perfused rat pancreatic islets. *Diabetologia* (1998) 41:1085–92. doi: 10.1007/s001250051034
152. Sadacca LA, Lamia KA, DeLemos AS, Blum B, Weitz CJ. An intrinsic circadian clock of the pancreas is required for normal insulin release and glucose homeostasis in mice. *Diabetologia* (2011) 54:120–4. doi: 10.1007/s00125-010-1920-8
153. Saini C, Petrenko V, Pulimeno P, Giovannoni L, Berney T, Hebrok M, et al. A functional circadian clock is required for proper insulin secretion by human pancreatic islet cells. *Diabetes Obes Metab* (2016) 18:355–65. doi: 10.1111/dom.12616
154. Lee J, Kim MS, Li R, Liu VY, Fu L, Moore DD, et al. Loss of Bmal1 leads to uncoupling and impaired glucose-stimulated insulin secretion in  $\beta$ -cells. *Islets* (2011) 3:381–8. doi: 10.4161/isl.3.6.18157
155. Laposky AD, Shelton J, Bass J, Dugovic C, Perrino N, Turek FW. Altered sleep regulation in leptin-deficient mice. *Am J Physiol - Regul Integr Comp Physiol* (2006) 290:R894–903. doi: 10.1152/ajpregu.00304.2005
156. Laposky AD, Bradley MA, Williams DL, Bass J, Turek FW. Sleep-wake regulation is altered in leptin-resistant (db/db) genetically obese and diabetic mice. *Am J Physiol - Regul Integr Comp Physiol* (2008) 295:R2059–66. doi: 10.1152/ajpregu.00026.2008
157. Lesauter J, Hoque N, Weintraub M, Pfaff DW, Silver R. Stomach ghrelin-secreting cells as food-entrainable circadian clocks. *Proc Natl Acad Sci USA* (2009) 106:13582–7. doi: 10.1073/pnas.0906426106
158. Bélanger M, Allaman I, Magistretti PJ. Brain energy metabolism: Focus on Astrocyte-neuron metabolic cooperation. *Cell Metab* (2011) 14:724–38. doi: 10.1016/j.cmet.2011.08.016
159. Leloup C, Allard C, Carneiro L, Fioramonti X, Collins S, Pénicaud L. Glucose and hypothalamic astrocytes: More than a fueling role? *Neuroscience* (2016) 323:110–20. doi: 10.1016/j.neuroscience.2015.06.007
160. Rey G, Cesbron F, Rougemont J, Reinke H, Brunner M, Naef F. Genome-wide and phase-specific DNA-binding rhythms of BMAL1 control circadian output functions in mouse liver. *PLoS Biol* (2011) 9:e1000595. doi: 10.1371/journal.pbio.1000595
161. Morgello S, Uson RR, Schwartz EJ, Haber RS. The human blood-brain barrier glucose transporter (GLUT1) is a glucose transporter of gray matter astrocytes. *Glia* (1995) 14:43–54. doi: 10.1002/glia.440140107
162. De los Angeles García M, Millán C, Balmaceda-Aguilera C, Castro T, Pastor P, Montecinos H, et al. Hypothalamic ependymal-glial cells express the glucose transporter GLUT2, a protein involved in glucose sensing. *J Neurochem* (2003) 86:709–24. doi: 10.1046/j.1471-4159.2003.01892.x
163. Young JK, McKenzie JC. GLUT2 immunoreactivity in Gomori-positive astrocytes of the hypothalamus. *J Histochem Cytochem* (2004) 52:1519–24. doi: 10.1369/jhc.4A6375.2004

164. Oomura Y, Kimura K, Ooyama H, Maeno T, Matasaburo I, Kuniyoshi M. Reciprocal activities of the ventromedial and lateral hypothalamic areas of cats. *Sci (80- )* (1964) 143:484–5. doi: 10.1126/science.143.3605.484
165. Marty N, Dallaporta M, Foretz M, Emery M, Tarussio D, Bady I, et al. Regulation of glucagon secretion by glucose transporter type 2 (glut2) and astrocyte-dependent glucose sensors. *J Clin Invest* (2005) 115:3545–53. doi: 10.1172/JCI26309
166. Bady I, Marty N, Dallaporta M, Emery M, Gyger J, Tarussio D, et al. Evidence from glut2-null mice that glucose is a critical physiological regulator of feeding. *Diabetes* (2006) 55:988–95. doi: 10.2337/diabetes.55.04.06.db05-1386
167. Stolarczyk E, Guissard C, Michau A, Even PC, Grosfeld A, Serradas P, et al. Detection of extracellular glucose by GLUT2 contributes to hypothalamic control of food intake. *Am J Physiol - Endocrinol Metab* (2010) 298:E1078–87. doi: 10.1152/ajpendo.00737.2009
168. Iwashina I, Mochizuki K, Inamochi Y, Goda T. Clock genes regulate the feeding schedule-dependent diurnal rhythm changes in hexose transporter gene expressions through the binding of BMAL1 to the promoter/enhancer and transcribed regions. *J Nutr Biochem* (2011) 22:334–43. doi: 10.1016/j.jnutbio.2010.02.012
169. Šoltésiová D, Veselá A, Mravec B, Herichová I. Daily profile of glut1 and glut4 expression in tissues inside and outside the blood-brain barrier in control and streptozotocin-treated rats. *Physiol Res* (2013) 62:S115–24. doi: 10.33549/physiolres.932596
170. Lam TKT, Gutierrez-Juarez R, Pocai A, Rossetti L. Medicine: Regulation of blood glucose by hypothalamic pyruvate metabolism. *Sci (80- )* (2005) 309:943–7. doi: 10.1126/science.1112085
171. Magistretti PJ, Pellerin L. Cellular Bases of Brain Energy Metabolism and Their Relevance to Functional Brain Imaging: Evidence for a Prominent Role of Astrocytes. *Cereb Cortex* (1996) 6:50–61. doi: 10.1093/cercor/6.1.50
172. Parsons MP, Hirasawa M. ATP-sensitive potassium channel-mediated lactate effect on orexin neurons: Implications for brain energetics during arousal. *J Neurosci* (2010) 30:8061–70. doi: 10.1523/JNEUROSCI.5741-09.2010
173. Burt J, Alberto CO, Parsons MP, Hirasawa M. Local network regulation of orexin neurons in the lateral hypothalamus. *Am J Physiol - Regul Integr Comp Physiol* (2011) 301:R572–80. doi: 10.1152/ajpregu.00674.2010
174. Lundgaard I, Lu ML, Yang E, Peng W, Mestre H, Hitomi E, et al. Glymphatic clearance controls state-dependent changes in brain lactate concentration. *J Cereb Blood Flow Metab* (2017) 37:2112–24. doi: 10.1177/0271678X16661202
175. Cespuoglio R, Netchiporouk L, Shram N. Glucose and lactate monitoring across the rat sleep-wake cycle. in: *Neuromethods* (2013) 80:241–56. doi: 10.1007/978-1-62703-370-1-11
176. Rutter J, Reick M, Wu LC, McKnight SL. Regulation of cAMP and NPAS2 DNA binding by the redox state of NAD cofactors. *Sci (80- )* (2001) 293:510–4. doi: 10.1126/science.1060698
177. Wieggers EC, Rooijackers HM, Tack CJ, Heerschap A, De Galan BE, Van Der Graaf M. Brain lactate concentration falls in response to hypoglycemia in patients with type 1 diabetes and impaired awareness of hypoglycemia. *Diabetes* (2016) 65:1601–5. doi: 10.2337/db16-0068
178. De Feyter HM, Mason GF, Shulman GI, Rothman DL, Petersen KF. Increased brain lactate concentrations without increased lactate oxidation during hypoglycemia in type 1 diabetic individuals. *Diabetes* (2013) 62:3075–80. doi: 10.2337/db13-0313
179. Geissler A, Fründ R, Schölmerich J, Feuerbach S, Zietz B. Alterations of Cerebral Metabolism in Patients with Diabetes Mellitus Studied by Proton Magnetic Resonance Spectroscopy. *Exp Clin Endocrinol Diabetes* (2003) 111:421–7. doi: 10.1055/s-2003-44289
180. George FC. Fuel metabolism in starvation. *Annu Rev Nutr* (2006) 26:1–22. doi: 10.1146/annurev.nutr.26.061505.111258
181. Le Foll C, Dunn-Meynell AA, Mizioro HM, Levin BE. Regulation of hypothalamic neuronal sensing and food intake by ketone bodies and fatty acids. *Diabetes* (2014) 63:1259–69. doi: 10.2337/db13-1090
182. Le Foll C, Dunn-Meynell AA, Mizioro HM, Levin BE. Role of VMH ketone bodies in adjusting caloric intake to increased dietary fat content in DIO and DR rats. *Am J Physiol - Regul Integr Comp Physiol* (2015) 308:R872–8. doi: 10.1152/ajpregu.00015.2015
183. Carneiro L, Geller S, Hébert A, Repond C, Fioramonti X, Leloup C, et al. Hypothalamic sensing of ketone bodies after prolonged cerebral exposure leads to metabolic control dysregulation. *Sci Rep* (2016) 6:34909. doi: 10.1038/srep34909
184. Hwang JJ, Jiang L, Hamza M, Sanchez Rangel E, Dai F, Belfort-DeAguiar R, et al. Blunted rise in brain glucose levels during hyperglycemia in adults with obesity and T2DM. *JCI Insight* (2017) 2:e95913. doi: 10.1172/jci.insight.95913
185. Kullmann S, Heni M, Hallschmid M, Fritsche A, Preissl H, Häring HU. Brain insulin resistance at the crossroads of metabolic and cognitive disorders in humans. *Physiol Rev* (2016) 96:1169–209. doi: 10.1152/physrev.00032.2015
186. Baker LD, Cross DJ, Minoshima S, Belongia D, Stennis Watson G, Craft S. Insulin resistance and alzheimer-like reductions in regional cerebral glucose metabolism for cognitively normal adults with prediabetes or early type 2 diabetes. *Arch Neurol* (2011) 68:51–7. doi: 10.1001/archneurol.2010.225
187. Weightman Potter PG, Vlachaki Walker JM, Robb JL, Chilton JK, Williamson R, Randall AD, et al. Basal fatty acid oxidation increases after recurrent low glucose in human primary astrocytes. *Diabetologia* (2019) 62:187–98. doi: 10.1007/s00125-018-4744-6
188. Dos Santos JPA, Vizuete A, Hansen F, Biasibetti R, Gonçalves CA. Early and Persistent O-GlcNAc Protein Modification in the Streptozotocin Model of Alzheimer's Disease. *J Alzheimer's Dis* (2018) 61:237–49. doi: 10.3233/JAD-170211
189. Dias WB, Hart GW. O-GlcNAc modification in diabetes and Alzheimer's disease. *Mol Biosyst* (2007) 3:766–72. doi: 10.1039/b704905f
190. Parker GJ, Lund KC, Taylor RP, McClain DA. Insulin resistance of glycogen synthase mediated by O-linked N-acetylglucosamine. *J Biol Chem* (2003) 278:10022–7. doi: 10.1074/jbc.M207787200
191. Parker G, Taylor R, Jones D, McClain D. Hyperglycemia and inhibition of glycogen synthase in streptozotocin-treated mice: Role of O-linked N-acetylglucosamine. *J Biol Chem* (2004) 279:20636–42. doi: 10.1074/jbc.M312139200
192. Dosch M, Gerber J, Jebbawi F, Beldi G. Mechanisms of ATP release by inflammatory cells. *Int J Mol Sci* (2018) 19:1222. doi: 10.3390/ijms19041222
193. Cai W, Xue C, Sakaguchi M, Konishi M, Shirazian A, Ferris HA, et al. Insulin regulates astrocyte gliotransmission and modulates behavior. *J Clin Invest* (2018) 128:2914–26. doi: 10.1172/JCI99366
194. Juaristi I, Llorente-Folch I, Satrustegui J, del Arco A. Extracellular ATP and glutamate drive pyruvate production and energy demand to regulate mitochondrial respiration in astrocytes. *Glia* (2019) 67:759–74. doi: 10.1002/glia.23574
195. Lemos C, Pinheiro BS, Beleza RO, Marques JM, Rodrigues RJ, Cunha RA, et al. Adenosine A2B receptor activation stimulates glucose uptake in the mouse forebrain. *Purinergic Signal* (2015) 11:561–9. doi: 10.1007/s11302-015-9474-3
196. Jiang LH, Mousawi F, Yang X, Roger S. ATP-induced Ca<sup>2+</sup>-signalling mechanisms in the regulation of mesenchymal stem cell migration. *Cell Mol Life Sci* (2017) 74:3697–710. doi: 10.1007/s00018-017-2545-6
197. Colldén G, Mangano C, Meister B. P2X2 purinoreceptor protein in hypothalamic neurons associated with the regulation of food intake. *Neuroscience* (2010) 171:62–78. doi: 10.1016/j.neuroscience.2010.08.036
198. Jo YH, Donier E, Martínez A, Garret M, Toulmé E, Boué-Grabot E. Cross-talk between P2X4 and  $\gamma$ -aminobutyric acid, type A receptors determines synaptic efficacy at a central synapse. *J Biol Chem* (2011) 286:19993–20004. doi: 10.1074/jbc.M111.231324
199. Marpean L, Swanson AE, Chung K, Simon T, Haydon PG, Khan SK, et al. Circadian regulation of ATP release in astrocytes. *J Neurosci* (2011) 31:8342–50. doi: 10.1523/JNEUROSCI.6537-10.2011
200. Mackiewicz M, Nikonova EV, Zimmerman JE, Galante RJ, Zhang L, Cater JR, et al. Enzymes of adenosine metabolism in the brain: Diurnal rhythm and the effect of sleep deprivation. *J Neurochem* (2003) 85:348–57. doi: 10.1046/j.1471-4159.2003.01687.x
201. Verkhratsky A, Nedergaard M. Physiology of astroglia. *Physiol Rev* (2018) 98:239–389. doi: 10.1152/physrev.00042.2016
202. Young JK, Baker JH, Montes MI. The brain response to 2-deoxy glucose is blocked by a glial drug. *Pharmacol Biochem Behav* (2000) 67:233–9. doi: 10.1016/S0091-3057(00)00315-4

203. Barca Mayo O, Berdondini L, De Pietri Tonelli D. "Astrocytes and circadian rhythms: An emerging astrocyte–neuron synergy in the timekeeping system," in. *Methods Mol Biol* (2019) 1938:131–54. doi: 10.1007/978-1-4939-9068-9\_10
204. Zhang Y, Reichel JM, Han C, Zuniga-Hertz JP, Cai D. Astrocytic Process Plasticity and IKK $\beta$ /NF- $\kappa$ B in Central Control of Blood Glucose, Blood Pressure, and Body Weight. *Cell Metab* (2017) 25:1091–102.e4. doi: 10.1016/j.cmet.2017.04.002
205. Chen N, Sugihara H, Kim J, Fu Z, Barak B, Sur M, et al. Direct modulation of GFAP-expressing glia in the arcuate nucleus bi-directionally regulates feeding. *Elife* (2016) 5:e18716. doi: 10.7554/eLife.18716
206. Chowdhury GMI, Wang P, Ciardi A, Mamillapalli R, Johnson J, Zhu W, et al. Impaired glutamatergic neurotransmission in the ventromedial hypothalamus may contribute to defective counterregulation in recurrently hypoglycemic rats. in. *Diabetes* (2017) 66:1979–89. doi: 10.2337/db16-1589
207. Guyenet SJ, Matsen ME, Morton GJ, Kaiyala KJ, Schwartz MW. Rapid glutamate release in the mediobasal hypothalamus accompanies feeding and is exaggerated by an obesogenic food. *Mol Metab* (2013) 2:116–22. doi: 10.1016/j.molmet.2013.02.001
208. Fuente-Martín E, García-Cáceres C, Granado M, De Ceballos ML, Sánchez-Garrido MÁ, Sarman B, et al. Leptin regulates glutamate and glucose transporters in hypothalamic astrocytes. *J Clin Invest* (2012) 122:3900–13. doi: 10.1172/JCI61402
209. Thaler JP, Yi CX, Schur EA, Guyenet SJ, Hwang BH, Dietrich MO, et al. Obesity is associated with hypothalamic injury in rodents and humans. *J Clin Invest* (2012) 122:153–62. doi: 10.1172/JCI59660
210. Reis WL, Yi CX, Gao Y, Tschöp MH, Stern JE. Brain innate immunity regulates hypothalamic arcuate neuronal activity and feeding behavior. *Endocrinology* (2015) 156:1303–15. doi: 10.1210/en.2014-1849
211. Chen Y, Liu G, He F, Zhang L, Yang K, Yu H, et al. MicroRNA 375 modulates hyperglycemia-induced enteric glial cell apoptosis and Diabetes-induced gastrointestinal dysfunction by targeting Pdk1 and repressing PI3K/Akt pathway. *Sci Rep* (2018) 8:12681. doi: 10.1038/s41598-018-30714-0
212. Konturek PC, Brzozowski T, Konturek SJ. Gut clock: Implication of circadian rhythms in the gastrointestinal tract. *J Physiol Pharmacol* (2011) 62:139–50. doi: 10.2337/db13-1501
213. Gil-Lozano M, Mingomataj EL, Wu WK, Ridout SA, Brubaker PL. Circadian secretion of the intestinal hormone GLP-1 by the rodent L cell. *Diabetes* (2014) 63:3674–85. doi: 10.2337/db13-1501
214. Brubaker PL, Gil-Lozano M. Glucagon-like peptide-1: The missing link in the metabolic clock? *J Diabetes Investig* (2016) 7:70–5. doi: 10.1111/jdi.12477
215. Martchenko A, Oh RH, Wheeler SE, Gurses P, Chalmers JA, Brubaker PL. Suppression of circadian secretion of glucagon-like peptide-1 by the saturated fatty acid, palmitate. *Acta Physiol* (2018) 222:e13007. doi: 10.1111/apha.13007
216. Thaiss CA, Levy M, Korem T, Dohnalová L, Shapiro H, Jaitin DA, et al. Microbiota Diurnal Rhythmicity Programs Host Transcriptome Oscillations. *Cell* (2016) 167:1495–510.e12. doi: 10.1016/j.cell.2016.11.003
217. Woon PY, Kaisaki PJ, Bragança J, Bihoreau MT, Levy JC, Farrall M, et al. Aryl hydrocarbon receptor nuclear translocator-like (BMAL1) is associated with susceptibility to hypertension and type 2 diabetes. *Proc Natl Acad Sci USA* (2007) 104:14412–7. doi: 10.1073/pnas.0703247104
218. Scott EM, Carter AM, Grant PJ. Association between polymorphisms in the Clock gene, obesity and the metabolic syndrome in man. *Int J Obes* (2008) 32:658–62. doi: 10.1038/sj.jco.0803778
219. Sookoian S, Gemma C, Gianotti TF, Burgueño A, Castaño G, Pirola CJ. Genetic variants of Clock transcription factor are associated with individual susceptibility to obesity. *Am J Clin Nutr* (2008) 87:1606–15. doi: 10.1093/ajcn/87.6.1606
220. Dupuis J, Langenberg C, Prokopenko I, Saxena R, Soranzo N, Jackson AU, et al. New genetic loci implicated in fasting glucose homeostasis and their impact on type 2 diabetes risk. *Nat Genet* (2010) 42:105–16. doi: 10.1038/ng.520
221. Barker A, Sharp SJ, Timpson NJ, Bouatia-Naji N, Warrington NM, Kanoni S, et al. Association of genetic loci with glucose levels in childhood and adolescence: A meta-analysis of over 6,000 children. *Diabetes* (2011) 60:1805–12. doi: 10.2337/db10-1575
222. Marcheva B, Ramsey KM, Buhr ED, Kobayashi Y, Su H, Ko CH, et al. Disruption of the clock components CLOCK and BMAL1 leads to hypoinsulinaemia and diabetes. *Nature* (2010) 466:627–31. doi: 10.1038/nature09253
223. Hogenboom R, Kalsbeek MJ, Korpel NL, de Goede P, Koenen M, Buijs RM, et al. Loss of arginine vasopressin- and vasoactive intestinal polypeptide-containing neurons and glial cells in the suprachiasmatic nucleus of individuals with type 2 diabetes. *Diabetologia* (2019) 62:2088–93. doi: 10.1007/s00125-019-4953-7
224. Fonken LK, Nelson RJ. The effects of light at night on circadian clocks and metabolism. *Endocr Rev* (2014) 35:648–70. doi: 10.1210/er.2013-1051
225. Fonken LK, Workman JL, Walton JC, Weil ZM, Morris JS, Haim A, et al. Light at night increases body mass by shifting the time of food intake. *Proc Natl Acad Sci USA* (2010) 107:18664–9. doi: 10.1073/pnas.1008734107
226. Obayashi K, Saeki K, Iwamoto J, Ikada Y, Kurumatani N. Independent associations of exposure to evening light and nocturnal urinary melatonin excretion with diabetes in the elderly. *Chronobiol Int* (2014) 31:394–400. doi: 10.3109/07420528.2013.864299
227. Obayashi K, Saeki K, Iwamoto J, Okamoto N, Tomioka K, Nezu S, et al. Exposure to light at night, nocturnal urinary melatonin excretion, and obesity/dyslipidemia in the elderly: A cross-sectional analysis of the HEIJO-KYO study. *J Clin Endocrinol Metab* (2013) 98:337–44. doi: 10.1210/jc.2012-2874
228. McFadden E, Jones ME, Schoemaker MJ, Ashworth A, Swerdlow AJ. The relationship between obesity and exposure to light at night: Cross-sectional analyses of over 100,000 women in the breakthrough generations study. *Am J Epidemiol* (2014) 180:245–50. doi: 10.1093/aje/kwu117
229. Cheung IN, Zee PC, Shalman D, Malkani RG, Kang J, Reid KJ. Morning and Evening Blue-Enriched Light Exposure Alters Metabolic Function in Normal Weight Adults. *PloS One* (2016) 11:e0155601. doi: 10.1371/journal.pone.0155601
230. Versteeg RI, Stenvers DJ, Visintainer D, Linnenbank A, Tanck MW, Zwanenburg G, et al. Acute Effects of Morning Light on Plasma Glucose and Triglycerides in Healthy Men and Men with Type 2 Diabetes. *J Biol Rhythms* (2017) 32:130–42. doi: 10.1177/0748730417693480
231. Aton SJ, Colwell CS, Harnar AJ, Waschek J, Herzog ED. Vasoactive intestinal polypeptide mediates circadian rhythmicity and synchrony in mammalian clock neurons. *Nat Neurosci* (2005) 8:476–83. doi: 10.1038/nn1419
232. Colwell CS, Michel S, Itri J, Rodriguez W, Tam J, Lelievre V, et al. Disrupted circadian rhythms in VIP- and PHI-deficient mice. *Am J Physiol - Regul Integr Comp Physiol* (2003) 285:R939–49. doi: 10.1152/ajpregu.00200.2003
233. Takahashi Y, Okamura H, Yanaiharu N, Hamada S, Fujita S, Ibata Y. Vasoactive intestinal peptide immunoreactive neurons in the rat suprachiasmatic nucleus demonstrate diurnal variation. *Brain Res* (1989) 497:374–7. doi: 10.1016/0006-8993(89)90283-7
234. Ohta H, Yamazaki S, McMahon DG. Constant light desynchronizes mammalian clock neurons. *Nat Neurosci* (2005) 8:267–9. doi: 10.1038/nn1395
235. Shan Z, Ma H, Xie M, Yan P, Guo Y, Bao W, et al. Sleep duration and risk of type 2 diabetes: A meta-analysis of prospective studies. *Diabetes Care* (2015) 38:529–37. doi: 10.2337/dc14-2073
236. Cappuccio FP, D'Elia L, Strazzullo P, Miller MA. Quantity and quality of sleep and incidence of type 2 diabetes: A systematic review and meta-analysis. *Diabetes Care* (2010) 33:414–20. doi: 10.2337/dc09-1124
237. Boley-Westphal A, Hinrichs S, Jauch-Chara K, Hitz B, Later W, Wilms B, et al. Influence of partial sleep deprivation on energy balance and insulin sensitivity in healthy women. *Obes Facts* (2008) 1:266–73. doi: 10.1159/000158874
238. Nedeltcheva AV, Kilkus JM, Imperial J, Kasza K, Schoeller DA, Penev PD. Sleep curtailment is accompanied by increased intake of calories from snacks. *Am J Clin Nutr* (2009) 89:126–33. doi: 10.3945/ajcn.2008.26574
239. Reutrakul S, Mokhlesi B. Obstructive Sleep Apnea and Diabetes: A State of the Art Review. *Chest* (2017) 152:1070–86. doi: 10.1016/j.chest.2017.05.009
240. Spiegel K, Leproult R, Van Cauter E. Impact of sleep debt on metabolic and endocrine function. *Lancet* (1999) 354:1435–9. doi: 10.1016/S0140-6736(99)01376-8
241. Stamatakis KA, Punjabi NM. Effects of sleep fragmentation on glucose metabolism in normal subjects. *Chest* (2010) 137:95–101. doi: 10.1378/chest.09-0791

242. Rao MN, Neylan TC, Grunfeld C, Mulligan K, Schambelan M, Schwarz JM. Subchronic sleep restriction causes tissue-specific insulin resistance. *J Clin Endocrinol Metab* (2015) 100:1664–71. doi: 10.1210/jc.2014-3911
243. Halassa MM, Fellin T, Haydon PG. Tripartite synapses: Roles for astrocytic purines in the control of synaptic physiology and behavior. *Neuropharmacology* (2009) 57:343–6. doi: 10.1016/j.neuropharm.2009.06.031
244. Vetter C, Dashti HS, Lane JM, Anderson SG, Schernhammer ES, Rutter MK, et al. Night shift work, genetic risk, and type 2 diabetes in the UK biobank. *Diabetes Care* (2018) 41:762–9. doi: 10.2337/dc17-1933
245. Gan Y, Yang C, Tong X, Sun H, Cong Y, Yin X, et al. Shift work and diabetes mellitus: A meta-analysis of observational studies. *Occup Environ Med* (2015) 72:72–8. doi: 10.1136/oemed-2014-102150
246. Leproult R, Holmbäck U, Van Cauter E. Circadian misalignment augments markers of insulin resistance and inflammation, independently of sleep loss. *Diabetes* (2014) 63:1860–9. doi: 10.2337/db13-1546
247. Qian J, Dalla Man C, Morris CJ, Cobelli C, Scheer FAJL. Differential effects of the circadian system and circadian misalignment on insulin sensitivity and insulin secretion in humans. *Diabetes Obes Metab* (2018) 20:2481–5. doi: 10.1111/dom.13391
248. Wefers J, Van Moorsel D, Hansen J, Connell NJ, Havekes B, Hoeks J, et al. Circadian misalignment induces fatty acid metabolism gene profiles and compromises insulin sensitivity in human skeletal muscle. *Proc Natl Acad Sci USA* (2018) 115:7789–94. doi: 10.1073/pnas.1722295115
249. Scheer FAJL, Hilton MF, Mantzoros CS, Shea SA. Adverse metabolic and cardiovascular consequences of circadian misalignment. *Proc Natl Acad Sci USA* (2009) 106:4453–8. doi: 10.1073/pnas.0808180106
250. Morris CJ, Purvis TE, Mistretta J, Scheer FAJL. Effects of the internal circadian system and circadian misalignment on glucose tolerance in chronic shift workers. *J Clin Endocrinol Metab* (2016) 101:1066–74. doi: 10.1210/jc.2015-3924

**Conflict of Interest:** The authors declare that the research was conducted in the absence of any commercial or financial relationships that could be construed as a potential conflict of interest.

Copyright © 2021 Barca-Mayo and López. This is an open-access article distributed under the terms of the Creative Commons Attribution License (CC BY). The use, distribution or reproduction in other forums is permitted, provided the original author(s) and the copyright owner(s) are credited and that the original publication in this journal is cited, in accordance with accepted academic practice. No use, distribution or reproduction is permitted which does not comply with these terms.



# Brain-Body Control of Glucose Homeostasis—Insights From Model Organisms

Alastair J. MacDonald, Yu Hsuan Carol Yang, Ana Miguel Cruz, Craig Beall and Kate L. J. Ellacott\*

*Institute of Biomedical and Clinical Sciences, University of Exeter Medical School, Exeter, United Kingdom*

## OPEN ACCESS

### Edited by:

Cristina García Cáceres,  
Ludwig Maximilian University of  
Munich, Germany

### Reviewed by:

Christelle Le Foll,  
University of Zurich, Switzerland  
Tim Gruber,  
Helmholtz Center Munich, Germany

### \*Correspondence:

Kate L. J. Ellacott  
k.ellacott@exeter.ac.uk

### Specialty section:

This article was submitted to  
Neuroendocrine Science,  
a section of the journal  
Frontiers in Endocrinology

**Received:** 01 February 2021

**Accepted:** 12 March 2021

**Published:** 31 March 2021

### Citation:

MacDonald AJ, Yang YHC, Cruz AM,  
Beall C and Ellacott KLJ (2021) Brain-  
Body Control of Glucose Homeostasis  
—Insights From Model Organisms.  
*Front. Endocrinol.* 12:662769.  
doi: 10.3389/fendo.2021.662769

Tight regulation of blood glucose is essential for long term health. Blood glucose levels are defended by the correct function of, and communication between, internal organs including the gastrointestinal tract, pancreas, liver, and brain. Critically, the brain is sensitive to acute changes in blood glucose level and can modulate peripheral processes to defend against these deviations. In this mini-review we highlight select key findings showcasing the utility, strengths, and limitations of model organisms to study brain-body interactions that sense and control blood glucose levels. First, we discuss the large platform of genetic tools available to investigators studying mice and how this field may yet reveal new modes of communication between peripheral organs and the brain. Second, we discuss how rats, by virtue of their size, have unique advantages for the study of CNS control of glucose homeostasis and note that they may more closely model some aspects of human (patho)physiology. Third, we discuss the nascent field of studying the CNS control of blood glucose in the zebrafish which permits ease of genetic modification, large-scale measurements of neural activity and live imaging in addition to high-throughput screening. Finally, we briefly discuss glucose homeostasis in drosophila, which have a distinct physiology and glucoregulatory systems to vertebrates.

**Keywords:** brain, glucose homeostasis, model organism, mouse, rat, zebrafish

## INTRODUCTION

The central nervous system has emerged as an important node in the coordinated control of blood glucose homeostasis. Maintenance of euglycemia is critical for health and the regulation of energy homeostasis. Extended periods of poor glycemic control drive disease pathology; for example, prolonged hyperglycemia in type-1 and type-2 diabetes can cause eye, kidney, and nerve damage over the longer term. Conversely, low blood glucose or hypoglycemia is also dangerous acutely, with recurrent bouts leading to deficits in hypoglycemia awareness, which can result in death in extreme but rare circumstances. Given this importance, in healthy individuals, highly sensitive feedback systems exist to regulate blood glucose within a tight window. Appropriate regulation of blood glucose is ultimately dependent on the correct balance between glucose ingestion, production, utilization, and storage. This control is achieved by communication between multiple organ systems, chiefly the gastrointestinal tract, pancreas, muscle, liver, adipose, adrenal glands, and brain.

When combined with classical physiological approaches, modern genetic manipulation technologies have refined our understanding of the critical role of the brain in overseeing glucose homeostasis and orchestrating appropriate physiological and behavioral responses (1, 2). In addition to well described endocrine inter-organ communication, cell populations in discrete brain nuclei are sensitive to acute deviations in tissue glucose levels and some are also capable of direct glucose sensing (3–6). Furthermore, sensory innervation of organs relays relevant information on peripheral glucose state to the brain (7, 8). By altering autonomic outflow, the brain drives responses to these deviations in blood glucose, helping to restore homeostasis (9, 10).

Much of what is known about crosstalk between the body and brain is the result of experimentation in model species. A simplified overview of the main brain regions and cell populations identified in blood glucose control in common model species is shown in **Figure 1**. Comprehensive reviews on both the different species used to model human metabolic disease and descriptions of glucoregulatory neurocircuitry are available elsewhere (11–13). Instead, in this mini-review, using select examples from the literature, we will focus on the utility of different model organisms to specifically elucidate neural circuits regulating glucose homeostasis.

## Mice

Mice have emerged as the most commonly used rodent species for neuroscience research (14). This is due, at least in part, to the suite of transgenic tools available. Furthermore, mice are amenable to measures of systemic glucose homeostasis, commonly glucose and insulin tolerance tests, but glucose clamps are also possible (15–17).

The combination of genetic tools and means for real-time measurement of changes in systemic glucose levels in mice permits the investigation of the role of the brain in control of blood glucose homeostasis. The ventromedial nucleus of the

hypothalamus (VMN) has long been implicated in the neural control of energy balance and blood glucose levels (3, 4, 18). Cre-lox recombination has been used to elegantly dissect the role of a defined neuronal population within this nucleus in glucose homeostasis: using a driver line expressing Cre recombinase in the VMN (Steroidogenic factor 1-Cre) to knock out vesicular glutamate transporter 2 selectively in VMN neurons (19). These mice lack VMN glutamatergic transmission and have impaired sensitivity to fasting, insulin and 2-deoxyglucose (2-DG). Taken together, this shows that glutamatergic transmission in VMN neurons is an essential component for the counter-regulatory response to hypoglycemia (CRR) (19). Thus, this approach can be used to generate causal evidence of a specific process (glutamatergic neurotransmission), in a defined brain area (VMN) required for a physiological process (CRR). Similarly, Cre-lox recombination can be used to selectively re-express a gene in genetically defined cells in knockout animals (20, 21). This permits testing of both necessity (knock-out) and sufficiency (selective re-expression) of a gene of interest in a specific cell population.

This recombination method can be refined with drug-inducible forms of Cre (e.g. tamoxifen inducible cre; CreERT2). The importance of temporal control of recombination is illustrated in the case of leptin receptor (LepR) expression on pro-opiomelanocortin cells (POMC cells). Embryonic deletion of *LepR* from POMC cells results in mice that have a greater body and fat mass than control animals with intact leptin signaling in POMC cells (22). However in adult mice where *LepR* is knocked out of adult POMC cells by providing tamoxifen to POMC<sup>CreERT2</sup> mice, this phenotype is absent (23). Instead, these mice show a hyperglycemic phenotype driven by increased hepatic glucose production and insulin resistance, while body weight and energy expenditure are normal (23). This reveals a glucoregulatory role of

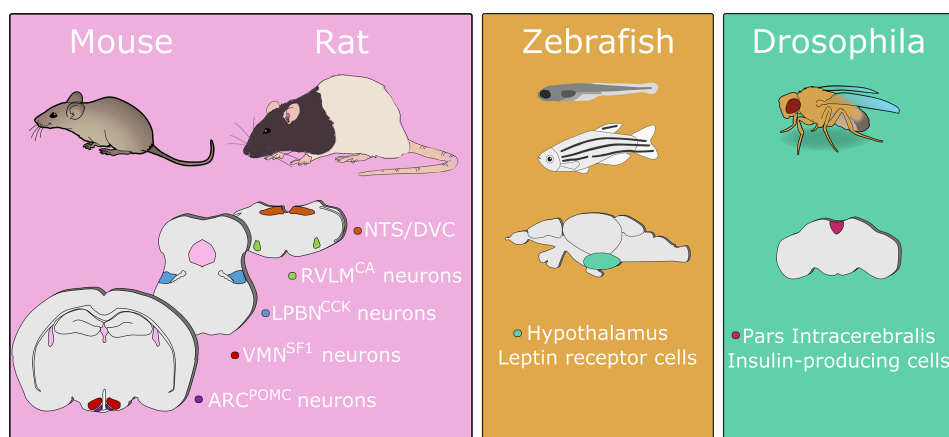


**FIGURE 1** | A simplified overview of primary brain sites regulating blood glucose identified in model organisms. This figure shows the cell populations discussed in this review and is not an exhaustive list. Numerous brain regions have been demonstrated to contribute to glucose regulation in mice and/or rats. In zebrafish disruption of leptin receptor signaling induces hyperglycemia. In drosophila, ablation of insulin-producing cells causes increases in hemolymph carbohydrate levels. Abbreviations: ARC, arcuate nucleus of the hypothalamus; CA, catecholamine; CCK, cholecystokinin; DVC, dorsal vagal complex; LPBN, lateral parabrachial nucleus; NTS, nucleus of the solitary tract; POMC, pro-opiomelanocortin; RVLM, rostral ventrolateral medulla; SF1, steroidogenic factor 1; VMN, ventromedial nucleus of the hypothalamus. Animal images adapted from Scidraw.io. Drawings not to scale.

LepR signaling in POMC cells in adult mice which may have been masked by the embryonic knockout and thus highlights potential developmental compensation as a caveat to Cre recombination without temporal control. Furthermore, it has been shown that a number of ventral hypothalamic cells transiently express POMC during development but not in adulthood, including functionally opposed agouti-related peptide (AgRP) expressing neurons (24). Thus, by using temporally restricted Cre-recombination, manipulations can be limited to cells of interest in adulthood rather than all cells derived from a POMC-expressing lineage.

In addition to the selective embryonic genetic (or inducible adult) knockout models described above, mice are also amenable for the selective stimulation or inhibition of defined neuronal populations in adult animals by optogenetic or chemogenetic methods (25, 26). For example, using chemogenetics, stimulation of neurons in the lateral parabrachial nucleus (LPBN) identified by their expression of cholecystokinin (CCK; LPBN<sup>CCK</sup> neurons) causes a CCK-dependent increase in blood glucose driven by increased plasma glucagon, corticosterone and epinephrine levels (27). Chemogenetic inhibition of this neuronal population leads to an attenuated blood glucose increase in response to 2-DG-induced glucoprivation. Using this methodology to selectively inhibit the VMN neurons, identified by their expression of steroidogenic factor 1 (SF1; VMN<sup>SF1</sup> neurons), while stimulating upstream LPBN<sup>CCK</sup> neurons occludes the rise in blood glucose induced by this stimulation. This suggests that LPBN<sup>CCK</sup> neurons are involved in hypoglycemia detection and relay this information to VMN<sup>SF1</sup> neurons to exert compensatory changes in blood glucose. This illustrates the power of experimental tools which enable bi-directional modulation of neuronal populations of interest (specific activation or inhibition) while measuring physiological parameters. In addition, it highlights how concomitant manipulation of pre- and post-synaptic neurons, respectively, can demonstrate the necessity of a given projection site for the observed effects. The same viral approach can be used to drive expression of fluorescent proteins in genetically defined cell populations. This expands the scope of this method to tracing anatomical circuits in addition to probing their function. These tools also have the advantage of being specific and targetable in adult animals, avoiding the potential developmental adaptations and complications associated with embryonic deletion of genes.

In recent years, studies in mice have characterized sensory neurons of the vagus nerves and their role in relaying information on internal state from the periphery to the brain (28–33) including cardiovascular, pulmonary, and gastrointestinal parameters. These signals appear to exist to drive appropriate autonomic responses (i.e., vago-vagal reflexes) in addition to modulating associated behavior. For example, stimulation of gut-innervating vagal sensory neurons elicits changes in gastric motility and pressure while also suppressing food intake (28, 31, 33). Given this evidence, the existence of a vagal sensory circuit monitoring blood glucose, communicating this to the brain and driving both appropriate autonomic and behavioral responses seems possible. Vagal sensory innervation of the liver and pancreas have been described in classical studies performed in rats (34, 35). With the

platform already developed for functional and genetic investigation of vagal sensory subtypes (28–32), this represents an area ripe for investigation using contemporary neuroscience techniques. However, a recent report suggests that the detection of ingested glucose by hypothalamic neurons is independent of the vagus nerve, instead this signal is relayed by spinal afferents monitoring the hepatic portal vein (36).

In complementary studies, vagal efferent pathways regulating blood glucose have been examined in mice. Vagal sensory neurons from peripheral organs terminate in the nucleus of the solitary tract (NTS), while vagal efferent neurons originate in the neighboring dorsal motor nucleus of the vagus (DMV). Vagal efferent neurons of the DMV are identified by expression of choline acetyltransferase (ChAT; DMV<sup>ChAT</sup> neurons). These DMV neurons are innervated by NTS neurons, providing an anatomical substrate for vago-vagal processes. Acute chemogenetic activation of inhibitory NTS neurons (NTS<sup>GABA</sup> neurons (10)), which receive direct vagal input (37), increases blood glucose by reducing the tonic activity of DMV<sup>ChAT</sup> neurons. This disinhibits hepatic glucose production (10). Thus, the cellular architecture of vago-vagal signaling loops are beginning to be elucidated in mice.

As described above, contemporary neuroscience technologies allow for the selective manipulation of activity and/or gene expression of spatially and genetically defined cell types, both in the brain and peripheral ganglia. Combined with standard tests of glucose homeostasis and the similarities between mouse and human physiology (11), this presents a powerful platform on which to examine neural circuits governing blood glucose homeostasis. However, this species and these approaches are not without their caveats. Strains and sub-strains of inbred mice have demonstrably different responses to modulation of blood glucose both in terms of glucose-stimulated insulin secretion and glucoprivic feeding (38–40). Some of these differences arise from known genetic mutations, for example the nicotinamide nucleotide transhydrogenase mutation in the C57Bl6/J sub-strain (41). As such, outbred strains may be more suitable for some experiments to reduce the impact of single mutations on observed measurements (38, 41).

Care should also be taken with respect to studies utilizing Cre-lox recombination. Mice expressing Cre recombinase can have phenotypes arising from off target recombination or integration of Cre into a functional gene (42). As such, it is important to consider the appropriate control groups, including littermates, to account for this [discussed in detail in (33)]. In addition, embryonic Cre recombination or transient expression in off target tissues may account for a phenotype in adult animals that does not represent the function of the gene in adult physiology. Finally, opto- or chemogenetic manipulations may induce artificial activity patterns that demonstrate the consequence of cellular activation, but should be interpreted with caution as may not reflect the “normal” function of those cells. Moreover, with chemogenetic experiments, it is important to control for both off target effects of chemogenetic ligands and expression of the receptor which may have constitutive activity in the cell type of interest (43, 44). These limitations and key experimental controls also apply to related studies in transgenic rats (see below).

## Rats

Rats offer some major advantages over mice, such as their larger size and the fact that many common strains (i.e., Sprague Dawley, Wistar) are outbred, increasing the generalizability of the data for human populations. This outbred nature can increase variability in a study and combined with the size can make studies more expensive. However, the greater size allows for collection of larger blood sample volumes, which can be advantageous for endocrine studies. For the advanced assessment of glucose homeostasis, it can be beneficial to surgically implant indwelling vascular catheters in a vein and/or an artery (i.e., jugular vein and carotid artery). This enables repeated sampling with a continuous infusion in conscious, freely moving rats, which is useful during hyperinsulinemic glucose clamping (45). However, protocols for clamping in mice are highly refined (46). From a rat, the larger blood samples volumes can be taken without the need for concomitant replacement of blood from donor animals (although blood cells can be re-suspended and re-infused during a clamp). Moreover, recent advances in indwelling vascular access buttons (VAB) have allowed for streamlined blood sampling, maintenance of catheter patency, and attachment of animals to the glucose clamping apparatus. This is advantageous over harnesses, which can cause chaffing as the rat moves and/or grows. These buttons also permit social housing immediately post-surgery if aluminum VAB caps are used. This may improve welfare by reducing post-surgical weight loss and improve overall recovery. This technology has also been adapted for use in mice, with some minor modifications.

Another recent technological advancement is the development of fully implantable glucose telemetry devices for continuous glucose monitoring in freely moving unrestrained rats (47). This permits glucose monitoring for up to 75 days and requires implantation of a ~2g device with a sensor tip placed in an artery. It should be noted that glucose measurements can differ between tail vein and arterial glucose, depending on the model of choice (48). These devices can also be adapted for use in mice; however, the cost of the telemetry devices and the advanced surgical procedures required have prevented widespread adoption of this technology, which is only likely to be beneficial for chronic studies.

The rat is a particularly useful model to study the neuroendocrine regulation of the CRR to acute and recurrent hypoglycemia, particularly the Sprague-Dawley and Wistar rats, which have been the workhorse of the hypoglycemia field for the last 30 years. The hyperinsulinemic-hypoglycemic clamp, together with insulin-induced hypoglycemia and 2-DG induced glucoprivation, have been extensively used in Sprague-Dawley rats to investigate CRR, glucoprivic feeding and impaired awareness of hypoglycemia (49–56). This latter aspect of hypoglycemia “awareness” can be studied using a conditioned place preference test, which has so far been validated in rats but not in mice (57), largely because of the more rapid induction of defective counter-regulation in rats and their tractability for behavioral tests. The species differences between rats and mice in the adaptation to recurrent hypoglycemia are important considerations when designing a study and have been previously discussed in detail elsewhere (58). Seminal studies in rats revealed the presence of glucosensors in the hindbrain that can mount responses to restore blood glucose in the face of a glucoprivic challenge

independent of forebrain structures or when the cerebral aqueduct is blocked (59, 60). Secondly, chemical lesion studies of hypothalamus-projecting catecholaminergic neurons implicates these cells as a class of neurons underlying glucoprivic feeding (61). However, evidence suggests that hindbrain-limited recurrent glucoprivation does not alter CRR (62), suggesting that adaptations to hypoglycemia that cause defective CRR are likely forebrain-mediated. Studies by the Levin lab mapped expression of the key glucosensor, glucokinase (GK), to neurons that exhibited both glucose sensing and non-glucose sensing properties (63). In support of the physiological data described above, they also noted a relative lack of GK expression in the NTS, despite neurons in this region playing a key role in neuroendocrine and behavioral responses to hypoglycemia (64). Other key components of glucosensing originally described in the beta-cell have also been shown to play a role in hypoglycemia detection in rats. For example, pharmacological and genetic manipulation of VMN ATP-sensitive potassium channels ( $K_{ATP}$ ) (65) or AMP-activated protein kinase activity (66, 67) can alter CRR in healthy, recurrently hypoglycemic and diabetic rats.

With the advent of genetic technologies and the ease of applying these approaches to mice, rats have been somewhat side-lined in neuroscientific research (14). However, the first Cre-driver rat lines were described a decade ago and many more are now available (68, 69), including some which have been used to demonstrate control of blood glucose by defined neuronal populations (70). In a pair of recent studies, chemogenetic receptors were expressed selectively in anatomically distinct subgroups of catecholaminergic neurons (identified by expression of tyrosine hydroxylase [TH]) in the rat ventrolateral medulla (VLM<sup>TH</sup> neurons). This was achieved by injection of Cre-dependent viral vectors into TH-Cre rats (68, 70, 71). Selective activation of these VLM-neuronal subgroups (distributed along the rostral-caudal axis) differentially increased food intake and corticosterone levels, but only in combination was activation sufficient to increase blood glucose (70). This anatomically precise modular viral transduction was facilitated by the larger size of the rat brain relative to the mouse; in a comparable study using similar methodology in dopamine-beta-hydroxylase-Cre mice the whole VLM was transduced and chemogenetic activation increased blood glucose (72). In a follow up study, again in TH-Cre rats, the same group showed that repeated glucoprivation by daily injection with 2-DG reduced the effects of chemogenetic stimulation of VLM<sup>TH</sup> neurons on food intake and corticosterone release. Importantly, repeated chemogenetic activation of these neurons blunted food intake and the corticosterone response to a single bout of glucoprivation, suggesting that prior activation of this neural circuit by any means, is sufficient to blunt subsequent activation (71).

## Zebrafish

Vertebrate genetics, embryonic development, and metabolic diseases can be modelled in zebrafish (73, 74), given the well conserved organ systems, lipid metabolism, hormone secretion, and glucose homeostasis (75–78). Indeed, zebrafish are emerging as a complementary model to understand analysis of glucoregulatory organs, like the liver (79–81), muscle (82, 83), adipose (84, 85), and pancreas (86, 87). Their small size and high fecundity also make

them suitable for compound screening (88) for regulators of beta cell mass and metabolism (89–97). Additionally, the major brain regions, while morphologically different, are well conserved in zebrafish (98, 99). Notably, the small size and optical transparency of larval zebrafish allows for *in vivo* activity recording of all neurons (100–102), and subsequent mapping of their anatomical brain regions (103, 104). Analogous neural circuits governing animal behavior can be found in zebrafish; including, the feeding and sleep/wake cycle associated neurotensin and hypocretin/orexin secreting neurons in the hypothalamus (105), the stress-associated hypothalamic-pituitary-adrenal axis (106), and learning and memory centers (107, 108).

While zebrafish behavioral research has been prolific, there have been few studies on the neural regulation of glucose homeostasis. Nonetheless, as in mammals, both leptin receptor and the central melanocortin systems are present in the zebrafish hypothalamus (109–111). The role of leptin in the maintenance of energy homeostasis is well studied in mammalian models (112, 113). Leptin receptor knockout (*lepr<sup>-/-</sup>*) zebrafish display altered glucose homeostasis, increased beta cell mass, but normal adiposity, feeding and fertility, highlighting potentially important differences in the function of this hormone in zebrafish compared to mammals (109). Two leptin genes (*lepa* and *lepb*) exist in zebrafish. In contrast to *lepr<sup>-/-</sup>* zebrafish, *lepa<sup>-/-</sup>* zebrafish display hyperglycemia, mild obesity, increased appetite, and decreased aggression (114). Therefore, it remains to be determined whether loss of leptin signaling in zebrafish can fully recapitulate mammalian phenotypes.

In the peripheral nervous system, recent studies have demonstrated the innervation of zebrafish pancreas early in development (115, 116). Our understanding of the neural regulation of glucoregulatory organs and the respective sensory feedback loops will be advanced by future studies in zebrafish combining optogenetic (117) and chemogenetic (43) approaches to control neural signaling and detailed *in vivo* analysis of the target organ of interest on the single cell level. Targeting the desired neural populations in zebrafish will be guided by topographic mapping, which has been elegantly studied for the vagus motor nucleus in the hindbrain (118–120), and retrograde neural tracing (121). Additionally, the GAL4-Upstream Activating Sequence (UAS) system provides a flexible toolbox for driving the expression of a range of transgenes in zebrafish in a tissue specific manner (122). Changes in glucose homeostasis could also be investigated in larval and adult zebrafish. Tracking changes in circulating glucose levels within the same animal remains difficult; however, due to the relatively low housing costs and high fecundity, glucose tolerance tests could be conducted in zebrafish by sampling different animals at various time points following exposure to a glucose bolus (75). Zebrafish could provide new insights in brain-body communication, especially on a single cell level, with live animal studies that are difficult to achieve in other vertebrate models.

## Drosophila

Despite stark differences in physiology, namely the absence of an organ equivalent to the pancreas and the predominant circulation of a non-reducing sugar trehalose instead of glucose, the invertebrate *Drosophila* has been used as a model organism to study diabetes (123). Crucially, these flies can distinguish nutritive sugars (e.g. *D*-





glucose) from non-nutritive sugars (e.g. *L*-glucose) independent of taste, indicating the existence of glucosensing mechanisms (124). Of interest to readers of this review, the *drosophila* brain contains a population of insulin-producing cells proposed to be functional equivalents of pancreatic beta cells in other species (125). When these cells are ablated in *drosophila* larvae the predominant phenotype is reduced growth. However, these larvae also show elevated carbohydrate (combined trehalose and glucose) levels (125). Ablation of these insulin-producing cells (IPCs) in adult flies increases hemolymph glucose levels in addition to other phenotypes including longer lifespan and stress resistance (126). These cells also share signal transduction mechanisms with mammalian beta cells including excitability increased by glucose and/or closure of the  $K_{ATP}$  channel (127, 128). This suggests that the brain may be the principal glucoregulatory site in *drosophila* although the functional importance of this to insect physiology is debated (123). The brain is not the sole site of glucose regulation in the *drosophila* however, since the *drosophila* equivalent of glucagon is produced by a group of neuroendocrine cells in the corpora cardiaca ([CC] analogous to the mammalian pituitary) (129). It was recently shown that both IPCs and CC cells are regulated by a pair of glucose excited neurons in the dorsolateral portion of the *drosophila* brain (130). These neurons, identified by co-incident expression of corazonin and short neuropeptide F, project to both IPCs and CC cells to stimulate insulin secretion and suppress glucagon secretion respectively (130).

*Drosophila* offer a low-cost high-throughput screening platform for disease-related genes. A recent relevant example is the description of a suite of behavioral assays in *drosophila* where neural expression of genes associated with appetite regulation, identified from genome wide association studies [GWAS], were disrupted (131). With available GWAS data, large-scale reverse genetic studies could potentially be adapted in *drosophila* to study genes regulating blood glucose (132).

To summarize, *drosophila* have distinct physiology from mammalian species and, while there is evidence for glucoregulatory neurocircuitry, it appears that these circuits are distinct from those in mammals, instead, resembling something closer to pancreatic cell types. This may preclude the use of *drosophila* to provide meaningful insight specifically into the control of glucose homeostasis by the brain but could be a useful reverse genetic screening tool for genes that impact systemic glucose homeostasis.

## Experimental Models of Diabetes

While it is beyond the scope of this review to discuss in great detail the strengths and weaknesses of these model organisms to recapitulate features of human diabetes (11) we can briefly outline these here (summarized in **Figure 2**). A range of mouse and rat strains with known, spontaneous, mutations are available each with distinct phenotypes that model type 1 or 2 diabetes, with and without obesity. Complementary to these lines, disease states can be induced by feeding with a high-fat, high-sugar diet, injection with streptozotocin or repeated bouts of hypoglycemia. The effectiveness of these protocols varies between mice and rats (and within strains of these species) with C57BL/6 mice being especially prone to diet-induced obesity (DIO) while inbred rat strains show both resistance or susceptibility to DIO (133, 134). Similarly, rats more readily develop impaired awareness of hypoglycemia with fewer

	 Mouse	 Rat	 Zebrafish	 Drosophila
Autoimmune diabetes	Non-obese diabetic (NOD)	BBDP, KDP, LEW.1AR1	No	No
STZ-induced diabetes	Yes	Yes	Yes	No
RH-induced defective CRR	Yes (more bouts required than rat)	Yes	Unknown	Unknown
High fat diet/diabetes susceptibility	Yes, variable across strains C57BL/6 particularly susceptible to DIO and insulin resistance	Sprague-Dawley, Long-Evans, Obese-prone CD, SHHF/obese	Yes with various overfeeding paradigms. Genetically obese transgenic strains e.g. Tg(b-actin:agrp)	Yes, insulin resistance on high fat diet or hyperglycemia following ablation of IPCs.
Glucose clamp	Yes	Yes	No	No
Optogenetics Chemogenetics	Yes	Yes	Yes	Yes
Cre-loxP KI/KO or Gal4-UAS	Cre and loxP strains widespread	Limited Cre and loxP strains	Cre, loxP, Gal4 and UAS strains widespread	Gal4 and UAS strains widespread

**FIGURE 2** | A summary of disease models and techniques available in each of the discussed organisms. BBDP, biobreeding diabetes-prone; DIO, diet-induced obesity; IPC, insulin-producing cell; KDP, Komeda diabetes prone; SHHF, spontaneously hypertensive heart failure; UAS, upstream activation sequence. This is a summary and is not intended as an exhaustive list. Animal images adapted from Scidraw.io.

hypoglycemic bouts required for induction than mice (58). Non-mammalian species including zebrafish and drosophila also have transgenic strains that can model some facets of human disease, however, their distinct physiology from humans means that these models do not recapitulate human disease as faithfully as rodent models (135, 136).

## CONCLUSION

A wide variety of approaches in diverse model species has begun to identify pathways by which the brain communicates with peripheral systems to control glucose homeostasis. The strengths and weaknesses of these models are summarized in **Figure 2**. The toolbox for manipulation and monitoring of genetically defined cell types in rodents affords the ability to characterize neural circuits in a high degree of detail. However, these techniques are not without their caveats and careful experimentation and selection of control groups is required (42, 137). The hyperinsulinemic-euglycemic clamp remains the gold standard technique for assessing whole-body insulin sensitivity *in vivo* (138). Not only is vascular catheterization less technically challenging in the rat compared to the mouse, but mice require infusion of donor blood to replace erythrocytes and sustain hematocrit during clamping procedures, which results in larger colony number and more complex experimental design (137). Independently of rodent model choice, however, blood glucose assessments must take into consideration; strain (40, 139), age (140, 141), sex (142–144), fasting length (137, 145) and husbandry (146–148) as all of these parameters differentially impact glucose homeostasis and the translatability of

each model to human physiology (discussed in detail in 7,9). Non-mammalian species, while having critical distinctions in their mechanisms of glucose homeostasis, particularly with respect to the brain, offer unique opportunities afforded by their genetic tractability, lower cost, and fecundity. In particular, zebrafish offer a powerful platform for genetic manipulation, live imaging, neural recording, and high throughput screening with some comparable neuroendocrine processes to mammals. Ultimately, the use of model organisms permits investigation into brain-body interactions underlying glucose homeostasis with a level of detail not achievable using studies in humans.

## AUTHOR CONTRIBUTIONS

All authors contributed to the article and approved the submitted version.

## FUNDING

This work was supported by grants from Diabetes UK (19/0006035 to KE and CB, which funds AM) and the Juvenile Diabetes Research Foundation (1-INO-2020-919-A-N to CB which funds AC). YY is supported by Expanding Excellence in England.

## ACKNOWLEDGMENTS

Some images were obtained/adapted from Scidraw.io, we thank the artists.

## REFERENCES

- Brown JM, Scarlett JM, Schwartz MW. Rethinking the role of the brain in glucose homeostasis and diabetes pathogenesis. *J Clin Invest* (2019) 129(8):3035–7. doi: 10.1172/JCI130904
- Deem JD, Muta K, Scarlett JM, Morton GJ, Schwartz MW. How should we think about the role of the brain in glucose homeostasis and diabetes? *Diabetes* (2017) 66(7):1758–65. doi: 10.2337/dbi16-0067
- Song Z, Levin BE, McArdle JJ, Bakhos N, Routh VH. Convergence of pre- and postsynaptic influences on glucosensing neurons in the ventromedial hypothalamic nucleus. *Diabetes* (2001) 50(12):2673–81. doi: 10.2337/diabetes.50.12.2673
- Ashford MLJ, Boden PR, Treherne JM. Glucose-induced excitation of hypothalamic neurones is mediated by ATP-sensitive K<sup>+</sup> channels. *Pflügers Arch Eur J Physiol* (1990) 415(4):479–83. doi: 10.1007/BF00373626
- Kang L, Dunn-Meynell AA, Routh VH, Gaspers LD, Nagata Y, Nishimura T, et al. Glucokinase is a critical regulator of ventromedial hypothalamic neuronal glucosensing. *Diabetes* (2006) 55(2):412–20. doi: 10.2337/diabetes.55.02.06.db05-1229
- Kang L, Routh VH, Kuzhikandathil EV, Gaspers LD, Levin BE. Physiological and Molecular Characteristics of Rat Hypothalamic Ventromedial Nucleus Glucosensing Neurons. *Diabetes* (2004) 53(3):549–59. doi: 10.2337/diabetes.53.3.549
- Matveyenko AV, Donovan CM. Metabolic sensors mediate hypoglycemic detection at the portal vein. *Diabetes* (2006) 55(5):1276–82. doi: 10.2337/db05-1665
- Raybould HE. Sensing of glucose in the gastrointestinal tract. *Auton Neurosci Basic Clin* (2007) 133(1):86–90. doi: 10.1016/j.autneu.2007.01.006
- Lamy CM, Sanno H, Labouëbe G, Picard A, Magnan C, Chatton JY, et al. Hypoglycemia-activated GLUT2 neurons of the nucleus tractus solitarius stimulate vagal activity and glucagon secretion. *Cell Metab* (2014) 19(3):527–38. doi: 10.1016/j.cmet.2014.02.003
- Boychuk CR, Smith KC, Peterson LE, Boychuk JA, Butler CR, Derera ID, et al. A hindbrain inhibitory microcircuit mediates vagally-coordinated glucose regulation. *Sci Rep* (2019) 9(1):2722. doi: 10.1038/s41598-019-39490-x
- Kleinert M, Clemmensen C, Hofmann SM, Moore MC, Renner S, Woods SC, et al. Animal models of obesity and diabetes mellitus. *Nat Rev Endocrinol* (2018) 14(3):140–62. doi: 10.1038/nrendo.2017.161
- Ruud J, Steculorum SM, Bruning JC. Neuronal control of peripheral insulin sensitivity and glucose metabolism. *Nat Commun* (2017) 8:15259. doi: 10.1038/ncomms15259
- Verberne AJM, Sabetghadam A, Korim WS. Neural pathways that control the glucose counterregulatory response. *Front Neurosci* (2014) 8(FEB):1–12. doi: 10.3389/fnins.2014.00038
- Ellenbroek B, Youn J. Rodent models in neuroscience research: Is it a rat race? *DMM Dis Model Mech* (2016) 9(10):1079–87. doi: 10.1242/dmm.026120
- Ayala JE, Samuel VT, Morton GJ, Obici S, Croniger CM, Shulman GI, et al. Standard operating procedures for describing and performing metabolic tests of glucose homeostasis in mice. *DMM Dis Model Mech* (2010) 3(9–10):525–34. doi: 10.1242/dmm.006239
- Alquier T, Poutout V. Considerations and guidelines for mouse metabolic phenotyping in diabetes research. *Diabetologia* (2018) 61(3):526–38. doi: 10.1007/s00125-017-4495-9
- Bowe JE, Franklin ZJ, Hauge-Evans AC, King AJ, Persaud SJ, Jones PM. Assessing glucose homeostasis in rodent models. *J Endocrinol* (2014) 222(3):13–25. doi: 10.1530/JOE-14-0182
- Steffens AB, Mogenson GJ, Stevenson JA. Blood glucose, insulin, and free fatty acids after stimulation and lesions of the hypothalamus. *Am J Physiol* (1972) 222(6):1446–52. doi: 10.1152/ajplegacy.1972.222.6.1446
- Tong Q, Ye CP, McCrimmon RJ, Dhillon H, Choi B, Kramer MD, et al. Synaptic Glutamate Release by Ventromedial Hypothalamic Neurons Is Part of the Neurocircuitry that Prevents Hypoglycemia. *Cell Metab* (2007) 5(5):383–93. doi: 10.1016/j.cmet.2007.04.001
- Balthasar N, Dalgaard LT, Lee CE, Yu J, Funahashi H, Williams T, et al. Divergence of melanocortin pathways in the control of food intake and energy expenditure. *Cell* (2005) 123(3):493–505. doi: 10.1016/j.cell.2005.08.035
- Rossi J, Balthasar N, Olson D, Scott M, Berglund E, Lee CE, et al. Melanocortin-4 Receptors Expressed by Cholinergic Neurons Regulate Energy Balance and Glucose Homeostasis. *Cell Metab* (2011) 13(2):195–204. doi: 10.1016/j.cmet.2011.01.010
- Balthasar N, Coppari R, McMinn J, Liu SM, Lee CE, Tang V, et al. Leptin receptor signaling in POMC neurons is required for normal body weight homeostasis. *Neuron* (2004) 42(6):983–91. doi: 10.1016/j.neuron.2004.06.004
- Caron A, Lemko HMD, Castorena CM, Fujikawa T, Lee S, Lord CC, et al. POMC neurons expressing leptin receptors coordinate metabolic responses to fasting via suppression of leptin levels. *Elife* (2018) 7:1–18. doi: 10.7554/eLife.33710
- Padilla SL, Carmody JS, Zeltser LM. Pomc-expressing progenitors give rise to antagonistic neuronal populations in hypothalamic feeding circuits. *Nat Med* (2010) 16(4):403–5. doi: 10.1038/nm.2126
- Sternson SM, Roth BL. Chemogenetic tools to interrogate brain functions. *Annu Rev Neurosci* (2014) 37:387–407. doi: 10.1146/annurev-neuro-071013-014048
- Boyden ES. A history of optogenetics: The development of tools for controlling brain circuits with light. *F1000 Biol Rep* (2011) 3(1):1–12. doi: 10.3410/B3-11
- Garfield AS, Shah BP, Madara JC, Burke LK, Patterson CM, Flak J, et al. A parabrachial-hypothalamic cholecystokinin neurocircuit controls counterregulatory responses to hypoglycemia. *Cell Metab* (2014) 20(6):1030–7. doi: 10.1016/j.cmet.2014.11.006
- Williams EKK, Chang RBB, Strohlic DEE, Umans BDD, Lowell BBB, Liberles SDD. Sensory neurons that detect stretch and nutrients in the digestive system. *Cell* (2016) 166(1):209–21. doi: 10.1016/j.cell.2016.05.011
- Min S, Chang RB, Prescott SL, Beeler B, Joshi NR, Strohlic DE, et al. Arterial baroreceptors sense blood pressure through decorated aortic claws. *Cell Rep* (2019) 29(8):2192–201. doi: 10.1016/j.celrep.2019.10.040
- Chang RB, Strohlic DE, Williams EK, Umans BD, Liberles SD. Vagal sensory neuron subtypes that differentially control breathing. *Cell* (2015) 161(3):622–33. doi: 10.1016/j.cell.2015.03.022
- Bai L, Mesgarzadeh S, Ramesh KS, Huey EL, Liu Y, Lindsay A, et al. Genetic identification of vagal afferents that control hunger. *Cell* (2019) 179:1129–43. doi: 10.1016/j.cell.2019.10.031
- Prescott SL, Umans BD, Williams EK, Brust RD, Liberles SD, Prescott SL, et al. An Airway Protection Program Revealed by Sweeping Genetic Control of Vagal Afferents Article An Airway Protection Program Revealed by Sweeping Genetic Control of Vagal Afferents. *Cell* (2020) 181(3):574–89. doi: 10.1016/j.cell.2020.03.004
- Han W, Tellez LA, Perkins MH, Perez IO, Qu T, Ferreira J, et al. A neural circuit for gut-induced reward. *Cell* (2018) 175(3):655–78. doi: 10.1016/j.cell.2018.08.049
- Berthoud HR, Kressel M, Neuhuber WL. An anterograde tracing study of the vagal innervation of rat liver, portal vein and biliary system. *Anat Embryol (Berl)* (1992) 186(5):431–42. doi: 10.1007/BF00185458
- Neuhuber WL. Vagal afferent fibers almost exclusively innervate islets in the rat pancreas as demonstrated by anterograde tracing. *J Auton Nerv Syst* (1989) 29(1):13–8. doi: 10.1016/0165-1838(89)90015-5
- Goldstein N, Mcknight AD, Carty JRE, Arnold M, Betley JN, Alhadeff AL. Hypothalamic detection of macronutrients via multiple gut-brain pathways. *Cell Metab* (2021) 33:1–12. doi: 10.1016/j.cmet.2020.12.018
- Bailey TW, Appleyard SM, Jin Y-H, Andresen MC. Organization and properties of GABAergic neurons in solitary tract nucleus (NTS). *J Neurophysiol* (2008) 99(4):1712–22. doi: 10.1152/jn.00038.2008
- Fergusson G, Éthier M, Guévremont M, Chrétien C, Attané C, Joly E, et al. Defective insulin secretory response to intravenous glucose in C57Bl/6J compared to C57Bl/6N mice. *Mol Metab* (2014) 3(9):848–54. doi: 10.1016/j.molmet.2014.09.006
- Lewis SR, Ahmed S, Khaimova E, Israel Y, Singh A, Kandov Y, et al. Genetic variance contributes to ingestive processes: A survey of 2-deoxy-D-glucose-induced feeding in eleven inbred mouse strains. *Physiol Behav* (2006) 87(3):595–601. doi: 10.1016/j.physbeh.2005.12.002
- Berglund ED, Li CY, Poffenberger G, Ayala JE, Fueger PT, Willis SE, et al. Glucose metabolism in vivo in a commonly used inbred mouse strains. *Diabetes* (2008) 57(7):1790–9. doi: 10.2337/db07-1615

41. Freeman HC, Hugill A, Dear NT, Ashcroft FM, Cox RD. Deletion of nicotinamide nucleotide transhydrogenase: A new quantitative trait locus accounting for glucose intolerance in C57BL/6J mice. *Diabetes* (2006) 55 (7):2153–6. doi: 10.2337/db06-0358
42. Harno E, Cottrell EC, White A. Metabolic pitfalls of CNS cre-based technology. *Cell Metab* (2013) 18(1):21–8. doi: 10.1016/j.cmet.2013.05.019
43. Roth BL. DREADDs for neuroscientists. *Neuron* (2016) 89(4):683–94. doi: 10.1016/j.neuron.2016.01.040
44. Gomez JL, Bonaventura J, Lesniak W, Mathews WB, Sysa-Shah P, Rodriguez LA, et al. Chemogenetics revealed: DREADD occupancy and activation via converted clozapine. *Science* (80- ) (2017) 357(6350):503–7. doi: 10.1126/science.aan2475
45. Hughey CC, Hittel DS, Johnsen VL, Shearer J. Hyperinsulinemic-euglycemic clamp in the conscious rat. *J Vis Exp* (2010) 7(48):2432. doi: 10.3791/2432
46. Ayala JE, Bracy DP, Malabanan C, James FD, Ansari T, Fueger PT, et al. Hyperinsulinemic-euglycemic clamps in conscious, unrestrained mice. *J Vis Exp* (2011). doi: 10.3791/3188
47. Brockway R, Tiesma S, Bogie H, White K, Fine M, O'Farrell L, et al. Fully implantable arterial blood glucose device for metabolic research applications in rats for two months. *J Diabetes Sci Technol* (2015). doi: 10.1177/1932296815586424
48. Chaudhary P, Schreihof AM. Improved glucose homeostasis in male obese Zucker rats coincides with enhanced baroreflexes and activation of the nucleus tractus solitarius. *Am J Physiol - Regul Integr Comp Physiol* (2018). doi: 10.1152/ajpregu.00195.2018
49. Sanders NM, Ritter S. Repeated 2-deoxy-D-glucose-induced glucoprivation attenuates Fos expression and glucoregulatory responses during subsequent glucoprivation. *Diabetes* (2000). doi: 10.2337/diabetes.49.11.1865
50. Hurst P, Garfield AS, Marrow C, Heisler LK, Evans ML. Recurrent hypoglycemia is associated with loss of activation in rat brain cingulate cortex. *Endocrinology* (2012). doi: 10.1210/en.2011-1827
51. Sanders NM, Figlewicz DP, Taborsky GJ, Wilkinson CW, Daumen W, Levin BE. Feeding and neuroendocrine responses after recurrent insulin-induced hypoglycemia. *Physiol Behav* (2006). doi: 10.1016/j.physbeh.2006.01.007
52. Osundiji MA, Hurst P, Moore SP, Markkula SP, Yueh CY, Swamy A, et al. Recurrent hypoglycemia increases hypothalamic glucose phosphorylation activity in rats. *Metabolism* (2011). doi: 10.1016/j.metabol.2010.05.009
53. Kakall ZM, Kavurma MM, Cohen EM, Howe PR, Nedoboy PE, Pilowsky PM. Repetitive hypoglycemia reduces activation of glucose-responsive neurons in C1 and C3 medullary brain regions to subsequent hypoglycemia. *Am J Physiol - Endocrinol Metab* (2019). doi: 10.1152/ajpendo.00051.2019
54. Sivitz WI, Herlein JA, Morgan DA, Fink BD, Phillips BG, Haynes WG. Effect of acute and antecedent hypoglycemia on sympathetic neural activity and catecholamine responsiveness in normal rats. *Diabetes* (2001). doi: 10.2337/diabetes.50.5.1119
55. Paranjape SA, Briski KP. Recurrent insulin-induced hypoglycemia causes site-specific patterns of habituation or amplification of CNS neuronal genomic activation. *Neuroscience* (2005). doi: 10.1016/j.neuroscience.2004.09.030
56. Chan O, Chan S, Inouye K, Shum K, Matthews SG, Vranic M. Diabetes impairs hypothalamo-pituitary-adrenal (HPA) responses to hypoglycemia, and insulin treatment normalizes HPA but not epinephrine responses. *Diabetes* (2002). doi: 10.2337/diabetes.51.6.1681
57. Otlivanchik O, Sanders NM, Dunn-Meynell A, Levin BE. Orexin signaling is necessary for hypoglycemia-induced prevention of conditioned place preference. *Am J Physiol - Regul Integr Comp Physiol* (2016) 310(1):66–73. doi: 10.1152/ajpregu.00066.2015
58. Sankar A, Khodai T, McNeilly AD, McCrimmon RJ, Luckman SM. Experimental Models of Impaired Hypoglycaemia-Associated Counter-Regulation. *Trends Endocrinol Metab* (2020) 31(9):691–703. doi: 10.1016/j.tem.2020.05.008
59. Ritter R, Slusser P, Stone S. Glucoreceptors controlling feeding and blood glucose: location in the hindbrain. *Science* (80- ) (1981) 213(4506):451–2. doi: 10.1126/science.6264602
60. Dirocco RJ, Grill HJ. The forebrain is not essential for sympathoadrenal hyperglycemic response to glucoprivation. *Science* (80- ) (1979) 204 (4397):1112–4. doi: 10.1126/science.451558
61. Ritter S, Dinh TT, Li AJ. Hindbrain catecholamine neurons control multiple glucoregulatory responses. *Physiol Behav* (2006) 89(4):490–500. doi: 10.1016/j.physbeh.2006.05.036
62. Sanders NM, Taborsky GJ, Wilkinson CW, Daumen W, Figlewicz DP. Antecedent hindbrain glucoprivation does not impair the counterregulatory response to hypoglycemia. *Diabetes* (2007) 56(1):217–23. doi: 10.2337/db06-1025
63. Lynch RM, Tompkins LS, Brooks HL, Dunn-Meynell AA, Levin BE. Localization of glucokinase gene expression in the rat brain. *Diabetes* (2000) 49(5):693–700. doi: 10.2337/diabetes.49.5.693
64. Aklan I, Atasoy NS, Yavuz Y, Ates T, Coban I, Koksalar F, et al. NTS catecholamine neurons mediate hypoglycemic hunger via medial hypothalamic feeding pathways. *Cell Metab* (2020) 31:313–26. doi: 10.1016/j.cmet.2019.11.016
65. McCrimmon RJ, Evans ML, Fan X, McNay EC, Chan O, Ding Y, et al. Activation of ATP-sensitive K<sup>+</sup> channels in the ventromedial hypothalamus amplifies counterregulatory hormone responses to hypoglycemia in normal and recurrently hypoglycemic rats. *Diabetes* (2005) 54(11):3169–74. doi: 10.2337/diabetes.54.11.3169
66. Alquier T, Kawashima J, Tsuji Y, Kahn BB. Role of hypothalamic adenosine 5'-monophosphate-activated protein kinase in the impaired counterregulatory response induced by repetitive neuroglucopenia. *Endocrinology* (2007). doi: 10.1210/en.2006-1039
67. McCrimmon RJ, Shaw M, Fan X, Cheng H, Ding Y, Vella MC, et al. Key Role for AMP-activated protein kinase in the ventromedial hypothalamus in regulating counterregulatory hormone responses to acute hypoglycemia. *Diabetes* (2008) 57(2):444–50. doi: 10.2337/db07-0837
68. Witten IB, Steinberg EE, Lee SY, Davidson TJ, Zalocusky KA, Brodsky M, et al. Recombinase-driver rat lines: Tools, techniques, and optogenetic application to dopamine-mediated reinforcement. *Neuron* (2011) 72 (5):721–33. doi: 10.1016/j.neuron.2011.10.028
69. Ikeda K, Takahashi M, Sato S, Igarashi H, Ishizuka T, Yawo H, et al. A Phox2b bac transgenic rat line useful for understanding respiratory rhythm generator neural circuitry. *PLoS One* (2015) 10(7):1–23. doi: 10.1371/journal.pone.0132475
70. Li AJ, Wang Q, Ritter S. Selective pharmacogenetic activation of catecholamine subgroups in the ventrolateral medulla elicits key glucoregulatory responses. *Endocrinology* (2018) 159(1):341–55. doi: 10.1210/en.2017-00630
71. Li AJ, Wang Q, Ritter S. Repeated pharmacogenetic catecholamine neuron activation in the ventrolateral medulla attenuates subsequent glucoregulatory responses. *Diabetes* (2020) 69(12):2747–55. doi: 10.2337/db20-0402
72. Zhao Z, Wang L, Gao W, Hu F, Zhang J, Ren Y, et al. A Central Catecholaminergic Circuit Controls Blood Glucose Levels during Stress. *Neuron* (2017) 95(1):138–52.e5. doi: 10.1016/j.neuron.2017.05.031
73. Gut P, Reischauer S, Stainier D, Arnaut R. Little fish, big data: Zebrafish as a model for cardiovascular and metabolic disease. *Physiol Rev* (2017) 97 (3):889–938. doi: 10.1152/physrev.00038.2016
74. Seth A, Stemple DL, Barroso I. The emerging use of zebrafish to model metabolic disease. *DMM Dis Model Mech* (2013) 6(5):1080–8. doi: 10.1242/dmm.011346
75. Eames SC, Philipson LH, Prince VE, Kinkel MD. Blood sugar measurement in zebrafish reveals dynamics of glucose homeostasis. *Zebrafish* (2010) 7 (2):205–13. doi: 10.1089/zeb.2009.0640
76. Jurczyk A, Roy N, Bajwa R, Gut P, Lipson K, Yang C, et al. Dynamic glucoregulation and mammalian-like responses to metabolic and developmental disruption in zebrafish. *Gen Comp Endocrinol* (2011) 170 (2):334–45. doi: 10.1016/j.ygcen.2010.10.010
77. Zang L, Shimada Y, Nishimura N. Development of a Novel Zebrafish Model for Type 2 Diabetes Mellitus. *Sci Rep* (2017) 7(1):1–11. doi: 10.1038/s41598-017-01432-w
78. Castillo J, Crespo D, Capilla E, Diaz M, Chauvigné F, Cerdà J, et al. Evolutionary structural and functional conservation of an ortholog of the GLUT2 glucose transporter gene (SLC2A2) in zebrafish. *Am J Physiol - Regul Integr Comp Physiol* (2009) 297(5):1570–81. doi: 10.1152/ajpregu.00430.2009
79. Cruz-Garcia L, Schlegel A. Lxr-driven enterocyte lipid droplet formation delays transport of ingested lipids. *J Lipid Res* (2014) 55(9):1944–58. doi: 10.1194/jlr.M052845

80. Carten JD, Bradford MK, Farber SA. Visualizing digestive organ morphology and function using differential fatty acid metabolism in live zebrafish. *Dev Biol* (2011) 360(2):276–85. doi: 10.1016/j.ydbio.2011.09.010
81. Field HA, Ober EA, Roeser T, Stainier DYR. Formation of the digestive system in zebrafish. I. Liver morphogenesis. *Dev Biol* (2003) 253(2):279–90. doi: 10.1016/S0012-1606(02)00017-9
82. Maddison LA, Joest KE, Kammeyer RM, Chen W. Skeletal muscle insulin resistance in Zebrafish induces alterations in  $\beta$ -cell number and glucose tolerance in an age- and diet-dependent manner. *Am J Physiol - Endocrinol Metab* (2015) 308(8):E662–9. doi: 10.1152/ajpendo.00441.2014
83. Faught E, Vijayan MM. Loss of the glucocorticoid receptor in zebrafish improves muscle glucose availability and increases growth. *Am J Physiol - Endocrinol Metab* (2019) 316(6):E1093–104. doi: 10.1152/ajpendo.00045.2019
84. Oka T, Nishimura Y, Zang L, Hirano M, Shimada Y, Wang Z, et al. Diet-induced obesity in zebrafish shares common pathophysiological pathways with mammalian obesity. *BMC Physiol* (2010) 10(1):21. doi: 10.1186/1472-6793-10-21
85. Minchin JEN, Rawls JF. A classification system for zebrafish adipose tissues. *DMM Dis Model Mech* (2017) 10(6):797–809. doi: 10.1242/dmm.025759
86. Prince VE, Anderson RM, Dalgin G. Zebrafish Pancreas Development and Regeneration: Fishing for Diabetes Therapies. *Curr Top Dev Biol* (2017) 124:235–76.
87. Field HA, Si Dong PD, Beis D, Stainier DYR. Formation of the digestive system in zebrafish. II. Pancreas morphogenesis. *Dev Biol* (2003) 261(1):197–208. doi: 10.1016/S0012-1606(03)00308-7
88. Rennekamp AJ, Peterson RT. 15 years of zebrafish chemical screening. *Curr Opin Chem Biol* (2015) 24(Feb):58–70. doi: 10.1016/j.cbpa.2014.10.025
89. Mullapudi ST, Helker CS, Boezio GL, Maischein H-M, Sokol AM, Guenther S, et al. Screening for insulin-independent pathways that modulate glucose homeostasis identifies androgen receptor antagonists. *Elife* (2018) 7(Dec 6):e42209. doi: 10.7554/eLife.42209
90. Rovira M, Huang W, Yusuf S, Shim JS, Ferrante AA, Liu JO, et al. Chemical screen identifies FDA-approved drugs and target pathways that induce precocious pancreatic endocrine differentiation. *Proc Natl Acad Sci U S A* (2011) 108(48):19264–9. doi: 10.1073/pnas.1113081108
91. Tsuji N, Ninov N, Delawary M, Osman S, Roh AS, Gut P, et al. Whole organism high content screening identifies stimulators of pancreatic beta-cell proliferation. *PLoS One* (2014) 9(8):e104112. doi: 10.1371/journal.pone.0104112
92. Wang G, Rajpurohit SK, Delaspre F, Walker SL, White DT, Ceasrine A, et al. First quantitative high-throughput screen in zebrafish identifies novel pathways for increasing pancreatic  $\beta$ -cell mass. *Elife* (2015) 28(4):e08261. doi: 10.7554/eLife.08261
93. Gut P, Stainier DYR. Whole-organism screening for modulators of fasting metabolism using transgenic zebrafish. *Methods Mol Biol* (2015) 1263:157–65. doi: 10.1007/978-1-4939-2269-7\_12
94. Ninov N, Hesselson D, Gut P, Zhou A, Fidelin K, Stainier DYR. Metabolic regulation of cellular plasticity in the pancreas. *Curr Biol* (2013) 23(13):1242–50. doi: 10.1016/j.cub.2013.05.037
95. Gut P, Baeza-Raja B, Andersson O, Hasenkamp L, Hsiao J, Hesselson D, et al. Whole-organism screening for gluconeogenesis identifies activators of fasting metabolism. *Nat Chem Biol* (2013) 9(2):97–104. doi: 10.1038/nchembio.1136
96. Andersson O, Adams BA, Yoo D, Ellis GC, Gut P, Anderson RM, et al. Adenosine signaling promotes regeneration of pancreatic  $\beta$  cells in vivo. *Cell Metab* (2012) 15(6):885–94. doi: 10.1016/j.cmet.2012.04.018
97. Matsuda H, Mullapudi ST, Yang YHC, Masaki H, Hesselson D, Stainier DYR. Whole-organism chemical screening identifies modulators of pancreatic B-cell function. *Diabetes* (2018) 67(11):2268–79. doi: 10.2337/db17-1223
98. Folgueira M, Bayley P, Navratilova P, Becker TS, Wilson SW, Clarke JDW. Morphogenesis underlying the development of the everted teleost telencephalon. *Neural Dev* (2012) 7:212. doi: 10.1186/1749-8104-7-32
99. Kozol RA, Abrams AJ, James DM, Buglo E, Yan Q, Dallman JE. Function over form: Modeling groups of inherited neurological conditions in zebrafish. *Front Mol Neurosci* (2016) 7(9):55. doi: 10.3389/fnfmol.2016.00055
100. Ahrens MB, Li JM, Orger MB, Robson DN, Schier AF, Engert F, et al. Brain-wide neuronal dynamics during motor adaptation in zebrafish. *Nature* (2012) 485(7399):471–7. doi: 10.1038/nature11057
101. Portugues R, Feierstein CE, Engert F, Orger MB. Whole-brain activity maps reveal stereotyped, distributed networks for visuomotor behavior. *Neuron* (2014) 81(6):1328–43. doi: 10.1016/j.neuron.2014.01.019
102. Pantoja C, Larsch J, Laurell E, Marquart G, Kunst M, Baier H. Rapid Effects of Selection on Brain-wide Activity and Behavior. *Curr Biol* (2020) 30(18):3647–56. doi: 10.1016/j.cub.2020.06.086
103. Randlett O, Wee CL, Naumann EA, Nnaemeka O, Schoppik D, Fitzgerald JE, et al. Whole-brain activity mapping onto a zebrafish brain atlas. *Nat Methods* (2015) 12(11):1039–46. doi: 10.1038/nmeth.3581
104. Kunst M, Laurell E, Mokayes N, Kramer A, Kubo F, Fernandes AM, et al. A Cellular-Resolution Atlas of the Larval Zebrafish Brain. *Neuron* (2019) 103(1):21–38. doi: 10.12139/ssrn.3257346
105. Levitas-Djerbi T, Yelin-Bekerman L, Lerer-Goldshtein T, Appelbaum L. Hypothalamic leptin-neurotensin-hypocretin neuronal networks in zebrafish. *J Comp Neurol* (2015) 523(5):831–48. doi: 10.1002/cne.23716
106. vom Berg-Maurer CM, Trivedi CA, Bollmann JH, De Marco RJ, Ryu S. The severity of acute stress is represented by increased synchronous activity and recruitment of hypothalamic CRH neurons. *J Neurosci* (2016) 36(11):3350–62. doi: 10.1523/JNEUROSCI.3390-15.2016
107. López-Schier H. Neuroplasticity in the acoustic startle reflex in larval zebrafish. *Curr Opin Neurobiol* (2019) 54(Feb):134–9. doi: 10.1016/j.conb.2018.10.004
108. Lovett-Barron M. Learning-dependent neuronal activity across the larval zebrafish brain. *Curr Opin Neurobiol* (2021) 67(4):42–9. doi: 10.1016/j.conb.2020.07.006
109. Michel M, Page-McCaw PS, Chen W, Cone RD. Leptin signaling regulates glucose homeostasis, but not adipostasis, in the zebrafish. *Proc Natl Acad Sci U S A* (2016) 113(11):3084–9. doi: 10.1073/pnas.1513212113
110. Zhang C, Forlano PM, Cone RD. AgRP and POMC neurons are hypophysiotropic and coordinately regulate multiple endocrine axes in a larval teleost. *Cell Metab* (2012) 15(2):256–64. doi: 10.1016/j.cmet.2011.12.014
111. Sebag JA, Zhang C, Hinkle PM, Bradshaw AM, Cone RD. Developmental control of the melanocortin-4 receptor by MRAP2 proteins in zebrafish. *Science* (80- ) (2013) 341(6143):278–81. doi: 10.1126/science.1232995
112. Pan WW, Myers MG. Leptin and the maintenance of elevated body weight. *Nat Rev Neurosci* (2018) 19(2):95–105. doi: 10.1038/nrn.2017.168
113. Friedman J. 20 YEARS OF LEPTIN: Leptin at 20: an overview. *J Endocrinol* (2014) 223(1):1–8. doi: 10.1530/JOE-14-0405
114. Audira G, Sarasamma S, Chen JR, Juniardi S, Sampurna BP, Liang ST, et al. Zebrafish mutants carrying leptin (a Lepa) gene deficiency display obesity, anxiety, less aggression and fear, and circadian rhythm and color preference dysregulation. *Int J Mol Sci* (2018) 19(12):4038. doi: 10.3390/ijms19124038
115. Yang YHC, Kawakami K, Stainier DYR. A new mode of pancreatic islet innervation revealed by live imaging in zebrafish. *Elife* (2018) 7:1–19. doi: 10.7554/eLife.34519
116. Podlasz P, Jakimiuk A, Chmielewska-Krzyszewska M, Kasica N, Nowik N, Kaleczyc J. Galanin regulates blood glucose level in the zebrafish: a morphological and functional study. *Histochem Cell Biol* (2016) 145(1):105–17. doi: 10.1007/s00418-015-1376-5
117. Antinucci P, Dumitrescu AS, Deleuze C, Morley HJ, Leung K, Hagley T, et al. A calibrated optogenetic toolbox of stable zebrafish opsin lines. *Elife* (2020) 9(Mar 27):e54937. doi: 10.1101/2020.01.13.904185
118. Ohata S, Kinoshita S, Aoki R, Tanaka H, Wada H, Tsuruoka-Kinoshita S, et al. Neuroepithelial cells require fucosylated glycans to guide the migration of vagus motor neuron progenitors in the developing zebrafish hindbrain. *Development* (2009) 136(10):1653–63. doi: 10.1242/dev.033290
119. Barsh GR, Isabella AJ, Moens CB. Vagus Motor Neuron Topographic Map Determined by Parallel Mechanisms of hox5 Expression and Time of Axon Initiation. *Curr Biol* (2017) 27(24):3812–25. doi: 10.1016/j.cub.2017.11.022
120. Isabella AJ, Barsh GR, Stonick JA, Dubrulle J, Moens CB. Retinoic Acid Organizes the Zebrafish Vagus Motor Topographic Map via Spatiotemporal Coordination of Hgf/Met Signaling. *Dev Cell* (2020) 53(3):344–57. doi: 10.1101/826735
121. Yáñez J, Souto Y, Piñeiro L, Folgueira M, Anadón R. Gustatory and general visceral centers and their connections in the brain of adult zebrafish: a carbocyanine dye tract-tracing study. *J Comp Neurol* (2017) 525(2):333–62. doi: 10.1002/cne.24068

122. Kawakami K, Asakawa K, Hibi M, Itoh M, Muto A, Wada H. Gal4 Driver Transgenic Zebrafish: Powerful Tools to Study Developmental Biology, Organogenesis, and Neuroscience. *Adv Genet* (2016) 95:65–87. doi: 10.1016/bs.adgen.2016.04.002
123. Graham P, Pick L. Drosophila as a model for diabetes and diseases of insulin resistance. *Curr Top Dev Biol* (2017) 121:397–419. doi: 10.1016/bs.ctdb.2016.07.011
124. Dus M, Min SH, Keene AC, Lee GY, Suh GSB. Taste-independent detection of the caloric content of sugar in Drosophila. *Proc Natl Acad Sci U S A* (2011) 108(28):11644–9. doi: 10.1073/pnas.1017096108
125. Rulifson EJ, Kim SK, Nusse R. Ablation of insulin-producing neurons in flies: Growth and diabetic phenotypes. *Science* (80-) (2002) 296(5570):1118–20. doi: 10.1126/science.1070058
126. Broughton SJ, Piper MDW, Ikeya T, Bass TM, Jacobson J, Driege Y, et al. Longer lifespan, altered metabolism, and stress resistance in Drosophila from ablation of cells making insulin-like ligands. *Proc Natl Acad Sci U S A* (2005) 102(8):3105–10. doi: 10.1073/pnas.0405775102
127. Kréneisz O, Chen X, Fridell YWC, Mulkey DK. Glucose increases activity and Ca<sup>2+</sup> in adult drosophila insulin producing cells. *Neuroreport* (2010) 21(17):1116–20. doi: 10.1097/WNR.0b013e3283409200
128. Fridell YWC, Hoh M, Kréneisz O, Hosier S, Chang C, Scantling D, et al. Increased uncoupling protein (UCP) activity in Drosophila insulin-producing neurons attenuates insulin signaling and extends lifespan. *Aging (Albany NY)* (2009) 1(8):699–713. doi: 10.18632/aging.100067
129. Kim SK, Rulifson EJ. Conserved mechanisms of glucose sensing and regulation by Drosophila corpora cardiaca cells. *Nature* (2004) 431(7006):316–20. doi: 10.1038/nature02897
130. Oh Y, Lai JSY, Mills HJ, Erdjument-Bromage H, Giammarinaro B, Saadipour K, et al. A glucose-sensing neuron pair regulates insulin and glucagon in Drosophila. *Nature* (2019) 574(7779):559–64. doi: 10.1038/s41586-019-1675-4
131. Chalmers J, Tung YCL, Liu CH, O’Kane CJ, O’Rahilly S, Yeo GSH. A multi-component screen for feeding behaviour and nutritional status in Drosophila to interrogate mammalian appetite-related genes. *Mol Metab* (2021) 43:101127. doi: 10.1016/j.molmet.2020.101127
132. Lagou V, Mägi R, Hottenga JJ, Gallert H, Perry JRB, Bouatia-Naji N, et al. Sex-dimorphic genetic effects and novel loci for fasting glucose and insulin variability. *Nat Commun* (2021) 12(1):1–18. doi: 10.1038/s41467-020-19366-9
133. Levin BE, Dunn-Meynell AA, Balkan B, Keeseey RE. Selective breeding for diet-induced obesity and resistance in Sprague-Dawley rats. *Am J Physiol - Regul Integr Comp Physiol* (1997). doi: 10.1152/ajpregu.1997.273.2.R725
134. Collins S, Martin TL, Surwit RS, Robidoux J. Genetic vulnerability to diet-induced obesity in the C57BL/6J mouse: Physiological and molecular characteristics. *Physiol Behav* (2004) 81(2):243–8. doi: 10.1016/j.physbeh.2004.02.006
135. Morris SNS, Coogan C, Chamseddin K, Fernandez-Kim SO, Kolli S, Keller JN, et al. Development of diet-induced insulin resistance in adult Drosophila melanogaster. *Biochim Biophys Acta - Mol Basis Dis* (2012) 1822(8):1230–7. doi: 10.1016/j.bbdis.2012.04.012
136. Zang L, Maddison LA, Chen W. Zebrafish as a model for obesity and diabetes. *Front Cell Dev Biol* (2018) 6(AUG):1–13. doi: 10.3389/fcell.2018.00091
137. Ayala JE, Bracy DP, McGuinness OP, Wasserman DH. Considerations in the design of hyperinsulinemic-euglycemic clamps in the conscious mouse. *Diabetes* (2006) 55(2):390–7. doi: 10.2337/diabetes.55.02.06.db05-0686
138. Kim JK. Hyperinsulinemic-euglycemic clamp to assess insulin sensitivity in vivo. *Methods Mol Biol* (2009) 560:221–38. doi: 10.1007/978-1-59745-448-3\_15
139. Mn M, Smvk P, Battula KK, Nv G, Kalashikam RR. Differential response of rat strains to obesogenic diets underlines the importance of genetic makeup of an individual towards obesity. *Sci Rep* (2017) 7(1):9162. doi: 10.1038/s41598-017-09149-6
140. Ghezzi AC, Cambri LT, Botezelli JD, Ribeiro C, Dalia RA, De Mello MAR. Metabolic syndrome markers in wistar rats of different ages. *Diabetol Metab Syndr* (2012) 4(1):16. doi: 10.1186/1758-5996-4-16
141. He W, Yuan T, Choezom D, Hunkler H, Annamalai K, Lupse B, et al. Ageing potentiates diet-induced glucose intolerance,  $\beta$ -cell failure and tissue inflammation through TLR4. *Sci Rep* (2018) 8(1):2767. doi: 10.1038/s41598-018-20909-w
142. Kim B, Kim YY, Nguyen PTT, Nam H, Suh JG. Sex differences in glucose metabolism of streptozotocin-induced diabetes inbred mice (C57BL/6J). *Appl Biol Chem* (2020) 63(1):59. doi: 10.1186/s13765-020-00547-5
143. Gustavsson C, Yassin K, Wahlström E, Cheung L, Lindberg J, Brismar K, et al. Sex-different hepatic glycogen content and glucose output in rats. *BMC Biochem* (2010) 11(Sep23):38. doi: 10.1186/1471-2091-11-38
144. Blesson CS, Schutt A, Chacko S, Marini JC, Mathew PR, Tanchico D, et al. Sex Dependent Dysregulation of Hepatic Glucose Production in Lean Type 2 Diabetic Rats. *Front Endocrinol (Lausanne)* (2019). doi: 10.3389/fendo.2019.00538
145. Rakvaag E, Lund MD, Wiking L, Hermansen K, Gregersen S. Effects of Different Fasting Durations on Glucose and Lipid Metabolism in Sprague Dawley Rats. *Horm Metab Res* (2019). doi: 10.1055/a-0897-2496
146. Balcombe JP, Barnard ND, Sandusky C. Laboratory routines cause animal stress. *Contemp Top Lab Anim Sci* (2004).
147. Ghosal S, Nunley A, Mahbod P, Lewis AG, Smith EP, Tong J, et al. Mouse handling limits the impact of stress on metabolic endpoints. *Physiol Behav* (2015). doi: 10.1016/j.physbeh.2015.06.021
148. Meijer MK, Sommer R, Spruijt BM, Van Zutphen LFM, Baumans V. Influence of environmental enrichment and handling on the acute stress response in individually housed mice. *Lab Anim* (2007) 41(2):161–73. doi: 10.1258/002367707780378168

**Conflict of Interest:** The authors declare that the research was conducted in the absence of any commercial or financial relationships that could be construed as a potential conflict of interest.

Copyright © 2021 MacDonald, Yang, Cruz, Beall and Ellacott. This is an open-access article distributed under the terms of the Creative Commons Attribution License (CC BY). The use, distribution or reproduction in other forums is permitted, provided the original author(s) and the copyright owner(s) are credited and that the original publication in this journal is cited, in accordance with accepted academic practice. No use, distribution or reproduction is permitted which does not comply with these terms.



# Obesity and Dietary Added Sugar Interact to Affect Postprandial GLP-1 and Its Relationship to Striatal Responses to Food Cues and Feeding Behavior

Sabrina Jones<sup>1,2</sup>, Shan Luo<sup>1,2,3</sup>, Hilary M. Dorton<sup>2,4</sup>, Alexandra G. Yunker<sup>1,2</sup>, Brendan Angelo<sup>1,2</sup>, Alexis Defendis<sup>1,2</sup>, John R. Monterosso<sup>3,4</sup> and Kathleen A. Page<sup>1,2,4\*</sup>

<sup>1</sup> Division of Endocrinology, Department of Medicine, Keck School of Medicine, University of Southern California, Los Angeles, CA, United States, <sup>2</sup> Keck School of Medicine, Diabetes and Obesity Research Institute, University of Southern California, Los Angeles, CA, United States, <sup>3</sup> Department of Psychology, University of Southern California, Los Angeles, CA, United States, <sup>4</sup> Neuroscience Graduate Program, University of Southern California, Los Angeles, CA, United States

## OPEN ACCESS

### Edited by:

Hubert Preissl,  
Institute for Diabetes Research and  
Metabolic Diseases (IDM), Germany

### Reviewed by:

Stephanie Kullmann,  
University of Tübingen, Germany  
Burkhard J. Göke,  
Medical School Hamburg, Germany

### \*Correspondence:

Kathleen A. Page  
kpage@usc.edu

### Specialty section:

This article was submitted to  
Clinical Diabetes,  
a section of the journal  
Frontiers in Endocrinology

**Received:** 06 December 2020

**Accepted:** 15 February 2021

**Published:** 31 March 2021

### Citation:

Jones S, Luo S, Dorton HM,  
Yunker AG, Angelo B, Defendis A,  
Monterosso JR and Page KA (2021)  
Obesity and Dietary Added Sugar  
Interact to Affect Postprandial GLP-1  
and Its Relationship to Striatal  
Responses to Food Cues and  
Feeding Behavior.  
Front. Endocrinol. 12:638504.  
doi: 10.3389/fendo.2021.638504

It has been hypothesized that the incretin hormone, glucagon-like peptide-1 (GLP-1), decreases overeating by influencing mesolimbic brain regions that process food-cues, including the dorsal striatum. We previously showed that habitual added sugar intake was associated with lower glucose-induced circulating GLP-1 and a greater striatal response to high calorie food cues in lean individuals. Less is known about how dietary added sugar and obesity may interact to affect postprandial GLP-1 and its relationship to striatal responses to food cues and feeding behavior. The current study aimed to expand upon previous research by assessing how circulating GLP-1 and striatal food cue reactivity are affected by acute glucose consumption in participants with varied BMIs and amounts of habitual consumption of added sugar. This analysis included 72 participants from the Brain Response to Sugar Study who completed two study visits where they consumed either plain water or 75g glucose dissolved in water (order randomized; both drinks were flavored with non-caloric cherry flavoring) and underwent repeated blood sampling, a functional magnetic resonance imaging (fMRI) based food-cue task, and an ad-libitum buffet meal. Correlations between circulating GLP-1 levels, striatal food-cue reactivity, and food intake were assessed, and interactions between obesity and added sugar on GLP-1 and striatal responses were examined. An interaction between BMI and dietary added sugar was associated with reduced post-glucose GLP-1 secretion. Participants who were obese and consumed high levels of added sugar had the smallest increase in plasma GLP-1 levels. Glucose-induced GLP-1 secretion was correlated with lower dorsal striatal reactivity to high-calorie versus low-calorie food-cues, driven by an increase in reactivity to low calorie food-cues. The increase in dorsal striatal reactivity to low calorie food-cues was negatively correlated with sugar consumed at the buffet. These findings suggest that an interaction between obesity and dietary added sugar intake is associated with additive reductions in postprandial GLP-1 secretion. Additionally, the results suggest that changes

to dorsal striatal food cue reactivity through a combination of dietary added sugar and obesity may affect food consumption.

**Keywords:** striatum, glucagon-like peptide-1, obesity, dietary sugar, fMRI, feeding behavior, appetite and food intake

## INTRODUCTION

Obesity among U.S. adults has reached over 40% of the total population (1). In order to combat this public health crisis, recent research has been aimed at identifying interactions between neural and hormonal mechanisms that underly energy regulation and the factors that can disrupt typical functioning, inducing a cycle of overeating and excess weight gain. One hormone that has been identified as a key influence in the control of consummatory behavior is glucagon-like peptide-1 (GLP-1). GLP-1 is an incretin hormone that is derived from preproglucagon and is predominantly produced in intestinal L-cells (2) and a subset of neurons in the nucleus tractus solitarius (NTS) (3). Endogenous GLP-1 is elevated following glucose consumption (4) and improves glucose metabolism by augmenting glucose stimulated insulin secretion (5) and decreasing glucagon levels (4).

Along with its effects on glucose metabolism, GLP-1 has been implicated in altering the brain's processing of both food and drug rewards (6) through its influence on the mesolimbic system (7–9). Activation of GLP-1 receptors using GLP-1 analogues decreases drug reward and striatal c-fos expression in mice (10). In humans, neuroimaging studies in humans have found that infusions of GLP-1 (11) and GLP-1 agonists (12), or glucose-induced GLP-1 increases (13, 14) alter brain responses to food cues in regions of the brain involved in the regulation of eating. A previous study from our laboratory (15) found a negative correlation between GLP-1 response to oral glucose and activation of the dorsal striatum in response to high-calorie food images, relative to nonfood images, in lean young adults.

In addition, this study showed that high levels of habitual added sugar consumption were associated with both a reduction in GLP-1 secretion in response to acute glucose ingestion and an increase in dorsal striatal food cue reactivity to palatable food cues. While this study provided new insights into relationships between consumption of dietary added sugars, GLP-1 secretion, and striatal food cue reactivity, these relationships were only examined in lean participants and the food cue task only included high-calorie food cues (15). Excess weight gain (e.g., obesity/overweight) has been associated with impairments in glucose-induced GLP-1 secretion (16–19) and alterations to dorsal striatal response to food cues (20–23), but no study that we are aware of has examined how an interactions between obesity and dietary added sugars are related to postprandial GLP-1 secretion or dorsal striatal food cue reactivity, despite the established potential comorbidity between these two factors (24, 25).

The current study aimed to extend findings from Dorton et al. (15) by examining if dietary added sugar interacts with overweight and/or obesity to alter glucose-induced GLP-1 and

striatal food cue reactivity. Additionally, the current study assessed if these relationships were specific to high-calorie, palatable food cues, like those used in Dorton et al. (15), or if they applied to low-calorie food cues. Finally, the current study examined if the observed relationships were associated with changes to consummatory behavior. Data was collected as part of a larger randomized cross-over study in which neuroimaging, blood sampling, and an ad-libitum buffet meal were performed to examine the neuroendocrine regulation of feeding behavior. Based on our previous findings, we expected post-glucose GLP-1 levels to be correlated with striatal food cue reactivity, but we predicted that the direction of this relationship could be food cue type specific as the striatum has been found to respond differentially to high calorie and low calorie food cues based on interoceptive state (26). We hypothesized that BMI, dietary added sugar, and/or the interaction between the two would be associated with reductions in postprandial GLP-1 secretion and increased striatal food cue reactivity. The behavioral relevance of dorsal striatal and/or GLP-1 alterations was also tested by correlating the neuroimaging and hormone data with food consumption at an ad-libitum buffet meal.

## SUBJECTS AND METHODS

### Participants

All participants from the parent study that completed either the water or glucose days were included in the present analysis. Using this inclusion criteria, data on 72 young adults (32 males, 40 females) were included in this analysis. Participants were right-handed, nonsmokers, weight stable for at least 3 months, non-dieters, not on any medication (except oral contraceptives), with normal or corrected-to-normal vision, and no history of diabetes, eating disorders, or other significant medical diagnoses. Recruitment occurred between July 2016 and January 2020. During the course of the study, participants were asked to adhere to their usual diet and physical activity levels. Participants provided written informed consent compliant in accordance with the Declaration of Helsinki. The protocol # HS-09-00395-CR011 was approved by the University of Southern California Institutional Review Board.

Three participants were excluded from the final analysis of dorsal striatal food cue reactivity on the glucose day: one because of  $\geq 5\%$  weight gain between the water and glucose sessions, one for scanner sequence error during the food cue task, and one for motion (larger than 2 mm or  $2^\circ$  in any direction). Four participants were excluded from analysis of food cue reactivity on the water day: one because of drop out, one because of scanner failure during data collection for the food cue task, and

two because of motion. Sixty-nine participants were included in the final glucose food cue reactivity analysis and sixty-eight were included in the final water food cue reactivity analysis. Sixty-six of these participants completed blood sampling on the glucose day and sixty-two completed blood draws on the water day. Problems with intravenous line insertion or blood sampling led to the lower numbers of participants who completed blood sampling procedures (for participant flowsheet for this sub-study see **Supplemental Figure 1**). There were no significant differences in demographics of the included vs excluded participants (see **Supplemental Results**).

## Experiment Overview

This study used data collected as part of a larger study aimed at examining the neural mechanisms for appetitive responses to food (Clinical Trial NCT02945475). In the larger parent study, each participant attended an initial screening visit and up to four functional magnetic resonance imaging (fMRI) test sessions. This analysis only included two of these fMRI sessions (i.e., water and glucose drinks) to specifically examine how obesity and dietary sugar affect the GLP-1 response to glucose and dorsal striatal responses to food cues. At the screening visit, demographic information was collected along with height (cm), weight (kg), and a 24h dietary intake recall. Height was measured to the nearest 0.1cm using a stadiometer and weight was measured to the nearest 0.1 kg using a calibrated digital scale (Model no.SC-331S, TANITA Corporation of America, Inc.). Using the anthropometric measures acquired at the screening visit, BMI was calculated as  $\text{weight (kg)}/\text{height(m)}^2$ . At each fMRI study session, height and weight were collected to confirm participants were weight stable (body weight change <5%). Additionally, a 24h dietary intake recall was collected along with fMRI scans, plasma GLP-1 levels, and calories consumed at a buffet. All females underwent study session days during the follicular phase of the menstrual cycle to control for potential confounding effects of cycle on appetitive behaviors (27, 28).

MRI scans were performed at the Dornsife Cognitive Neuroimaging Center of the University of Southern California. For each test session day, participants arrived at approximately 8:00 a.m. after a 12h overnight fast. Upon arrival, participants were asked to complete a 24h dietary recall and a baseline blood draw was performed. The MRI scan began with a T1 structural scan (used for anatomical registration). Participants then received one of two standard drinks to consume within 2 minutes. One drink was a 75g glucose load dissolved in 300ml of water along with .45g of non-sweetened, zero calorie, cherry flavoring and the other

drink was a noncaloric 300ml of water with .45g of non-sweetened, zero calorie, cherry flavoring [drinks based on (15)]. The order of the drink days was randomized for each individual using a computer-generated sequence and the time interval between the two drinks days ranged from 2 days-2 months. Both participants and experimenters were blinded to the drink provided during the study sessions. Following drink consumption, a second blood draw was performed (10min post-drink), participants returned to the scanner for the food cue task (20min post-drink). Blood draws were performed again at 35min and 120 min post-drink. The study ended with a food buffet (125min post-drink) (for study sessions overview see **Figure 1**).

## 24h Dietary Recall

To assess dietary intake, we used the validated multiple-pass 24h dietary recall (29, 30). A trained staff member interviewed participants on all food and beverage items consumed during the prior 24h period. Participants were asked to provide the amount of each item consumed, time of consumption, how each item was prepared, and additional details (e.g., brand name). Recall interviews typically lasted between 30-60min. Dietary recalls were performed during the screening visit and each MRI visit. Data from dietary recalls were manually checked for quality. To determine outliers, we performed a linear regression analysis, using body weight to predict caloric intake. Residuals were standardized and examined for any values that were >3 SDs from the mean (15). Using this method, 359 dietary recalls were included in this analysis (an average of 5 recalls per participant), and 5 recalls were excluded. Participant's dietary data was averaged across all available recall days.

Dietary data was analyzed using Nutrition Data Systems for Research (NDSR) software version 2015, developed by the Nutrition Coordinating Center, University of Minnesota, Minneapolis, MN, USA. The output from the software provided intake of overall calories and the breakdown of macronutrients. For the purpose of this study, we analyzed the amount of added sugar in the diet as a percent of total calories. Based on the World Health Organization's dietary recommendations,  $\geq 10\%$  added sugar was considered a high amount of added sugar and <10% was considered a low amount of added sugar based.

## Food-Cue Task

Participants completed the food-cue task in the MRI scanner by viewing stimuli through a mirror mounted over the head coil. In a randomized block design, participants were asked to watch a



**FIGURE 1** | Visualization of the study visits. \*300ml noncaloric cherry flavored drink. Either water or 75g of glucose dissolved in water. Order of drinks were counterbalanced.

total of 12 visual food cue and non-food cue blocks using Matlab (MathWorks, Inc., Natick, MA, USA) and Psychtoolbox on a 13-in, 2.5 GHz Intel Core i5 processor MacBook Pro. Four images per block were presented in random order, each appearing immediately after the last. Within a block, each image was presented for 4 s. An 8s questioning period followed each block where participants were asked to rate their hunger along with their wanting and liking for the food cues; however, these data were not included in this analysis. There were different food cue types presented: 4 high-calorie (e.g., pizza, ice cream) food image blocks, 4 low-calorie (e.g., carrots, apples) food image blocks, and 4 non-food (buses, staircase) image blocks (for a full list of visual cues see **Supplemental Table 1**). The set of food and non-food cue images was gathered from the food-pics database (31) and prior published work (15). The total running time of this task was ~6 min.

## Hormone Analysis

Blood samples were assessed for GLP-1 (7–35) (active) using Luminex multiplex technology (Millipore, Billerica, MA). Circulating insulin and glucose were also assessed as both would be expected to be altered, along with GLP-1, by acute glucose ingestion. Plasma glucose was measured enzymatically using glucose oxidase (YSI 2300 STAT PLUS Enzymatic Electrode-YSI analyzer, Yellow Springs Instruments), and plasma insulin was measured *via* Luminex multiplex technology (Millipore, Billerica, MA). Insulin and blood glucose levels were controlled for in the data analysis to examine if any observed relationships were GLP-1-dependent or due to confounding hormones. Plasma glucose and hormones were assessed at each time point (baseline/0 min and 10, 35, 120 min post-drink) and area under the curve (AUC) was calculated using the trapezoid method (32).

## MRI Imaging Parameters and Analysis

Imaging data were collected using a 3T Siemens MAGNETOM Prismafit MRI System, with a 32-channel head coil. A high-resolution 3D magnetization prepared rapid gradient echo sequence (TR=1950ms; TE=2.26ms; bandwidth=200Hz/pixel; flip angle=9°; slice thickness=1mm; FOV=224mm×256mm; matrix=224×256) was used to acquire structural images for multi-subject registration. Food cue reactivity was measured by functional BOLD signals, acquired with a multi-band interleaved gradient echo planar imaging sequence. Eighty-eight 1.5-mm thick slices covering the whole brain were acquired using the following parameters: repetition time (TR)=1,000ms, echo time (TE)=43.20ms, bandwidth=2,055Hz/pixel, flip angle=52°, field of view (FOV)=128mm×112mm, matrix=128×112.

To analyze the fMRI data, we used tools from the Oxford University Centre for Functional MRI of the Brain Software Library (FMRIB). MRI data were processed using the fMRI Expert Analysis Tool (FEAT) version 6.00. Eight functional volumes (8 TRs) acquired at the beginning of each MRI session were discarded to account for magnetic saturation effects. fMRI data were preprocessed using motion correction, high-pass filtering (100s), and spatial smoothing with a Gaussian kernel of full width at half-maximum = 5 mm. Functional data

were first mapped to each participant's anatomical image and then registered into standard space [Montreal Neurological Institute (MNI)] using affine transformation with FMRIB's Linear Image Registration Tool to the avg152 T1 MNI template. Explanatory variables were added to the general linear model after convolution with a canonical hemodynamic response function. Temporal derivatives and temporal filtering were added to increase statistical sensitivity. Motion confounds were generated using the tool "fsl\_motion\_outliers" to be used as regressors of no-interest in the general linear model. For each participant, contrast maps were created on the first-level analysis for: high-calorie food vs nonfood, low-calorie food vs nonfood, and high-calorie food vs low-calorie food images.

To specifically test the relationship between postprandial GLP-1, BMI, dietary added sugar, food consumption and the dorsal striatum food cue reactivity, we used an *a priori* ROI-based approach. An anatomical, bilateral ROI of the striatum (including caudate and putamen) was created using the Harvard-Oxford subcortical atlas with a probability threshold over 50% (**Supplemental Figure 2**). Percent signal change was extracted from the striatal ROI for contrasts for each participant using FSL's FEATquery.

Additional arterial spin labeling scans were conducted pre-drink and 5 and 26min post-drink, but this data was not analyzed in the current sub-study.

## Buffet Meal

Study sessions ended with the presentation of an ad libitum buffet meal given 125min post-drink. The buffet meal consisted of 32 pre-measured food and drink items, including high-calorie foods, such as potato chips and cookies, and lower calorie foods, such as apple slices and carrots. Total energy available from the buffet meal was 4650kcal (for a full list of foods at the buffet and the calorie content of each food cue see **Supplemental Table 2**). Caloric value per gram or fluid ounce of each item was calculated using the NDSR. Participants were given 20 minutes to eat any quantity they desired and instructed not to leave the room with any items. After the participant exited, each buffet item was re-weighed. Calorie and nutrient intake during the buffet meal were calculated using the difference between the pre-meal and post-meal weight for each buffet item.

## Statistical Analysis

All statistical tests were corrected for age and gender. Alpha levels were set at .05 for all tests, except where alpha was adjusted using Bonferroni corrections, and all confidence intervals (CI) were set at 95%. Partial  $\eta^2$  were used to calculate effect size. Statistical analyses were run using Statistica Academic 13.3.0 (Tibco).

## Relationship Between BMI, Dietary Added Sugar and GLP-1 or Striatal Food Cue Reactivity

Simple regressions were run using BMI or percent calories from added sugar as the regressor and GLP-1 AUC (pg/ml) or striatal food cue reactivity (% signal change) as the dependent variables. Factorial regressions were then run to examine interactions between BMI and dietary added sugar on striatal food cue

reactivity. The striatal food cue reactivity (measured as percent signal change) contrasts assessed were: high-calorie food vs nonfood, low-calorie food vs nonfood, and high-calorie food vs low-calorie food images. These tests were run on striatal food cue reactivity separately for water and glucose days. Findings were controlled for age and gender.

### Correlations Between GLP-1 and Striatal Food Cue Reactivity

Multiple regression analyses were run using GLP-1 AUC on water or glucose days as the primary regressor, and BMI, percent calories from added sugar, age, and gender as co-variate regressors and striatal food cue reactivity (following water or glucose) as the dependent variable. Findings were further corrected for potentially confounding hormones that are also altered by glucose consumption (plasma insulin and circulating glucose AUC) and differences in insulin sensitivity [calculated as the Matsuda Index (33)]. All striatal contrasts listed above were tested.

### Striatal Food Cue Reactivity and Consumption at a Buffet

Paired t-tests were run to assess if differences in buffet consumption on water and glucose days. Simple regressions were run using BMI or percent calories from added sugar as the regressor and consumption at a food buffet at the dependent variables. Buffet consumption measures that were tested included total calories consumed and calories consumed of macronutrients (sugar, fat, protein, total carbohydrates). Factorial regressions were also run to test for an interaction between BMI and dietary added sugar on food consumption. To assess the role of circulating GLP-1 and striatal food cue reactivity multiple regressions were used. Striatal food cue reactivity contrasts found to significantly correlate with plasma GLP-1 following glucose consumption, GLP-1 AUC, BMI, percent calories from added sugar, age, and gender were co-variate regressors and consumption measures as the dependent variable.

## RESULTS

### Participants

Mean Age ( $23.22 \pm 3.73$  years), Body mass index (BMI) ( $27.33 \pm 5.13$  kg/m<sup>2</sup>), and Consumption of Dietary Added Sugar ( $9.31 \pm 4.47\%$ )

**TABLE 1** | Characteristics for all participants (N=72).

CHARACTERISTIC	Mean $\pm$ SD
SEX	Male: n=32 Female: n=40
AGE (YEARS)	$23.22 \pm 3.73$
BMI (KG/M <sup>2</sup> )	$27.33 \pm 5.13$
LEAN (>18.5 AND <24.9)	n=25; $22.13 \pm 1.67$
OVERWEIGHT (>25.0 AND <29.9)	n=25; $26.93 \pm 1.28$
OBESE (>30.0)	n=22; $33.68 \pm 3.05$
PERCENT CALORIES FROM ADDED SUGAR	$9.31 \pm 4.47$
LOW (<10%)	n=42; $6.59 \pm 2.38$
HIGH ( $\geq 10\%$ )	n=30; $13.16 \pm 3.88$

for the overall cohort of 72 (32 males, 40 females) participants are described in **Table 1**. Independent samples t-tests found no significant differences in age, BMI, or percent calories from added sugar in the participants that completed all measurements (food cue task on the glucose and water days and hormone on glucose and water days) and the participants that either did not completed all assays or were removed from data analysis for confound, like motion. For detailed t-test findings and descriptive statistics stratified by BMI and Added Sugar see **Supplemental Results**.

### GLP-1 Following Drink

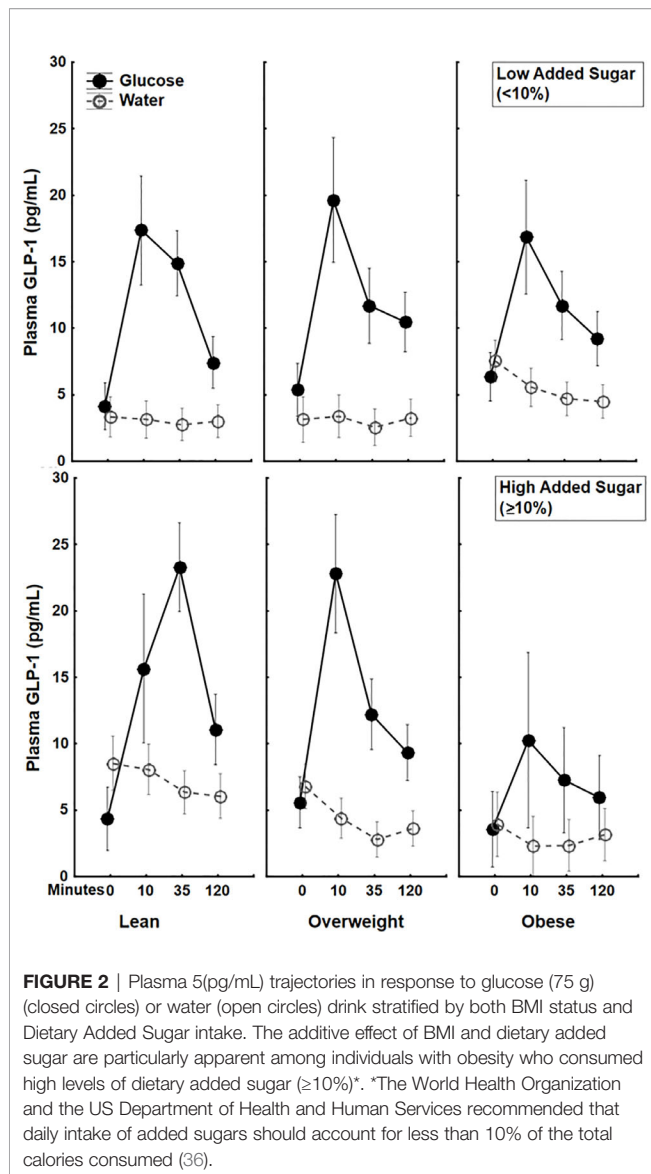
Across all participants, paired t-tests showed that circulating GLP-1 levels significantly increased 10 min ( $t(65)=6.26$ , 95%CI [8.01, 15.5],  $p<.001$ ), 35 ( $t(65)=6.55$ , 95%CI: [5.71, 10.72],  $p<.001$ ), and 120 min ( $t(65)=4.72$ , CI [2.57, 6.34],  $p<.001$ ) post-glucose drink relative to pre-drink. Conversely, GLP-1 levels significantly decreased 10 min ( $t(61)=-2.69$ , 95%CI [-1.8, -.26],  $p<.01$ ), 35 ( $t(61)=-3.98$ , 95%CI [-2.8, -.93],  $p<.001$ ), and 120 min ( $t(61)=-2.69$ , 95%CI [-2.51, -.37],  $p<.01$ ) post-water drink relative to pre-drink. T-tests also revealed that GLP-1 AUC was significantly greater following a glucose versus water drink ( $t(58)=9.65$ , 95%CI [1179.9, 774.414],  $p<.001$ ).

### Relationship Between BMI and Dietary Added Sugar on Circulating GLP-1

Simple regressions showed a trend towards a negative correlation between BMI and circulating GLP-1 (AUC) ( $\beta=-.21$ ,  $p=.08$ ), but no significant correlation between percent calories from added sugar and circulating GLP-1 (AUC) ( $\beta=.09$ ,  $p=.49$ ) following a glucose drink. Interestingly, a factorial ANOVA examining the interaction between BMI and dietary added sugar showed a significant BMI  $\times$  percent calories from added sugar interaction ( $\beta=-1.87 \pm .85$ , 95% CI [-3.56, -.18],  $p<.05$ , partial  $\eta^2=.07$ ) on circulating GLP-1 (AUC) following the oral glucose load. The increase in GLP-1 secretion following glucose was markedly lower among participants with both high BMI and high percent calories from added sugar in their diet (see **Figure 2**). There were no significant correlations between BMI ( $p=.41$ ) or percent calories from added sugar ( $p=.8$ ) as well as no significant interaction between BMI and percent calories from added sugar on circulating GLP-1 following water ingestion ( $p=.76$ ) (**Figure 2**). These findings are the first to illustrate that the interaction between BMI and percent calories from added sugar is associated with decreased GLP-1 secretion following glucose ingestion. The interaction of BMI and dietary added sugar on GLP-1 secretion demonstrated that individuals with obesity who consumed higher levels of dietary added sugar had the lowest postprandial GLP-1 response.

### Associations Between BMI and Dietary Added Sugar on Striatal Food Cue Reactivity Following Glucose or Water

Simple regressions showed no correlations between BMI (all  $p>.15$ ) or percent calories from added sugar (all  $p>.1$ ) and striatal food cue reactivity following glucose or water consumption. Additionally, a factorial regression examining the interaction



between BMI and percent calories from added sugar yielded no significant correlations between the interaction term and striatal food cue reactivity to any food cue type following glucose or water (all  $p > .2$ ).

### GLP-1 and Striatal Food Cue Reactivity

To examine if circulating GLP-1 is related to food cue processing, we ran a multiple regression with GLP-1, BMI, and percent calories from added sugar as regressors and striatal food cue reactivity following either water or glucose as the dependent variable. We found that GLP-1 secretion following glucose, but not BMI or Percent Calories from Added Sugar, was positively correlated with striatal food cue reactivity to low-calorie food cues vs non-food cues ( $\beta = .4 \pm .12$ , 95%CI [.15, .64],  $p < .01$ , partial  $\eta^2 = .15$ ) (Figure 3A) and negatively correlated with striatal food cue reactivity to high-calorie relative to low-calorie food cues ( $\beta = -.37 \pm .13$ , 95%CI [-.62, -.11],

$p < .01$ , partial  $\eta^2 = .13$ ) (Figure 3B). These results were adjusted for age and gender, which also did not have significant correlations with striatal food cue reactivity. There were no correlations between GLP-1, BMI and/or percent calories from added sugar and striatal food cue reactivity after water consumption. The positive correlation between GLP-1 and dorsal striatal responding to low calorie food cues relative to nonfood cues ( $\beta = .49 \pm .14$ , 95%CI [.15, .68],  $p < .01$ , partial  $\eta^2 = .15$ ) and the negative correlation between GLP-1 and dorsal striatal responding to high calorie food cues relative to low calorie food cues ( $\beta = -.40 \pm .14$ , 95%CI [-.67, -.11],  $p < .01$ , partial  $\eta^2 = .13$ ) remained significant after further adjusting for changes in circulating insulin and glucose levels in response to glucose ingestion and further adjusting for insulin sensitivity. Additionally, these findings remained significant after adjusting the alpha level using Bonferroni corrections to account for repeated measures ( $\alpha = .016$ ). Taken together, the data suggest that following glucose consumption, increases in circulating GLP-1 are associated with an increased preferential response to low- vs high-calorie foods driven by increased reactivity to low-calorie food cues.

### Consummatory Behaviors

Overall caloric consumption at the buffet was greater on water relative to glucose days ( $t(68) = 3.94$ , 95%CI [63.61, 194.01],  $p < .001$ ), and consumption of all macronutrients was greater on water vs. glucose days (all  $p < .05$ ).

BMI and percent calories from added sugar were not independently correlated with any food consumption measures on water or glucose days (all  $ps > .2$ ), and there was no interaction between BMI and percent calories from added sugar on food consumption at the buffet on water or glucose days (all  $ps > .3$ ).

Using multiple regression analyses, striatal food cue reactivity to low-calorie food cues (vs. non-food cues) was negatively correlated with sugar (kcal) consumed at the food buffet following a glucose drink, even when adjusting for age, gender, BMI, percent calories from added sugar, and postprandial GLP-1 ( $\beta = -.32 \pm .14$ , 95%CI [-.59, -.05],  $p < .05$ , partial  $\eta^2 = .09$ ) (Figure 4). There were no significant relationships between BMI, percent calories from added sugar, post-prandial GLP-1 levels, or interactions between these variables with consumption of sugar at the buffet, indicating that changes in striatal food cue reactivity, rather than body weight, dietary added sugars, or circulating GLP-1, may be driving the changes in consummatory behaviors. There were no correlations between striatal food cue reactivity to low-calorie food cues and total carbohydrates, fat, protein, or total calories consumed. There were also no correlations between striatal reactivity to high vs low calorie food cues, GLP-1, BMI, or percent calories from added sugar and total caloric intake at the buffet after glucose consumption. There were also no correlations between striatal food cue reactivity, GLP-1, BMI, percent calories from added sugar, and food consumption at the buffet after consumption of water (control). These findings suggest a potential shift of striatal food cue reactivity from high-calories food cues to low-calorie food cues after glucose consumption and this shift is related to a reduction in ad-libitum sugar intake.

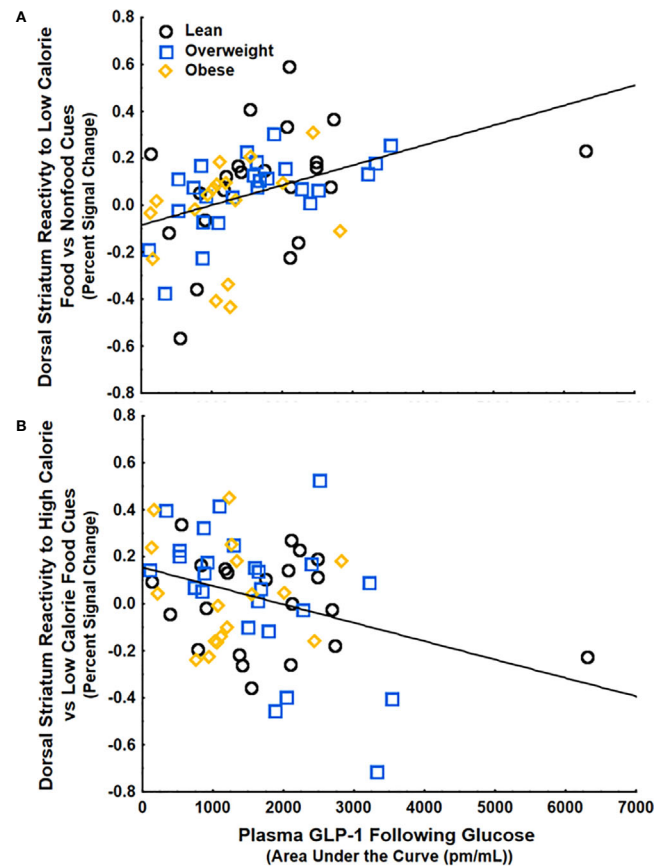


**FIGURE 3** | GLP-1 secretion following glucose ingestion was (A) positively correlated with striatal food cue reactivity to low-calorie food vs nonfood cues ( $p < .01$ ) and (B) negatively correlated with striatal food cue reactivity to high-calorie relative to low-calorie food cues ( $p < .05$ ). These findings were controlled for BMI, percent calories from added sugar, age, and gender.

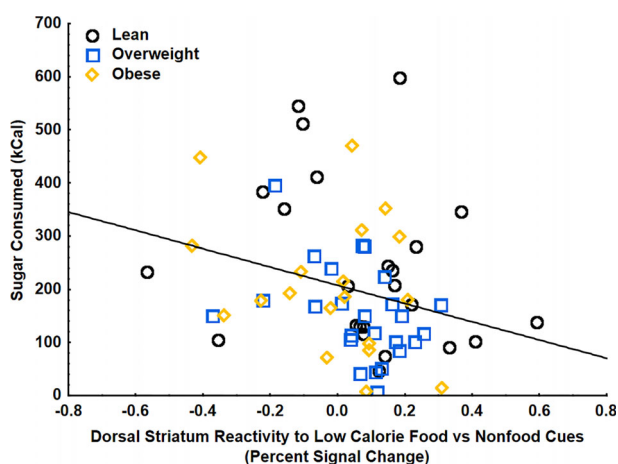


**FIGURE 4** | Striatal food cue reactivity to low-calorie food vs nonfood cues was negatively correlated with sugar (kcal) consumed at the food buffet on the glucose day ( $p < .05$ ). These findings were controlled for age, gender, BMI, percent calories from added sugar, and glucose-induced increases in GLP-1.

## DISCUSSION

The current paper supports a potential indirect pathway by which GLP-1 regulates appetitive behaviors through its impacts on dorsal striatal food cue reactivity. Furthermore, the present findings help to describe how the interaction between BMI and dietary added sugars may be associated with disruptions in this mechanism. To our knowledge this is the first study to illustrate that an interaction between BMI and dietary added sugar intake is associated with altered postprandial GLP-1 secretion. Post-glucose circulating GLP-1 levels were positively correlated with dorsal striatal food cue reactivity to low-calorie food vs nonfood cues and negatively correlated with dorsal striatal food cue reactivity to high-calorie vs low-calorie food cues, independent of BMI and dietary added sugar. The relationship between glucose-induced GLP-1 secretion and dorsal striatum food cue reactivity suggests that increases in plasma GLP-1 following glucose consumption may shift dorsal striatum food cue reactivity from high-calorie food cues toward low-calorie food cues. This potential shift, represented by the increase in dorsal striatal response to low-calorie food cues, was associated with a decrease in sugar intake at the buffet meal. These results suggest that postprandial increases in GLP-1 may play an

indirect role in regulating eating behaviors through preferential striatal responsivity to low-calorie (healthier) foods. How these findings relate to signaling between other brain regions and networks involved in appetite regulation remains to be elucidated. Future studies should assess how the current findings may be related to other food cue reactivity alterations in other appetite processing regions of the brain.

Taken together, the current study suggests a potential GLP-1 and dorsal striatal mechanism for how dietary added sugar may affect eating behavior in individuals with overweight and obesity, but the correlational nature of these findings prevents the conclusion of directionality. While the present experiment cannot rule out other confounding factors that may be associated with glucose ingestion, the observed association between increases in circulating GLP-1 and dorsal striatal activation to low-calorie food cues was independent of postprandial increases in plasma glucose or insulin levels or insulin sensitivity. However, to address the directionality question and rule out third variable effects, an experimental design assessing the effect of GLP-1 administration or a GLP-1 antagonist on food cue reactivity and eating behavior is necessary.

GLP-1 analogues have been found to be associated with weight loss in clinical populations with obesity and overweight with or without diabetes (34, 35, 37), but individual effectiveness of these weight loss therapies is highly variable. These findings could suggest that GLP-1 analogues, such as liraglutide and exendin-4, may be especially successful weight loss therapies in individuals more likely to exhibit decreases in GLP-1 secretion (e.g., people with obesity and those who habitually consume high levels of dietary added sugar), but this prediction requires further investigation with randomized controlled studies. Identifying at risk populations may help inform individualized treatment strategies and improve the success rate of weight loss and weight loss maintenance interventions.

## DATA AVAILABILITY STATEMENT

Imaging data is available at Open Source Framework (OSF) <https://osf.io/E7B9F/>. Additional data generated and analyzed during the current study are available from the corresponding author (KP), on reasonable request. Further inquiries can be directed to the corresponding author.

## ETHICS STATEMENT

The studies involving human participants were reviewed and approved by # HS-09-00395-CR011 was approved by the University of Southern California Institutional Review Board.

## REFERENCES

1. Hales CM, Fryar CD, Carroll MD, Freedman DS, Ogden CL. Trends in Obesity and Severe Obesity Prevalence in US Youth and Adults by Sex and Age, 2007-2016 to 2015-2016. *JAMA* (2018) 319:1723. doi: 10.1001/jama.2018.3060
2. Kauth TH, Metz J. Immunohistochemical localization of glucagon-like peptide 1. *Histochemistry* (1987) 86:509-15. doi: 10.1007/BF00500625

The patients/participants provided their written informed consent to participate in this study.

## AUTHOR CONTRIBUTIONS

SJ, SL, HD, JM, and KP were responsible for conceptualization of the study. SJ and BA contributed to methodology and formal analysis. HD, AY, BA, and AD were responsible for management and coordination of the study execution. KP was responsible for supervision of the research activities. SJ and KP wrote the original draft. SJ, SL, AY, JM, and KP provided critical review, commentary, and revisions to the manuscript. KP provided funding for this study. All authors contributed to the article and approved the submitted version.

## FUNDING

This work was supported by the National Institutes of Health (NIH) National Institute of Diabetes and Digestive and Kidney Diseases R01DK102794 (PI: KP). A Research Electronic Data Capture, REDCap, database was used for this study, which is supported by the Southern California Clinical and Translational Science Institute (SC CTSI) through NIH UL1TR001855. American Heart Association 14BGIA18720032 (PI: KP).

## ACKNOWLEDGMENTS

The authors would like to thank the volunteers who participated in this study. The authors would also like to thank Ana Romero, Enrique Trigo, Lloyd Nate Overholtzer, Jada Hislop, Martina Erdstein, Esther Jahng, Priyanka Dave, and Brandon Ge for assisting with study visits and recruiting volunteers, and the staff at the Dornsife Cognitive Neuroimaging Center and Diabetes and Obesity Research Institute of the University of Southern California.

## SUPPLEMENTARY MATERIAL

The Supplementary Material for this article can be found online at: <https://www.frontiersin.org/articles/10.3389/fendo.2021.638504/full#supplementary-material>

3. Trapp S, Richards JE. The gut hormone glucagon-like peptide-1 produced in brain: is this physiologically relevant? *Curr Opin Pharmacol* (2013) 13:964-9. doi: 10.1016/j.coph.2013.09.006
4. Kreyman B, Ghatei MA, Williams G, Bloom SR. GLUCAGON-LIKE PEPTIDE-1 7-36: A PHYSIOLOGICAL INCRETIN IN MAN. *Lancet* (1987) 330:1300-4. doi: 10.1016/S0140-6736(87)91194-9
5. Mojsov S, Weir GC, Habener JF. Insulinotropin: glucagon-like peptide I (7-37) co-encoded in the glucagon gene is a potent stimulator of insulin release

- in the perfused rat pancreas. *J Clin Invest* (1987) 79:616–9. doi: 10.1172/JCI112855
6. Hayes MR, Schmidt HD. GLP-1 influences food and drug reward. *Curr Opin Behav Sci* (2016) 9:66–70. doi: 10.1016/j.cobeha.2016.02.005
  7. Richard JE, Anderberg RH, Göteson A, Gribble FM, Reimann F, Skibicka KP. Activation of the GLP-1 Receptors in the Nucleus of the Solitary Tract Reduces Food Reward Behavior and Targets the Mesolimbic System. *PloS One* (2015) 10:e0119034. doi: 10.1371/journal.pone.0119034
  8. Wang X-F, Liu J-J, Xia J, Liu J, Mirabella V, Pang ZP. Endogenous Glucagon-like Peptide-1 Suppresses High-Fat Food Intake by Reducing Synaptic Drive onto Mesolimbic Dopamine Neurons. *Cell Rep* (2015) 12:726–33. doi: 10.1016/j.celrep.2015.06.062
  9. Zanchi D, Depoorter A, Egloff L, Haller S, Mählmann L, Lang UE, et al. The impact of gut hormones on the neural circuit of appetite and satiety: A systematic review. *Neurosci Biobehav Rev* (2017) 80:457–75. doi: 10.1016/j.neubiorev.2017.06.013
  10. Sørensen G, Reddy IA, Weikop P, Graham DL, Stanwood GD, Wortwein G, et al. The glucagon-like peptide 1 (GLP-1) receptor agonist exendin-4 reduces cocaine self-administration in mice. *Physiol Behav* (2015) 149:262–8. doi: 10.1016/j.physbeh.2015.06.013
  11. De Silva A, Salem V, Long CJ, Makwana A, Newbould RD, Rabiner EA, et al. The gut hormones PYY 3–36 and GLP-1 7–36 amide reduce food intake and modulate brain activity in appetite centers in humans. *Cell Metab* (2011) 14:700–6. doi: 10.1016/j.cmet.2011.09.010
  12. van Bloemendaal L, IJzerman RG, ten Kulve JS, Barkhof F, Konrad RJ, Drent ML, et al. GLP-1 Receptor Activation Modulates Appetite- and Reward-Related Brain Areas in Humans. *Diabetes* (2014) 63:4186–96. doi: 10.2337/db14-0849
  13. Heni M, Kullmann S, Ketterer C, Guthoff M, Bayer M, Staiger H, et al. Differential effect of glucose ingestion on the neural processing of food stimuli in lean and overweight adults. *Hum Brain Mapp* (2014) 35:918–28. doi: 10.1002/hbm.22223
  14. Maurer L, Mai K, Krude H, Haynes J-D, Weygandt M, Spranger J. Interaction of circulating GLP-1 and the response of the dorsolateral prefrontal cortex to food-cues predicts body weight development. *Mol Metab* (2019) 29:136–44. doi: 10.1016/j.molmet.2019.08.014
  15. Dorton HM, Luo S, Monterosso JR, Page KA. Influences of Dietary Added Sugar Consumption on Striatal Food-Cue Reactivity and Postprandial GLP-1 Response. *Front Psychiatry* (2018) 8:297. doi: 10.3389/fpsy.2017.00297
  16. Carr RD, Larsen MO, Jelic K, Lindgren O, Vikman J, Holst JJ, et al. Secretion and Dipeptidyl Peptidase-4-Mediated Metabolism of Incretin Hormones after a Mixed Meal or Glucose Ingestion in Obese Compared to Lean, Nondiabetic Men. *J Clin Endocrinol Metab* (2010) 95:872–8. doi: 10.1210/jc.2009-2054
  17. Færch K, Torekov SS, Vistisen D, Johansen NB, Witte DR, Jonsson A, et al. GLP-1 Response to Oral Glucose Is Reduced in Prediabetes, Screen-Detected Type 2 Diabetes, and Obesity and Influenced by Sex: The ADDITION-PRO Study. *Diabetes* (2015) 64:2513–25. doi: 10.2337/db14-1751
  18. Galderisi A, Giannini C, Van Name M, Caprio S. Fructose consumption contributes to hyperinsulinemia in obese adolescents through a GLP-1 mediated mechanism. *J Clin Endocrinol Metab* (2019) 104(8):3481–90. doi: 10.1210/jc.2019-00161
  19. Ranganath LR, Beety JM, Morgan LM, Wright JW, Howland R, Marks V. Attenuated GLP-1 secretion in obesity: cause or consequence? *Gut* (1996) 38:916–9. doi: 10.1136/gut.38.6.916
  20. Contreras-Rodríguez O, Martín-Pérez C, Vilar-López R, Verdejo-García A. Ventral and Dorsal Striatum Networks in Obesity: Link to Food Craving and Weight Gain. *Biol Psychiatry* (2017) 81:789–96. doi: 10.1016/j.biopsych.2015.11.020
  21. Rothmund Y, Preuschhof C, Bohnert G, Bauknecht H-C, Klingebiel R, Flor H, et al. Differential activation of the dorsal striatum by high-calorie visual food stimuli in obese individuals. *NeuroImage* (2007) 37:410–21. doi: 10.1016/j.neuroimage.2007.05.008
  22. Stice E, Yokum S, Blum K, Bohon C. Weight gain is associated with reduced striatal response to palatable food. *J Neurosci* (2010) 30:13105–9. doi: 10.1523/JNEUROSCI.2105-10.2010
  23. Stoeckel LE, Weller RE, Cook EWII, Twieg DB, Knowlton RC, Cox JE. Widespread reward-system activation in obese women in response to pictures of high-calorie foods. *Neuroimage* (2008) 41:636–47. doi: 10.1016/j.neuroimage.2008.02.031
  24. Bray GA, Popkin BM. Dietary Sugar and Body Weight: Have We Reached a Crisis in the Epidemic of Obesity and Diabetes?: Health Be Damned! Pour on the Sugar. *Diabetes Care* (2014) 37:950–6. doi: 10.2337/dc13-2085
  25. Malik VS, Willett WC, Hu FB. Sugar-sweetened beverages and BMI in children and adolescents: reanalyses of a meta-analysis. *Am J Clin Nutr* (2009) 89:438–9. doi: 10.3945/ajcn.2008.26980
  26. Fletcher PC, Napolitano A, Skeggs A, Miller SR, Delafont B, Cambridge VC, et al. Distinct Modulatory Effects of Satiety and Sibutramine on Brain Responses to Food Images in Humans: A Double Dissociation across Hypothalamus, Amygdala, and Ventral Striatum. *J Neurosci* (2010) 30:14346–55. doi: 10.1523/JNEUROSCI.3323-10.2010
  27. Dye L, Blundell JE. Menstrual cycle and appetite control: implications for weight regulation. *Hum Reprod* (1997) 12:1142–51. doi: 10.1093/humrep/12.6.1142
  28. Krishnan S, Tryon RR, Horn WF, Welch L, Keim NL. Estradiol, SHBG and leptin interplay with food craving and intake across the menstrual cycle. *Physiol Behav* (2016) 165:304–12. doi: 10.1016/j.physbeh.2016.08.010
  29. Biro B, Hulshof KFAM, Ovesen L, Cruz JA. Selection of methodology to assess food intake. *Eur J Clin Nutr* (2002) 56:S25. doi: 10.1038/sj.ejcn.1601426
  30. Johnson RK, Driscoll P, Goran MI. Comparison of Multiple-Pass 24-Hour Recall Estimates of Energy Intake With Total Energy Expenditure Determined By the Doubly Labeled Water Method in Young Children. *J Am Dietetic Assoc* (1996) 96:1140–4. doi: 10.1016/S0002-8223(96)00293-3
  31. Blechert J, Meule A, Busch NA, Ohla K. Food-pics: An image database for experimental research on eating and appetite. *Front Psychol* (2014) 5:617. doi: 10.3389/fpsyg.2014.00617
  32. Tai MM. A mathematical model for the determination of total area under glucose tolerance and other metabolic curves. *Diabetes Care* (1994) 17:152–4. doi: 10.2337/diacare.17.2.152
  33. DeFronzo RA, Matsuda M. Reduced Time Points to Calculate the Composite Index. *Diabetes Care* (2010) 33:e93–3. doi: 10.2337/dc10-0646
  34. Potts JE, Gray LJ, Brady EM, Khunti K, Davies MJ, Bodicoat DH. The Effect of Glucagon-Like Peptide 1 Receptor Agonists on Weight Loss in Type 2 Diabetes: A Systematic Review and Mixed Treatment Comparison Meta-Analysis. *PloS One* (2015) 10:e0126769. doi: 10.1371/journal.pone.0126769
  35. Vilsboll T, Christensen M, Junker AE, Knop FK, Gluud LL. Effects of glucagon-like peptide-1 receptor agonists on weight loss: systematic review and meta-analyses of randomised controlled trials. *BMJ* (2012) 344:d7771–1. doi: 10.1136/bmj.d7771
  36. McGuire S. US department of agriculture and US department of health and human services, dietary guidelines for Americans, 2010.7th Edition, Washington, DC: U.S. Government Printing Office, January 2011. *Adv Nutr* (2011) 2:293–4. doi: 10.3945/an.111.000430
  37. on behalf of the NN8022-1807 Investigators, Astrup A, Carraro R, Finer N, Harper A, Kunesova M, et al. Safety, tolerability and sustained weight loss over 2 years with the once-daily human GLP-1 analog, liraglutide. *Int J Obes* (2012) 36:843–54. doi: 10.1038/ijo.2011.158

**Conflict of Interest:** The authors declare that the research was conducted in the absence of any commercial or financial relationships that could be construed as a potential conflict of interest.

Copyright © 2021 Jones, Luo, Dorton, Yunker, Angelo, Defendis, Monterosso and Page. This is an open-access article distributed under the terms of the Creative Commons Attribution License (CC BY). The use, distribution or reproduction in other forums is permitted, provided the original author(s) and the copyright owner(s) are credited and that the original publication in this journal is cited, in accordance with accepted academic practice. No use, distribution or reproduction is permitted which does not comply with these terms.



# Vildagliptin Has a Neutral Association With Dementia Risk in Type 2 Diabetes Patients

Chin-Hsiao Tseng<sup>1,2,3\*</sup>

<sup>1</sup> Department of Internal Medicine, National Taiwan University College of Medicine, Taipei, Taiwan, <sup>2</sup> Division of Endocrinology and Metabolism, Department of Internal Medicine, National Taiwan University Hospital, Taipei, Taiwan, <sup>3</sup> Division of Environmental Health and Occupational Medicine of the National Health Research Institutes, Zhunan, Taiwan

## OPEN ACCESS

### Edited by:

Szu-Tah Chen,  
Linkou Chang Gung Memorial  
Hospital, Taiwan

### Reviewed by:

Jung Lung Hsu,  
Chang Gung University, Taiwan  
Horng-Yih Ou,  
National Cheng Kung University  
Hospital, Taiwan

### \*Correspondence:

Chin-Hsiao Tseng  
ccktsh@ms6.hinet.net

### Specialty section:

This article was submitted to  
Clinical Diabetes,  
a section of the journal  
Frontiers in Endocrinology

Received: 04 December 2020

Accepted: 12 April 2021

Published: 30 April 2021

### Citation:

Tseng C-H (2021) Vildagliptin Has a  
Neutral Association With Dementia  
Risk in Type 2 Diabetes Patients.  
Front. Endocrinol. 12:637392.  
doi: 10.3389/fendo.2021.637392

**Background and aims:** Animal studies suggested that vildagliptin might exert a beneficial effect on cognitive function. The present study evaluated whether the use of vildagliptin in patients with type 2 diabetes mellitus might affect dementia risk.

**Methods:** The database of Taiwan's National Health Insurance was used to enroll an unmatched cohort and a propensity score-matched-pair cohort of ever and never users of vildagliptin from patients with newly diagnosed diabetes mellitus during 2002-2014. The patients should be alive on January 1, 2015 and were followed up for dementia diagnosis until December 31, 2016. Unadjusted and multivariate-adjusted hazard ratios (HR) and their 95% confidence intervals (CI) were estimated for vildagliptin ever *versus* never users, for cumulative duration and cumulative dose of vildagliptin therapy categorized into tertiles *versus* never users, and for cumulative duration and cumulative dose treated as continuous variables.

**Results:** There were 355610 never users and 43196 ever users in the unmatched cohort and 40489 never users and 40489 ever users in the matched cohort. In the unmatched cohort, unadjusted HR (95% CI) was 0.929 (0.683-1.264) and the multivariate-adjusted HR (95% CI) was 0.922 (0.620-1.372). In the matched cohort, the unadjusted HR (95% CI) was 0.930 (0.616-1.402) and the multivariate-adjusted HR (95% CI) was 0.825 (0.498-1.367). None of the analyses conducted for cumulative duration and cumulative dose was significant, either being treated as tertile cutoffs or as continuous variables, in either the unmatched cohort or the matched cohort.

**Conclusions:** This study showed a neutral effect of vildagliptin on dementia risk.

**Keywords:** vildagliptin, dementia, diabetes mellitus, pharmacoepidemiology, Taiwan

## INTRODUCTION

Both diabetes and dementia affect hundreds of millions of the world population. The International Diabetes Federation estimates that 463 million people or 1 in every 11 adults aged 20 to 79 years have diabetes mellitus over the world (1). On the other hand, the World Health Organization estimates that around 50 million people are suffering from dementia over the world and every year

there are nearly 10 million new cases of dementia (2). Diabetes mellitus and dementia are closely linked and diabetes patients may have a significantly higher risk of dementia. According to a meta-analysis that included 20 studies, diabetes mellitus is associated with an approximately 70% higher risk of all types of dementia (3). Studies conducted in Taiwan using the reimbursement database of the National Health Insurance (NHI) showed a similarly increased risk of dementia of 50% (4) to 60% (5) in the diabetes patients. Dementia can be resulted from either a vascular etiology or a neurodegenerative disease known as Alzheimer's disease (which contributes to 60-70% of the cases of dementia) (2). The two disease entities may share common pathophysiological changes of impaired insulin expression and insulin resistance, leading to the coining of "type 3 diabetes" for Alzheimer's disease (6). The higher risk of dementia in diabetes patients may also be explained by vascular and metabolic changes associated with hyperglycemia and diabetes-related comorbidities, including atherosclerosis, increased deposition of advanced glycation end-products, dysregulation of lipid metabolism, and augmented status of inflammation and oxidative stress (6, 7).

Dipeptidyl peptidase-4 (DPP4) inhibitors are commonly used oral antidiabetic drugs that stimulate insulin secretion by prolonging the half-life of glucagon like peptide-1 and glucose dependent insulinotropic polypeptide (8). Vildagliptin is one of the drugs in the class of DPP4 inhibitors. Previous *in vitro* and animal studies suggested that vildagliptin might improve cognitive dysfunction, exert neuroprotective effect and prevent the development of Alzheimer's disease or dementia (9–17). A recent animal study from China suggested that vildagliptin might alleviate cognitive deficits of spatial learning and memory by using the Morris water maze in streptozotocin-induced diabetes in male Wistar rats (18). Such a beneficial effect might be exerted through reducing the levels of apoptosis-related proteins in the hippocampus, probably *via* reversing diabetes-induced decrease in the phosphorylated (p)-protein kinase B (Akt) and p-glycogen synthase kinase  $\beta$  (18). However, whether this neuroprotective effect observed in *in vitro* and animal studies could be applied to millions of patients with type 2 diabetes mellitus who had been treated with vildagliptin has not been answered. The purpose of the present study was to compare the dementia risk in patients with type 2 diabetes mellitus who had been treated with vildagliptin to those who had never been treated with vildagliptin by using the reimbursement database of the Taiwan's NHI.

## MATERIALS AND METHODS

This is a retrospective cohort study that used the longitudinal reimbursement database of Taiwan's NHI, which has been implemented since March 1995. The NHI is a unique and compulsive healthcare system covering >99.9% of Taiwan's population. The Bureau of NHI signed contracts with all in-hospitals and 93% of all medical settings throughout Taiwan.

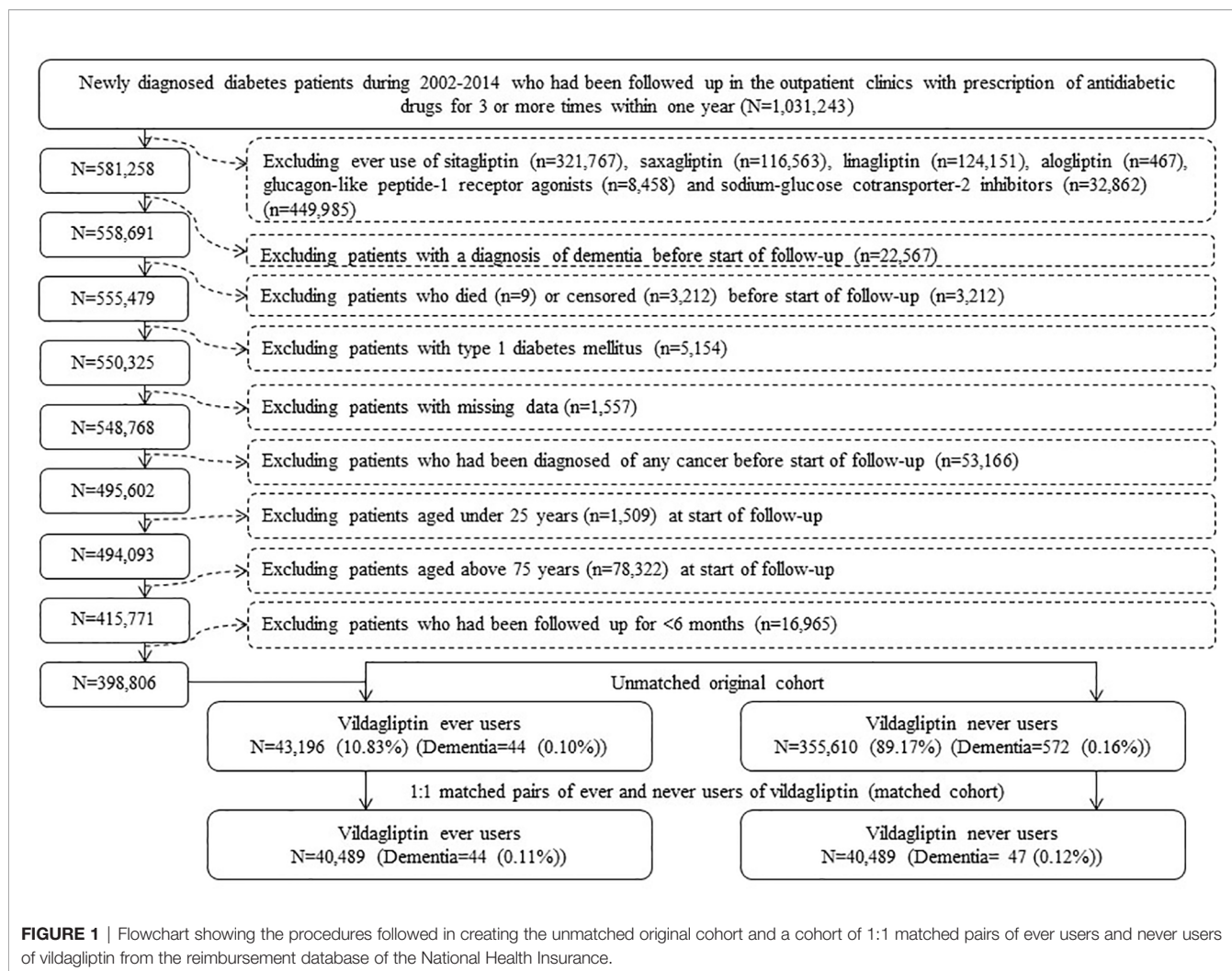
The database is managed by the Ministry of Health and Welfare and keeps all records of disease diagnoses, medication

prescriptions and performed procedures. It can be used for academic research after ethics review and the study was approved by the Research Ethics Committee C of the National Taiwan University Hospital (NTUH-REC No. 201805002WC). On-site analyses were conducted at the Health and Welfare Data Center of the Ministry. Informed consent was not required according to local regulations because the database had been de-identified before release for analyses for the protection of privacy.

Throughout the study period, diabetes mellitus was coded 250.XX according to the International Classification of Diseases, Ninth Revision, Clinical Modification (ICD-9-CM) and dementia was coded as abridged codes of A210 or A222, or as ICD-9-CM codes of 290.0, 290.1, 290.2, 290.4, 294.1, 331.0–331.2, or 331.7–331.9.

The procedures used to create an unmatched cohort and a cohort of 1:1 matched pairs of ever and never users of vildagliptin are shown in **Figure 1**. At first, 1,031,243 patients who had newly diagnosed diabetes mellitus during 2002–2014 and had been prescribed antidiabetic drugs for 3 or more times within one year were identified from the outpatient clinics. Patients who had a diagnosis of diabetes mellitus in 2001 or before were excluded to ensure a new diagnosis after 2002. The following patients were then excluded: 1) 449,985 patients who had ever used other incretin-based therapies [including sitagliptin ( $n = 321,767$ ), saxagliptin ( $n = 116,563$ ), linagliptin ( $n = 124,151$ ), alogliptin ( $n = 467$ ) and glucagon like peptide-1 receptor agonists ( $n = 8,458$ )] and/or sodium-glucose cotransporter-2 inhibitors ( $n = 32,862$ ); 2) 22,567 patients with a diagnosis of dementia before start of follow-up; 3) 3,212 patients who died ( $n = 9$ ) or censored ( $n = 3,212$ ) before start of follow-up; 4) 5,154 patients with type 1 diabetes mellitus; 5) 1,557 patients with missing data; 6) 53,166 patients who had been diagnosed of any cancer before start of follow-up (cancer patients were excluded because they might have shortened lifespan and might have distorted follow-up time, and dementia could be misdiagnosed from the clinical presentations of malignancy); 7) 1,509 patients aged <25 years at start of follow-up; 8) 78,322 patients aged >75 years at start of follow-up [the life expectancy of the Taiwan population at the beginning of the study in the year 2000 was approximately 75 years (19), therefore inclusion of older patients might tend to suffer from "healthy survivor" bias (20)]; and 9) 16,965 patients with a follow-up duration <6 months. As a result, 43,196 ever users and 355,610 never users of vildagliptin were identified (unmatched original cohort). A cohort of 1:1 matched pairs of 40,489 ever users and 40,489 never users (the matched cohort) was created by matching on propensity score based on the Greedy 8→1 digit match algorithm (21). Logistic regression was used to create the propensity score from all characteristics listed in **Table 1**.

Cumulative duration (in months) and cumulative dose (in mg) of vildagliptin therapy were calculated from the database. Potential confounders included the following categories: basic data, major comorbidities associated with diabetes mellitus, diabetes-related complications, major risk factors of dementia, potential risk factors of cancer, antidiabetic drugs and medications commonly used in diabetes patients. Basic data



included age, diabetes duration, sex, occupation and living region (classified as Taipei, Northern, Central, Southern, and Kao-Ping/Eastern). Occupation was classified as class I (civil servants, teachers, employees of governmental or private businesses, professionals and technicians), class II (people without a specific employer, self-employed people or seamen), class III (farmers or fishermen) and class IV (low-income families supported by social welfare, or veterans). Major comorbidities associated with diabetes mellitus included hypertension (ICD-9-CM 401-405), dyslipidemia (272.0-272.4) and obesity (278). Major diabetes-related complications included nephropathy (580-589), eye diseases (250.5: diabetes with ophthalmic manifestations, 362.0: diabetic retinopathy, 369: blindness and low vision, 366.41: diabetic cataract, and 365.44: glaucoma associated with systemic syndromes), stroke (430-438), ischemic heart disease (410-414) and peripheral arterial disease (250.7, 785.4, 443.81 and 440-448). Potential risk factors of dementia included head injury (959.01), Parkinson's disease (332), hypoglycemia (251.0, 251.1 and 251.2), encephalitis and/or meningoencephalitis (323, 062, 063, 064 and 054.3),

osteoporosis (733.00), muscular wasting (728.2) and accidental falls (E880-E888). Potential risk factors of cancer included chronic obstructive pulmonary disease (a surrogate for smoking, 490-496), tobacco abuse (305.1, 649.0 and 989.84), alcohol-related diagnoses (291, 303, 535.3, 571.0-571.3 and 980.0), gallstone (574.00, 574.01, 574.10, 574.11, 574.20, 574.21 and A348), diseases of the digestive system (520-579), hepatitis B virus infection (070.22, 070.23, 070.32, 070.33 and V02.61), hepatitis C virus infection (070.41, 070.44, 070.51, 070.54 and V02.62), and liver cirrhosis (571.5). Antidiabetic drugs included sulfonylurea, metformin, meglitinide, acarbose and thiazolidinediones. Commonly used medications in diabetes patients included angiotensin converting enzyme inhibitor/angiotensin receptor blocker, calcium channel blocker, statin, fibrate and aspirin.

Student's t test compared the difference of age and diabetes duration between never and ever users and Chi-square test was used for other variables.

Incidence density of dementia was calculated for never users, ever users and tertiles of cumulative duration and cumulative dose of vildagliptin therapy. The numerator was the case number of

**TABLE 1 |** Characteristics of never users and ever users of vildagliptin in the unmatched original cohort and in the matched cohort.

Variable	Unmatched cohort					Matched cohort				
	Never users		Ever users		P value	Never users		Ever users		P value
	(n = 355610)		(n = 43196)			(n = 40489)		(n = 40489)		
	n	%	n	%		n	%	n	%	
Basic data										
Age (years)	59.10	9.19	58.19	9.37	<0.0001	58.43	9.63	58.16	9.36	<0.0001
Diabetes duration (years)	5.26	3.47	6.02	3.61	<0.0001	5.59	3.49	6.00	3.62	<0.0001
Sex (men)	160756	45.21	18769	43.45	<0.0001	17854	44.10	17616	43.51	0.0918
Occupation										
I	149742	42.11	18650	43.18	<0.0001	16854	41.63	17515	43.26	<0.0001
II	73458	20.66	9027	20.90		8419	20.79	8499	20.99	
III	62847	17.67	7333	16.98		6962	17.19	6831	16.87	
IV	69563	19.56	8186	18.95		8254	20.39	7644	18.88	
Living region										
Taipei	114624	32.23	13080	30.28	<0.0001	13146	32.47	12453	30.76	<0.0001
Northern	47693	13.41	5200	12.04		5480	13.53	4876	12.04	
Central	63151	17.76	11437	26.48		7286	18.00	10611	26.21	
Southern	57087	16.05	5798	13.42		6364	15.72	5369	13.26	
Kao-Ping and Eastern	73055	20.54	7681	17.78		8213	20.28	7180	17.73	
Major comorbidities										
Hypertension	186307	52.39	23212	53.74	<0.0001	21474	53.04	21383	52.81	0.5217
Dyslipidemia	177612	49.95	22271	51.56	<0.0001	20558	50.77	20537	50.72	0.8827
Obesity	10325	2.90	1407	3.26	<0.0001	1215	3.00	1363	3.37	0.0031
Diabetes-related complications										
Nephropathy	62464	17.57	8271	19.15	<0.0001	7562	18.68	7735	19.10	0.1204
Eye disease	53665	15.09	7119	16.48	<0.0001	6458	15.95	6684	16.51	0.0312
Stroke	65665	18.47	8569	19.84	<0.0001	7895	19.50	8018	19.80	0.2767
Ischemic heart disease	87513	24.61	11286	26.13	<0.0001	10394	25.67	10466	25.85	0.5629
Peripheral arterial disease	45352	12.75	6038	13.98	<0.0001	5486	13.55	5690	14.05	0.0377
Major risk factors of dementia										
Head injury	13719	3.86	1898	4.39	<0.0001	1663	4.11	1800	4.45	0.0173
Parkinson's disease	11482	3.23	1574	3.64	<0.0001	1354	3.34	1511	3.73	0.0028
Hypoglycemia	40255	11.32	5389	12.48	<0.0001	4729	11.68	5090	12.57	0.0001
Encephalitis and/or meningoencephalitis	657	0.18	122	0.28	<0.0001	76	0.19	122	0.30	0.0011
Osteoporosis	32089	9.02	4358	10.09	<0.0001	3837	9.48	4115	10.16	0.0010
Muscular wasting	3240	0.91	465	1.08	0.0007	402	0.99	465	1.15	0.0315
Accidental falls	1088	0.31	176	0.41	0.0004	126	0.31	176	0.43	0.0039
Potential risk factors of cancer										
Chronic obstructive pulmonary disease	91784	25.81	11881	27.50	<0.0001	10928	26.99	10982	27.12	0.6693
Tobacco abuse	10173	2.86	1423	3.29	<0.0001	1223	3.02	1369	3.38	0.0036
Alcohol-related diagnoses	12699	3.57	1703	3.94	<0.0001	1496	3.69	1634	4.04	0.0119
Gallstone	23425	6.59	3213	7.44	<0.0001	2802	6.92	3001	7.41	0.0067
Diseases of the digestive system	226288	63.63	28000	64.82	<0.0001	26058	64.36	25675	63.41	0.0051
Hepatitis B virus infection	15351	4.32	2129	4.93	<0.0001	1808	4.47	1808	4.47	0.0005
Hepatitis C virus infection	14779	4.16	1983	4.59	<0.0001	1730	4.27	1885	4.66	0.0084
Liver cirrhosis	14651	4.12	1984	4.59	<0.0001	1733	4.28	1885	4.66	0.0097
Antidiabetic drugs										
Sulfonylurea	85333	24.00	10738	24.86	<0.0001	10258	25.34	10519	25.98	0.0357
Metformin	10738	3.02	14829	34.33	<0.0001	16013	39.55	14829	36.62	<0.0001
Meglitinide	8068	2.27	1182	2.74	<0.0001	2490	6.15	1031	2.55	<0.0001
Acarbose	12797	3.60	1754	4.06	<0.0001	4018	9.92	1527	3.77	<0.0001
Thiazolidinediones	16605	4.67	1461	3.38	<0.0001	4705	11.62	1275	3.15	<0.0001
Medications commonly used in diabetes patients										
Angiotensin converting enzyme inhibitor/angiotensin receptor blocker	207170	58.26	28050	64.94	<0.0001	23458	57.94	26051	64.34	<0.0001
Calcium channel blocker	186126	52.34	22377	51.80	0.0350	21172	52.29	20885	51.58	0.0435
Statin	230140	64.72	30442	70.47	<0.0001	26078	64.41	28487	70.36	<0.0001
Fibrate	99162	27.89	13790	31.92	<0.0001	11624	28.71	11624	28.71	<0.0001
Aspirin	117604	33.07	16909	39.14	<0.0001	13520	33.39	15715	38.81	<0.0001

Age and diabetes duration are expressed as mean and standard deviation.

newly diagnosed dementia identified during follow-up and the denominator was the follow-up duration in person-years. Follow-up started on January 1, 2015 and ended on December 31,

2016, at the time of a new diagnosis of dementia, or on the date of death or the last reimbursement record, whichever occurred first.

Cox proportional hazards model was used to estimate the unadjusted and multivariate-adjusted hazard ratios and their 95% confidence intervals for ever users *versus* never users, for users categorized according to tertiles of cumulative duration and cumulative dose *versus* never users, and for cumulative duration (every 1-month increment) and cumulative dose (every 1-mg increment) of vildagliptin therapy being treated as continuous variables. Analyses were conducted in the unmatched cohort and the matched cohort, respectively. In the multivariate-adjusted models, all characteristics listed in **Table 1** were considered as potential confounders.

To examine whether the findings might be consistent for patients enrolled during three different periods of time, i.e., 2002-2005, 2006-2009 and 2010-2014, multivariate-adjusted models were created for the unmatched cohort enrolled during the three periods.

Analyses were conducted using SAS statistical software, version 9.4 (SAS Institute, Cary, NC).  $P < 0.05$  was considered statistically significant.

## RESULTS

**Table 1** shows the characteristics of never users and ever users of vildagliptin in the unmatched cohort and the matched cohort, respectively.

The incidence of dementia and the unadjusted and multivariate-adjusted hazard ratios by vildagliptin exposure are shown in **Table 2**. The overall hazard ratio comparing ever *versus* never users suggested a null association. Neither the cumulative duration nor the cumulative dose of vildagliptin therapy was

**TABLE 2 |** Incidence rates and hazard ratios of dementia by vildagliptin exposure.

Vildagliptin use	n	N	Person-year	Incidence rate	Unadjusted model			Multivariate-adjusted model		
				(per 100,000 person-years)	Hazard ratio	95% Confidence interval	P value	Hazard ratio	95% Confidence interval	P value
Unmatched cohort										
Vildagliptin never users	572	355610	620302.42	92.21	1.000			1.000		
Vildagliptin ever users	44	43196	64874.08	67.82	0.929	(0.683-1.264)	0.6379	0.922	(0.620-1.372)	0.6905
Tertiles of cumulative duration of vildagliptin therapy (months)										
Never users	572	355610	620302.42	92.21	1.000			1.000		
<1.87	6	15914	19428.75	30.88	0.723	(0.321-1.631)	0.4351	0.684	(0.287-1.630)	0.3918
1.87-7.47	15	12882	19812.75	75.71	0.990	(0.593-1.654)	0.9695	0.983	(0.552-1.750)	0.9545
>7.47	23	14400	25632.58	89.73	0.959	(0.632-1.455)	0.8429	0.956	(0.593-1.540)	0.8522
Cumulative duration of vildagliptin therapy treated as a continuous variable										
For every 1-month increment of vildagliptin use					0.997	(0.975-1.019)	0.7578	0.997	(0.974-1.021)	0.8299
Tertiles of cumulative dose of vildagliptin (mg)										
Never users	572	355610	620302.42	92.21	1.000			1.000		
<3,000	6	14105	17112.33	35.06	0.847	(0.375-1.911)	0.6887	0.771	(0.324-1.834)	0.5565
3,000-14,400	17	14378	21589.67	78.74	1.076	(0.663-1.744)	0.7674	1.045	(0.603-1.809)	0.8757
>14,400	21	14713	26172.08	80.24	0.858	(0.555-1.326)	0.4895	0.885	(0.540-1.450)	0.6284
Cumulative dose of vildagliptin treated as a continuous variable										
For every 1-mg increment of vildagliptin use					1.000	(1.000-1.000)	0.5452	1.000	(1.000-1.000)	0.6806
Matched cohort										
Vildagliptin never users	47	40489	61777.58	76.08	1.000			1.000		
Vildagliptin ever users	44	40489	62779.58	70.09	0.930	(0.616-1.402)	0.7281	0.825	(0.498-1.367)	0.4560
Tertiles of cumulative duration of vildagliptin therapy (months)										
Never users	47	40489	61777.58	76.08	1.000			1.000		
<1.87	6	13901	17876.92	33.56	0.714	(0.300-1.697)	0.4457	0.607	(0.238-1.543)	0.2939
1.87-8.37	16	12823	20339.42	78.66	0.996	(0.565-1.756)	0.9883	0.914	(0.482-1.734)	0.7839
>8.37	22	13765	24563.25	89.56	0.962	(0.578-1.599)	0.8806	0.836	(0.466-1.498)	0.5463
Cumulative duration of vildagliptin therapy treated as a continuous variable										
For every 1-month increment of vildagliptin use					0.998	(0.973-1.024)	0.8701	0.993	(0.966-1.020)	0.6131
Tertiles of cumulative dose of vildagliptin (mg)										
Never users	47	40489	61777.58	76.08	1.000			1.000		
<3,150	6	13361	17103.92	35.08	0.763	(0.321-1.816)	0.5414	0.623	(0.245-1.582)	0.3194
3,150-16,500	18	13357	21103.33	85.29	1.088	(0.632-1.872)	0.7621	0.957	(0.516-1.775)	0.8885
>16,500	20	13771	24572.33	81.39	0.872	(0.516-1.475)	0.6103	0.794	(0.436-1.446)	0.4515
Cumulative dose of vildagliptin treated as a continuous variable										
For every 1-mg increment of vildagliptin use					1.000	(1.000-1.000)	0.6062	1.000	(1.000-1.000)	0.5243

*n*, incident cases of dementia; *N*, cases followed.

significantly associated with the risk of dementia when these parameters were categorized into tertiles or treated as continuous variables. The findings consistently supported a null association in the unmatched cohort and the matched cohort.

**Table 3** shows the overall multivariate-adjusted hazard ratios comparing ever *versus* never users of vildagliptin analyzed in patients enrolled during three different periods, i.e., 2002-2005, 2006-2009 and 2010-2014. The results suggested a null association in all subgroups.

## DISCUSSION

The findings suggested that vildagliptin use has a null association with dementia risk in patients with type 2 diabetes mellitus (**Tables 2 and 3**).

Antidiabetic drugs are being used by thousands of millions of diabetes patients. Therefore, the safety and potential pleiotropic effects or benefits of antidiabetic drugs are clinically important, especially for dementia, a disease that affects millions of patients and has a close link with diabetes mellitus. This study may have some clinical and research significance. First, neuroprotective findings of vildagliptin observed in *in vitro*, *in vivo* and animal studies should not be readily interpreted as a potential protection against dementia in humans without consideration of its accessibility to human brain. It is interesting that vildagliptin alleviated cognitive deficits of spatial learning and memory in rats with streptozotocin-induced diabetes (18), but this benefit could not be similarly demonstrated in humans in the present study (**Tables 2 and 3**). One of the possible explanations is that most DPP4 inhibitors cannot readily pass through the blood-brain barrier in humans (22). However, vildagliptin, a small molecule with a molecular weight of 303.4 Daltons (g/mol) (23), might cross the blood-brain barrier more efficiently in streptozotocin-induced diabetes rats because streptozotocin administration may cause a progressive increase in the blood-brain barrier permeability (especially significant in the midbrain) of small molecules [using vascular space markers ranging from 342 to 65,000 Daltons (g/mol) from 28 to 90 days] (24). In the animal study conducted by Zhang et al., vildagliptin was administered for 4 consecutive weeks after successful induction of diabetes by streptozotocin for 10 weeks (18). This time frame just met the time of streptozotocin-induced progressive increase of blood-brain barrier permeability observed by Huber et al. (24). Although diabetes mellitus has been claimed to affect the permeability of blood-brain barrier, findings derived from

human studies are still lacking and the conclusions remain controversial (25). Therefore, the findings derived from streptozotocin-induced diabetes might not be readily applied to patients with diabetes mellitus if the blood-brain barrier remains intact. More in-depth studies are required to explore the possible effect of vildagliptin on the risk of dementia in humans. Second, patients with type 2 diabetes mellitus in East Asia are characterized by more remarkable  $\beta$ -cell dysfunction and less insulin resistance than in Caucasians, and DPP4 inhibitors seem to exert better glycemic control in East Asians (26). In Japan, DPP4 inhibitors have become the first-line antidiabetic drugs and more than 70% of the diabetes patients are being treated with incretin-based therapies (26). Although major clinical trials suggested a neutral cardiovascular effect of DPP4 inhibitors (27) and the present study did not favor a beneficial effect of vildagliptin on dementia, DPP4 inhibitors can at least be safely used for glycemic control in older patients because of a high tolerability and a lack of hypoglycemic risk (28). Third, recent studies suggested that DPP4 inhibitors (especially vildagliptin and linagliptin) are associated with a higher risk of bullous pemphigoid (29–31). According to an observational study conducted in Taiwan, the risk factors of bullous pemphigoid in patients with type 2 diabetes mellitus seemed to be associated with using DPP4 inhibitors, having dementia and taking spironolactone (32). Therefore, DPP4 inhibitors should better be avoided in diabetes patients with dementia and/or taking spironolactone.

Some potential biases commonly seen in pharmacoepidemiological studies such as selection bias, prevalent user bias, immortal time bias and confounding by indication have been addressed in the present study. Selection bias would not be a problem because of the use of the nationwide database that covers more than 99.9% of the population. Prevalent user bias was avoided by including patients with new-onset type 2 diabetes mellitus and new users of vildagliptin (**Figure 1**).

Immortal time refers to the follow-up period when the outcome cannot happen. When the treatment status or follow-up time is inappropriately assigned, immortal time bias can be introduced (33). We tried to exclude patients with ambiguous diagnosis of diabetes mellitus by enrolling only patients who had been prescribed antidiabetic drugs for 3 or more times within one year (**Figure 1**). In the universal healthcare system in Taiwan, the information of all prescriptions in the NHI was complete during the whole follow-up period and misclassification of treatment status was not likely. Therefore, inappropriate assignment of treatment status was unlikely in the present study.

**TABLE 3 |** Incidence of dementia comparing ever *versus* never users of vildagliptin in patients enrolled during three different periods of time in the unmatched cohort.

Year	Ever users		Never users		Multivariate-adjusted model		
	<i>n</i>	<i>N</i>	<i>n</i>	<i>N</i>	Hazard ratio	95% Confidence interval	<i>P</i> value
2002-2005	13	8628	125	55931	1.019	(0.529-1.963)	0.9541
2006-2009	17	13059	182	98103	1.070	(0.562-2.036)	0.8369
2010-2014	14	21509	265	201576	0.651	(0.289-1.469)	0.3016

*n*, incident cases of dementia; *N*, cases followed.

To avoid the inappropriate assignment of follow-up time, we first enrolled only patients who had been treated with antidiabetic drugs and they were followed up only after a certain period of antidiabetic treatment (**Figure 1**). This avoided the immortal time between diabetes diagnosis and the start of the use of antidiabetic drugs (i.e., a certain period when the patients could have been put on diet control or exercise and antidiabetic drugs were not used). We then excluded patients with a short follow-up duration of <6 months (**Figure 1**) to avoid the enrollment of patients with such an immortal time in the calculation of person-years. It should be pointed out that the immortal time during the waiting period between drug prescription and dispense at hospital discharge as described by Lévesque et al. (33) would not happen in Taiwan because all discharge drugs can be obtained at the hospital when the patient is discharged.

To examine whether the results might be affected by potential confounding by indication, we compared the findings between the unmatched cohort and the matched cohort based on propensity score and between the unadjusted and multivariate-adjusted models (**Table 2**). The findings seemed to be very consistent in different analyses. Analyses in subgroups of patients categorized by the tertiles of exposure parameters and by treating these parameters as continuous variables (**Table 2**) also supported a lack of association between vildagliptin and dementia. The indications and recommendations for the use of antidiabetic drugs for the treatment of type 2 diabetes mellitus have evolved over the past decades following the introduction of newer classes of antidiabetic drugs and according to the results of novel clinical trials. The ever-changing recommendations for the indications and uses of different classes of antidiabetic drugs would not confound the finding of a neutral effect of vildagliptin on dementia risk while patients enrolled during three different periods of time were analyzed separately (**Table 3**).

The present study has some other merits. First, the findings can be readily generalized to the whole population because the NHI database covers >99.9% of the Taiwan's population. Second, self-reporting bias and recall bias could be avoided by using the medical records. Third, although detection bias because of different socioeconomic status could be a severe problem in some countries, this would not be the case in our study because the drug cost-sharing is low and can always be waived in patients with low-income, in veterans and when the patients receive prescription refills for chronic disease in our NHI healthcare system.

There are several limitations in the present study. First, we could only use the ICD-9-CM codes for disease diagnoses and no additional support from laboratory examinations was available in the database. The accuracy of the diagnosis of dementia was not known. If the misdiagnosis was non-differential between ever users and never users of vildagliptin, the estimated effect would be expected to bias towards to null (34) and a true positive or negative effect could not be shown. Therefore, the findings of the present study should better be considered as preliminary and future studies with well-verified cases are required to confirm our findings of a null effect. Second, we did not have measured data

of some confounders like blood levels of glucose and insulin, fluctuation of blood glucose, indicators of insulin resistance and  $\beta$ -cell function, anthropometric factors, dietary pattern, nutritional status, lifestyle, smoking, alcohol drinking, family history and genetic parameters. It is recognized that the application of propensity score matching in a retrospective cohort study can never adjust for unmeasured confounders as a randomized control trial can do (35). It is impossible for the present study to assess whether the impact of unmeasured confounders could be substantial and the estimates could be misleading. Therefore, if possible, the findings of the present study should better be confirmed by a randomized control trial in the future. Third, we were not able to discern the two major types of dementia, i.e., vascular or degenerative type, because of lack of sufficient laboratory data. If the effects of vildagliptin were not the same for these two types of dementia, the estimates would be misleading by including different types of dementia. Additionally, to our knowledge, although the accuracy of diabetes diagnosis and most other comorbidities in the NHI database has been validated in previous studies (36, 37), the accuracy of dementia diagnosis remains to be validated. It would be a good future research topic to validate the related diagnostic codes of dementia in the database. Fourth, the mean age of the patients was around 58–59 years old at the start of follow-up (**Table 1**). The incidence of dementia in these patients might not be high enough to have sufficient power to detect a significant difference. It would be better to include a cohort of older age for additional study in the future. Fifth, the follow-up duration might be too short and therefore the findings should be confirmed by studies with longer follow-up duration. Finally, because the study excluded users of other incretin-based therapies, whether the findings can be applied to other DPP4 inhibitors or to glucagon like peptide-1 receptor agonists is not known.

In conclusion, the present study finds a neutral effect of vildagliptin on the association with dementia risk in Taiwanese patients with type 2 diabetes mellitus. More studies are warranted to clarify the neuroprotective effects of vildagliptin or other DPP4 inhibitors observed in *in vitro* or animal studies.

## DATA AVAILABILITY STATEMENT

The datasets presented in this article are not readily available because public availability of the dataset is restricted by local regulations to protect privacy. Requests to access the datasets should be directed to C-HT, ccktsh@ms6.hinet.net.

## ETHICS STATEMENT

The studies involving human participants were reviewed and approved by The Research Ethics Committee C of the National Taiwan University Hospital (NTUH-REC No. 201805002WC). Written informed consent for participation was not required for

this study in accordance with the national legislation and the institutional requirements.

## AUTHOR CONTRIBUTIONS

The author confirms being the sole contributor of this work and has approved it for publication.

## FUNDING

The study was supported partly by the Ministry of Science and Technology (MOST 107-2221-E-002-129-MY3) of Taiwan and

by Novartis Taiwan. The funders had no role in study design, data collection and analysis, decision to publish, or preparation of the manuscript.

## ACKNOWLEDGMENTS

The study is based in part on data from the National Health Insurance Research Database provided by the Bureau of National Health Insurance, Department of Health and managed by National Health Research Institutes. The interpretation and conclusions contained herein do not represent those of Bureau of National Health Insurance, Department of Health or National Health Research Institutes.

## REFERENCES

1. IDF Diabetes Atlas 9th edition (2019). Available at: <https://www.diabetesatlas.org/en/> (Accessed April 2, 2021).
2. World Health Organization. Available at: <https://www.who.int/news-room/fact-sheets/detail/dementia> (Accessed April 2, 2021).
3. Gudala K, Bansal D, Schifano F, Bhansali A. Diabetes Mellitus and Risk of Dementia: A Meta-Analysis of Prospective Observational Studies. *J Diabetes Investig* (2013) 4:640–50. doi: 10.1111/jdi.12087
4. Fan YC, Hsu JL, Tung HY, Chou CC, Bai CH. Increased Dementia Risk Predominantly in Diabetes Mellitus Rather Than in Hypertension or Hyperlipidemia: A Population-Based Cohort Study. *Alzheimers Res Ther* (2017) 9:7. doi: 10.1186/s13195-017-0236-z
5. Cheng PY, Sy HN, Wu SL, Wang WF, Chen YY. Newly Diagnosed Type 2 Diabetes and Risk of Dementia: A Population-Based 7-Year Follow-Up Study in Taiwan. *J Diabetes Complicat* (2012) 26:382–7. doi: 10.1016/j.jdiacomp.2012.06.003
6. de la Monte SM, Tong M, Wands JR. The 20-Year Voyage Aboard the Journal of Alzheimer's Disease: Docking At 'Type 3 Diabetes', Environmental/Exposure Factors, Pathogenic Mechanisms, and Potential Treatments. *J Alzheimers Dis* (2018) 62:1381–90. doi: 10.3233/JAD-170829
7. Li X, Song D, Leng SX. Link Between Type 2 Diabetes and Alzheimer's Disease: From Epidemiology to Mechanism and Treatment. *Clin Interv Aging* (2015) 10:549–60. doi: 10.2147/CIA.S74042
8. Mulvihill EE. Dipeptidyl Peptidase Inhibitor Therapy in Type 2 Diabetes: Control of the Incretin Axis and Regulation of Postprandial Glucose and Lipid Metabolism. *Peptides* (2018) 100:158–64. doi: 10.1016/j.peptides.2017.11.023
9. D'Amico M, Di Filippo C, Marfella R, Abbatecola AM, Ferraraccio F, Rossi F, et al. Long-Term Inhibition of Dipeptidyl Peptidase-4 in Alzheimer's Prone Mice. *Exp Gerontol* (2010) 45:202–7. doi: 10.1016/j.exger.2009.12.004
10. Matteucci E, Giampietro O. Mechanisms of Neurodegeneration in Type 2 Diabetes and the Neuroprotective Potential of Dipeptidyl Peptidase 4 Inhibitors. *Curr Med Chem* (2015) 22:1573–81. doi: 10.2174/0929867322666150227153308
11. Pintana H, Tanajak P, Pratchayasakul W, Sa-Nguanmoo P, Chunchai T, Satjaritanun P, et al. Energy Restriction Combined With Dipeptidyl Peptidase-4 Inhibitor Exerts Neuroprotection in Obese Male Rats. *Br J Nutr* (2016) 117:1–9. doi: 10.1017/S0007114516003871
12. Sripecthwanee J, Pipatpiroon N, Pratchayasakul W, Chattipakorn N, Chattipakorn SC. DPP-4 Inhibitor and PPAR $\gamma$  Agonist Restore the Loss of CA1 Dendritic Spines in Obese Insulin-Resistant Rats. *Arch Med Res* (2014) 45:547–52. doi: 10.1016/j.arcmed.2014.09.002
13. Kosaraju J, Murthy V, Khatwal RB, Dubala A, Chinni S, Muthureddy Nataraj SK, et al. Vildagliptin: An Anti-Diabetes Agent Ameliorates Cognitive Deficits and Pathology Observed in Streptozotocin-Induced Alzheimer's Disease. *J Pharm Pharmacol* (2013) 65:1773–84. doi: 10.1111/jph.12148
14. Pipatpiroon N, Pratchayasakul W, Chattipakorn N, Chattipakorn SC. Ppar $\gamma$  Agonist Improves Neuronal Insulin Receptor Function in Hippocampus and Brain Mitochondria Function in Rats With Insulin Resistance Induced by Long Term High-Fat Diets. *Endocrinology* (2012) 153:329–38. doi: 10.1210/en.2011-1502
15. Pipatpiroon N, Pintana H, Pratchayasakul W, Chattipakorn N, Chattipakorn SC. DPP4-Inhibitor Improves Neuronal Insulin Receptor Function, Brain Mitochondrial Function and Cognitive Function in Rats With Insulin Resistance Induced by High-Fat Diet Consumption. *Eur J Neurosci* (2013) 37:839–49. doi: 10.1111/ejn.12088
16. Zheng T, Qin L, Chen B, Hu X, Zhang X, Liu Y, et al. Association of Plasma DPP4 Activity With Mild Cognitive Impairment in Elderly Patients With Type 2 Diabetes: Results From the GDMD Study in China. *Diabetes Care* (2016) 39:1594–601. doi: 10.2337/dc16-0316
17. Nath S, Ghosh SK, Choudhury Y. A Murine Model of Type 2 Diabetes Mellitus Developed Using a Combination of High Fat Diet and Multiple Low Doses of Streptozotocin Treatment Mimics the Metabolic Characteristics of Type 2 Diabetes Mellitus in Humans. *J Pharmacol Toxicol Methods* (2017) 84:20–30. doi: 10.1016/j.vascn.2016.10.007
18. Zhang DD, Shi N, Fang H, Ma L, Wu WP, Zhang YZ, et al. Vildagliptin, a DPP4 Inhibitor, Alleviates Diabetes-Associated Cognitive Deficits by Decreasing the Levels of Apoptosis-Related Proteins in the Rat Hippocampus. *Exp Ther Med* (2018) 15:5100–6. doi: 10.3892/etm.2018.6016
19. Taiwan Life Expectancy 1950–2021. Available at: <https://www.macrotrends.net/countries/TWN/taiwan/life-expectancy> (Accessed April 2, 2021).
20. Galatas C, Afilalo J. Transcatheter Aortic Valve Replacement Over Age 90: Risks vs Benefits. *Clin Cardiol* (2020) 43:156–62. doi: 10.1002/clc.23310
21. Parsons LS. *Performing a 1:N Case-Control Match on Propensity Score*. Available at: <http://www2.sas.com/proceedings/sugi29/165-29.pdf> (Accessed April 2, 2021).
22. Deacon CF. Dipeptidyl Peptidase-4 Inhibitors in the Treatment of Type 2 Diabetes: A Comparative Review. *Diabetes Obes Metab* (2011) 13:7–18. doi: 10.1111/j.1463-1326.2010.01306.x
23. PubChem. *US National Library of Medicine*. Available at: <https://pubchem.ncbi.nlm.nih.gov/compound/cid-5251896> (Accessed April 2, 2021).
24. Huber JD, VanGilder RL, Houser KA. Streptozotocin-Induced Diabetes Progressively Increases Blood-Brain Barrier Permeability in Specific Brain Regions in Rats. *Am J Physiol Heart Circ Physiol* (2006) 291:H2660–8. doi: 10.1152/ajpheart.00489.2006
25. Prasad S, Sajja RK, Naik P, Cucullo L. Diabetes Mellitus and Blood-Brain Barrier Dysfunction: An Overview. *J Pharmacovigil* (2014) 2:125. doi: 10.4172/2329-6887.1000125
26. Seino Y, Kuwata H, Yabe D. Incretin-Based Drugs for Type 2 Diabetes: Focus on East Asian Perspectives. *J Diabetes Investig* (2016) Suppl 1:102–9. doi: 10.1111/jdi.12490
27. Home P. Cardiovascular Outcome Trials of Glucose-Lowering Medications: An Update. *Diabetologia* (2019) 62:357–69. doi: 10.1007/s00125-018-4801-1
28. Ling J, Cheng P, Ge L, Zhang DH, Shi AC, Tian JH, et al. The Efficacy and Safety of Dipeptidyl Peptidase-4 Inhibitors for Type 2 Diabetes: A Bayesian Network Meta-Analysis of 58 Randomized Controlled Trials. *Acta Diabetol* (2019) 56:249–72. doi: 10.1007/s00592-018-1222-z

29. Tasanen K, Varpuluoma O, Nishie W. Dipeptidyl Peptidase-4 Inhibitor-Associated Bullous Pemphigoid. *Front Immunol* (2019) 10:1238. doi: 10.3389/fimmu.2019.01238
30. Nishie W. Dipeptidyl Peptidase IV Inhibitor-Associated Bullous Pemphigoid: A Recently Recognized Autoimmune Blistering Disease With Unique Clinical, Immunological and Genetic Characteristics. *Immunol Med* (2019) 42:22–8. doi: 10.1080/25785826.2019.1619233
31. Kridin K, Bergman R. Association of Bullous Pemphigoid With Dipeptidyl-Peptidase 4 Inhibitors in Patients With Diabetes: Estimating the Risk of the New Agents and Characterizing the Patients. *JAMA Dermatol* (2018) 154:1152–8. doi: 10.1001/jamadermatol.2018.2352
32. Guo JY, Chen HH, Yang YC, Wu PY, Chang MP, Chen CC. The Association of Dipeptidyl Peptidase IV Inhibitors and Other Risk Factors With Bullous Pemphigoid in Patients With Type 2 Diabetes Mellitus: A Retrospective Cohort Study. *J Diabetes Complicat* (2020) 34:107515. doi: 10.1016/j.jdiacomp.2019.107515
33. Lévesque LE, Hanley JA, Kezouh A, Suissa S. Problem of Immortal Time Bias in Cohort Studies: Example Using Statins for Preventing Progression of Diabetes. *BMJ* (2010) 340:b5087. doi: 10.1136/bmj.b5087
34. Kesmodel US. Information Bias in Epidemiological Studies With a Special Focus on Obstetrics and Gynecology. *Acta Obstet Gynecol Scand* (2018) 97:417–23. doi: 10.1111/aogs.13330
35. Reiffel JA. Propensity Score Matching: The ‘Devil is in the Details’ Where More may be Hidden Than You Know. *Am J Med* (2020) 133:178–81. doi: 10.1016/j.amjmed.2019.08.055
36. Lin CC, Lai MS, Syu CY, Chang SC, Tseng FY. Accuracy of Diabetes Diagnosis in Health Insurance Claims Data in Taiwan. *J Formos Med Assoc* (2005) 104:157–63.
37. Cheng CL, Kao YH, Lin SJ, Lee CH, Lai ML. Validation of the National Health Insurance Research Database With Ischemic Stroke Cases in Taiwan. *Pharmacoepidemiol Drug Saf* (2011) 20:236–42. doi: 10.1002/pds.2087

**Conflict of Interest:** The author declares that the research was conducted in the absence of any commercial or financial relationships that could be construed as a potential conflict of interest.

Copyright © 2021 Tseng. This is an open-access article distributed under the terms of the Creative Commons Attribution License (CC BY). The use, distribution or reproduction in other forums is permitted, provided the original author(s) and the copyright owner(s) are credited and that the original publication in this journal is cited, in accordance with accepted academic practice. No use, distribution or reproduction is permitted which does not comply with these terms.



# Altered White Matter Microstructures in Type 2 Diabetes Mellitus: A Coordinate-Based Meta-Analysis of Diffusion Tensor Imaging Studies

## OPEN ACCESS

### Edited by:

Hubert Preissl,  
Institute for Diabetes Research and  
Metabolic Diseases (IDM), Germany

### Reviewed by:

Onno Meijer,  
Leiden University, Netherlands  
Jorge Miguel Amaya Fernandez,  
Leiden University, Netherlands, in  
collaboration with reviewer OM  
Erwin Lemche,  
King's College London,  
United Kingdom

### \*Correspondence:

Cong Zhou  
doctorzhoucong@163.com

### Specialty section:

This article was submitted to  
Neuroendocrine Science,  
a section of the journal  
Frontiers in Endocrinology

**Received:** 25 January 2021

**Accepted:** 07 April 2021

**Published:** 03 May 2021

### Citation:

Zhou C, Li J, Dong M, Ping L, Lin H,  
Wang Y, Wang S, Gao S, Yu G,  
Cheng Y and Xu X (2021) Altered  
White Matter Microstructures in Type 2  
Diabetes Mellitus: A Coordinate-  
Based Meta-Analysis of Diffusion  
Tensor Imaging Studies.  
Front. Endocrinol. 12:658198.  
doi: 10.3389/fendo.2021.658198

Cong Zhou<sup>1\*</sup>, Jie Li<sup>2</sup>, Man Dong<sup>1</sup>, Liangliang Ping<sup>3</sup>, Hao Lin<sup>1</sup>, Yuxin Wang<sup>1</sup>,  
Shuting Wang<sup>1</sup>, Shuo Gao<sup>1</sup>, Ge Yu<sup>1</sup>, Yuqi Cheng<sup>4</sup> and Xiufeng Xu<sup>4</sup>

<sup>1</sup> School of Mental Health, Jining Medical University, Jining, China, <sup>2</sup> Department of Psychiatry, Jining Psychiatric Hospital, Jining, China, <sup>3</sup> Department of Psychiatry, Xiamen Xianyue Hospital, Xiamen, China, <sup>4</sup> Department of Psychiatry, The First Affiliated Hospital of Kunming Medical University, Kunming, China

**Objective:** Type 2 diabetes mellitus (T2DM) is often accompanied by cognitive decline and depressive symptoms. Numerous diffusion tensor imaging (DTI) studies revealed microstructural white matter (WM) abnormalities in T2DM but the findings were inconsistent. The present study aimed to conduct a coordinate-based meta-analysis (CBMA) to identify statistical consensus of DTI studies in T2DM.

**Methods:** We performed a systematic search on relevant studies that reported fractional anisotropy (FA) differences between T2DM patients and healthy controls (HC). The anisotropic effect size seed-based d mapping (AES-SDM) approach was used to explore WM alterations in T2DM. A meta-regression was then used to analyze potential influences of sample characteristics on regional FA changes.

**Results:** A total of eight studies that comprised 245 patients and 200 HC, along with 52 coordinates were extracted. The meta-analysis identified FA reductions in three clusters including the left inferior network, the corpus callosum (CC), and the left olfactory cortex. Besides, FA in the CC was negatively correlated with body mass index (BMI) in the patients group.

**Conclusions:** T2DM could lead to subtle WM microstructural alterations, which might be associated with cognitive deficits or emotional distress symptoms. This provides a better understanding of the pathophysiology of neurodegeneration and complications in T2DM.

**Systematic Review Registration:** Registered at PROSPERO (<http://www.crd.york.ac.uk/PROSPERO>), registration number: CRD42020218737.

**Keywords:** type 2 diabetes mellitus, diffusion tensor imaging, fractional anisotropy, white matter, meta-analysis

## INTRODUCTION

The International Diabetes Federation estimates that 415 million people have diabetes mellitus worldwide, with 90% of these individuals having T2DM (1). Type 2 diabetes mellitus (T2DM) is a chronic metabolic disorder characterized by reduced insulin sensitivity, followed by a compensatory increase in insulin secretion (2). The disease has become a critical health concern worldwide owing to its high prevalence and related disability and mortality (3). T2DM usually leads to various complications in multiple organs, including impairments in the brain (4). People with type 2 diabetes are at an increased risk of cognitive decline and dementia (including Alzheimer's disease, AD) (5, 6), which is related with worse diabetes management, more frequent occurrence of severe hypoglycemic episodes, and an increased risk of cardiovascular events, and death (7). Earlier meta-analyses showed that the presence of diabetes in older adults was associated with 47% increased risk of all dementia, 39% increased risk of AD, and 138% increased risk of vascular dementia (8, 9). Existing evidence indicated that microstructural brain atrophy contributed to poor cognitive function (10–13). Several neuroimaging studies with different modalities have demonstrated that T2DM is accompanied with structural and functional abnormalities in various regions of the brain (2, 14, 15). Moreover, T2DM and mood disorders share pathophysiological commonalities in the central nervous system (16, 17). The prevalence of depression among T2DM is quite high (18–21), which is considered to be related with cerebral microvascular dysfunction (22). However, the specific neurobiological mechanisms underlying the cognitive impairment and emotional distress of T2DM patients remain unclear for now.

Advances in MRI techniques make it possible to investigate subtle structural alterations of the brain. Among them, diffusion tensor imaging (DTI) is able to detect white matter (WM) microstructure characteristics by estimating random movement of water molecules in the brain (23). The most widely used parameter to study DTI is fractional anisotropy (FA), which reflects diffusion direction and is related to fiber orientation. Any reduction in white matter anisotropy indicates an alteration in the degree of tissue order or integrity (24). DTI approach is widely applied in the evaluation of WM microstructure in various central nervous system disorders. Specially, DTI metrics appears to be a more sensitive marker of cognitive decline due to aging and AD, even when there is no sign of microstructural gray matter (GM) volume alterations and atrophy of brain structures (25, 26). The two most widely used methods of DTI to achieve whole-brain analysis were voxel-based analysis (VBA) and tract-based spatial statistics (TBSS) (27). The former involves analyzing all white matter voxels and correcting for multiple comparisons and noise by reporting only contiguous clusters of significant voxels, while the latter isolates the central core of white matter tracts with the highest FA and reports significant clusters within that white matter skeleton (28, 29). Findings from numerous studies have suggested widespread white matter abnormalities in T2DM patients. However, the results are inconsistent and controversial. According to previous studies, significantly decreased in FA has been observed in

patients with T2DM in widespread WM regions such as the frontal lobe (15, 30, 31), temporal region (15, 30–33), corpus callosum (CC) (34–36), cingulum bundle (15, 35, 37), uncinate fasciculus (UF) (35, 36, 38), and corticospinal tract (CST) (35, 36). The inconsistencies of different studies were probably owing to small sample size, heterogeneous demographic characteristics of the patients, and the diversity of methodological techniques.

The coordinate-based meta-analysis (CBMA) is a widely used method to solve the discrepancies of regional alterations among various neuroimaging studies (39). The anisotropic effect size seed-based d mapping (AES-SDM) is an advanced statistical technique for CBMA on different neuroimaging techniques such as structural MRI, functional MRI, DTI, or PET (40). Compared with earlier methods such as activation likelihood estimation and multilevel kernel density analysis (41, 42), the AES-SDM has strengths as below: (a) In the AES-SDM, both positive and negative differences in the same map are combined to avoid a particular voxel from appearing to be significant in opposite directions (43); (b) The AES-SDM approach allows reported peak coordinates to be combined with statistical parametric maps, thus ensuring more exhaustive and accurate meta-analyses (44); (c) SDM enables several complementary analyses, such as jack-knife, subgroup, and meta-regression analyses, which can be used to evaluate the robustness and heterogeneity of the results (40). The AES-SDM method has been fully validated in several neuropsychiatric disorders including Parkinson's disease (45, 46), major depressive disorder (MDD) (29), bipolar disorder (47), obsessive-compulsive disorder (43, 48, 49), autism spectrum disorder (50), type 1 diabetes mellitus (T1DM) (51), and also in voxel-based morphometry (VBM) studies in T2DM patients (52, 53).

A recently published systematic review of DTI studies (54) comprehensively and systematically summarized previous DTI findings of brain microstructural abnormalities in T2DM. However, this review study is not able to detect the discrepancies of regional alterations with reported coordinates and anisotropic effect size. Thus, a CBMA using AES-SDM is required to identify consistent results from DTI studies in patients with T2DM. The first objective of this present research was to investigate the most robust FA alterations in T2DM compared with healthy controls (HC). Secondly, we intended to explore the potential effects of demographics and clinical characteristics including mean age, duration of disease, body mass index (BMI), and HbA1c% on WM changes by using meta-regression approach. We hypothesized that patients with T2DM would exhibit microarchitecture alterations in core WM tracts such as the CC, as well as regions related with cognitive functions and emotional regulations.

## MATERIALS AND METHODS

### Literature Search Strategy

This meta-analysis was conducted according to the Preferred Reporting Items for Systematic Reviews and Meta-Analyses (PRISMA) guidelines (55–57). The protocol of this CBMA was

registered at PROSPERO (<http://www.crd.york.ac.uk/PROSPERO>) (registration number: CRD42020218737). Systematic and comprehensive searches were used to acquire relevant literatures from the PubMed and Web of Science databases published (or “in press”) up to October 31, 2020. The search keywords were (“type 2 diabetes mellitus” or “T2DM” or “type 2 diabetes”) and (“diffusion tensor” or “DTI” or “diffusion magnetic resonance imaging”). Additionally, the reference lists of identified studies and relevant reviews were manually checked to avoid omitting.

## Study Selection

Studies which met the following criteria were included (1): studies compared FA value differences between T2DM and HC in whole-brain analyses (2); reported results in Talairach or Montreal Neurological Institute (MNI) coordinates; (3) used a threshold for significance; (4) articles written in the English language and published in peer-reviewed journals. Exclusion criteria were: (1) meta-analysis, reviews, case reports, or tractography-based only study; (2) studies with no direct between-group comparison; (3) studies from which peak coordinates or parametric maps were unavailable.

## Quality Assessment and Data Extraction

Two authors (ZC and LJ) independently searched the literatures, assessed the quality of the retrieved articles, extracted and cross-checked the data from eligible articles. The quality of the final studies was also independently checked by both authors following guidelines for neuroimaging meta-analyses promoted by Müller and colleagues (58). For each study the following data were recorded: first author, cohort size, demographics (age and gender), illness duration, BMI, HbA1c%, imaging parameters, data processing method and statistical threshold, as well as the three-dimensional peak coordinates of case-control differences in each study.

## AES-SDM Meta-Analysis

Regional FA differences between T2DM patients and HC were performed using the SDM software v5.15 (<http://www.sdmproject.com>) (43, 59) in a voxel-based meta-analysis approach. We conducted the analysis according to the SDM tutorial and previous meta-analytic studies. The AES-SDM technique uses effect sizes combining with reported peak coordinates which are extracted from databases with statistical parametric maps, and recreates maps of the original maps of the effect size of FA between patients and controls, rather than just assessing the probability or likelihood of a peak (40).

The AES-SDM procedures have been described in detail elsewhere (29, 46, 60), and were briefly summarized as follows: (1) The peak coordinates of all white-matter from each data set were extracted at the level of *t*-statistics (*Z*- or *P*- values for significant clusters which were then converted to *t*-statistics using the SDM online converter); (2) The peak coordinates for each study were recreated using a standard MNI map of the effect size of the group differences in FA by means of an anisotropic Gaussian kernel (44). A relatively wide full width at half maximum (20 mm) and DTI templates were used to control

false-positive results; (3) The standard meta-analysis was conducted to create a mean map *via* voxel-wise calculation of the random-effects mean of the study maps. According to Radua et al. (40), an uncorrected *P* = 0.005 using the AES-SDM software is approximately equivalent to a corrected *P* = 0.025. Here, we used more stringent thresholds as follows: uncorrected *P* value < 0.001, peak height threshold *Z* = 1.00, and cluster size threshold = 10 voxels.

## Sensitivity Analyses

To assess the replicability of the results, we performed a systematic whole-brain voxel-based jackknife sensitivity analysis. This procedure involved repeating the main statistical analysis for each result eight times, discarding a different study each time. If a brain region remains significant after running jackknife sensitivity in all or most of the combinations of studies, the finding is considered highly replicable (43).

## Meta-Regression Analysis

Considering the potential influences of mean age, duration of disease, BMI, and HbA1c% on WM abnormalities, a more conservative threshold (*P* < 0.0005) was adopted in consistent with previous meta-analyses and the recommendations of the AES-SDM authors (43), and only brain regions identified in the main effect were considered.

## RESULTS

### Included Studies and Sample Characteristics

The flow diagram of the identification and the attributes of the studies is presented in **Figure 1**. The demographics of the samples are summarized in **Table 1**. The search strategy identified 90 studies, eight of which met the inclusion criteria (15, 30, 32, 34–36, 61, 62). One study contained two different subgroups of T2DM patients (T2DM patients with mild cognitive impairment and T2DM patients with normal cognition), but only the coordinates of significantly different clusters in T2DM patients with mild cognitive impairment were reported. We treated this study as one single dataset. Thus, our final sample comprised 245 T2DM patients and 200 HC, along with 52 coordinates extracted from eight datasets. The scanning methods and FA alterations of the eight datasets are shown in **Table 2**.

### Regional Differences in FA

The meta-analysis revealed that patients with T2DM exhibited significant FA reductions in three clusters relative to HC, including the left inferior network, the CC and left olfactory cortex (BA 25), as illustrated in **Figure 2** and **Table 3**. No region with higher FA was identified in the current meta-analysis.

### Jackknife Sensitivity Analysis

The whole-brain jackknife sensitivity analysis revealed that decreased FA in T2DM patients in the left inferior network

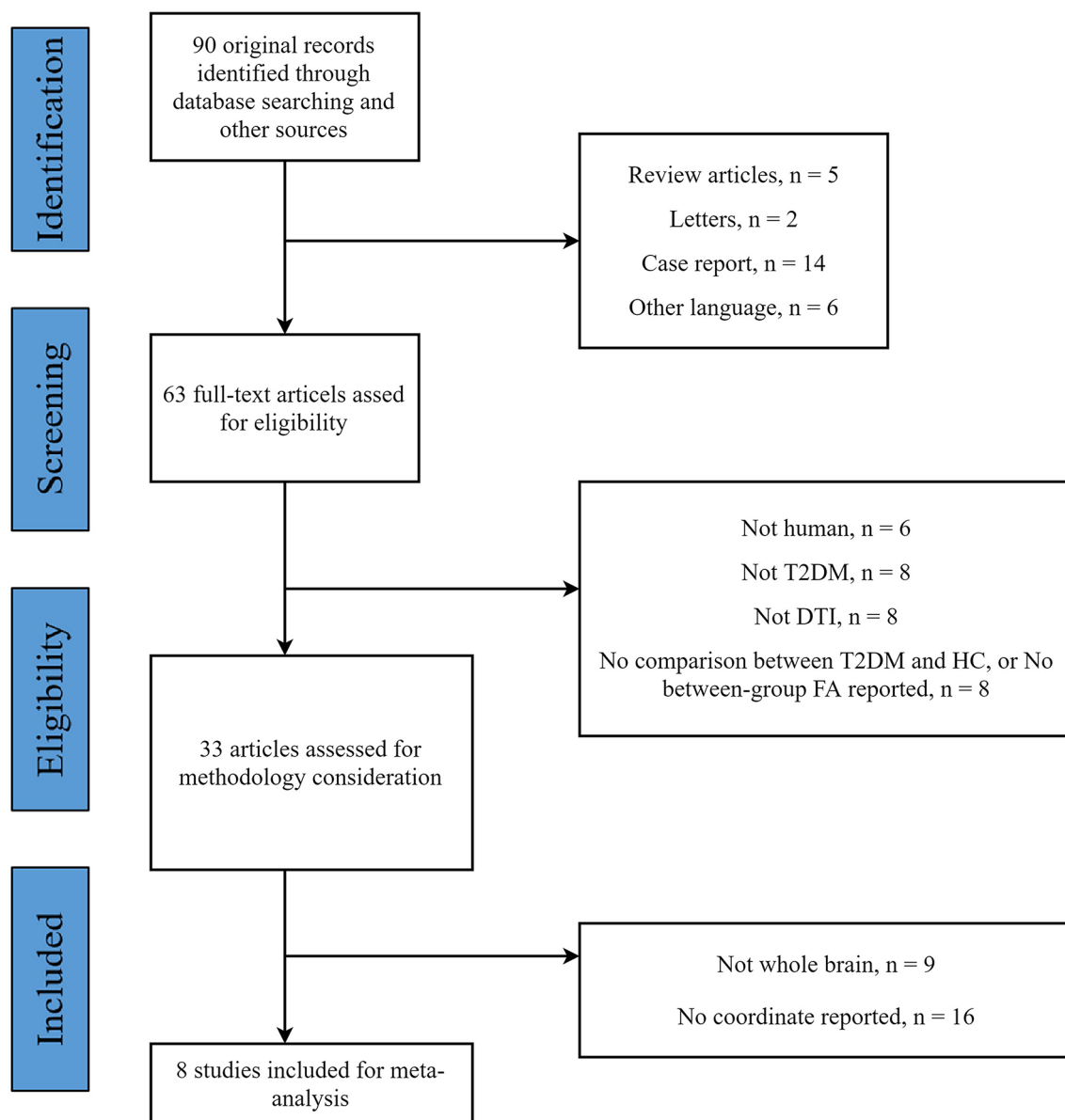


**FIGURE 1** | Flow diagram for the identification and exclusion of studies.

and the CC was highly replicable, as these findings were preserved throughout all but one combination of the datasets. FA reduction in the left olfactory cortex remained significant in all but two combinations (Table 3).

### Meta-Regression Analysis

At a stringent threshold of  $P < 0.0005$ , meta-regression analysis found a negative correlation between FA in the CC and BMI in the patients group (Table 4). The mean age of patients, illness duration, and HbA1c% were not linearly associated with FA changes.

### DISCUSSION

To our knowledge, this study is the first coordinate-based meta-analysis (CBMA) of DTI studies in T2DM patients investigating microstructural WM abnormalities and examining how clinical features affect WM morphometry. Using the AES-SDM meta-analytical approach, this study identified decreased FA in three clusters, and these three regional differences remained replicable in the Jackknife sensitivity analyses. The largest cluster exhibited a peak coordinate in the left inferior network mainly consisted of left inferior fronto-occipital fasciculus (IFOF), left inferior longitudinal

**TABLE 1 |** Demographic and clinical characteristics of the participants in eight studies included in the meta-analysis.

Study	Subjects, n (female, n)		Age, years		Diabetes duration, years	HbA1c%	BMIkg/m <sup>2</sup>	Comorbidity (number of patients)
	T2DM	HC	T2DM	HC				
Yau et al. (30)	24 (11)	17 (9)	57.2	56.4	7.9	7.8	32.1	Hypertension (16)
Yau et al. (15)	18 (N/A)	18 (N/A)	16.5	17.2	2.6	8.3	37.7	Obesity (18)
Kim et al. (34)	20 (11)	20 (11)	54.6	54.3	12.1	10.7	24.7	Hypertension (5)
								Diabetic retinopathy (9)
								Diabetic nephropathy (4)
van Bloemendaal et al. (61)	16 (8)	15 (7)	61.4	57.3	7.0	6.9	34.0	Diabetic peripheral neuropathy (7)
								Obesity (16)
								N/A
Nouwen et al. (35)	13 (13)	20 (14)	16.0	16.1	2.6	7.8	N/A	N/A
Yoon et al. (36)	100 (50)	50 (25)	49.2	49.0	1.8	7.1	25.5	Overweight/obesity (50)
Liang et al. (62)	34 (24)	32 (14)	58.3	56.3	6.9	7.9	24.4	Overweight (20)
								Obesity (1)
								Hypertension (9)
Xiong et al. (32)	20 (12)	28 (18)	63.6	59.7	9.1	8.2	24.4	Mild cognitive impairment (20)

T2DM, type 2 diabetes mellitus; HC, healthy controls; N/A, not available; BMI, body mass index.

**TABLE 2 |** Scanning methods and FA alterations of the eight studies included in this meta-analysis.

Study	Scanner	Diffusion encoding directions	Type of analysis	Statistical threshold	Number of coordinates	FA alterations
Yau et al. (30)	1.5 T	6	VBA	$P < 0.005$ , uncorrected	6	Decrease observed in L temporal stem, R prefrontal region, L frontal temporal region, R external capsule, L parietal region, and L middle temporal region
Yau et al. (15)	1.5 T	6	VBA	$P < 0.005$ , uncorrected	3	Decrease observed in R cingulate WM, L cerebral peduncle, and L temporal stem
Kim et al. (34)	3.0 T	30	TBSS	$P < 0.05$ , FWE corrected	10	Decrease observed in bilateral posterior thalamic radiation, R retrolenticular part of internal capsule, R splenium of CC, R fornix (cres)/stria terminalis, R sagittal stratum, R external capsule
van Bloemendaal et al. (61)	3.0 T	30	TBSS	$P < 0.05$ , FWE corrected	0	–
Nouwen et al. (35)	3.0 T	61	TBSS	$P < 0.05$ , TFCE corrected	9	Decrease observed in L CST, medial corpus callosum, L fornix, L thalamic radiation, L retrolenticular internal capsule, L IFOF, R anterior corona radiata, the genu of CC, L uncinate, L callosal body and cingulum, L anterior external capsule, and uncinate fasciculus
Yoon et al. (36)	1.5 T	N/A	VBA	$P < 0.05$ , corrected	22	Decrease observed in L fornix sagittal stratum, L IFOF, L uncinate fasciculus, bilateral CST, CC, bilateral anterior thalamic radiation fornix, R superior corona radiata, bilateral cerebellar WM, bilateral forceps minor, bilateral optic radiation, bilateral anterior corona radiata, L external capsule, R parietal WM, and R temporal WM
Liang et al. (62)	3.0 T	25	VBA	$P < 0.05$ , AlphaSim corrected	1	L corona
Xiong et al. (32)	3.0 T	25	TBSS	$P < 0.05$ , FWE corrected	1	R temporal lobe

CC, corpus callosum; CST, corticospinal tract; FA, fractional anisotropy; FWE, family-wise error; IFOF, inferior fronto-occipital fasciculus; N/A, not available; L, left; R, right; T, Tesla; TBSS, tract-based spatial statistics; TFCE, threshold-free cluster enhancement; VBA, voxel-based analysis; WM, white matter.

fasciculus (ILF), left uncinate fasciculus (UF), and anterior commissure. Other clusters exhibited FA reductions in the CC and the left olfactory cortex (BA25). Besides, according to the meta-regression, FA in the CC was negatively correlated with BMI in the patients group. These findings enhanced our understanding of the underlying neurodegeneration in T2DM.

Our meta-analysis only identified lower FA rather than higher FA in T2DM patients. This is in accordance with most published DTI studies of T2DM (54). As FA presents the anisotropic diffusion of water molecules and can reflect the underlying characteristics of microstructure, such as fiber density, axonal diameter, thickness of the myelin sheaths, and directionality of the fibers (27, 63), decreased FA in our findings represented disrupted WM microarchitecture in

the brain. One of the core characteristics of T2DM is insulin resistance, which interferes with glucose metabolism and even can lead to increased plasma glucose in regional brain areas in T2DM patients (52). From the microscopic point of view, hyperglycemia is considered to be related with various metabolic and molecular alterations and could result in brain cell dysfunction, degeneration, or death ultimately (52, 64). And from the macroscopic perspective, brain atrophy might be the neurobiological basis of cognitive decline (5, 6, 11). This was also in agreement with previous VBM meta-analyses of T2DM (52, 53).

The left inferior network mainly comprised the left IFOF, left ILF, left UF, and anterior commissure. Several studies support the extension of WM impairments in T2DM to other association fibers,

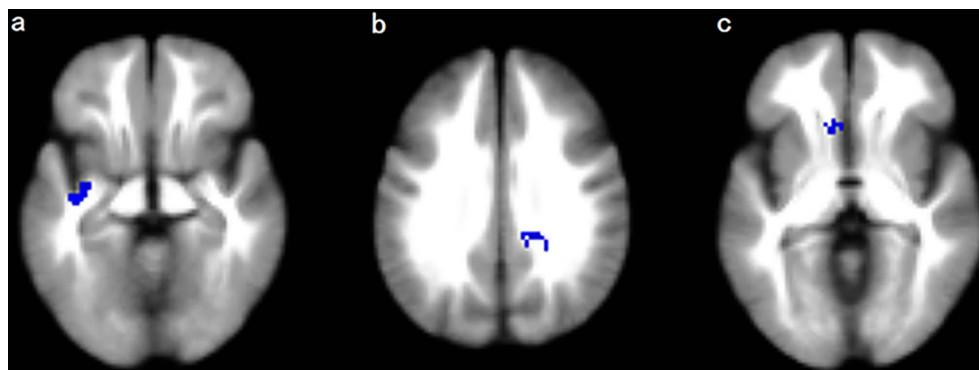


**FIGURE 2** | Regions showing FA reductions in **(A)** the left inferior network; **(B)** the corpus callosum; and **(C)** the left olfactory cortex. Significant clusters are overlaid on MNI template for Windows for display purposes only.

**TABLE 3** | White Matter Regions of FA reductions in T2DM Patients compared to healthy controls in the coordinate-based meta-analysis.

Regions	Maximum					Cluster	Jackknife sensitivity analysis		
	MNI coordinates			SDM Value	P			Number of voxels*	Breakdown (number of voxels)
	X	Y	Z						
Left inferior network, inferior fronto-occipital fasciculus	-38	-16	-10	-2.279	0.000032604	97	Left inferior network, inferior fronto-occipital fasciculus (28) Left inferior network, inferior longitudinal fasciculus (20) Anterior commissure (8) Left inferior network, uncinate fasciculus (7) Left insula, BA 48 (2) Left amygdala, BA 34 (1) Left superior temporal gyrus, BA 48 (1) BA 48 (20) BA 34 (3) BA 36 (3) BA 20 (3) BA 21 (1)	7/8	
Corpus callosum	14	-34	32	-2.107	0.000091314	55	Corpus callosum (46) Right median network, cingulum (9)	7/8	
Left olfactory cortex, BA 25	-4	20	4	-1.999	0.000228226	28	Corpus callosum (12) Left striatum (9) Left caudate nucleus, BA 25 (3) Left olfactory cortex, BA 25 (3) BA 25 (1)	6/8	

\*All voxels with  $P < 0.001$  uncorrected.

BA, Brodmann area; FA, fractional anisotropy; MNI, Montreal Neurological Institute; SDM, seed-based  $d$  mapping; T2DM, type 2 diabetes.

**TABLE 4** | Correlation between FA alterations and BMI in T2DM revealed by Meta-regression analyses.

Factor	Anatomic label	MNI coordinates			SDM Value	P	Number of voxels
		X	Y	Z			
BMI	Corpus callosum	14	-32	30	-2.390	0.000045657	58

BMI, body mass index; FA, fractional anisotropy; MNI, Montreal Neurological Institute; SDM, seed-based  $d$  mapping; T2DM, type 2 diabetes.

which pass through the temporal lobe, such as IFOF and ILF (33, 36, 54). Besides, some fibers of IFOF and UF are located in the external capsule, which associates the hippocampus and amygdala with prefrontal and orbitofrontal cortices (54, 65). Previous studies

already indicated that atrophy in temporal lobe, hippocampus, and orbitofrontal regions occurred in T2DM (2, 13, 54), and also evidence has shown that atrophy in these areas is one of the earliest neuroanatomical changes in Alzheimer's dementia (2, 36, 53).

Among the eight studies included in our meta-analysis, four of them reported microstructural abnormalities in temporal regions. Given that the vital role that the temporal lobe, the hippocampus, and the orbitofrontal cortex play in cognitive processes such as learning, memory, and decision making (66, 67), we conjectured that disruptions of WM in IFOF, ILF, and UF might be related with cognitive function deficits in T2DM patients. Besides, the comorbidity of depression and T2DM is quite common (18–21), and disrupted WM connectivity in inferior network has also been constantly found in MDD patients (29, 68, 69). Thus, microarchitecture alterations in the inferior network might also underlie potential affective changes in T2DM.

The CC is the largest interhemispheric WM commissure connecting the cerebral hemispheres, and plays crucial role in interhemispheric communication and cognitive processes (70). Microstructural changes in this core WM tract were found not only in T2DM patients in numerous research (34–36, 38, 54), but also in patients with cognitive impairment (38, 71, 72) and patients with MDD (29, 68, 73, 74). Therefore, decreased FA in the CC observed in our meta-analysis may underlie the deficits in cognitive processing and emotional modulation in patients with T2DM. Besides, there was a negative correlation between FA in the CC and BMI in T2DM patients revealed by meta-regression analysis. This was consistent with previous findings that higher BMI was associated with FA reductions in the CC in healthy cohorts (75, 76). There were DTI studies on BMI-related WM abnormalities suggesting a primordial effect of BMI on brain circuits involved in reward processing and emotion regulation (77), or even on the entire brain (75). Furthermore, there was evidence that alterations in white matter were associated with several obesity-related conditions such as cardiovascular risk factors including metabolic syndrome (78). Therefore, our finding might suggest disrupted CC microstructures as an BMI-related neurobiological marker of T2DM. The other WM tracts showed non-significant regression results, probably due to a relatively strict *P*-value in the process of statistics. Neurologic changes in the left inferior network and the left olfactory cortex might also be associated with metabolic syndrome related symptoms and these regions should receive full considerations.

It is particularly noteworthy that the left olfactory cortex exhibited decreased FA in T2DM patients. Current evidence implied that olfactory function is associated with the emergence of prodromal AD (79, 80). Scholars assumed that olfactory impairments might reflect the onset of AD, amnesic mild cognitive impairment (MCI), and the presence of amyloid- $\beta$  (A $\beta$ ) and tau pathology (79, 81–86). Thus, FA reductions in the left olfactory cortex might be served as an early prediction of cognitive impairment in T2DM patients. This was of great significance for early detection of potential cognitive decline and dementia in T2DM patients. Moreover, olfactory function was also found to be related to the pathogenesis of MDD (87). Olfactory sulcus structural abnormality might be a trait-related marker of vulnerability to MDD (88). In consideration of the high prevalence of comorbidity of depression and T2DM, olfactory cortex alterations might be involved in the pathophysiology of the co-morbidity.

Several limitations of this study should be noted. Firstly, as the number of studies included in our meta-analysis was small,

we were not able to perform separate subgroup meta-analyses for clinical variables such as cognition status, depression severity, and BMI, or methodological differences such as VBA and TBSS, which would likely diversify the results. Secondly, the data acquisition parameters, participants characteristics and clinical variables in the included studies were heterogeneous. It is not possible to eliminate these differences by statistical means. Thirdly, our analysis was limited to WM diffusion changes thereby not including the large amount of research on GM volume or WM volume. Future meta-analysis could include VBM studies for a more comprehensive perspective of the brain microarchitecture. Last but not least, it is meaningful to work on the reversibility of nerve damage, but the present meta-analysis and the literatures included in our research are all cross-sectional design. Longitudinal studies with respect to reversibility of the neurodegeneration of T2DM is of great importance and should be addressed in the future.

## CONCLUSION

The present meta-analysis indicated that T2DM patients demonstrated significant FA reductions in the left inferior network, the CC and the left olfactory cortex. Among them, FA of the CC had a negative correlation with BMI in the patients group. These findings supported the opinion that T2DM could lead to subtle WM structural alterations, which might be associated with cognitive deficits or emotional distress in T2DM patients. This helps us better understand the neural mechanism underlying neurodegeneration in T2DM.

## DATA AVAILABILITY STATEMENT

The original contributions presented in the study are included in the article/supplementary material. Further inquiries can be directed to the corresponding author.

## AUTHOR CONTRIBUTIONS

CZ designed the study and revised the manuscript. CZ wrote the initial manuscript. CZ and JL collected the data and undertook the statistical analysis. MD and LP assisted with data collection and statistical analysis and modified the paper. HL, YW, SW, SG, and GY assisted with data collection and data analysis. YC and XX critically reviewed and modified the paper. All authors contributed to the article and approved the submitted version.

## FUNDING

This study was supported by the Medical and Health Science and Technology Development Plan of Shandong Province (202003061210), and the Supporting Fund for Teachers' Research of Jining Medical University. The Supporting Fund for Teachers' Research of Jining Medical University (600903001).

## REFERENCES

- Krentz N, Gloy A. Insights Into Pancreatic Islet Cell Dysfunction From Type 2 Diabetes Mellitus Genetics. *Nat Rev Endocrinol* (2020) 16(4):202–12. doi: 10.1038/s41574-020-0325-0
- Brundel M, Kappelle LJ, Biessels GJ. Brain Imaging in Type 2 Diabetes. *Eur Neuropsychopharmacol* (2014) 24(12):1967–81. doi: 10.1016/j.euroneuro.2014.01.023
- Li Y, Teng D, Shi X, Qin G, Qin Y, Quan H, et al. Prevalence of Diabetes Recorded in Mainland China Using 2018 Diagnostic Criteria From the American Diabetes Association: National Cross Sectional Study. *Bmj* (2020) 369. doi: 10.1136/bmj.m997
- Klein JP, Waxman SG. The Brain in Diabetes: Molecular Changes in Neurons and Their Implications for End-Organ Damage. *Lancet Neurol* (2003) 2(9):548–54. doi: 10.1016/s1474-4422(03)00503-9
- Biessels GJ, Strachan MWJ, Visseren FLJ, Kappelle LJ, Whitmer RA. Dementia and Cognitive Decline in Type 2 Diabetes and Prediabetic Stages: Towards Targeted Interventions. *Lancet Diabetes Endocrinol* (2014) 2(3):246–55. doi: 10.1016/s2213-8587(13)70088-3
- Ryan JP, Fine DF, Rosano C. Type 2 Diabetes and Cognitive Impairment: Contributions From Neuroimaging. *J Geriatr Psychiatry Neurol* (2014) 27(1):47–55. doi: 10.1177/0891988713516543
- Biessels GJ, Nobili F, Teunissen CE, Simó R, Scheltens P. Understanding Multifactorial Brain Changes in Type 2 Diabetes: A Biomarker Perspective. *Lancet Neurol* (2020) 19(8):699–710. doi: 10.1016/s1474-4422(20)30139-3
- Lu FP, Lin KP, Kuo HK. Diabetes and the Risk of Multi-System Aging Phenotypes: A Systematic Review and Meta-Analysis. *PloS One* (2009) 4(1):e4144. doi: 10.1371/journal.pone.0004144
- Danna SM, Graham E, Burns RJ, Deschenes SS, Schmitz N. Association Between Depressive Symptoms and Cognitive Function in Persons With Diabetes Mellitus: A Systematic Review. *PloS One* (2016) 11(8):e0160809. doi: 10.1371/journal.pone.0160809
- Moran C, Beare R, Wang W, Callisaya M, Srikanth V. Alzheimer's Disease Neuroimaging I. Type 2 Diabetes Mellitus, Brain Atrophy, and Cognitive Decline. *Neurology* (2019) 92(8):e823–e30. doi: 10.1212/WNL.0000000000006955
- Callisaya ML, Beare R, Moran C, Phan T, Wang W, Srikanth VK. Type 2 Diabetes Mellitus, Brain Atrophy and Cognitive Decline in Older People: A Longitudinal Study. *Diabetologia* (2019) 62(3):448–58. doi: 10.1007/s00125-018-4778-9
- Shi L, Cheng Y, Xu Y, Shen Z, Lu Y, Zhou C, et al. Effects of Hypertension on Cerebral Cortical Thickness Alterations in Patients With Type 2 Diabetes. *Diabetes Res Clin Pract* (2019) 157:107872. doi: 10.1016/j.diabres.2019.107872
- Rosenberg J, Lechea N, Pentang GN, Shah NJ. What Magnetic Resonance Imaging Reveals - A Systematic Review of the Relationship Between Type II Diabetes and Associated Brain Distortions of Structure and Cognitive Functioning. *Front Neuroendocrinol* (2019) 52:79–112. doi: 10.1016/j.yfrne.2018.10.001
- Brundel M, van den Heuvel M, de Bresser J, Kappelle LJ, Biessels GJ. Utrecht Diabetic Encephalopathy Study G. Cerebral Cortical Thickness in Patients With Type 2 Diabetes. *J Neurol Sci* (2010) 299(1-2):126–30. doi: 10.1016/j.jns.2010.08.048
- Yau PL, Javier DC, Ryan CM, Tsui WH, Ardekani BA, Ten S, et al. Preliminary Evidence for Brain Complications in Obese Adolescents With Type 2 Diabetes Mellitus. *Diabetologia* (2010) 53(11):2298–306. doi: 10.1007/s00125-010-1857-y
- Pouwer F. Should We Screen for Emotional Distress in Type 2 Diabetes Mellitus? *Nat Rev Endocrinol* (2009) 5(12):665–71. doi: 10.1038/nrendo.2009.214
- Xia W, Luo Y, Chen YC, Zhang D, Bo F, Zhou P, et al. Disrupted Functional Connectivity of the Amygdala is Associated With Depressive Mood in Type 2 Diabetes Patients. *J Affect Disord* (2018) 228:207–15. doi: 10.1016/j.jad.2017.12.012
- Darwish L, Beroncal E, Sison MV, Swardfager W. Depression in People With Type 2 Diabetes: Current Perspectives. *Diabetes Metab Syndr Obes* (2018) 11:333–43. doi: 10.2147/DMSO.S106797
- Huang CJ, Hsieh HM, Tu HP, Jiang HJ, Wang PW, Lin CH. Major Depressive Disorder in Patients With Type 2 Diabetes Mellitus: Prevalence and Clinical Characteristics. *J Affect Disord* (2018) 227:141–8. doi: 10.1016/j.jad.2017.09.044
- Hussain S, Habib A, Singh A, Akhtar M, Najmi AK. Prevalence of Depression Among Type 2 Diabetes Mellitus Patients in India: A Meta-Analysis. *Psychiatry Res* (2018) 270:264–73. doi: 10.1016/j.psychres.2018.09.037
- Salinero-Fort MA, Gomez-Campelo P, San Andres-Rebollo FJ, Cardenas-Valladolid J, Abanades-Herranz JC, Carrillo de Santa Pau E, et al. Prevalence of Depression in Patients With Type 2 Diabetes Mellitus in Spain (the DIADEMA Study): Results From the MADIABETES Cohort. *BMJ Open* (2018) 8(9):e020768. doi: 10.1136/bmjopen-2017-020768
- van Sloten TT, Sedaghat S, Carnethon MR, Launer LJ, Stehouwer CDA. Cerebral Microvascular Complications of Type 2 Diabetes: Stroke, Cognitive Dysfunction, and Depression. *Lancet Diabetes Endocrinol* (2020) 8(4):325–36. doi: 10.1016/s2213-8587(19)30405-x
- Le Bihan D, Mangin JF, Poupon C, Clark CA, Pappata S, Molko N, et al. Diffusion Tensor Imaging: Concepts and Applications. *J Magnet Resonance Imaging: JMIR* (2001) 13(4):534–46. doi: 10.1002/jmri.1076
- Beaulieu C. The Basis of Anisotropic Water Diffusion in the Nervous System - a Technical Review. *NMR Biomed* (2002) 15(7-8):435–55. doi: 10.1002/nbm.782
- Schiavone F, Charlton RA, Barrick TR, Morris RG, Markus HS. Imaging Age-Related Cognitive Decline: A Comparison of Diffusion Tensor and Magnetization Transfer MRI. *J Magnet Resonance Imaging: JMIR* (2009) 29(1):23–30. doi: 10.1002/jmri.21572
- Zhuang L, Sachdev PS, Trollor JN, Kochan NA, Reppermund S, Brodaty H, et al. Microstructural White Matter Changes in Cognitively Normal Individuals At Risk of Amnesic MCI. *Neurology* (2012) 79(8):748–54. doi: 10.1212/WNL.0b013e3182661f4d
- Koch K, Reess TJ, Rus OG, Zimmer C, Zaudig M. Diffusion Tensor Imaging (DTI) Studies in Patients With Obsessive-Compulsive Disorder (OCD): A Review. *J Psychiatr Res* (2014) 54:26–35. doi: 10.1016/j.jpsychires.2014.03.006
- Smith SM, Jenkinson M, Johansen-Berg H, Rueckert D, Nichols TE, Mackay CE, et al. Tract-Based Spatial Statistics: Voxelwise Analysis of Multi-Subject Diffusion Data. *NeuroImage* (2006) 31(4):1487–505. doi: 10.1016/j.neuroimage.2006.02.024
- Jiang J, Zhao YJ, Hu XY, Du MY, Chen ZQ, Wu M, et al. Microstructural Brain Abnormalities in Medication-Free Patients With Major Depressive Disorder: A Systematic Review and Meta-Analysis of Diffusion Tensor Imaging. *J Psychiatry Neurosci: JPN* (2017) 42(3):150–63. doi: 10.1503/jpn.150341
- Yau PL, Javier D, Tsui W, Sweat V, Bruehl H, Borod JC, et al. Emotional and Neutral Declarative Memory Impairments and Associated White Matter Microstructural Abnormalities in Adults With Type 2 Diabetes. *Psychiatry Res* (2009) 174(3):223–30. doi: 10.1016/j.psychres.2009.04.016
- Hsu JL, Chen YL, Leu JG, Jaw FS, Lee CH, Tsai YF, et al. Microstructural White Matter Abnormalities in Type 2 Diabetes Mellitus: A Diffusion Tensor Imaging Study. *NeuroImage* (2012) 59(2):1098–105. doi: 10.1016/j.neuroimage.2011.09.041
- Xiong Y, Zhang S, Shi J, Fan Y, Zhang Q, Zhu W. Application of Neurite Orientation Dispersion and Density Imaging to Characterize Brain Microstructural Abnormalities in Type-2 Diabetics With Mild Cognitive Impairment. *J Magnet Resonance Imaging: JMIR* (2019) 50(3):889–98. doi: 10.1002/jmri.26687
- Zhang JH, Xu HZ, Shen QF, Lin YZ, Sun CK, Sha L, et al. Nepsilon-(Carboxymethyl)-Lysine, White Matter, and Cognitive Function in Diabetes Patients. *Can J Neurol Sci Le J Canadien Des Sci Neurol* (2016) 43(4):518–22. doi: 10.1017/cjn.2015.398
- Kim DJ, Yu JH, Shin MS, Shin YW, Kim MS. Hyperglycemia Reduces Efficiency of Brain Networks in Subjects With Type 2 Diabetes. *PloS One* (2016) 11(6):e0157268. doi: 10.1371/journal.pone.0157268
- Nouwen A, Chambers A, Chechla M, Higgs S, Blissett J, Barrett TG, et al. Microstructural Abnormalities in White and Gray Matter in Obese Adolescents With and Without Type 2 Diabetes. *NeuroImage Clin* (2017) 16:43–51. doi: 10.1016/j.nicl.2017.07.004
- Yoon S, Cho H, Kim J, Lee DW, Kim GH, Hong YS, et al. Brain Changes in Overweight/Obese and Normal-Weight Adults With Type 2 Diabetes Mellitus. *Diabetologia* (2017) 60(7):1207–17. doi: 10.1007/s00125-017-4266-7
- Hoogenboom WS, Marder TJ, Flores VL, Huisman S, Eaton HP, Schneiderman JS, et al. Cerebral White Matter Integrity and Resting-State

- Functional Connectivity in Middle-Aged Patients With Type 2 Diabetes. *Diabetes* (2014) 63(2):728–38. doi: 10.2337/db13-1219
38. Zhang J, Wang Y, Wang J, Zhou X, Shu N, Wang Y, et al. White Matter Integrity Disruptions Associated With Cognitive Impairments in Type 2 Diabetic Patients. *Diabetes* (2014) 63(11):3596–605. doi: 10.2337/db14-0342
  39. Fox PT, Lancaster JL, Laird AR, Eickhoff SB. Meta-Analysis in Human Neuroimaging: Computational Modeling of Large-Scale Databases. *Annu Rev Neurosci* (2014) 37:409–34. doi: 10.1146/annurev-neuro-062012-170320
  40. Radua J, Mataix-Cols D, Phillips ML, El-Hage W, Kronhaus DM, Cardoner N, et al. A New Meta-Analytic Method for Neuroimaging Studies That Combines Reported Peak Coordinates and Statistical Parametric Maps. *Eur Psychiatry: J Assoc Eur Psychiatrists* (2012) 27(8):605–11. doi: 10.1016/j.eurpsy.2011.04.001
  41. Turkeltaub PE, Eden GF, Jones KM, Zeffiro TA. Meta-Analysis of the Functional Neuroanatomy of Single-Word Reading: Method and Validation. *NeuroImage* (2002) 16(3-part-PA):765–80. doi: 10.1006/nimg.2002.1131
  42. Wager TD, Lindquist M, Kaplan L. Meta-Analysis of Functional Neuroimaging Data: Current and Future Directions. *Soc Cogn Affect Neurosci* (2007) 2(2):150. doi: 10.1093/scan/nsm015
  43. Radua J, Mataix-Cols D. Voxel-Wise Meta-Analysis of Grey Matter Changes in Obsessive-Compulsive Disorder. *Br J Psychiatry: J Ment Sci* (2009) 195(5):393–402. doi: 10.1192/bjp.bp.108.055046
  44. Radua J, Rubia K, Canales-Rodriguez EJ, Pomarol-Clotet E, Fusar-Poli P, Mataix-Cols D. Anisotropic Kernels for Coordinate-Based Meta-Analyses of Neuroimaging Studies. *Front Psychiatry* (2014) 5:13. doi: 10.3389/fpsy.2014.00013
  45. Suo X, Lei D, Li W, Li L, Dai J, Wang S, et al. Altered White Matter Microarchitecture in Parkinson's Disease: A Voxel-Based Meta-Analysis of Diffusion Tensor Imaging Studies. *Front Med* (2020) 15(1):125–38. doi: 10.1007/s11684-019-0725-5
  46. Mihaescu AS, Masellis M, Graff-Guerrero A, Kim J, Criaud M, Cho SS, et al. Brain Degeneration in Parkinson's Disease Patients With Cognitive Decline: A Coordinate-Based Meta-Analysis. *Brain Imaging Behav* (2019) 13(4):1021–34. doi: 10.1007/s11682-018-9922-0
  47. Nortje G, Stein DJ, Radua J, Mataix-Cols D, Horn N. Systematic Review and Voxel-Based Meta-Analysis of Diffusion Tensor Imaging Studies in Bipolar Disorder. *J Affect Disord* (2013) 150(2):192–200. doi: 10.1016/j.jad.2013.05.034
  48. Hu X, Zhang L, Bu X, Li H, Gao Y, Lu L, et al. White Matter Disruption in Obsessive-Compulsive Disorder Revealed by Meta-Analysis of Tract-Based Spatial Statistics. *Depress Anxiety* (2020) 37(7):620–31. doi: 10.1002/da.23008
  49. Zhang Z, Ping L, Zhai A, Zhou C. Microstructural White Matter Abnormalities in Obsessive-Compulsive Disorder: A Coordinate-Based Meta-Analysis of Diffusion Tensor Imaging Studies. *Asian J Psychiatry* (2020) 55. doi: 10.1016/j.ajp.2020.102467
  50. Radua J, Via E, Catani M, Mataix-Cols D. Voxel-Based Meta-Analysis of Regional White-Matter Volume Differences in Autism Spectrum Disorder Versus Healthy Controls. *psychol Med* (2011) 41(7):1539–50. doi: 10.1017/S0033291710002187
  51. Liu J, Fan W, Jia Y, Su X, Wu W, Long X, et al. Altered Gray Matter Volume in Patients With Type 1 Diabetes Mellitus. *Front Endocrinol* (2020) 11:45. doi: 10.3389/fendo.2020.00045
  52. Liu J, Liu T, Wang W, Ma L, Ma X, Shi S, et al. Reduced Gray Matter Volume in Patients With Type 2 Diabetes Mellitus. *Front Aging Neurosci* (2017) 9:161. doi: 10.3389/fnagi.2017.00161
  53. Wu G, Lin L, Zhang Q, Wu J. Brain Gray Matter Changes in Type 2 Diabetes Mellitus: A Meta-Analysis of Whole-Brain Voxel-Based Morphometry Study. *J Diabetes its Complications* (2017) 31(12):1698–703. doi: 10.1016/j.jdiacomp.2017.09.001
  54. Sanjari Moghaddam H, Ghazi Sherbaf F, Aarabi MH. Brain Microstructural Abnormalities in Type 2 Diabetes Mellitus: A Systematic Review of Diffusion Tensor Imaging Studies. *Front Neuroendocrinol* (2019) 55:100782. doi: 10.1016/j.yfrne.2019.100782
  55. Moher D, Liberati A, Tetzlaff J, Altman DG, Group P. Preferred Reporting Items for Systematic Reviews and Meta-Analyses: The PRISMA Statement. *J Clin Epidemiol* (2009) 62(10):1006–12. doi: 10.1016/j.jclinepi.2009.06.005
  56. Liberati A, Altman DG, Tetzlaff J, Mulrow C, Gotzsche PC, Ioannidis JP, et al. The PRISMA Statement for Reporting Systematic Reviews and Meta-Analyses of Studies That Evaluate Healthcare Interventions: Explanation and Elaboration. *Bmj* (2009) 339:b2700. doi: 10.1136/bmj.b2700
  57. Moher D, Liberati A, Tetzlaff J, Altman DG. Preferred Reporting Items for Systematic Reviews and Meta-Analyses: The PRISMA Statement. *PloS Med* (2009) 6(10):1006–12. doi: 10.1371/journal.pmed.1000097
  58. Muller VI, Cieslik EC, Laird AR, Fox PT, Radua J, Mataix-Cols D, et al. Ten Simple Rules for Neuroimaging Meta-Analysis. *Neurosci Biobehav Rev* (2018) 84:151–61. doi: 10.1016/j.neubiorev.2017.11.012
  59. Albajes-Eizaguirre A, Solanes A, Vieta E, Radua J. Voxel-Based Meta-Analysis Via Permutation of Subject Images (PSI): Theory and Implementation for SDM. *NeuroImage* (2019) 186:174–84. doi: 10.1016/j.neuroimage.2018.10.077
  60. Yang C, Hu X, Luo Q, Kuang W, Lui S, Huang X, et al. Psychoradiologic Abnormalities of White Matter in Patients With Bipolar Disorder: Diffusion Tensor Imaging Studies Using Tract-Based Spatial Statistics. *J Psychiatry Neurosci* (2019) 44(1):32–44. doi: 10.1503/jpn.170221
  61. van Bloemendaal L, Ijzerman RG, Ten Kulve JS, Barkhof F, Diamant M, Veltman DJ, et al. Alterations in White Matter Volume and Integrity in Obesity and Type 2 Diabetes. *Metab Brain Dis* (2016) 31(3):621–9. doi: 10.1007/s11011-016-9792-3
  62. Liang Y, Zhang H, Tan X, Liu J, Qin C, Zeng H, et al. Local Diffusion Homogeneity Provides Supplementary Information in T2DM-Related Wm Microstructural Abnormality Detection. *Front Neurosci* (2019) 13:63. doi: 10.3389/fnins.2019.00063
  63. Alger JR. The Diffusion Tensor Imaging Toolbox. *J Neurosci* (2012) 32(22):7418–28. doi: 10.1523/JNEUROSCI.4687-11.2012
  64. Tomlinson DR, Gardiner NJ. Glucose Neurotoxicity. *Nat Rev Neurosci* (2008) 9(1):36–45. doi: 10.1038/nrn2294
  65. Shott ME, Cornier MA, Mittal VA, Pryor TL, Orr JM, Brown MS, et al. Orbitofrontal Cortex Volume and Brain Reward Response in Obesity. *Int J Obes* (2015) 39(2):214–21. doi: 10.1038/ijo.2014.121
  66. Bell B, Lin JJ, Seidenberg M, Hermann B. The Neurobiology of Cognitive Disorders in Temporal Lobe Epilepsy. *Nat Rev Neurol* (2011) 7(3):154–64. doi: 10.1038/nrneurol.2011.3
  67. Wikenheiser AM, Schoenbaum G. Over the River, Through the Woods: Cognitive Maps in the Hippocampus and Orbitofrontal Cortex. *Nat Rev Neurosci* (2016) 17(8):513–23. doi: 10.1038/nrn.2016.56
  68. Liao Y, Huang X, Wu Q, Yang C, Kuang W, Du M, et al. Is Depression a Disconnection Syndrome? Meta-analysis of Diffusion Tensor Imaging Studies in Patients With MDD. *J Psychiatry Neurosci JPN* (2013) 38(1):49–56. doi: 10.1503/jpn.110180
  69. Chen G, Guo Y, Zhu H, Kuang W, Bi F, Ai H, et al. Intrinsic Disruption of White Matter Microarchitecture in First-Episode, Drug-Naive Major Depressive Disorder: A Voxel-Based Meta-Analysis of Diffusion Tensor Imaging. *Prog Neuropsychopharmacol Biol Psychiatry* (2017) 76:179–87. doi: 10.1016/j.pnpbp.2017.03.011
  70. Saito Y, Nobuhara K, Okugawa G, Takase K, Sugimoto T, Horiuchi M, et al. Corpus Callosum in Patients With Obsessive-Compulsive Disorder: Diffusion-Tensor Imaging Study. *Radiology* (2008) 246(2):536–42. doi: 10.1148/radiol.2462061469
  71. Brueggen K, Dyrba M, Cardenas-Blanco A, Schneider A, Fließbach K, Buerger K, et al. Structural Integrity in Subjective Cognitive Decline, Mild Cognitive Impairment and Alzheimer's Disease Based on Multicenter Diffusion Tensor Imaging. *J Neurol* (2019) 266(10):2465–74. doi: 10.1007/s00415-019-09429-3
  72. Lo Buono V, Palmeri R, Corallo F, Allone C, Pria D, Bramanti P, et al. Diffusion Tensor Imaging of White Matter Degeneration in Early Stage of Alzheimer's Disease: A Review. *Int J Neurosci* (2020) 130(3):243–50. doi: 10.1080/00207454.2019.1667798
  73. Xu K, Jiang W, Ren L, Ouyang X, Jiang Y, Wu F, et al. Impaired Interhemispheric Connectivity in Medication-Naive Patients With Major Depressive Disorder. *J Psychiatry Neurosci JPN* (2013) 38(1):43–8. doi: 10.1503/jpn.110132
  74. Wise T, Radua J, Nortje G, Cleare A, Young A, Arnott D. Voxel-Based Meta-Analytical Evidence of Structural Disconnectivity in Major Depression and Bipolar Disorder. *Biol Psychiatry* (2016) 79(4):293–302. doi: 10.1016/j.biopsych.2015.03.004
  75. Repple J, Opel N, Meinert S, Redlich R, Hahn T, Winter NR, et al. Elevated Body-Mass Index is Associated With Reduced White Matter Integrity in Two

- Large Independent Cohorts. *Psychoneuroendocrinology* (2018) 91:179–85. doi: 10.1016/j.psyneuen.2018.03.007
76. Xu J, Li Y, Lin H, Sinha R, Potenza MN. Body Mass Index Correlates Negatively With White Matter Integrity in the Fornix and Corpus Callosum: A Diffusion Tensor Imaging Study. *Hum Brain Mapp* (2013) 34 (5):1044–52. doi: 10.1002/hbm.21491
  77. Papageorgiou I, Astrakas LG, Xydis V, Alexiou GA, Bargiotas P, Tzarouchi L, et al. Abnormalities of Brain Neural Circuits Related to Obesity: A Diffusion Tensor Imaging Study. *Magnet Resonance Imaging* (2017) 37:116–21. doi: 10.1016/j.mri.2016.11.018
  78. Alfaro FJ, Gavrieli A, Saade-Lemus P, Lioutas VA, Upadhyay J, Novak V. White Matter Microstructure and Cognitive Decline in Metabolic Syndrome: A Review of Diffusion Tensor Imaging. *Metabol: Clin Exp* (2018) 78:52–68. doi: 10.1016/j.metabol.2017.08.009
  79. Murphy C. Olfactory and Other Sensory Impairments in Alzheimer Disease. *Nat Rev Neurol* (2019) 15(1):11–24. doi: 10.1038/s41582-018-0097-5
  80. Swan GE, Carmelli D. Impaired Olfaction Predicts Cognitive Decline in Nondemented Older Adults. *Neuroepidemiology* (2002) 21(2):58–67. doi: 10.1159/000048618
  81. Dhillon Albers A, Asafu-Adjei J, Delaney MK, Kelly KE, Gomez-Isla T, Blacker D, et al. Episodic Memory of Odors Stratifies Alzheimer Biomarkers in Normal Elderly. *Ann Neurol* (2016) 80(6):846–57. doi: 10.1002/ana.24792
  82. Vassilaki M, Christianson TJ, Mielke MM, Geda YE, Kremers WK, Machulda MM, et al. Neuroimaging Biomarkers and Impaired Olfaction in Cognitively Normal Individuals. *Ann Neurol* (2017) 81(6):871–82. doi: 10.1002/ana.24960
  83. Murphy C, Jernigan TL, Fennema-Notestine C. Left Hippocampal Volume Loss in Alzheimer's Disease is Reflected in Performance on Odor Identification: A Structural MRI Study. *J Int Neuropsychol Soc* (2003) 9 (3):459–71. doi: 10.1017/S1355617703930116
  84. Growdon ME, Schultz AP, Dagley AS, Amariglio RE, Hedden T, Rentz DM, et al. Odor Identification and Alzheimer Disease Biomarkers in Clinically Normal Elderly. *Neurology* (2015) 84(21):2153. doi: 10.1212/WNL.0000000000001614
  85. Lafaille-Magnan M-E, Poirier J, Etienne P, Tremblay-Mercier J, Frenette J, Rosa-Neto P, et al. Odor Identification as a Biomarker of Preclinical AD in Older Adults At Risk. *Neurology* (2017) 89(4):327–35. doi: 10.1212/WNL.0000000000004159
  86. Attems J, Walker L, Jellinger KA. Olfactory Bulb Involvement in Neurodegenerative Diseases. *Acta Neuropathol* (2014) 127(4):459–75. doi: 10.1007/s00401-014-1261-7
  87. Wang F, Wu X, Gao J, Li Y, Zhu Y, Fang Y. The Relationship of Olfactory Function and Clinical Traits in Major Depressive Disorder. *Behav Brain Res* (2020) 386:112594. doi: 10.1016/j.bbr.2020.112594
  88. Takahashi T, Nishikawa Y, Yucel M, Whittle S, Lorenzetti V, Walterfang M, et al. Olfactory Sulcus Morphology in Patients With Current and Past Major Depression. *Psychiatry Res Neuroimaging* (2016) 255:60–5. doi: 10.1016/j.pscychres.2016.07.008

**Conflict of Interest:** The authors declare that the research was conducted in the absence of any commercial or financial relationships that could be construed as a potential conflict of interest.

Copyright © 2021 Zhou, Li, Dong, Ping, Lin, Wang, Wang, Gao, Yu, Cheng and Xu. This is an open-access article distributed under the terms of the Creative Commons Attribution License (CC BY). The use, distribution or reproduction in other forums is permitted, provided the original author(s) and the copyright owner(s) are credited and that the original publication in this journal is cited, in accordance with accepted academic practice. No use, distribution or reproduction is permitted which does not comply with these terms.



# Attenuated Induction of the Unfolded Protein Response in Adult Human Primary Astrocytes in Response to Recurrent Low Glucose

## OPEN ACCESS

### Edited by:

Cristina García Cáceres,  
Ludwig Maximilian University of  
Munich, Germany

### Reviewed by:

Ophélie Le Thuc,  
Helmholtz Center Munich, Germany  
Ismael González-García,  
Helmholtz-Gemeinschaft Deutscher  
Forschungszentren (HZ), Germany

### \*Correspondence:

Emma L. Dempster  
e.l.dempster@exeter.ac.uk  
Craig Beall  
c.beall@exeter.ac.uk

<sup>†</sup>These authors have contributed  
equally to this work

<sup>‡</sup>These authors share  
senior authorship

### Specialty section:

This article was submitted to  
Diabetes: Molecular Mechanisms,  
a section of the journal  
Frontiers in Endocrinology

**Received:** 24 February 2021

**Accepted:** 03 May 2021

**Published:** 26 May 2021

### Citation:

Weightman Potter PG, Washer SJ,  
Jeffries AR, Holley JE, Gutowski NJ,  
Dempster EL and Beall C (2021)  
*Attenuated Induction of the Unfolded  
Protein Response in Adult Human  
Primary Astrocytes in Response  
to Recurrent Low Glucose.*  
*Front. Endocrinol.* 12:671724.  
doi: 10.3389/fendo.2021.671724

Paul G. Weightman Potter<sup>1†</sup>, Sam J. Washer<sup>1†</sup>, Aaron R. Jeffries<sup>1</sup>, Janet E. Holley<sup>2</sup>,  
Nick J. Gutowski<sup>2</sup>, Emma L. Dempster<sup>1\*‡</sup> and Craig Beall<sup>1\*‡</sup>

<sup>1</sup> Institute of Biomedical and Clinical Sciences, University of Exeter Medical School, Exeter, United Kingdom, <sup>2</sup> Royal Devon  
and Exeter Hospital, University of Exeter Medical School and the Department of Neurology, Exeter, United Kingdom

**Aims/hypothesis:** Recurrent hypoglycaemia (RH) is a major side-effect of intensive insulin therapy for people with diabetes. Changes in hypoglycaemia sensing by the brain contribute to the development of impaired counterregulatory responses to and awareness of hypoglycaemia. Little is known about the intrinsic changes in human astrocytes in response to acute and recurrent low glucose (RLG) exposure.

**Methods:** Human primary astrocytes (HPA) were exposed to zero, one, three or four bouts of low glucose (0.1 mmol/l) for three hours per day for four days to mimic RH. On the fourth day, DNA and RNA were collected. Differential gene expression and ontology analyses were performed using DESeq2 and GSeq, respectively. DNA methylation was assessed using the Infinium MethylationEPIC BeadChip platform.

**Results:** 24 differentially expressed genes (DEGs) were detected (after correction for multiple comparisons). One bout of low glucose exposure had the largest effect on gene expression. Pathway analyses revealed that endoplasmic-reticulum (ER) stress-related genes such as *HSPA5*, *XBP1*, and *MANF*, involved in the unfolded protein response (UPR), were all significantly increased following low glucose (LG) exposure, which was diminished following RLG. There was little correlation between differentially methylated positions and changes in gene expression yet the number of bouts of LG exposure produced distinct methylation signatures.

**Conclusions/interpretation:** These data suggest that exposure of human astrocytes to transient LG triggers activation of genes involved in the UPR linked to endoplasmic reticulum (ER) stress. Following RLG, the activation of UPR related genes was diminished, suggesting attenuated ER stress. This may be a consequence of a successful metabolic adaptation, as previously reported, that better preserves intracellular energy levels and a reduced necessity for the UPR.

**Keywords:** recurrent low glucose, unfolded protein response, ER stress, human primary astrocytes, transcriptome (RNA-seq)

## INTRODUCTION

Iatrogenic hypoglycaemia is a limiting factor to optimal glycaemic control in people with type 1 (T1D) and insulin/sulphonylurea-treated type 2 diabetes [T2D (1)]. Acutely, severe hypoglycaemia, defined as requiring help from a third party for recovery, can lead to brain damage or death, in extreme but rare circumstances. Importantly the detection of hypoglycaemia and activation of appropriate counterregulatory responses (CRR) to reverse hypoglycaemia, are mediated to large extent by the central detection of hypoglycaemia (2). Moreover, frequent exposure to hypoglycaemia leads to defective CRR. Specifically the magnitude of the glucose-raising catecholamine response during hypoglycaemia is suppressed and triggered at a lower plasma glucose level, combined with an often absent glucagon response (3). These changes are, at least in part, driven by changes in brain hypoglycaemia-sensing nuclei, including the ventromedial hypothalamus [VMH (4)] and hindbrain (5).

Activation of CRR can be induced by administration of glucoprivic agents such as 2-deoxy-glucose [2DG (6)] and 5-thio-D-glucose (7) to discrete brain nuclei. Glucose sensing neurons found in nuclei of the hypothalamus and hindbrain detect changes in glucose concentration (8, 9). However, recently astrocytes have been implicated in direct glucose sensing and altering neuronal output (10, 11). For example, the expression of the glucose transporter GLUT2 is required in astrocytes but not neurons for a robust response to glucoprivation (12). Moreover, astrocytes in *ex vivo* brain slices containing the nucleus of the tractus solaris [NTS (6)], were activated by low glucose or 2DG. Furthermore, blocking astrocytic metabolism with fluorocitrate prevented increases in gastric motility normally associated with hypoglycaemia (13). In response to low glucose, astrocytes in the NTS increase intracellular calcium levels which occur before and independently of neuronal activity (14). Recently it has also been

shown that blockade of purinergic signalling from astrocytes also blocks 2DG-induced CRR (11, 15). In addition, astrocytic glutamate uptake is impaired following RH, contributing to counterregulatory failure (16). Together these data suggest an active role of astrocytes in glucose detection, despite this evidence little is known about the intrinsic changes within astrocytes, especially human astrocytes, following recurrent low glucose (RLG). In this study, we used both RNA sequencing and an epigenome-wide association study (EWAS) of DNA methylation (DNAm) to examine for the first time, changes to the human astrocyte transcriptome and methylome following acute and recurrent low glucose exposure.

## RESEARCH DESIGN AND METHODS

### Astrocyte Isolation and Cell Culture

HPA cells were isolated from post-mortem sub-ventricular deep white matter following consent from next-of-kin, and with ethical approval from the North and East Devon Research Ethics Committee and confirmed as glial fibrillary and acidic protein (GFAP) and vimentin positive, as previously described (17), confirming astrocyte identity. The recurrent low glucose (RLG) model has been previously described [(18); **Figure 1**]. Each day cells were cultured in 2.5 mmol/L glucose-containing media for 2 hours before being changed for media containing 0.1 (low) or 2.5 (normal) mmol/L glucose for 3 hours. Overnight, cells were recovered in stock media containing 5.5 mmol/L glucose. This was repeated for four days. Control and low glucose (LG) treated cells had 2.5 mmol/L glucose for three days and on the fourth day the LG group received low glucose for 3 hours. The antecedent RLG (aRLG) and RLG groups had 0.1 mmol/L glucose for 3 hours on three consecutive days, on the fourth day the aRLG group was exposed to 2.5 mmol/L glucose,

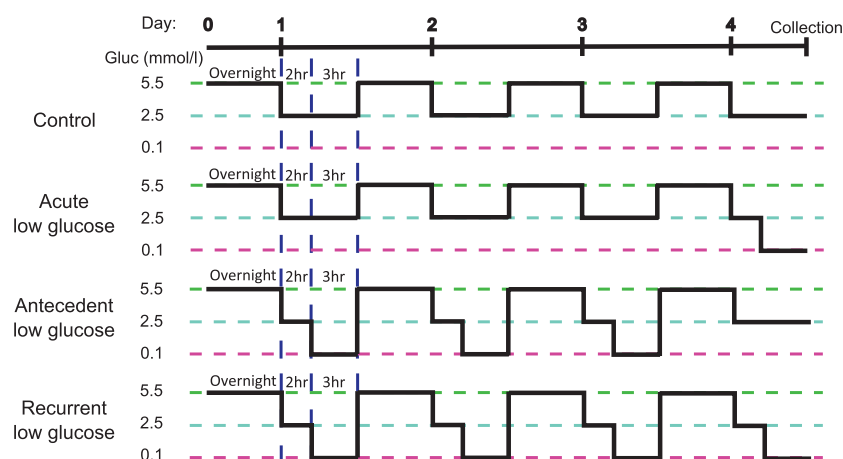


**FIGURE 1** | Schematic of the recurrent low glucose model. Human primary astrocytes were exposed to 0, 1, 3, or 4, three-hour long bouts of 0.1 mmol/l glucose; control (C), acute low glucose (LG), antecedent recurrent low glucose (aRLG), and recurrent low glucose (RLG) respectively. Each day cells were first incubated in 2.5 mmol/l glucose for 2 hours as a step down from overnight/stock media of 5.5 mmol/l glucose. Adapted from (18).

whereas RLG was exposed to 0.1 mmol/L glucose for 3 hours. Mannitol was added to maintain osmolarity (see ESM for details). Samples were split for RNA extraction and DNA extraction, with a total of five and six replicates for RNA sequencing and DNA methylation studies, respectively. Cells were confirmed as mycoplasma free using the MycoAlert kit (Lonza, Slough, UK).

## RNA Sequencing

Briefly, RNA was extracted using TRIzol and Direct-zol miniprep kit (Invitrogen, Carlsbad, CA, USA), according to manufacturers' instructions. cDNA libraries were generated using the TruSeq DNA HT Library Preparation Kit (Illumina Inc., San Diego, CA, USA). Sequencing reads were generated using the Illumina HiSeq 2500 and fastq sequence quality was checked using MultiQC before alignment to the human genome (Build GRCh38.p12) using STAR. Mapped reads were counted using the FeatureCounts function of the subread package. Differential gene expression was calculated using DESeq2 (19) using the Likelihood ratio test function to analyse all groups together followed by the Wald-test for pairwise analysis. Genes with a false discovery rate (FDR)  $\leq 0.05$  were considered differentially expressed. For a principal component analysis plot see ESM **Figure 1**. Functional gene ontology analysis was performed using GOSep. Gene length was accounted for during GO analysis. Raw RNAseq files are available through GEO accession number GSE166848.

## DNA Methylation Analysis

DNA was extracted using a modified phenol:chloroform protocol and DNA methylation (DNAm) examined using the Infinium MethylationEPIC BeadChip platform (Illumina Inc.; EPIC). 729727 probes remained after QC processes. The one-way analysis of variance (ANOVA) test was used to test for differentially methylated sites associated across the three groups: LG, aRLG, RLG compared to control. To determine which group was driving the association behind the significant ANOVA results, the *T* statistics for control versus each of the three groups were extracted from the regression model. Unprocessed array data is available through GEO accession number GSE166848.

## RESULTS

### Low Glucose-Induced Changes in Gene Expression in Human Astrocytes

In HPA cells, expression of 1240 genes were significantly ( $p < 0.05$ ) altered in response to glucose variation; 24 of which were significantly differentially expressed (DE) after FDR correction (adjusted  $p < 0.05$ ; **Figure 2A**). Volcano plots displaying the pairwise comparisons of each treatment group versus control shows that LG (**Figure 2Ai**) produced the largest effect on gene expression, whereas changes induced by aRLG (**Figure 2Aii**) and RLG (**Figure 2Aiii**) were more modest. LG and RLG shared similar DE patterns (**Figure 2B**) and importantly *TXNIP*, regulated by glucose (20), was significantly downregulated in both LG (log2 fold-

change -2.16,  $p = 1.09E-5$ ) and RLG (log2 fold-change -1.46,  $p = 2.91E-3$ ; **Figure 2C**). Of the other DE genes there was a predominance of genes related to endoplasmic reticulum (ER)-stress. X-box binding protein 1 (*XBPI1*; log2 fold-change 0.28,  $p = 1.56E-4$ ; **Figure 2D**), heat shock protein family A member 5 (*HSPA5*; log2 fold-change 0.34,  $p = 3.55E-6$ ; **Figure 2E**), and mesencephalic astrocyte-derived neurotrophic factor (*MANF*; log2 fold-change 0.41,  $p = 7.55E-6$ ; **Figure 2F**) showed increased expression following LG exposure which was blunted following RLG. Similarly, mitochondrially encoded NADH:ubiquinone oxidoreductase core, subunit 4 and subunit 4L (*ND4* and *ND4L*) had increased gene expression in acute LG (*ND4*; log2 fold-change 0.37,  $p = 3.5E-6$ ; *ND4L*; log2 fold-change 0.47,  $p = 5.75E-7$ ) and a diminished, but still significant increase following RLG (**Figures 2G, H**). Pathway analysis of the DE genes identified seven gene ontology (GO) terms that were significantly altered after correction for multiple comparisons, which were related to the unfolded protein response (UPR) and ER-stress (**Table 1**).

### LG and RLG Produce Distinct DNA Methylation Profiles

Our analyses did not identify any differential methylated positions (DMP) that reached genome-wide significance for DNA methylation association analyses (**Figures 3Ai-iii**;  $p < 9.42 \times 10^{-8}$  (21)). However, 65 probes reached nominal significance of  $p < 0.0001$ . Hierarchical clustering of these top probes showed four distinct groups that matched with the four experimental conditions suggesting a DNA methylation profile specific to each condition (**Figure 3B**). Of the differentially methylated CpG sites, several were related to energy or ion homeostasis. *SLC19A3* (cg07417745,  $p = 5.16E-7$ ,  $\beta\Delta = 0.23$ ), encoding the thiamine transporter was hypermethylated after LG showing a linear relationship with the number of bouts of LG exposure (**Figure 3C**). Similarly, methylation of the *GRID1* gene, encoding the ionotropic glutamate receptor  $\delta 1$  (cg16777181) was hypermethylated following LG exposure ( $p = 1.90E-3$ ,  $\beta\Delta = 0.18$ ) and this remained elevated following RLG (**Figure 3D**). In contrast, cg1102254 (*NIPA1*,  $p = 2.65E-6$ ,  $\beta\Delta = -0.02$ ), cg11692715 (*SLC8B1*;  $p = 1.61E-5$ ,  $\beta\Delta = -0.16$ ) and cg22467827 (*CLHC1*,  $p = 4.28E-4$ ,  $\beta\Delta = -0.03$ ), which encode a  $Mg^{2+}$  transporter (22), a  $Na^+/Ca^{2+}$  antiporter, and clathrin heavy chain linker domain containing 1 respectively, were hypomethylated following RLG (**Figures 3E-G**). The probe cg22467827 (annotated to the gene *CLHC1*) was also differentially expressed (log2 fold-change 0.80,  $p = 1.03E-4$ ) in relation to RLG (**Figure 3H**). The two datasets (RNAseq and EPIC) were integrated resulting in 28 DE genes that overlapped with 31 differentially methylated positions (**Figure 3I**).

## DISCUSSION

The central adaptations in response to RH that mediates defective CRR require further investigation, with little known about how astrocytes respond or adapt to RH. We sought to examine changes in HPA gene expression and DNA methylation to determine which,

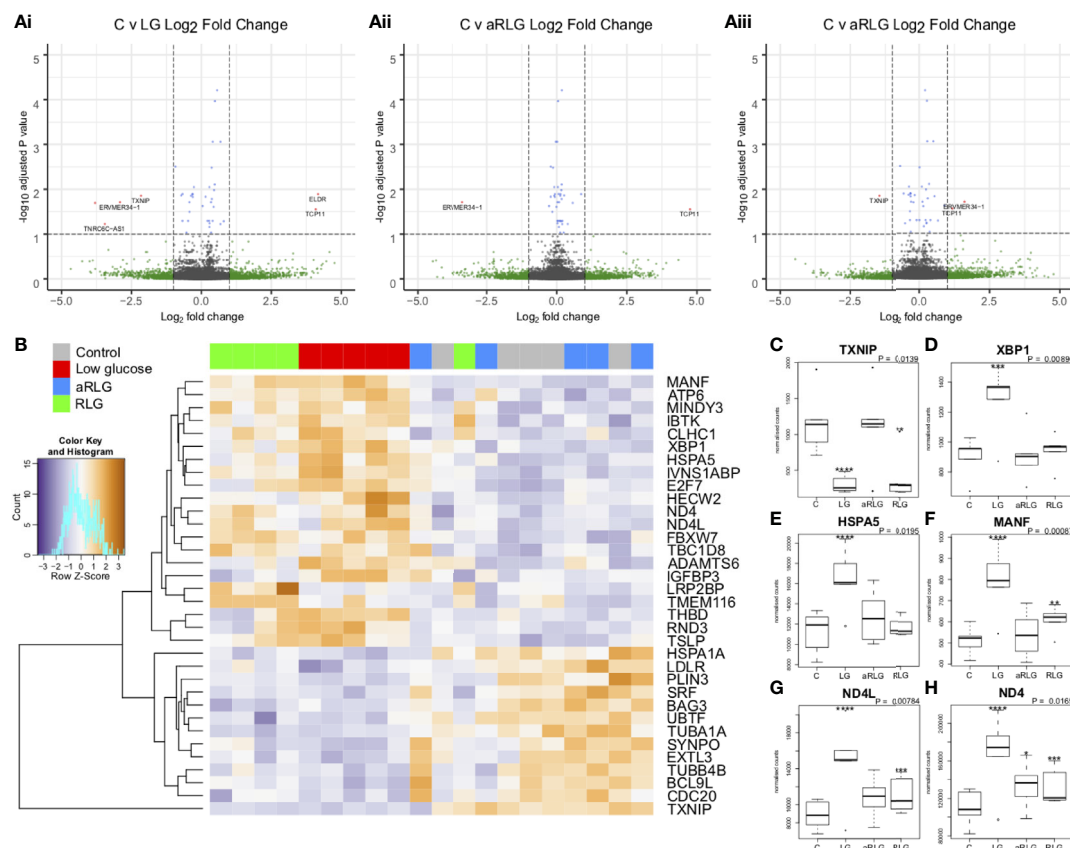


**FIGURE 2** | Glucose variation alters expression of genes involved in endoplasmic-reticulum stress. Volcano plots on the pairwise differential expression analysis between control cells (C) versus (Ai) low glucose (LG), (Aii) antecedent RLG, and (Aiii) recurrent low glucose (RLG), the red points on the plots represent genes  $\text{padj} < 0.05$ . **(B)** Heatmap of hierarchical clustering of LRT analysis  $\text{FDR} \leq 0.1$  indicates differentially expressed genes (rows) between the four groups ( $\text{padj} < 0.1$ ). Orange indicates up-regulation and blue indicates down-regulation. The LG and RLG groups cluster together. *TXNIP* **(C)**, *XBP1* **(D)**, *HSPA5* **(E)**, *MANF* **(F)**, *ND4* **(G)**, *ND4* **(H)** expression profiles, selected for their functional relevance to hypoglycaemia ( $p$ -value is the adjusted result of the likelihood ratio test).  $n=5$ ; \* $p < 0.05$ , \*\* $p < 0.01$ , \*\*\* $p < 0.001$ , \*\*\*\* $p < 0.0001$ . Data presented as Mean  $\pm$  SD.

**TABLE 1** | Glucose variation significantly enriched gene ontologies related to endoplasmic-reticulum stress.

GO term ID	GO term full name	Number of DEGs in the category	Total number of genes in the category	corrected $p$ value
GO:0006986	response to unfolded protein	8	160	0.0159
GO:1905897	regulation of response to endoplasmic reticulum stress	6	72	0.0159
GO:0006984	ER-nucleus signalling pathway	5	45	0.0159
GO:0035966	response to topologically incorrect protein	8	179	0.0159
GO:0034620	cellular response to unfolded protein	7	125	0.0159
GO:0035967	cellular response to topologically incorrect protein	7	143	0.0329
GO:0036498	IRE1-mediated unfolded protein response	5	59	0.0440

Gene ontologies that were significantly enriched by the differentially expressed genes. All seven of the GO terms were related to endoplasmic-reticulum stress and the unfolded protein response.

if any, pathways were altered by acute and RLG exposure. DE and GO pathway analyses revealed that the major pathway altered by acute LG was the UPR. Protein folding within the ER requires hydrolysis of ATP (for review see (23)) and reductions in ATP content driven by energy stress increases protein misfolding to activate the UPR (24). ER stress, *via* ATF6 promotes the production

of XBP1 (25), which is spliced by IRE1 $\alpha$ , to produce a potent transcriptional activator, XBP1s that increases HSPA5 (25) and MANF expression (26)). MANF is upregulated by UPR to inhibit cell proliferation and prevent ER-stress-related cell death (27, 28). Interestingly, here expression of *XBP1*, *HSPA5*, and *MANF* were increased following a single bout of LG. Similar ER stress responses

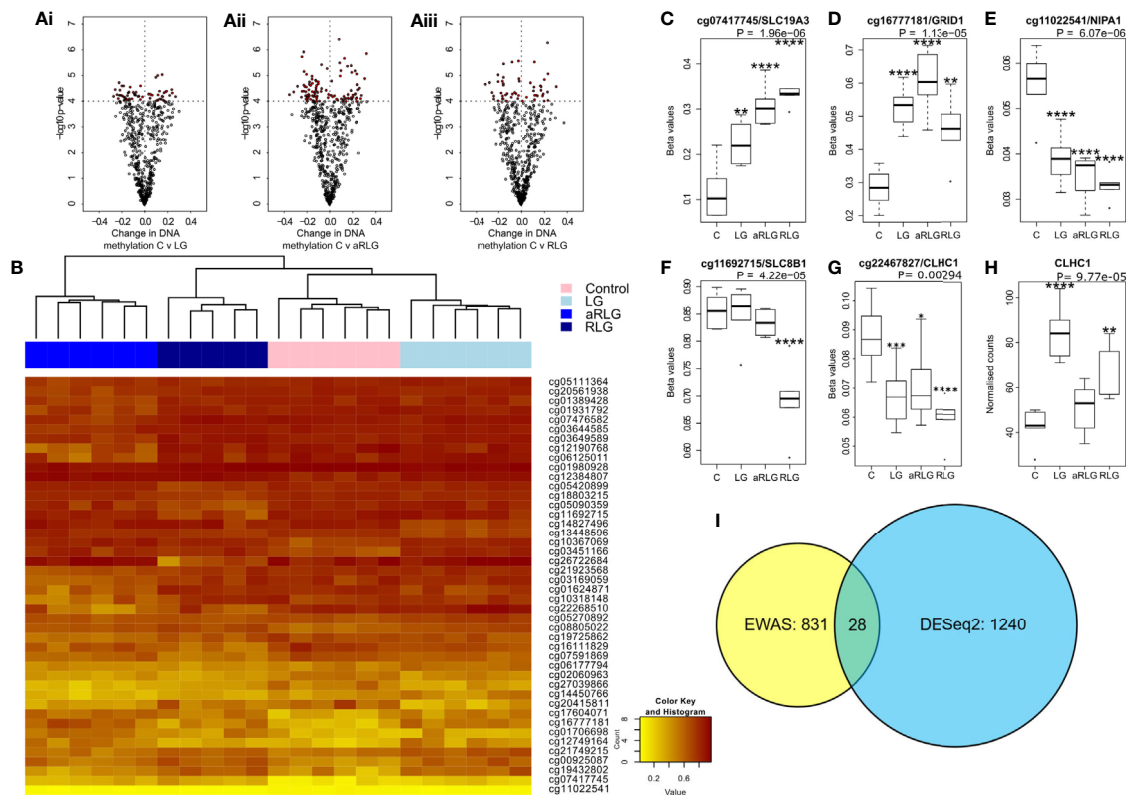


**FIGURE 3 |** Effect of glucose variation on DNA methylation. **(A)** The most differentially methylated genes (ANOVA  $p \leq 0.001$ ) in pairwise comparison (red points are  $p < 0.0001$ ) between control treated HPA cells (C) versus (Ai) low glucose (LG), (Aii) antecedent recurrent low glucose (aRLG), and (Aiii) recurrent low glucose (RLG). **(B)** Heatmap of hierarchical clustering using probes ANOVA  $p < 0.001$  indicates differentially methylated cg sites (rows) between the four groups. Orange indicates hypermethylation and yellow indicates hypomethylation. Box plots of some of the most differentially methylated CpG sites labelled by their associated gene, selected for functional importance **(C)**, cg07417745/SLC19A3, **(D)**, cg16777181/GRID1, **(E)**, cg11022541/NIPA1, **(F)**, cg11692715/SLC8B1 **(G)**, cg22467827/CLHC1 ( $p$ -value is the adjusted result of the ANOVA). **(H)**, *CLHC1* gene expression increases. Error bars represent standard deviation **(I)**, Venn diagram of differentially methylated cg sites in yellow and differentially expressed genes (blue) and overlap between the two data sets, 28 genes. Data presented as Mean  $\pm$  SD. \* $p < 0.05$ , \*\* $p < 0.01$ , \*\*\* $p < 0.001$ , \*\*\*\* $p < 0.0001$ .  $n = 6$  for methylation data and  $n = 5$  for gene expression changes.

have been reported in pericytes (29), cardiac tissue (30), rat primary astrocytes (31) and primary hippocampal neurons (24) in response to LG. Following RLG, the increase in UPR-related gene expression was substantially diminished. Given that energy deficiency increases ER stress, it is plausible that acute LG exposure causes poor folding of proteins leading to a marked increase in ER stress. Following successive bouts of LG, a concomitant metabolic adaptation, as previously reported (18), better preserves cellular (or intra-ER) ATP levels, thus attenuating (or delaying) subsequent LG-induced ER stress, reducing the necessity of the UPR. This is supported by the observation that expression levels of *ND4L* and *ND4* following RLG remained elevated above control. These mitochondrial genes encode two subunits of complex I (NADH dehydrogenase) and the continued elevation of expression following RLG suggests a persistent adaptation. This correlates with our previous data in the same cell type demonstrating increased basal mitochondrial oxygen consumption following RLG, mediated by an increased reliance on fatty acid oxidation for ATP generation (18). It is worth noting that in our previous study, we did not observe any reduction in total intracellular ATP content following acute or recurrent low

glucose exposure. When combined with our data presented here, it is possible that normal ER functions are transiently reduced during acute low glucose exposure in order to maintain intracellular ATP levels. Whether any metabolic adaptation following RLG leads to better preservation of intra-ER ATP levels remains to be determined.

The EWAS identified 65 DMPs associated with LG/RLG that reached nominal significance, while we did not identify any DMPs that reached the suggested array-wide significance ( $p < 9.42 \times 10^{-8}$ ). Hierarchical clustering revealed distinct patterns of DNA methylation across the four conditions. One of the most significant DMPs (cg07417745) is located in intron 1 of the *SLC19A3* gene, which encodes a thiamine transporter (32), and showed a linear relationship between increased DNA methylation and the number of LG exposures. Interestingly, expression of this gene has previously been found to be modulated by hyperglycaemic-like conditions (33). Conversely, methylation of cg11022541 and cg11692715 located within the genes *NIPA1* and *SLC8B1* respectively, decreased following RLG. As these genes encode a  $Mg^{2+}$  transporter (22) and a  $Na^+/Ca^+$

exchanger (34), this may indicate the energetic cost of ion handling within the cell, which requires further investigation. The main limitation in this study was that we were underpowered in the DNA methylation analyses as power analysis indicated we had 50% power to detect a difference of 10% in half of all the sites on the EPIC array. Moreover, the relationship between DNA methylation and gene expression is complex, with the direction of effect dictated by sequence context (35). Furthermore, the annotation of DNAm sites to genes is purely based on proximity rather than empirically derived data (36), both of these factors make inferences between DMPs and gene expression complicated. Despite these challenges we looked for overlapping genes between the datasets and identified 28 that were significantly altered ( $p < 0.05$ ) in both analyses. For example, *CLHC1* gene expression was significantly increased and a DMP (cg22467827) located in intron 1 was hypomethylated. This tentatively suggests that DNA methylation within the first intron may be mediating the upregulation of this gene in the response to LG glucose.

These data demonstrate the intrinsic response of adult human primary astrocytes to acute and recurrent low glucose exposure. Despite the advantages of the high resolution information obtained from primary astrocyte cultures, whether these responses are shared by astrocytes across different brain regions remains unknown, especially given the emerging evidence of astrocyte heterogeneity. In addition, the influence of neighbouring cells such as neurons, pericytes and microglia would be interesting to examine. Therefore, expanding these findings to a more replete setting will be important for future studies using for example human inducible pluripotent stem cells *in vitro* or *ex vivo/in vivo* rodent models.

In summary, there are both shared and unique gene expression and DNA methylation profiles in human astrocytes following LG and RLG exposure. A single bout of LG exposure induced expression of genes associated with the UPR linked to ER stress. This response diminished after four bouts of LG exposure, suggesting an attenuated stress response. Taken together with previous observations that astrocytes adapt to RLG by increasing reliance on fatty acid oxidation to maintain intracellular ATP levels, activation of the UPR by glucose deprivation may be attenuated following RLG exposure.

## DATA AVAILABILITY STATEMENT

The datasets presented in this study can be found in online repositories. The names of the repository/repositories and accession number(s) can be found in the article/**Supplementary Material**.

## REFERENCES

1. Cryer PE. Hypoglycemia: Still the Limiting Factor in the Glycemic Management of Diabetes. *Endocrine Practice: Off J Am Coll Endocrinol Am Assoc Clin Endocrinol* (2008) 14(6):750–6. doi: 10.4158/EP.14.6.750
2. Arbelaez AM, Powers WJ, Videen TO, Price JL, Cryer PE. Attenuation of Counterregulatory Responses to Recurrent Hypoglycemia by Active Thalamic

## AUTHOR CONTRIBUTIONS

AJ, ED, and CB conceived the project. PW, SW, AJ, and ED contributed to data acquisition, analyses and writing of the manuscript. JH and NG obtained human post mortem tissue from which astrocytes were isolated, cultured, and characterised as the stable human primary astrocyte population, thus permitting the investigation of intrinsic changes in human astrocyte responses to be undertaken. CB wrote and edited the manuscript and accepts full responsibility for the work and/or conduct of the study, had access to the data and controlled the decision to publish. All authors contributed to the article and approved the submitted version.

## FUNDING

This work was funded by a Novo Nordisk UK Research Foundation grant to CB, AJ, and ED, Mary Kinross Charitable Trust PhD studentship to CB for PWP, a European Foundation for the Study of Diabetes/Novo Nordisk Programme for Diabetes Research in Europe, a Diabetes UK RD Lawrence Fellowship to CB (13/0004647) and a JDRF postdoctoral fellowship (3-PDF-2020-941-A-N) to PWP. The University of Exeter Sequencing service is funded by Medical Research Council Clinical Infrastructure award (MR/M008924/1), Wellcome Trust Institutional Strategic Support Fund (WT097835MF), Wellcome Trust Multi-User Equipment Award (WT101650MA), and BBSRC LOLA award (BB/K003240/1). This study represents independent research supported by the National Institute of Health Research Exeter Clinical Research facility. The views expressed are those of the author(s) and not necessarily those of the NHS, the NIHR or the Department of Health and Social care.

## ACKNOWLEDGMENTS

We thank the family of the donor for making this research possible. RNA library preparation and sequencing were performed by the Exeter Sequencing Service and Computational Core facilities at the University of Exeter.

## SUPPLEMENTARY MATERIAL

The Supplementary Material for this article can be found online at: <https://www.frontiersin.org/articles/10.3389/fendo.2021.671724/full#supplementary-material>

Inhibition: A Mechanism for Hypoglycemia-Associated Autonomic Failure. *Diabetes* (2008) 57(2):470–5. doi: 10.2337/db07-1329

3. Segel SA, Paramore DS, Cryer PE. Hypoglycemia-Associated Autonomic Failure in Advanced Type 2 Diabetes. *Diabetes* (2002) 51(3):724–33. doi: 10.2337/diabetes.51.3.724
4. McCrimmon RJ, Song Z, Cheng H, McNay EC, Weikart-Yeckel C, Fan X, et al. Corticotrophin-Releasing Factor Receptors Within the Ventromedial

- Hypothalamus Regulate Hypoglycemia-Induced Hormonal Counterregulation. *J Clin Invest* (2006) 116(6):1723–30. doi: 10.1172/JCI27775
5. Sanders NM, Taborsky GJ, Wilkinson CW, Daumen W, Figlewicz DP. Antecedent Hindbrain Glucoprivation Does Not Impair the Counterregulatory Response to Hypoglycemia. *Diabetes* (2007) 56(1):217–23. doi: 10.2337/db06-1025
  6. Ritter S, Llewellyn-Smith I, Dinh TT. Subgroups of Hindbrain Catecholamine Neurons are Selectively Activated by 2-deoxy-D-glucose Induced Metabolic Challenge. *Brain Res* (1998) 805(1-2):41–54. doi: 10.1016/S0006-8993(98)00655-6
  7. Ritter S, Dinh TT, Zhang Y. Localization of Hindbrain Glucoreceptive Sites Controlling Food Intake and Blood Glucose. *Brain Res* (2000) 856(1-2):37–47. doi: 10.1016/S0006-8993(99)02327-6
  8. Song Z, Levin BE, McArdle JJ, Bakhs N, Routh VH. Convergence of Pre- and Postsynaptic Influences on Glucosensing Neurons in the Ventromedial Hypothalamic Nucleus. *Diabetes* (2001) 50(12):2673–81. doi: 10.2337/diabetes.50.12.2673
  9. Levin BE, Routh VH, Kang L, Sanders NM, Dunn-Meynell AA. Neuronal Glucosensing: What do We Know After 50 Years? *Diabetes* (2004) 53(10):2521–8. doi: 10.2337/diabetes.53.10.2521
  10. McDougal DH, Hermann GE, Rogers RC. Vagal Afferent Stimulation Activates Astrocytes in the Nucleus of the Solitary Tract Via AMPA Receptors: Evidence of an Atypical Neural-Glia Interaction in the Brainstem. *J Neurosci* (2011) 31(39):14037–45. doi: 10.1523/JNEUROSCI.2855-11.2011
  11. Rogers RC, McDougal DH, Ritter S, Qualls-Creekmore E, Hermann GE. Response of Catecholaminergic Neurons in the Mouse Hindbrain to Glucoprivic Stimuli is Astrocyte Dependent. *Am J Physiol Regul Integr Comp Physiol* (2018) 315(1):R153–r64. doi: 10.1152/ajpregu.00368.2017
  12. Marty N, Dallaporta M, Foretz M, Emery M, Tarussio D, Bady I, et al. Regulation of Glucagon Secretion by Glucose Transporter Type 2 (glut2) and Astrocyte-Dependent Glucose Sensors. *J Clin Invest* (2005) 115(12):3545–53. doi: 10.1172/JCI26309
  13. McDougal DH, Viard E, Hermann GE, Rogers RC. Astrocytes in the Hindbrain Detect Glucoprivation and Regulate Gastric Motility. *Autonomic Neurosci* (2013) 175(1-2):61–9. doi: 10.1016/j.autneu.2012.12.006
  14. McDougal D, Hermann G, Rogers R. Astrocytes in the Nucleus of the Solitary Tract are Activated by Low Glucose or Glucoprivation: Evidence for Glial Involvement in Glucose Homeostasis. *Front Neurosci* (2013) 7(249):1–10. doi: 10.3389/fnins.2013.00249
  15. Rogers RC, Ritter S, Hermann GE. Hindbrain Cytochrome P-450-Induced Increases in Systemic Blood Glucose Levels by 2-Deoxyglucose Depend on Intact Astrocytes and Adenosine Release. *Am J Physiol-Regulatory Integr Comp Physiol* (2016) 310(11):R1102–8. doi: 10.1152/ajpregu.00493.2015
  16. Chowdhury GMI, Wang P, Ciardi A, Mamillapalli R, Johnson J, Zhu W, et al. Impaired Glutamatergic Neurotransmission in the VMH may Contribute to Defective Counterregulation in Recurrently Hypoglycemic Rats. *Diabetes* (2017) 66(7):1979–89. doi: 10.2337/db16-1589
  17. Holley JE, Gveric D, Whatmore JL, Gutowski NJ. Tenascin C Induces a Quiescent Phenotype in Cultured Adult Human Astrocytes. *Glia* (2005) 52(1):53–8. doi: 10.1002/glia.20231
  18. Weightman Potter PG, Vlachaki Walker JM, Robb JL, Chilton JK, Williamson R, Randall AD, et al. Basal Fatty Acid Oxidation Increases After Recurrent Low Glucose in Human Primary Astrocytes. *Diabetologia* (2019) 62(1):187–98. doi: 10.1007/s00125-018-4744-6
  19. Love MI, Huber W, Anders S. Moderated Estimation of Fold Change and Dispersion for RNA-seq Data With Deseq2. *Genome Biol* (2014) 15(12):550. doi: 10.1186/s13059-014-0550-8
  20. Parikh H, Carlsson E, Chutkow WA, Johansson LE, Storgaard H, Poulsen P, et al. Txnip Regulates Peripheral Glucose Metabolism in Humans. *PloS Med* (2007) 4(5):e158. doi: 10.1371/journal.pmed.0040158
  21. Mansell G, Gorrie-Stone TJ, Bao Y, Kumari M, Schalkwyk LS, Mill J, et al. Guidance for DNA Methylation Studies: Statistical Insights From the Illumina EPIC Array. *BMC Genomics* (2019) 20(1):366. doi: 10.1186/s12864-019-5761-7
  22. Goytain A, Hines RM, El-Husseini A, Quamme GA. NIPA1 (SPG6), the Basis for Autosomal Dominant Form of Hereditary Spastic Paraplegia, Encodes a Functional Mg<sup>2+</sup> Transporter. *J Biol Chem* (2007) 282(11):8060–8. doi: 10.1074/jbc.M610314200
  23. Braakman I, Hebert DN. Protein Folding in the Endoplasmic Reticulum. *Cold Spring Harbor Perspect Biol* (2013) 5(5):1–19. doi: 10.1101/cshperspect.a013201
  24. de la Cadena SG, Hernández-Fonseca K, Camacho-Arroyo I, Massieu L. Glucose Deprivation Induces Reticulum Stress by the PERK Pathway and caspase-7- and Calpain-Mediated caspase-12 Activation. *Apoptosis* (2014) 19(3):414–27. doi: 10.1007/s10495-013-0930-7
  25. Yoshida H, Matsui T, Yamamoto A, Okada T, Mori K. Xbp1 mRNA is Induced by ATF6 and Spliced by IRE1 in Response to ER Stress to Produce a Highly Active Transcription Factor. *Cell* (2001) 107(7):881–91. doi: 10.1016/S0092-8674(01)00611-0
  26. Oh-Hashi K, Hirata Y, Kiuchi K. Transcriptional Regulation of Mouse Mesencephalic Astrocyte-Derived Neurotrophic Factor in Neuro2a Cells. *Cell Mol Biol Lett* (2013) 18(3):398–415. doi: 10.2478/s11658-013-0096-x
  27. Apostolou A, Shen Y, Liang Y, Luo J, Fang S. Armet, a UPR-upregulated Protein, Inhibits Cell Proliferation and ER Stress-Induced Cell Death. *Exp Cell Res* (2008) 314(13):2454–67. doi: 10.1016/j.yexcr.2008.05.001
  28. Huang J, Chen C, Gu H, Li C, Fu X, Jiang M, et al. Mesencephalic Astrocyte-Derived Neurotrophic Factor Reduces Cell Apoptosis Via Upregulating GRP78 in SH-SY5Y Cells. *Cell Biol Int* (2016) 40(7):803–11. doi: 10.1002/cbin.10621
  29. Ikesugi K, Mulhern ML, Madson CJ, Hosoya K, Terasaki T, Kador PF, et al. Induction of Endoplasmic Reticulum Stress in Retinal Pericytes by Glucose Deprivation. *Curr Eye Res* (2006) 31(11):947–53. doi: 10.1080/02713680600966785
  30. Barnes JA, Smoak IW. Glucose-Regulated Protein 78 (GRP78) is Elevated in Embryonic Mouse Heart and Induced Following Hypoglycemic Stress. *Anat Embryol* (2000) 202(1):67–74. doi: 10.1007/s004290000090
  31. Lind KR, Ball KK, Cruz NF, Diemel GA. The Unfolded Protein Response to Endoplasmic Reticulum Stress in Cultured Astrocytes and Rat Brain During Experimental Diabetes. *Neurochem Int* (2013) 62(5):784–95. doi: 10.1016/j.neuint.2013.02.009
  32. Eudy JD, Spiegelstein O, Barber RC, Wlodarczyk BJ, Talbot J, Finnell RH. Identification and Characterization of the Human and Mouse Slc19a3 Gene: A Novel Member of the Reduced Folate Family of Micronutrient Transporter Genes. *Mol Genet Metab* (2000) 71(4):581–90. doi: 10.1006/mgme.2000.3112
  33. Beltramo E, Mazzeo A, Lopatina T, Trento M, Porta M. Thiamine Transporter 2 is Involved in High Glucose-Induced Damage and Altered Thiamine Availability in Cell Models of Diabetic Retinopathy. *Diabetes Vasc Dis Res* (2020) 17(1):1479164119878427. doi: 10.1177/1479164119878427
  34. Palty R, Silverman WF, Hershfinkel M, Caporale T, Sensi SL, Parnis J, et al. NCLX is an Essential Component of Mitochondrial Na<sup>+</sup>/Ca<sup>2+</sup> Exchange. *Proc Natl Acad Sci USA* (2010) 107(1):436–41. doi: 10.1073/pnas.0908099107
  35. Jones PA. Functions of DNA Methylation: Islands, Start Sites, Gene Bodies and Beyond. *Nat Rev Genet* (2012) 13(7):484–92. doi: 10.1038/nrg3230
  36. Hannon E, Gorrie-Stone TJ, Smart MC, Burrage J, Hughes A, Bao Y, et al. Leveraging DNA-Methylation Quantitative-Trait Loci to Characterize the Relationship Between Methylation Variation, Gene Expression, and Complex Traits. *Am J Hum Genet* (2018) 103(5):654–65. doi: 10.1016/j.ajhg.2018.09.007

**Conflict of Interest:** The authors declare that the research was conducted in the absence of any commercial or financial relationships that could be construed as a potential conflict of interest.

Copyright © 2021 Weightman Potter, Washer, Jeffries, Holley, Gutowski, Dempster and Beall. This is an open-access article distributed under the terms of the Creative Commons Attribution License (CC BY). The use, distribution or reproduction in other forums is permitted, provided the original author(s) and the copyright owner(s) are credited and that the original publication in this journal is cited, in accordance with accepted academic practice. No use, distribution or reproduction is permitted which does not comply with these terms.



# Microglial Lipid Biology in the Hypothalamic Regulation of Metabolic Homeostasis

Andrew Folick<sup>1,2</sup>, Suneil K. Koliwad<sup>1,2</sup> and Martin Valdearcos<sup>1\*</sup>

<sup>1</sup> Diabetes Center, University of California, San Francisco, San Francisco, CA, United States, <sup>2</sup> Department of Medicine, University of California, San Francisco, San Francisco, CA, United States

## OPEN ACCESS

### Edited by:

Rachel Nicole Lippert,  
German Institute of Human Nutrition  
Potsdam-Rehbruecke (DIfE), Germany

### Reviewed by:

Alexandre Benani,  
Centre National de la Recherche  
Scientifique (CNRS), France  
Xavier Fioramonti,  
INRA UMR1286 Laboratoire  
NutriNeuro, France

### \*Correspondence:

Martin Valdearcos  
martin.valdearcoscontreras@ucsf.edu

### Specialty section:

This article was submitted to  
Neuroendocrine Science,  
a section of the journal  
Frontiers in Endocrinology

**Received:** 16 February 2021

**Accepted:** 05 May 2021

**Published:** 27 May 2021

### Citation:

Folick A, Koliwad SK and  
Valdearcos M (2021) Microglial  
Lipid Biology in the Hypothalamic  
Regulation of Metabolic Homeostasis.  
Front. Endocrinol. 12:668396.  
doi: 10.3389/fendo.2021.668396

In mammals, myeloid cells help maintain the homeostasis of peripheral metabolic tissues, and their immunologic dysregulation contributes to the progression of obesity and associated metabolic disease. There is accumulating evidence that innate immune cells also serve as functional regulators within the mediobasal hypothalamus (MBH), a critical brain region controlling both energy and glucose homeostasis. Specifically, microglia, the resident parenchymal myeloid cells of the CNS, play important roles in brain physiology and pathology. Recent studies have revealed an expanding array of microglial functions beyond their established roles as immune sentinels, including roles in brain development, circuit refinement, and synaptic organization. We showed that microglia modulate MBH function by transmitting information resulting from excess nutrient consumption. For instance, microglia can sense the excessive consumption of saturated fats and instruct neurons within the MBH accordingly, leading to responsive alterations in energy balance. Interestingly, the recent emergence of high-resolution single-cell techniques has enabled specific microglial populations and phenotypes to be profiled in unprecedented detail. Such techniques have highlighted specific subsets of microglia notable for their capacity to regulate the expression of lipid metabolic genes, including lipoprotein lipase (LPL), apolipoprotein E (APOE) and Triggering Receptor Expressed on Myeloid Cells 2 (TREM2). The discovery of this transcriptional signature highlights microglial lipid metabolism as a determinant of brain health and disease pathogenesis, with intriguing implications for the treatment of brain disorders and potentially metabolic disease. Here we review our current understanding of how changes in microglial lipid metabolism could influence the hypothalamic control of systemic metabolism.

**Keywords:** microglia, hypothalamus, lipids, obesity, diabetes

## INTRODUCTION

The brain contains the second highest lipid concentration in the body, behind adipose tissue, and lipids constitute 50% of the brain's dry weight (1). Beyond serving as energy substrates, brain lipids play a wide range of roles in cellular physiology, including membrane organization, protein modification, cell-cell interactions, membrane trafficking, energy storage and signal transduction.

Lipid metabolism within the brain is therefore highly regulated, and disruption of central nervous system (CNS) lipid homeostasis can produce devastating neurological consequences. For instance, impaired cholesterol or fatty acid metabolism leads to severe neurodevelopmental defects, intellectual disabilities, and motor dysfunction (2, 3). Neurons themselves engage in relatively low levels of lipid synthesis, in contrast to recent studies which suggest that glial cells are critical for both the synthesis and metabolism of lipids in the brain (4). For example, an “astrocyte-neuron lactate shuttle” has been postulated, in which astrocytes metabolize lipids in order to provide energy substrates for neurons (5) and regulate neurite outgrowth and synaptogenesis (6). Oligodendrocytes are also highly active in lipid metabolism, and have been shown to synthesize the cholesterol necessary for myelin sheath formation (7). Importantly, microglia can both synthesize and accumulate lipids, and both microglial lipid composition and lipid metabolic capability are increasingly implicated in determining their ability to regulate neuronal functions as well as their contributions to brain pathology (8–10).

Integration of lipidomic and genomic datasets can elucidate gene-environment (e.g. diet) interactions regulating lipid metabolism as a means to reveal biomarkers predictive of metabolic disease (11). Recent studies utilizing lipidomics and single-cell RNA sequencing (scRNA-seq) have revealed intriguing heterogeneity among microglia, and the importance of lipid and lipoprotein metabolism in microglial physiology (12, 13). This work had been done primarily in the context of specific neurodegenerative diseases, while our lab and others have investigated the role of dietary lipids in the immunological activation of microglia in the context of obesity and metabolism (14–16). This review summarizes our current knowledge of lipid metabolism in microglia, with a focus on its potential contribution to hypothalamic physiology and dysfunction in the context of metabolic disease.

## LIPID METABOLISM IN THE BRAIN

The brain has a high energy demand, and historical consensus has been that its energy requirements are almost entirely satisfied by glucose metabolism. However, this dogma has been recently challenged, as it was shown that approximately 20% of the brain’s total energy requirement is met through the oxidation of fatty acids (FAs) (17). Additionally, FA oxidation by cultured mouse brain slices is increased by withdrawing extracellular glucose (18). Astrocytes and microglia likely contribute significantly to brain utilization of FAs as energy substrates (18, 19). Astrocytes express higher levels of key FA oxidation enzymes, however detailed cell-type specific experiments comparing the capacity to oxidize fatty acids *in vivo* have not been reported (18). Neurons may have also the capacity to utilize FAs as an energy source, as a recent study using rat brain demonstrated that isolated neuronal mitochondria utilize FAs as an energy source even in the presence of other mitochondrial substrates (20). By contrast, the capacity of neurons to oxidize

FAs for energy is known to be quite limited (21). One reason for this limited capacity may be that neurons are highly susceptible to reactive oxygen stress (ROS) generated by FA oxidation, and it is widely accepted that mitochondrial oxidative stress and dysfunction contribute to neurologic disorders (22). Thus, the selective pressure to avoid oxidative stress may underlie the neuronal preference to oxidize glucose as their primary fuel source (21).

## Neuron-Glia Interactions in Brain Lipid Metabolism

Given the importance of lipids to overall brain physiology, the limited lipid metabolic capacity of neurons themselves has prompted exploration into the essential roles of glial cells in lipid metabolism, storage and synthesis. This effort has revealed the importance of coordinated lipid metabolism and trafficking between neurons and glia, as exemplified by work done to establish a genetic link between Parkinson’s disease (PD) and genes controlling lipid metabolism (23, 24). Indeed, both PD patients and experimental animal models of PD exhibit abnormal lipid accumulation in dopaminergic neurons and their surrounding microglia, but have a reduced lipid load in adjacent astrocytes. One recent study found that a Western diet impairs recovery from demyelinating injuries, by inhibiting microglial phagocytosis and clearance of lipid debris (25). Another study found that in the setting of demyelination, microglia synthesize desmosterol, the immediate cholesterol precursor and liver X receptor (LXR) agonist, and that microglial sterol synthesis is essential for efficient remyelination (26). As oligodendrocytes were thought to be the primary synthesizers of sterols in the brain, and require sterols for myelination, this indicates a new role for intercellular trafficking of sterols. Together, these findings indicate that a disturbance in the multicellular handling and trafficking of lipids plays may play a key role in PD pathogenesis (27).

However a broader, more systematic understanding of the regulation of lipid metabolism and flux between brain cell types in different physiological and pathological states is limited, with few detailed lipidomic profiles of CNS cell types having been published to date. However, recent studies have revealed that certain lipid species are enriched in distinct cell types and brain regions. For instance, microglia are enriched in sphingolipids and characterized by high levels of sphingomyelin species, which are almost absent in neurons and oligodendrocytes (13). Microglia in particular are essential for the clearance and recycling of lipid debris, and recent work has shown that aging-related defects in microglial lipid handling contribute both to their inflammatory activation and to the impairment of their response to demyelination (28). Further insights into microglial lipid metabolism will be essential to understanding how lipids impact brain function.

## Effects of Diet on Brain Lipid Composition and Metabolism

In addition to having a relatively high absolute lipid content, the composition of brain lipids is also distinct from that of other

tissues in the body. Indeed, 75% of lipids in mammals are present exclusively in neural tissues, underscoring that brain function has unique lipid requirements (29). The brain is the most cholesterol-rich organ in the body, and brain cholesterol is primarily supplied by local *de novo* synthesis (30). Cholesterol is essential for neuronal physiology, and defects in cholesterol metabolism leads to neurological diseases (31). Despite the primary *de novo* synthesis, diet may also affect sterol metabolism in the brain. The cholesterol metabolite 27-hydroxycholesterol (27-OHC) can pass through the BBB, and 27-OHC is significantly increased in plasma and adipose tissue of animals on HFD (32). Excess 27-OHC impairs brain glucose uptake (33). Additionally, peripheral cholesterol contained in circulating HDL, undergoes selective uptake mediated by the scavenger receptor class B type 1 for entry into the brain (34). In humans, low HDL levels are associated with increased risk for PD (35). Interestingly, genetic HDL deficiency caused increased astrogliosis, but not microgliosis, in the hypothalamus (36).

On the other hand, some FAs must be transported into the brain from the systemic circulation in a dynamic process (37). For instance, the brain is rich in long-chain polyunsaturated fatty acids (LC-PUFAs), particularly arachidonic acid (AA), eicosapentaenoic acid (EPA), and docosahexaenoic acid (DHA) but the brain has limited capacity to synthesize LC-PUFAs (38, 39). These have to therefore be provided through the diet, either as precursors, n-6 linoleic acid (LA) and n-3  $\alpha$ -linolenic acid (ALA), or as preformed AA and DHA (40, 41). Indeed, several radiolabeled studies have shown incorporation of circulating FAs into neurons (37). FAs could passively diffuse across the blood brain barrier (BBB), as shown for palmitate (PA), AA and DHA (42–44), however FA transporters such as FAT/CD36 may also play a key role in promoting the dissociation of FAs albumin in order to facilitate their diffusion across the BBB (45). In summary, brain lipid composition is highly regulated, and while distinct from peripheral lipid composition, is importantly influenced by circulating lipids including those from dietary sources.

The obesogenic high-fat diets (HFD) commonly used in mice, including the so-called “Western” diet with increased cholesterol levels, are characterized by a markedly high saturated fatty acid (SFA) content and a relatively low n-3 polyunsaturated fatty acids (PUFA) content, resulting in a high n-6/n-3 ratio (46). Given this, it is notable that studies suggest that not every type of fat is equally obesogenic when consumed in an isocaloric manner. Indeed, the profile of consumed fats, rather than strictly the energy they contain, may be critical for the development of obesity (47). Circulating lipid levels are affected by dietary fat composition; for example, one lipidomic analysis of postprandial plasma showed significant changes in the levels of 316 different lipids species after an individual switched from eating a breakfast based on dairy foods to one that was soy oil-based (48). Recent studies have also investigated the effect of dietary fat on the brain lipidome. Mice consuming a HFD have reduced EPA content in cerebral phospholipids and sphingolipids, in association with increased inflammation and consequently impaired brain function (49). By contrast, diets

enriched in the n-3 fatty acids EPA and DHA induce a different set of alterations in the FA composition of brain phospholipids, including increasing the number of double bonds in several phospholipid species (13). Indeed, supplementing a standard saturated fat-rich HFD with a daily gavage of fish oil rich in EPA and DHA is sufficient to increase brain PUFAs and reduce brain gliosis in obese mice (50). In probing this further, it is notable that both EPA and DHA are precursors of pro-resolving lipid mediators with anti-inflammatory properties (51). In contrast, n-3 deficient neonatal mice exhibit increased microglial phagocytosis of synaptic elements resulting in altered neuronal morphology and function (10). Thus, dietary changes in EPA and DHA, as detected by monitoring dietary n-6/n-3 ratios, may directly modulate microglial polarization states in a manner relevant to CNS diseases associated with microglial dysfunction.

## INTEGRATION OF LIPID SIGNALS BY THE MEDIOBASAL HYPOTHALAMUS (MBH)

The MBH, defined here as the hypothalamic region containing the arcuate nucleus (ARC) and median eminence (ME), is strategically located to directly sense and coordinate a response to nutritional signals. The structure and function of the BBB within the ME and ventromedial ARC, as a circumventricular organs, is unique, being supplied by fenestrated capillaries (52–55). Thus, substances that do not cross into the brain parenchyma in other regions of the brain may pass into the ME and ARC with relative ease (56, 57). For example, very low density lipoproteins (VLDL) are not thought to cross the BBB (34), however we demonstrated rapid accumulation of VLDL within the MBH after intravenous administration, and this was predominantly localized to microglia in the ME and ARC (14). Indeed, a recent study showed that triglyceride (TG)-rich lipoproteins are sensed in the hypothalamus by an LPL-dependent mechanism (58), and the uptake of dietary PA, a common SFA, into the hypothalamus is remarkably higher than for other brain regions (59). Thus, specialized fuel-sensing neurons that form critical hypothalamic circuits are uniquely positioned to sense circulating glucose and lipid species, including FAs (60).

Whereas lipid sensing in the MBH may create responsiveness to nutritional lipids, there may be roles for lipid sensing in other brain regions as well. For instance, recent work has shown that both nutritional and parenteral TG exposure modulated activity of neurons in the mesocorticolimbic system (MCL) and affects behavioral and reward responses (61, 62). These effects were dependent on neuronal lipoprotein lipase, suggesting a direct response to TGs (61, 62). Radiolabeled triolein was able to be detected in whole brain after peripheral injection, suggesting that some intact TG may pass through the BBB, however the location of triolein accumulation within the brain was not determined (63). This sensing capacity may play a role in the context of autophagy, lipids housed within locally-generated lipoproteins (e.g. APOE), or perhaps by context-specific selective permeability of the vasculature in certain brain regions to

circulating lipids. Further research is needed to tease apart these possibilities.

## Lipid Sensing by Hypothalamic Neurons

Circulating FA levels are increased after consumption of a HFD (64, 65) and the rate of entry of FAs into the brain is proportional to their plasma concentration (59). Indeed, hypothalamic levels of free FAs are increased by HFD feeding, suggesting an important role for these FAs in hypothalamic lipid-sensing pathways (66). Supporting this, it has been shown that FAs modify neuronal firing rates in the ARC (67). Moreover, intracerebroventricular (ICV) infusion of the monounsaturated FA, oleic acid (OA), suppresses food intake and hepatic glucose production (68) indicating that FAs can signal nutrient availability to the brain. Furthermore, increased LCFA-CoA levels in hypothalamic neurons suppress endogenous glucose production suggesting that hypothalamic lipid sensing regulates glucose homeostasis through a mechanism involving the esterification of LCFAs to LCFA-CoAs (69). Also, ICV infusions of OA or DHA, but not PA, reduce food intake and body weight indicating a selective hypothalamic response to specific unsaturated fatty acids (UFAs). However, ICV and direct infusions of FAs into the brain are not physiological. Short-term (3 days) of HFD can cause rewiring of anorexigenic proopiomelanocortin (POMC) neurons in the ARC, suggesting a physiological role for lipid sensing in the hypothalamus (70). In further support of this concept, a recent elegant study found that intragastric administration of lipids inhibited the activity of hunger-promoting Agouti-related protein (AgRP) neurons in the MBH (71). Furthermore, the ability of lipid infusion to inhibit the activity of AgRP neurons was blunted in HFD-fed animals, suggesting a reduction in the lipid sensitivity of AgRP neurons in this context (72). In summary, there is clear evidence that a HFD, in particular dietary FAs, is sensed by hypothalamic neuronal pathways to regulate energy homeostasis. The precise mechanisms of lipid sensing by hypothalamic neurons have been well studied, and have been recently reviewed (73–75).

Dysregulated lipid metabolism in the hypothalamus may affect neuronal FA sensing and therefore contribute to the development of metabolic diseases. In particular, excessive lipid accumulation and resultant activation of cellular stress pathways can lead to disruption of hypothalamic function. During both acute and chronic HFD feeding, multiple inflammatory and stress response pathways are activated in the hypothalamus, leading the dysfunction of hypothalamic circuits regulating energy and glucose homeostasis, resulting in leptin and insulin resistance (76). In evaluating the specific changes in hypothalamic lipid composition induced by overconsumption, specific attention has been paid to how excess lipid accumulation drives ER stress in the hypothalamus (77). Rodent studies have shown that HFD feeding induces ER stress in multiple metabolic tissues including the hypothalamus (78). This response is not uniform across all hypothalamic nuclei and seems to be specific to the ARC but not other regions such as the paraventricular nucleus (PVN) (78). Induction of hypothalamic ER stress leads to increased food intake, reduced energy expenditure and resultant obesity, and this is mediated at least in part by

defective  $\alpha$ -MSH production among POMC neurons (79) and development of leptin resistance (80). Fat composition is important in this regard, because saturated fats (e.g., PA) are more deleterious than unsaturated fats to hypothalamic neurons (81), and ER stress sensors are specifically activated by increasing ER membrane lipid saturation (82). Interestingly, PA-induced ER stress in hypothalamic neurons decreases protein abundance and function of the melanocortin 4 receptor (MC4R) (83), and central inhibition of lipid oxidation and ER stress is sufficient to restore hypothalamic lipid sensing and energy homeostasis in mice (84).

ER stress and inflammatory pathways are functionally coupled, and induction of CNS ER stress in lean mice is sufficient to activate NF- $\kappa$ B signaling (85). Furthermore, there is convincing evidence that ER stress activates the NLRP3 inflammasome in myeloid cells through different pathways in a context-dependent manner. We demonstrated that IRE1 $\alpha$ , a critical ER sensor of both unfolded protein and saturated lipid stress, mediates SFA-induced IL-1 $\beta$  secretion in macrophages upon sensing increasing saturation of cellular phospholipids (86). However, most metabolic studies in the hypothalamus have focused on neuronal ER stress, and the potential contribution of ER stress in glial cells to hypothalamic dysfunction has not been explored yet. However, a recent study did show that disrupting proteasome activity in microglia triggers the induction of a type I interferon (IFN) response in an IRE1-dependent manner (87), suggesting that microglial ER stress is worth studying in the context of hypothalamic regulation.

## Lipid Sensing by Non-Neuronal Cells

Hypothalamic neurons are critical to the regulation of energy and glucose homeostasis, and our understanding of neuronal circuits controlling metabolism has advanced greatly over the past decade. However, recent studies implicate non-neuronal cells, including microglia, as physiologic regulators of hypothalamic function as well. For instance, astrocytes are the most abundant glial cells in the CNS and are involved in multiple fundamental processes, including metabolic homeostasis, neurovascular coupling, and BBB maintenance (88). Recent studies show that disrupting astrocyte lipid homeostasis may contribute to neurological disorders (89, 90). In addition, astrocytes participate in immune responses, and HFD consumption induces morphological changes in hypothalamic astrocytes (91). Astrocytes can influence hypothalamic circuits involved in the control of feeding and energy metabolism, at least in part by regulating extracellular levels of adenosine (92, 93). Furthermore, a recent study suggested that astrocytic insulin signaling regulates hypothalamic glucose sensing and systemic glucose metabolism (94). Also, astrocytes in the MBH can respond to acute changes in nutritional exposure, with morphological changes after overnight fasting (91), or as soon as 1-hr post-prandially (95). Interestingly, post-prandial retraction of astrocytes surrounding POMC neurons was only seen with standard chow diet, but not HFD (95). Tanycytes are radial glia-like cells that line the wall of the third ventricle in the brain, a privileged position to integrate multiple peripheral

inputs (96, 97). Tanycytes can sense nutrients such as FAs in the cerebrospinal fluid (CSF), facilitate the transport of metabolic hormones across the BBB, and integrate signals to regulate appetite and energy balance (98, 99).

Microglia are increasingly being recognized as highly dynamic cells that continuously monitor for alterations to their environment, and assume different states of activation according to the unique CNS microenvironment in which they reside. Within the hypothalamus, microglia are emerging as key physiological mediators, both in the context of normal hypothalamic function and regulating the metabolic response to HFD. As such, key details of microglial lipid sensing and metabolic regulation have gained considerable interest, and are therefore reviewed below.

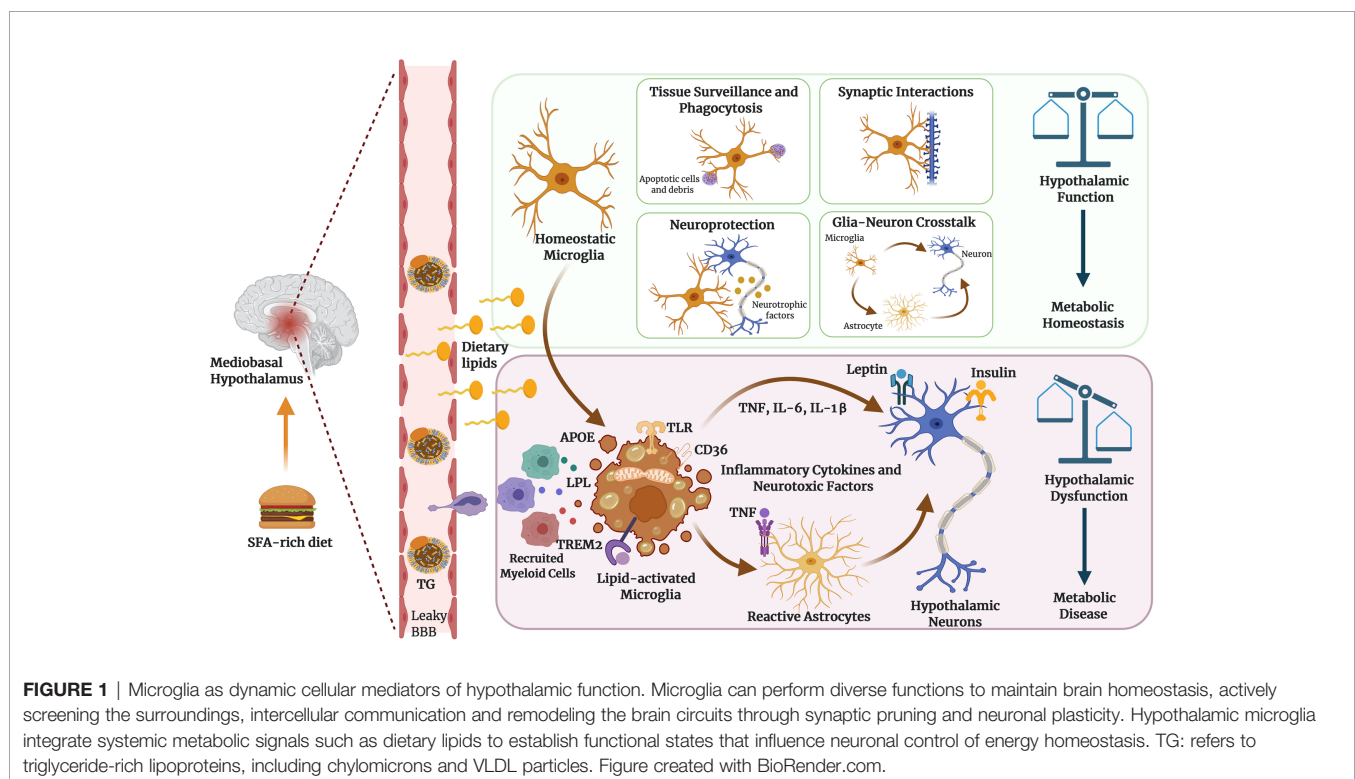
## MICROGLIA AS NOVEL REGULATORS OF HYPOTHALAMIC FUNCTION

Recent findings reveal an expanding array of functions for microglia, beyond their established roles as immune sentinels and phagocytic removers of cellular debris. These include roles in synaptic organization (100), neuronal excitability (101) and trophic support for brain repair (102) (**Figure 1**). Given the vital role of microglia in maintaining CNS homeostasis, it is not surprising that several brain disorders are associated with microglial dysfunction (103). Disrupting the interactions between neurons and microglia has devastating effects on memory, anxiety and other behavioral domains, demonstrating

the importance of myeloid cells in brain physiology (104). Furthermore, interactions between microglia and astrocytes have been implicated in brain health and disease (105), and their cross-talk may play an important role in HFD-induced hypothalamic dysfunction. Activated microglia can induce reactive astrocytes by secreting proinflammatory molecules, such as IL-1 $\alpha$ , TNF and C1q as previously demonstrated in a lipopolysaccharide (LPS)-induced murine neuroinflammation model (106). In addition, recent work suggests that microglial activity is directly regulated by metabolites of dietary tryptophan metabolism produced by commensal flora, and that this response controls a downstream inflammatory response among astrocytes (107). Recently, we showed that the inflammatory signaling of microglia dictates susceptibility to diet-induced hypothalamic dysfunction and obesity (15).

## Microglial Inflammatory Signaling Regulates Hypothalamic Immune Response to Dietary Excess

Chronic low-grade inflammation is considered one of the hallmarks of metabolic disease, and activation of inflammatory pathways have been described in several metabolic tissues. Animal and human studies have identified white adipose tissue (WAT) as the primary site where inflammation is initiated and exacerbated in response to weight gain (108). Obesity promotes drastic changes in the resident immune cell profile and function in WAT. Adipose tissue macrophages adopt a metabolically activated (MMe) phenotype distinct from that associated with classical “M1” activation, upregulating proteins involved in lipid processing



including ABCA1, PLIN2 and CD36 to maintain adipose tissue homeostasis (109). Moreover, a novel and conserved macrophage population called lipid-associated macrophages (LAMs) is involved in controlling WAT lipid homeostasis has been recently described in multiple obesity-related mouse models (110).

Interestingly, recent studies have provided evidence that HFD consumption also increases the expression of genes governing inflammatory signaling in the hypothalamus (111–113). This phenomenon has also been described in human obesity, and obese individuals without a systemic disease showed markedly increased levels of inflammatory markers in the hypothalamus compared to healthy non-obese individuals (114, 115). With this in mind, it is notable that HFD consumption in mice rapidly increases the accumulation and activation of microglial populations secreting inflammatory cytokines specifically in the MBH (14). Moreover, the activation of hypothalamic inflammatory pathways in response to HFD consumption is much more rapid than it is in peripheral tissues such as WAT, even preceding any significant diet-induced weight gain, suggesting that the inflammatory response of the MBH to dietary excess is a cause, rather than a consequence, of obesity (113). Indeed, a single high-fat meal is sufficient to induce morphological changes and increased *Iba1* expression in hypothalamic microglia (16).

We have shown that either pharmacologically depleting resident microglia, or genetically restraining their inflammatory

capacity *via* NF- $\kappa$ B signaling, protects mice from diet-induced hyperphagia and weight gain, whereas specifically forcing NF- $\kappa$ B-dependent microglial inflammatory activation reduces energy expenditure and increases both food intake and weight gain even in absence of a dietary challenge (15). Microglial inflammatory signaling may induce obesity by causing hypothalamic neuronal dysfunction, including the induction of neuronal insulin and leptin resistance (76). Moreover, prolonged microglial activation may also induce apoptosis of anorexigenic/catabolic POMC neurons (116).

## Metabolic Plasticity of Microglia

Microglia have the ability to adapt their metabolic pathways to use the energy substrates available in their local environment, and to acquire diverse and complex phenotypes during inflammatory activation in response to an insult or injury (18) (Figure 2). A comparative transcriptional profiling of genes related to energy metabolism in different brain cell types revealed that microglia express specific sets of genes required for both glycolytic and oxidative energy metabolism (117). For instance, microglia express the long-chain fatty acyl-CoA synthetase, which catalyzes the formation of fatty acyl-CoAs that are, in turn,  $\beta$ -oxidized into acetyl-CoA units and can be further metabolized in the TCA cycle. Additionally, a recent study showed that microglia are able to maintain oxidative

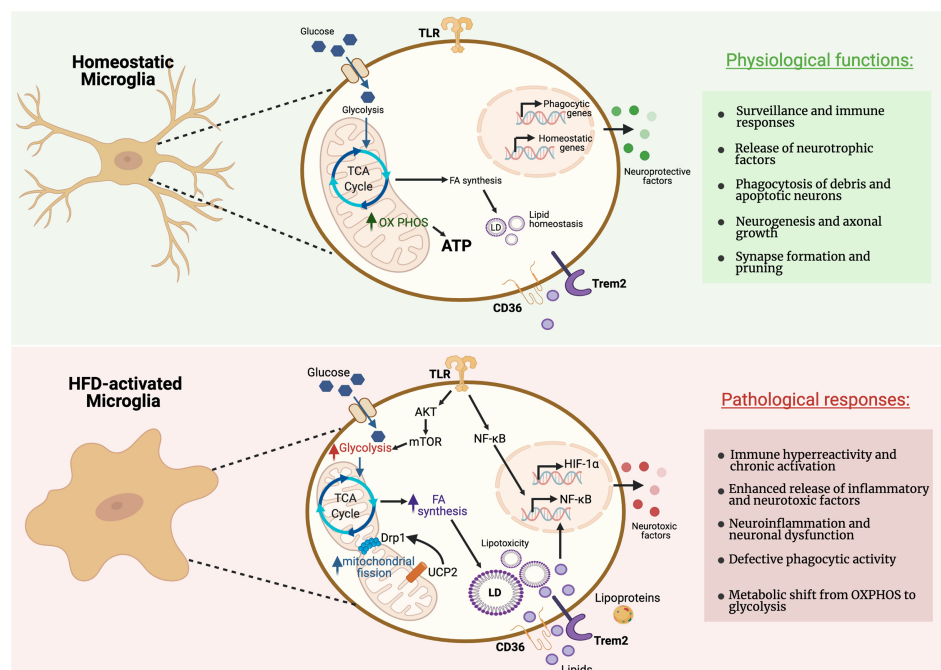


**FIGURE 2 |** Metabolic pathways regulating microglial activity during homeostasis and pathological responses. Microglia can rapidly adapt their energy metabolism to nutrient availability and transcriptomic analyses revealed that microglia express genes necessary for both glycolysis and oxidative metabolism. Microglia in their homeostatic status show reliance on oxidative metabolism to maintain their neuroprotective properties. However, microglia in proinflammatory states preferentially use glycolysis for energy production. This metabolic switch towards glycolysis allows microglia to produce ATP rapidly, despite being comparatively less efficient, for the secretion of inflammatory cytokines. High-fat diet (HFD) triggers a microglial inflammatory response leading to neuronal dysfunction in the MBH. Figure created with BioRender.com.

phosphorylation and homeostatic function during periods of hypoglycemia by shifting fuel utilization to glutamine (18). Homeostatic microglia, which are tasked with regulating day-to-day aspects of tissue homeostasis throughout the CNS, rely mainly on oxidative phosphorylation for ATP production, while microglia activated in the context of pro-inflammatory circumstances favor glycolysis (118, 119). When specifically activated, microglia are able to release several metabolites into the extracellular milieu (e.g.: succinate, itaconate, lactate) that modulate neuronal functionality and survival. For instance, a recent study showed that succinate produced by CNS myeloid cells is sensed by neural stem cells during the chronic phase of a mouse model of experimental autoimmune encephalitis (EAE) to ameliorate neuroinflammation *via* succinate-dependent mechanisms (120). Experiments on cultured microglia consistently show that they respond to proinflammatory stimuli by increasing glycolytic flux (121, 122). The metabolic alterations of isolated cells *in vitro* may differ from those *in vivo*. However, a novel approach to image NADH fluorescence has been recently employed to detect an enhanced glycolytic response of microglia to LPS treatment in mouse brain slices (18). Glycolysis is less efficient than oxidative phosphorylation (OXPHOS), however this glycolytic shift may redirect metabolites to provide the cell with precursor molecules for the production of inflammatory factors. Indeed, it has been shown that glycolysis is indispensable to stimulate secretion of pro-inflammatory cytokines by macrophages, the peripheral tissue analogs of microglia (123). Conversely, fatty acid  $\beta$ -oxidation and mitochondrial function are necessary for microglia to manifest relatively anti-inflammatory polarization states (124).

In considering what might control broad shifts in fuel metabolism among microglia, it is notable that epigenetic changes, including histone modifications and DNA methylation, are important modifiers of gene expression and are known to mediate the metabolic reprogramming of myeloid cells. For instance, feeding mice a HFD for 4 weeks is sufficient to induce lasting epigenetic modifications in myeloid progenitor cells in the bone marrow, leading to increased immune responses to LPS challenge even after the mice were returned to a regular low-fat chow diet (125). Despite the fact that metabolic alterations have been implicated in several disease models (126), more knowledge is needed to understand which specific metabolic pathways can be targeted to restore the homeostatic microglia phenotype in chronic inflammatory diseases, including obesity.

Recent studies have shed light on how changes in mitochondrial morphology and function may impact microglia polarization and function. Microglia stimulated with LPS, demonstrate increased mitochondrial fragmentation, which was dependent on ROS-mediated activation of adenosine monophosphate-activated protein kinase (AMPK) (127). Mitochondrial fragmentation in reactive microglia requires dynamin-related protein 1 (DRP1), an essential component of mitochondrial fission (127). Short-term HFD (3 days) caused decreased size and increased number of mitochondria in microglia in the MBH, associated with increased levels of activation of DRP1 (128) (**Figure 2**).

Mitochondrial uncoupling protein 2 (UCP2) plays a key role in reactive microglia. Knockdown of UCP2 modulates microglia response to both LPS and IL-4 (129). Deletion of microglial UCP2 prevented HFD-induced increases in mitochondrial fission in MBH microglia, and reduced microglial activation in the MBH and HFD-induced obesity (128). UCP2 has been shown to effect both ROS production (130, 131) and fuel utilization (132). Microglia in culture showed increased mitochondrial respiration in the presence of high glucose and palmitate, dependent on the presence of UCP2 (128). Further mechanistic studies are necessary to explore the impact of mitochondrial function and fuel utilization in the regulation of MBH microglia.

## The Impact of Sex on Microglial Phenotypes in Metabolic Regulation

The study of sex differences in physiology has gained attention, and sexual dimorphism in obesity and metabolic disease has been described (133, 134). HFD induces activation of microglia in the MBH of rodents, in a sexually dimorphic manner, affecting male differently than females (135). However, the mechanism underlying these differences are not well understood. Interestingly, recent studies suggest that male and female mice differentially metabolize lipids acquired from the diet. For instance, HFD feeding increases PA and sphingolipids levels in the hypothalamic tissue of male mice but not in the females (135). Alterations in sphingolipid-mediated signaling pathways might provide an additional mechanism by which SFAs induce hypothalamic dysfunction in the MBH (136). On the other hand, microglia in the adult mouse brain have sex-specific features and that could explain sex differences in neurological disease susceptibility (137). Moreover, it has been recently shown that microbiota influences adult microglia in a sex-specific manner (138). For instance, short-chain fatty acids (SCFAs) are the main metabolites produced by bacterial fermentation of dietary fiber in the gastrointestinal tract, and these SCFAs influence gut-brain communication and brain function directly or indirectly through immune, endocrine, and vagal pathways (139). Although the SCFAs have been shown to protect against diet-induced obesity in mice (140) and overweight humans (141), the underlying mechanisms are not well understood. SCFAs are important regulators of innate immune responses and recently have been involved in the regulation of microglial function (142). Thus, regulating CNS myeloid cell functions by manipulating the gut microbiota may represent a promising therapeutic approach to mitigate metabolic diseases.

## DIETARY LIPIDS REGULATE MICROGLIAL POLARIZATION AND RESPONSES IN THE MBH

Bioactive dietary FAs are potent modulators of microglial inflammatory responses. Lipid accumulation in myeloid cell types more broadly, is well demonstrated to be associated with

the activation of inflammatory signaling cascades (143). Moreover, microglia express a wide range of lipid metabolism-related genes such as those encoding fatty acid oxidation enzymes (144), lipoprotein lipases, lipid transporters, and lipid-sensitive receptors (e.g. receptors for endocannabinoids, prostaglandins or phospholipids), suggesting that lipids are important regulators of microglial physiology. Microglia can store FAs within lipid droplets, which are known to control their inflammatory responsiveness and phagocytic activity (145). Some reports suggest that dietary lipids in the context of the whole mammal, can also influence microglial function through indirect mechanisms including microbially-derived metabolites, hormonal control, and gut and systemically-derived inflammatory signals. For instance, treating microglia with insulin *in vitro* decreases LPS-induced TNF production and phagocytic activity in a dose-dependent manner (146). Moreover, ghrelin, an orexigenic hormone produced by the stomach and duodenum, directly exerts anti-inflammatory and anti-oxidative effects on LPS-activated microglia when introduced to them in culture (147).

In particular, long-chain SFAs have emerged as a potential nutritional triggers of microglial activation in the MBH, exerting effects in the brain analogous to those documented for peripheral tissues. HFD intake increases brain SFA levels, and more specifically those of lipids containing PA (14). Indeed, PA levels are increased in the CSF of overweight and obese humans (148). We showed that microglia in the MBH can sense rising levels of saturated fats, when consumed in excess, and transduce this to instruct local neurons. Moreover, enteric isocaloric gavage of SFAs, but not UFAs, for only 3 days is sufficient to induce microglial activation in the MBH, reproducing the response seen in the MBH of mice fed a HFD (14). These findings support the idea that SFAs trigger this response. However, the HFD commonly used for animal studies also contains high amounts of sugars, and another study suggested that dietary sugars, instead of fat, drive hypothalamic inflammation (149). One caveat of this study was that the authors did not control for calories and the sources of fat vs. carbohydrates across diets. Intriguingly, a recent comprehensive study of 29 different diets with different macronutrient compositions showed that only dietary fat, but not protein or carbohydrates, regulates hypothalamic control of energy intake and promotes adiposity (150). Besides macronutrient distribution, the specific source of dietary FA is can modulate microglial inflammatory responses. For instance, the substitution of dietary lard for flaxseed oil or olive oil reduced food intake and inflammatory markers in the MBH, highlighting a specific pro-inflammatory impact of SFAs (151).

SFAs were initially thought to induce inflammation as direct agonists of the toll-like receptor 4 (TLR4), a member of the interleukin-1 receptor superfamily with a prominent role in innate immune responses. In support of this hypothesis, pharmacological and genetic approaches to inhibit hypothalamic TLR4 signaling suppressed SFA-induced microglial activation and inflammatory cytokines expression in rodent models fed a HFD (112, 152). However, a recent study

showed that TLR4 is not the receptor for SFAs. Rather, TLR4-dependent priming alters cellular metabolism, lipid metabolic pathways and membrane lipid composition, changes that are required for engagement of SFA-induced inflammatory pathways (153). The fatty acid translocase CD36 is another potential mediator of microglial lipid-sensing. Indeed, CD36 has been shown to be essential for microglia-mediated uptake of myelin debris (154), and microglia response to beta-amyloid (155). However, while CD36 is known to be involved in long-chain fatty acid uptake and sensing in other tissues, its role in lipid-sensing in microglia has not been reported. Unlike SFAs, PUFAs have beneficial effects on the brain and reduce neuroinflammation. PUFAs, when incorporated into cell membranes, increasing membrane fluidity in a manner that was shown to help microglia engage in phagocytosis (156). Microglial movement was remarkably impaired in mice fed a diet deficient in n-3 PUFAs (157). Also, PUFAs are endogenous ligands of the G-couple receptor GPR120, which may explain, at least in part, how they activate anti-inflammatory signaling pathways (158). Moreover, GPR120 is primarily expressed by microglia in the hypothalamus and is suggested to be involved in regulating microglial inflammatory responses that influence energy homeostasis (159).

## LIPOPROTEIN METABOLISM AND LIPID MEDIATORS REGULATING MICROGLIAL PHENOTYPES

The emergence of new technology such as scRNA-seq has enabled the identification and characterization of the diversity of microglial populations. These studies have revealed that the heterogeneity of microglia in both normal and disease states exists beyond the simplistic M1/M2 paradigm, with a spectrum of cellular states existing from homeostatic microglia to pathology-associated microglia (160, 161). In addition, scRNA-seq of myeloid cells has revealed extensive regional heterogeneity in both microglia and non-parenchymal brain myeloid cells including so-called “border-associated” macrophages found proximal to, and within, meningeal lining tissue (162). Recently, several comprehensive *ex vivo* scRNA-seq analyses of microglia have defined specific transcriptional clusters with common metabolic characteristics. For instance, a novel microglial population called disease-associated microglia (DAM) was recently identify in a mouse models of AD and amyotrophic lateral sclerosis (ALS) expressing a distinct set of genes associated with lipid and lipoprotein metabolism (163). This transcriptional signature represents a preference for lipids as fuel substrates, ostensibly to meet the increased bioenergetic demands of this form of activated microglia (163). A similar signature is also observed in microglia in the context of demyelination, suggesting engagement of a transcriptional microglial phenotype that enables the ability to phagocytose and clear lipid debris (164). Moreover, human microglia from white matter adjacent to chronic multiple sclerosis (MS) lesions

showed upregulation of scavenger receptor and lipid metabolism genes including *LPL* and *PPARG* (165). Additionally, analyses of non-diseased human brain revealed clusters of microglia enriched for expression of metabolism-encoding genes, including *APOE* and *LPL*, in white- vs. grey matter, and increased with aging (166). While the transcriptional signature of activated microglial populations in these studies have shown variability in the response to different stimuli and experimental conditions, there is a clear consistent implication of alterations in lipid metabolism in analyses of microglia activated by stimuli other than those associated with acute infection.

## Lipoprotein Lipase (LPL)

Lipoprotein lipase (LPL), an enzyme needed for the hydrolytic cleavage and release of FAs from TGs, and a number of recent reports have highlighted LPL as a key feature of reparative microglia, which are recruited to restore tissue homeostasis in the context of injury, for example. scRNA-seq of DAM, in a murine model of Alzheimer's disease (AD), revealed that *LPL* levels are markedly increased in a unique microglial subset associated with phagocytosis and protection in AD (163). Furthermore, *LPL* gene transcription is elevated in a cuprizone model of demyelination (167), and a recent study suggested that LPL is a novel feature of a the supportive microglial phenotype that emerges during remyelination and repair *via* clearance of lipid debris (9).

LPL is expressed in the brain, spinal cord, and peripheral nerves but is predominantly expressed by macrophages and microglia in the human and murine brain (117, 168). Although the function of LPL in the microglial response to neurodegenerative disease is not well understood, *LPL* polymorphisms are been implicated in disease risk, such as an association with AD risk. For instance, loss-of-function *LPL* polymorphisms with reduced enzymatic activity are associated with increased AD risk as well as with increased VLDL-TG levels (169). Conversely, patients with *LPL* polymorphisms leading to increased LPL activity have reduced hippocampal amyloid plaque formation (170). Microglia-specific knockdown of *Lpl* exhibited decreased cell number and soma size of microglia in the ARC of mice fed a hypercaloric diet (168), supporting the hypothesis that lipoprotein metabolism is important in the regulation of MBH microglial function. In these mice, POMC neuronal loss was accelerated and they gained more weight than control mice. Microglia lacking *Lpl* demonstrated a shift in fuel utilization towards glutamine and decreased phagocytic capacity, suggestive of an immunometabolic shift (168). Taken together, these data suggest that LPL regulates lipid and lipoprotein uptake, which may provide the lipids needed to maintain homeostatic microglial functions in the MBH.

## Apolipoprotein E (APOE)

Apolipoprotein E (APOE) is the major carrier for lipids in the brain, and *APOE* genotype is the most profound genetic risk factor for AD, predominantly by modulating microglial activation (171). In the brain, APOE is expressed predominantly by astrocytes and microglia and a major role for APOE in the brain is to maintain a consistent supply of essential lipids to

neurons (172). Extensive studies have established the role of APOE in mediating inter-cellular cholesterol transport from glia to neuronal cells (173). The human APOE gene exists as three different alleles,  $\epsilon 2$ ,  $\epsilon 3$  and  $\epsilon 4$  and these isoforms change the lipid and receptor binding ability of APOE.

Microglial APOE production is strongly induced during injury and disease, including in AD (174). APOE is a key component of transcriptional signature of activated microglia, as demonstrated in post-mortem human brain studies, AD mouse models and studies of cultured microglia (163, 171). APOE induces an anti-inflammatory phenotype in macrophages and similarly an APOE peptide inhibits inflammatory processes in isolated microglia through the APOE receptor, LRP1 (175). In APOE-deficient mouse models, peptides based on the APOE receptor-binding domain prevent LPS-induced inflammation (176). Interestingly, blocking inflammatory signaling increases APOE expression in microglia (177), suggesting a negative feedback loop between APOE levels and inflammation.

The mechanistic role of APOE expression in hypothalamic microglia has not been explored in models of diet-induced obesity, but data from studies in neurodegenerative disease lend clues towards the potential function.

## Triggering Receptor Expressed on Myeloid Cells 2 (TREM2)

The Triggering Receptor Expressed on Myeloid Cells 2 (TREM2) is a type 1 transmembrane receptor protein expressed on myeloid cells. This receptor binds a wide array of ligands including extracellular lipids and lipoproteins, and loss of function variants in TREM2 are also associated with increased risk of AD. TREM2 modulates inflammatory signaling in myeloid cells, and in the brain is primarily expressed by microglia. TREM2 is crucial for induction of the transcriptomic and functional program of DAMs, by activation of phagocytosis and lipid metabolism-related pathways. TREM2-deficient microglia have strong metabolic defects, characterized by impaired lipid metabolism, accumulation of cholesterol esters, aberrant autophagy, altered mTOR signaling, and reduced ATP production (8, 178). Also, TREM2-deficient microglia have reduced mitochondrial mass and increased phosphorylation of AMPK (178), a key regulator of energy metabolism that is activated in response to low glucose and inhibits a shift in the cellular metabolism from oxidative phosphorylation to glycolysis (179). A recent study revealed that TREM2 activation by APOE, drives a neurodegenerative phenotype in microglia, characterized by suppression of transcription factors regulating homeostatic microglia (171). Thus, targeting of the TREM2-APOE pathway may represent a novel therapeutic approach to restore homeostatic microglia in neurological disease.

TREM2 signaling in peripheral macrophages has recently been linked to metabolic disease. TREM2 KO mice exhibit increased obesity, insulin resistance and altered adipose tissue remodeling in response to HFD feeding (180). TREM2 is required for induction of monocyte-derived LAMs, in which LPL and APOE are induced by a TREM2-dependent mechanism as a consequence of HFD-induced obesity in mice (110). Similar

transcriptional signatures were also identified in aortic macrophages during atherosclerosis (181) and fatty livers of mice fed a HFD (110). TREM2 activation *via* DAP12 antagonizes TLR signaling and inflammatory cytokine production in cultured macrophages and, conversely, TREM2 expression is abrogated by pro-inflammatory signaling (182, 183). However, the role of TREM2 in lipid-induced microglial activation in the MBH has not been investigated.

## CONCLUDING REMARKS AND FUTURE PERSPECTIVES

Both microglia and lipid metabolism are now known to play key roles in the onset and progression of the pathology of a wide variety of neurological diseases. The traditional view of the brain as an immune privileged organ has undergone a paradigm shift. In recent years, it has become increasingly clear that immune cells actively contribute to homeostatic processes in the CNS. Furthermore, dysfunctional microglial subsets characterized by excessive droplet- and membrane-associated lipid accumulation and attenuated lipid efflux have recently been the subject of considerable investigation (28, 184). Based on exciting data from other fields, it is increasingly becoming likely that a better understanding of how lipid mediators regulate the interaction between the immune and nervous systems may help uncover novel therapeutic targets to prevent and treat metabolic diseases as well. Indeed, many of the advances in determining the role of lipid and lipoprotein metabolism that have occurred in the context of neurodegenerative disease (12) have the capacity to provide direct insight into the mechanisms by which microglia are activated in the MBH by nutritional signals.

The CNS hosts a heterogeneous population of myeloid cells, including parenchymal homeostatic microglia, and perivascular and meningeal border-associated macrophages. These myeloid cells share the expression of numerous markers, and a major obstacle has been the lack of tools to discriminate between specific microglial as well as other brain myeloid populations. However, new approaches for single-cell profiling have revealed a remarkable functional complexity in the CNS myeloid compartment in both homeostatic and disease contexts. Microglia are highly dependent on environmental signals to maintain their polarization. Given that such signals may vary across brain regions, it is notable that immune profiling of human brain microglia by single-cell proteomics revealed

remarkable regional heterogeneity (185). Myeloid cells strategically located in close proximity to fenestrated blood vessels in the MBH may be able to sense metabolic factors including circulating lipids. To this end, we showed that HFD feeding induces the accumulation of a unique mix of myeloid cells in the MBH (15). This immunological response also includes the accumulation of perivascular macrophages involved in alterations systemic glucose metabolism (186). However, methods using marker-based analyses have technical limitations, and unbiased approaches are needed to resolve the heterogeneity and complexity of myeloid cell types within different CNS regions. Understanding the contribution of individual diet-responsive myeloid cell types will be critical for the development of novel therapeutics for obesity and T2D.

In summary, the emergence of a new field focused on microglial function, heterogeneity, and cell-cell crosstalk is providing us with an unprecedented understanding of how dietary lipids modulate microglial functions and their engagement with other cell types within the brain, including the MBH. This information has tremendous potential to help us identify new therapeutic targets to prevent overnutrition-induced hypothalamic dysfunction and metabolic disease.

## AUTHOR CONTRIBUTIONS

All authors listed have made a substantial, direct, and intellectual contribution to the work and approved it for publication.

## FUNDING

This work was funded by the NIDDK (Diabetes, Endocrinology & Metabolism Training Grant T32DK007418 to AF, R01DK103175 to SK, K01DK113064, and R03DK125627 to MV).

## ACKNOWLEDGMENTS

The authors thank members of their laboratories for helpful discussions on the topic and the Nutrition Obesity Research Centers at UCSF (DK098722).

## REFERENCES

- Hamilton JA, Hillard CJ, Spector AA, Watkins PA. Brain Uptake and Utilization of Fatty Acids, Lipids and Lipoproteins: Application to Neurological Disorders. *J Mol Neurosci* (2007) 33:2–11. doi: 10.1007/s12031-007-0060-1
- Karasinska JM, Hayden MR. Cholesterol Metabolism in Huntington Disease. *Nat Rev Neurol* (2011) 7:561–72. doi: 10.1038/nrneurol.2011.132
- Van Veldhoven PP. Biochemistry and Genetics of Inherited Disorders of Peroxisomal Fatty Acid Metabolism. *J Lipid Res* (2010) 51:2863–95. doi: 10.1194/jlr.R005959
- Barber CN, Raben DM. Lipid Metabolism Crosstalk in the Brain: Glia and Neurons. *Front Cell Neurosci* (2019) 13:212. doi: 10.3389/fncel.2019.00212
- Pellerin L, Bouzier-Sore A-K, Aubert A, Serres S, Merle M, Costalat R, et al. Activity-Dependent Regulation of Energy Metabolism by Astrocytes: An Update. *Glia* (2007) 55:1251–62. doi: 10.1002/glia.20528
- Bazan NG. Synaptic Lipid Signaling: Significance of Polyunsaturated Fatty Acids and Platelet-Activating Factor. *J Lipid Res* (2003) 44:2221–33. doi: 10.1194/jlr.R300013-JLR200
- Saher G, Brügger B, Lappe-Siefke C, Möbius W, Tozawa R, Wehr MC, et al. High Cholesterol Level Is Essential for Myelin Membrane Growth. *Nat Neurosci* (2005) 8:468–75. doi: 10.1038/nn1426

8. Nugent AA, Lin K, van Lengerich B, Lianoglou S, Przybyla L, Davis SS, et al. Trem2 Regulates Microglial Cholesterol Metabolism Upon Chronic Phagocytic Challenge. *Neuron* (2020) 105:837–54.e9. doi: 10.1016/j.neuron.2019.12.007
9. Bruce KD, Gorkhali S, Given K, Coates AM, Boyle KE, Macklin WB, et al. Lipoprotein Lipase Is a Feature of Alternatively-Activated Microglia and May Facilitate Lipid Uptake in the CNS During Demyelination. *Front Mol Neurosci* (2018) 11:57. doi: 10.3389/fnmol.2018.00057
10. Madore C, Leyrolle Q, Morel L, Rossitto M, Greenhalgh AD, Delpech JC, et al. Essential Omega-3 Fatty Acids Tune Microglial Phagocytosis of Synaptic Elements in the Mouse Developing Brain. *Nat Commun* (2020) 11:6133. doi: 10.1038/s41467-020-19861-z
11. Jha P, McDewitt MT, Halilbasic E, Williams EG, Quiros PM, Gariani K, et al. Genetic Regulation of Plasma Lipid Species and Their Association With Metabolic Phenotypes. *Cell Syst* (2018) 6:709–21.e6. doi: 10.1016/j.cels.2018.05.009
12. Loving BA, Bruce KD. Lipid and Lipoprotein Metabolism in Microglia. *Front Physiol* (2020) 11:393. doi: 10.3389/fphys.2020.00393
13. Fitzner D, Bader JM, Penkert H, Bergner CG, Su M, Weil M-T, et al. Cell-Type- and Brain-Region-Resolved Mouse Brain Lipidome. *Cell Rep* (2020) 32:108132. doi: 10.1016/j.celrep.2020.108132
14. Valdearcos M, Robblee MM, Benjamin DI, Nomura DK, Xu AW, Koliwad SK. Microglia Dictate the Impact of Saturated Fat Consumption on Hypothalamic Inflammation and Neuronal Function. *Cell Rep* (2014) 9:2124–38. doi: 10.1016/j.celrep.2014.11.018
15. Valdearcos M, Douglass JD, Robblee MM, Dorfman MD, Stifler DR, Bennett ML, et al. Microglial Inflammatory Signaling Orchestrates the Hypothalamic Immune Response to Dietary Excess and Mediates Obesity Susceptibility. *Cell Metab* (2017) 26:185–97.e3. doi: 10.1016/j.cmet.2017.05.015
16. Cansell C, Stobbe K, Sanchez C, Le Thuc O, Mosser C-A, Ben-Fradj S, et al. Dietary Fat Exacerbates Postprandial Hypothalamic Inflammation Involving Glial Fibrillary Acidic Protein-Positive Cells and Microglia in Male Mice. *Glia* (2020) 69(1):42–60. doi: 10.1002/glia.23882
17. Ebert D, Haller RG, Walton ME. Energy Contribution of Octanoate to Intact Rat Brain Metabolism Measured by <sup>13</sup>C Nuclear Magnetic Resonance Spectroscopy. *J Neurosci* (2003) 23:5928–35. doi: 10.1523/JNEUROSCI.23-13-05928.2003
18. Bernier L-P, York EM, Kamyabi A, Choi HB, Weilinger NL, MacVicar BA. Microglial Metabolic Flexibility Supports Immune Surveillance of the Brain Parenchyma. *Nat Commun* (2020) 11:1559. doi: 10.1038/s41467-020-15267-z
19. Bouyakdan K, Taib B, Budry L, Zhao S, Rodaros D, Neess D, et al. A Novel Role for Central ACBP/DBI as a Regulator of Long-Chain Fatty Acid Metabolism in Astrocytes. *J Neurochem* (2015) 133:253–65. doi: 10.1111/jnc.13035
20. Panov A, Orynbayeva Z, Vavilin V, Vyakhovich V. Fatty Acids in Energy Metabolism of the Central Nervous System. *BioMed Res Int* (2014) 2014:472459. doi: 10.1155/2014/472459
21. Schönfeld P, Reiser G. Why Does Brain Metabolism Not Favor Burning of Fatty Acids to Provide Energy? Reflections on Disadvantages of the Use of Free Fatty Acids as Fuel for Brain. *J Cereb Blood Flow Metab* (2013) 33:1493–9. doi: 10.1038/jcbfm.2013.128
22. Waldbaum S, Patel M. Mitochondria, Oxidative Stress, and Temporal Lobe Epilepsy. *Epilepsy Res* (2010) 88:23–45. doi: 10.1016/j.eplepsyres.2009.09.020
23. Alecu I, Bennett SAL. Dysregulated Lipid Metabolism and Its Role in  $\alpha$ -Synucleinopathy in Parkinson's Disease. *Front Neurosci* (2019) 13:328. doi: 10.3389/fnins.2019.00328
24. Billingsley KJ, Bandres-Ciga S, Saez-Atienzar S, Singleton AB. Genetic Risk Factors in Parkinson's Disease. *Cell Tissue Res* (2018) 373:9–20. doi: 10.1007/s00441-018-2817-y
25. Bosch-Queralt M, Cantuti-Castelvetri L, Damkou A, Schifferer M, Schlepckow K, Alexopoulos I, et al. Diet-Dependent Regulation of Tgfb $\beta$  Impairs Reporative Innate Immune Responses After Demyelination. *Nat Metab* (2021) 3:211–27. doi: 10.1038/s42255-021-00341-7
26. Berghoff SA, Spieth L, Sun T, Hosang L, Schlaphoff L, Depp C, et al. Microglia Facilitate Repair of Demyelinated Lesions Via Post-Squalene Sterol Synthesis. *Nat Neurosci* (2021) 24:47–60. doi: 10.1038/s41593-020-00757-6
27. Brekk OR, Honey JR, Lee S, Hallett PJ, Isacson O. Cell Type-Specific Lipid Storage Changes in Parkinson's Disease Patient Brains Are Recapitulated by Experimental Glycolipid Disturbance. *Proc Natl Acad Sci USA* (2020) 117:27646–54. doi: 10.1073/pnas.2003021117
28. Cantuti-Castelvetri L, Fitzner D, Bosch-Queralt M, Weil M-T, Su M, Sen P, et al. Defective Cholesterol Clearance Limits Remyelination in the Aged Central Nervous System. *Science* (2018) 359:684–8. doi: 10.1126/science.aan4183
29. Bozek K, Wei Y, Yan Z, Liu X, Xiong J, Sugimoto M, et al. Organization and Evolution of Brain Lipidome Revealed by Large-Scale Analysis of Human, Chimpanzee, Macaque, and Mouse Tissues. *Neuron* (2015) 85:695–702. doi: 10.1016/j.neuron.2015.01.003
30. Zhang J, Liu Q. Cholesterol Metabolism and Homeostasis in the Brain. *Protein Cell* (2015) 6:254–64. doi: 10.1007/s13238-014-0131-3
31. Petrov AM, Kasimov MR, Zefirov AL. Brain Cholesterol Metabolism and Its Defects: Linkage to Neurodegenerative Diseases and Synaptic Dysfunction. *Acta Naturae* (2016) 8:58–73. doi: 10.32607/20758251-2016-8-1-58-73
32. Wooten JS, Wu H, Raya J, Perrard XD, Gaubatz J, Hoogveen RC. The Influence of an Obesogenic Diet on Oxysterol Metabolism in C57BL/6J Mice. *Cholesterol* (2014) 2014:843468. doi: 10.1155/2014/843468
33. Ismail M-A-M, Mateos L, Maioli S, Merino-Serrais P, Ali Z, Lodeiro M, et al. 27-Hydroxycholesterol Impairs Neuronal Glucose Uptake Through an IRAP/GLUT4 System Dysregulation. *J Exp Med* (2017) 214:699–717. doi: 10.1084/jem.20160534
34. Wang H, Eckel RH. What Are Lipoproteins Doing in the Brain? *Trends Endocrinol Metab* (2014) 25:8–14. doi: 10.1016/j.tem.2013.10.003
35. Park J-H, Lee C-W, Nam MJ, Kim H, Kwon D-Y, Yoo JW, et al. Association of High-Density Lipoprotein Cholesterol Variability and the Risk of Developing Parkinson Disease. *Neurology* (2021) 96:e1391–401. doi: 10.1212/WNL.0000000000011553
36. Götz A, Lehti M, Donelan E, Striese C, Cucuruz S, Sachs S, et al. Circulating HDL Levels Control Hypothalamic Astroglialosis Via ApoA-I. *J Lipid Res* (2018) 59:1649–59. doi: 10.1194/jlr.M085456
37. Rapoport SI, Chang MC, Spector AA. Delivery and Turnover of Plasma-Derived Essential PUFAs in Mammalian Brain. *J Lipid Res* (2001) 42:678–85. doi: 10.1016/S0022-2275(20)31629-1
38. Plourde M, Cunnane SC. Extremely Limited Synthesis of Long Chain Polyunsaturates in Adults: Implications for Their Dietary Essentiality and Use as Supplements. *Appl Physiol Nutr Metab* (2007) 32:619–34. doi: 10.1139/H07-034
39. DeMar JC, Lee H-J, Ma K, Chang L, Bell JM, Rapoport SI, et al. Brain Elongation of Linoleic Acid Is a Negligible Source of the Arachidonate in Brain Phospholipids of Adult Rats. *Biochim Biophys Acta* (2006) 1761:1050–9. doi: 10.1016/j.bbalip.2006.06.006
40. Alashmali SM, Hopperton KE, Bazinet RP. Lowering Dietary N-6 Polyunsaturated Fatty Acids: Interaction With Brain Arachidonic and Docosahexaenoic Acids. *Curr Opin Lipidol* (2016) 27:54–66. doi: 10.1097/MOL.0000000000000255
41. Domenichiello AF, Kitson AP, Chen CT, Trépanier M-O, Stavro PM, Bazinet RP. The Effect of Linoleic Acid on the Whole Body Synthesis Rates of Polyunsaturated Fatty Acids From  $\alpha$ -Linolenic Acid and Linoleic Acid in Free-Living Rats. *J Nutr Biochem* (2016) 30:167–76. doi: 10.1016/j.jnutbio.2015.11.016
42. Ouellet M, Emond V, Chen CT, Julien C, Bourasset F, Oddo S, et al. Diffusion of Docosahexaenoic and Eicosapentaenoic Acids Through the Blood-Brain Barrier: An in Situ Cerebral Perfusion Study. *Neurochem Int* (2009) 55:476–82. doi: 10.1016/j.neuint.2009.04.018
43. Williams WM, Chang MC, Hayakawa T, Grange E, Rapoport SI. In Vivo Incorporation From Plasma of Radiolabeled Palmitate and Arachidonate Into Rat Brain Microvessels. *Microvasc Res* (1997) 53:163–6. doi: 10.1006/mvre.1996.1984
44. Spector R. Fatty Acid Transport Through the Blood-Brain Barrier. *J Neurochem* (1988) 50:639–43. doi: 10.1111/j.1471-4159.1988.tb02958.x
45. Le Foll C, Dunn-Meynell A, Musatov S, Magnan C, Levin BE. FAT/CD36: A Major Regulator of Neuronal Fatty Acid Sensing and Energy Homeostasis in Rats and Mice. *Diabetes* (2013) 62:2709–16. doi: 10.2337/db12-1689
46. Simopoulos AP. The Importance of the omega-6/omega-3 Fatty Acid Ratio in Cardiovascular Disease and Other Chronic Diseases. *Exp Biol Med* (2008) 233:674–88. doi: 10.3181/0711-MR-311
47. Hariri N, Thibault L. High-Fat Diet-Induced Obesity in Animal Models. *Nutr Res Rev* (2010) 23:270–99. doi: 10.1017/S0954422410000168

48. Sun T, Wang X, Cong P, Xu J, Xue C. Mass Spectrometry-Based Lipidomics in Food Science and Nutritional Health: A Comprehensive Review. *Comp Rev Food Sci Food Saf* (2020) 19:2530–58. doi: 10.1111/1541-4337.12603
49. Pakiet A, Jakubiak A, Czumaj A, Sledzinski T, Mika A. The Effect of Western Diet on Mice Brain Lipid Composition. *Nutr Metab (Lond)* (2019) 16:81. doi: 10.1186/s12986-019-0401-4
50. Demers G, Roy J, Machuca-Parra AI, Dashtehei Pour Z, Bairamian D, Daneault C, et al. Fish Oil Supplementation Alleviates Metabolic and Anxiodepressive Effects of Diet-Induced Obesity and Associated Changes in Brain Lipid Composition in Mice. *Int J Obes* (2020) 44:1936–45. doi: 10.1038/s41366-020-0623-6
51. Serhan CN, Chiang N, Van Dyke TE. Resolving Inflammation: Dual Anti-Inflammatory and Pro-Resolution Lipid Mediators. *Nat Rev Immunol* (2008) 8:349–61. doi: 10.1038/nri2294
52. Sánchez-Lasheras C, Könnner AC, Brüning JC. Integrative Neurobiology of Energy Homeostasis-Neurocircuits, Signals and Mediators. *Front Neuroendocrinol* (2010) 31:4–15. doi: 10.1016/j.yfrne.2009.08.002
53. Lechan RM, Toni R. Functional Anatomy of the Hypothalamus and Pituitary. In: Feingold KR, Anawalt B, Boyce A, Chrousos G, de Herder WW, Dhatariya K, et al, editors. *Endotext*. South Dartmouth, MA: MDText.com, Inc (2016).
54. Cheunsuang O, Stewart AL, Morris R. Differential Uptake of Molecules From the Circulation and CSF Reveals Regional and Cellular Specialisation in CNS Detection of Homeostatic Signals. *Cell Tissue Res* (2006) 325:397–402. doi: 10.1007/s00441-006-0162-z
55. Campbell JN, Macosko EZ, Fenselau H, Pers TH, Lyubetskaya A, Tenen D, et al. A Molecular Census of Arcuate Hypothalamus and Median Eminence Cell Types. *Nat Neurosci* (2017) 20:484–96. doi: 10.1038/nn.4495
56. Ciofi P, Garret M, Lapirot O, Lafon P, Loyens A, Prévot V, et al. Brain-Endocrine Interactions: A Microvascular Route in the Mediobasal Hypothalamus. *Endocrinology* (2009) 150:5509–19. doi: 10.1210/en.2009-0584
57. Ciofi P. The Arcuate Nucleus as a Circumventricular Organ in the Mouse. *Neurosci Lett* (2011) 487:187–90. doi: 10.1016/j.neulet.2010.10.019
58. Wang H, Astarita G, Taussig MD, Bharadwaj KG, DiPatrizio NV, Nave K-A, et al. Deficiency of Lipoprotein Lipase in Neurons Modifies the Regulation of Energy Balance and Leads to Obesity. *Cell Metab* (2011) 13:105–13. doi: 10.1016/j.cmet.2010.12.006
59. Rapoport SI. In Vivo Labeling of Brain Phospholipids by Long-Chain Fatty Acids: Relation to Turnover and Function. *Lipids* (1996) 31 Suppl:S97–101. doi: 10.1007/BF02637059
60. Jordan SD, Könnner AC, Brüning JC. Sensing the Fuels: Glucose and Lipid Signaling in the CNS Controlling Energy Homeostasis. *Cell Mol Life Sci* (2010) 67:3255–73. doi: 10.1007/s00018-010-0414-7
61. Cansell C, Castel J, Denis RGP, Rouch C, Delbes AS, Martinez S, et al. Dietary Triglycerides Act on Mesolimbic Structures to Regulate the Rewarding and Motivational Aspects of Feeding. *Mol Psychiatry* (2014) 19:1095–105. doi: 10.1038/mp.2014.31
62. Berland C, Montalban E, Perrin E, Di Miceli M, Nakamura Y, Martinat M, et al. Circulating Triglycerides Gate Dopamine-Associated Behaviors Through DRD2-Expressing Neurons. *Cell Metab* (2020) 31:773–90. doi: 10.1016/j.cmet.2020.02.010
63. Banks WA, Farr SA, Salameh TS, Niehoff ML, Rhea EM, Morley JE, et al. Triglycerides Cross the Blood-Brain Barrier and Induce Central Leptin and Insulin Receptor Resistance. *Int J Obes* (2018) 42:391–7. doi: 10.1038/ijo.2017.231
64. Weigert C, Brodbeck K, Staiger H, Kausch C, Machicao F, Häring HU, et al. Palmitate, But Not Unsaturated Fatty Acids, Induces the Expression of Interleukin-6 in Human Myotubes Through Proteasome-Dependent Activation of Nuclear Factor- $\kappa$ B. *J Biol Chem* (2004) 279:23942–52. doi: 10.1074/jbc.M312692200
65. Roberts R, Bickerton AS, Fielding BA, Blaak EE, Wagenmakers AJ, Chong MF-F, et al. Reduced Oxidation of Dietary Fat After a Short Term High-Carbohydrate Diet. *Am J Clin Nutr* (2008) 87:824–31. doi: 10.1093/ajcn/87.4.824
66. Yue JTY, Lam TKT. Lipid Sensing and Insulin Resistance in the Brain. *Cell Metab* (2012) 15:646–55. doi: 10.1016/j.cmet.2012.01.013
67. Wang R, Cruciani-Guglielmacci C, Migrenne S, Magnan C, Cotero VE, Routh VH. Effects of Oleic Acid on Distinct Populations of Neurons in the Hypothalamic Arcuate Nucleus Are Dependent on Extracellular Glucose Levels. *J Neurophysiol* (2006) 95:1491–8. doi: 10.1152/jn.00697.2005
68. Obici S, Feng Z, Morgan K, Stein D, Karkanas G, Rossetti L. Central Administration of Oleic Acid Inhibits Glucose Production and Food Intake. *Diabetes* (2002) 51:271–5. doi: 10.2337/diabetes.51.2.271
69. Obici S, Feng Z, Arduini A, Conti R, Rossetti L. Inhibition of Hypothalamic Carnitine Palmitoyltransferase-1 Decreases Food Intake and Glucose Production. *Nat Med* (2003) 9:756–61. doi: 10.1038/nm873
70. Benani A, Hryhorczuk C, Gouzé A, Fioramonti X, Brenachot X, Guissard C, et al. Food Intake Adaptation to Dietary Fat Involves PSA-Dependent Rewiring of the Arcuate Melanocortin System in Mice. *J Neurosci* (2012) 32:11970–9. doi: 10.1523/JNEUROSCI.0624-12.2012
71. Beutler LR, Chen Y, Ahn JS, Lin Y-C, Essner RA, Knight ZA. Dynamics of Gut-Brain Communication Underlying Hunger. *Neuron* (2017) 96:461–75. doi: 10.1016/j.neuron.2017.09.043
72. Beutler LR, Corpuz TV, Ahn JS, Kosar S, Song W, Chen Y, et al. Obesity Causes Selective and Long-Lasting Desensitization of AgRP Neurons to Dietary Fat. *Elife* (2020) 9. doi: 10.7554/eLife.55909
73. Dragano NR, Monfort-Pires M, Velloso LA. Mechanisms Mediating the Actions of Fatty Acids in the Hypothalamus. *Neuroscience* (2020) 447:15–27. doi: 10.1016/j.neuroscience.2019.10.012
74. Magnan C, Levin BE, Luquet S. Brain Lipid Sensing and the Neural Control of Energy Balance. *Mol Cell Endocrinol* (2015) 418(Pt 1):3–8. doi: 10.1016/j.mce.2015.09.019
75. Bruce KD, Zsombok A, Eckel RH. Lipid Processing in the Brain: A Key Regulator of Systemic Metabolism. *Front Endocrinol (Lausanne)* (2017) 8:60. doi: 10.3389/fendo.2017.00060
76. Jais A, Brüning JC. Hypothalamic Inflammation in Obesity and Metabolic Disease. *J Clin Invest* (2017) 127(1):24–32. doi: 10.1172/JCI88878
77. Volmer R, Ron D. Lipid-Dependent Regulation of the Unfolded Protein Response. *Curr Opin Cell Biol* (2015) 33:67–73. doi: 10.1016/j.ccb.2014.12.002
78. Cakir I, Cyr NE, Perello M, Litvinov BP, Romero A, Stuart RC, et al. Obesity Induces Hypothalamic Endoplasmic Reticulum Stress and Impairs Proopiomelanocortin (POMC) Post-Translational Processing. *J Biol Chem* (2013) 288:17675–88. doi: 10.1074/jbc.M113.475343
79. Schneeberger M, Dietrich MO, Sebastián D, Imbernón M, Castaño C, Garcia A, et al. Mitofusin 2 in POMC Neurons Connects ER Stress With Leptin Resistance and Energy Imbalance. *Cell* (2013) 155:172–87. doi: 10.1016/j.cell.2013.09.003
80. Hosoi T, Sasaki M, Miyahara T, Hashimoto C, Matsuo S, Yoshii M, et al. Endoplasmic Reticulum Stress Induces Leptin Resistance. *Mol Pharmacol* (2008) 74:1610–9. doi: 10.1124/mol.108.050070
81. Tse EK, Belsham DD. Palmitate Induces Neuroinflammation, ER Stress, and Pomc mRNA Expression in Hypothalamic mHypoA-POMC/GFP Neurons Through Novel Mechanisms That Are Prevented by Oleate. *Mol Cell Endocrinol* (2018) 472:40–9. doi: 10.1016/j.mce.2017.11.017
82. Volmer R, van der Ploeg K, Ron D. Membrane Lipid Saturation Activates Endoplasmic Reticulum Unfolded Protein Response Transducers Through Their Transmembrane Domains. *Proc Natl Acad Sci USA* (2013) 110:4628–33. doi: 10.1073/pnas.1217611110
83. Cragle FK, Baldini G. Mild Lipid Stress Induces Profound Loss of MC4R Protein Abundance and Function. *Mol Endocrinol* (2014) 28:357–67. doi: 10.1210/me.2013-1357
84. Ozcan L, Ergin AS, Lu A, Chung J, Sarkar S, Nie D, et al. Endoplasmic Reticulum Stress Plays a Central Role in Development of Leptin Resistance. *Cell Metab* (2009) 9:35–51. doi: 10.1016/j.cmet.2008.12.004
85. Zhang X, Zhang G, Zhang H, Karin M, Bai H, Cai D. Hypothalamic IKK $\beta$ /NF- $\kappa$ B and ER Stress Link Overnutrition to Energy Imbalance and Obesity. *Cell* (2008) 135:61–73. doi: 10.1016/j.cell.2008.07.043
86. Robblee MM, Kim CC, Porter Abate J, Valdearcos M, Sandlund KLM, Shenoy MK, et al. Saturated Fatty Acids Engage an IRE1 $\alpha$ -Dependent Pathway to Activate the NLRP3 Inflammasome in Myeloid Cells. *Cell Rep* (2016) 14:2611–23. doi: 10.1016/j.celrep.2016.02.053

87. Studencka-Turski M, Çetin G, Junker H, Ebstein F, Krüger E. Molecular Insight Into the IRE1 $\alpha$ -Mediated Type I Interferon Response Induced by Proteasome Impairment in Myeloid Cells of the Brain. *Front Immunol* (2019) 10:2900. doi: 10.3389/fimmu.2019.02900
88. Sofroniew MV, Vinters HV. Astrocytes: Biology and Pathology. *Acta Neuropathol* (2010) 119:7–35. doi: 10.1007/s00401-009-0619-8
89. Liu L, Zhang K, Sandoval H, Yamamoto S, Jaiswal M, Sanz E, et al. Glial Lipid Droplets and ROS Induced by Mitochondrial Defects Promote Neurodegeneration. *Cell* (2015) 160:177–90. doi: 10.1016/j.cell.2014.12.019
90. Ioannou MS, Jackson J, Sheu S-H, Chang C-L, Weigel AV, Liu H, et al. Neuron-Astrocyte Metabolic Coupling Protects Against Activity-Induced Fatty Acid Toxicity. *Cell* (2019) 177:1522–35.e14. doi: 10.1016/j.cell.2019.04.001
91. Zhang Y, Reichel JM, Han C, Zuniga-Hertz JP, Cai D. Astrocytic Process Plasticity and Ikk $\beta$ /Nf-kb in Central Control of Blood Glucose, Blood Pressure, and Body Weight. *Cell Metab* (2017) 25:1091–102.e4. doi: 10.1016/j.cmet.2017.04.002
92. Kim JG, Suyama S, Koch M, Jin S, Argente-Arizon P, Argente J, et al. Leptin Signaling in Astrocytes Regulates Hypothalamic Neuronal Circuits and Feeding. *Nat Neurosci* (2014) 17:908–10. doi: 10.1038/nn.3725
93. Yang L, Qi Y, Yang Y. Astrocytes Control Food Intake by Inhibiting AGRP Neuron Activity Via Adenosine A1 Receptors. *Cell Rep* (2015) 11:798–807. doi: 10.1016/j.celrep.2015.04.002
94. García-Cáceres C, Quarta C, Varela L, Gao Y, Gruber T, Legutko B, et al. Astrocytic Insulin Signaling Couples Brain Glucose Uptake With Nutrient Availability. *Cell* (2016) 166:867–80. doi: 10.1016/j.cell.2016.07.028
95. Nuzzaci D, Cansell C, Liénard F, Nédélec E, Ben Fradj S, Castel J, et al. Postprandial Hyperglycemia Stimulates Neuroglial Plasticity in Hypothalamic Pomc Neurons After a Balanced Meal. *Cell Rep* (2020) 30:3067–78.e5. doi: 10.1016/j.celrep.2020.02.029
96. Bolborea M, Dale N. Hypothalamic Tanycytes: Potential Roles in the Control of Feeding and Energy Balance. *Trends Neurosci* (2013) 36:91–100. doi: 10.1016/j.tins.2012.12.008
97. Rodríguez E, Guerra M, Peruzzo B, Blázquez JL. Tanycytes: A Rich Morphological History to Underpin Future Molecular and Physiological Investigations. *J Neuroendocrinol* (2019) 31:e12690. doi: 10.1111/jne.12690
98. Bolborea M, Pollatzek E, Benford H, Sotelo-Hitschfeld T, Dale N. Hypothalamic Tanycytes Generate Acute Hyperphagia Through Activation of the Arcuate Neuronal Network. *Proc Natl Acad Sci USA* (2020) 117:14473–81. doi: 10.1073/pnas.1919887117
99. Gao Y, Tschöp MH, Luquet S. Hypothalamic Tanycytes: Gatekeepers to Metabolic Control. *Cell Metab* (2014) 19:173–5. doi: 10.1016/j.cmet.2014.01.008
100. Paolicelli RC, Bolasco G, Pagani F, Maggi L, Scianni M, Panzanelli P, et al. Synaptic Pruning by Microglia Is Necessary for Normal Brain Development. *Science* (2011) 333:1456–8. doi: 10.1126/science.1202529
101. Coull JAM, Beggs S, Boudreau D, Boivin D, Tsuda M, Inoue K, et al. BDNF From Microglia Causes the Shift in Neuronal Anion Gradient Underlying Neuropathic Pain. *Nature* (2005) 438:1017–21. doi: 10.1038/nature04223
102. Lalancette-Hébert M, Gowing G, Simard A, Weng YC, Kriz J. Selective Ablation of Proliferating Microglial Cells Exacerbates Ischemic Injury in the Brain. *J Neurosci* (2007) 27:2596–605. doi: 10.1523/JNEUROSCI.5360-06.2007
103. Bachiller S, Jiménez-Ferrer I, Paulus A, Yang Y, Swanberg M, Deierborg T, et al. Microglia in Neurological Diseases: A Road Map to Brain-Disease Dependent-Inflammatory Response. *Front Cell Neurosci* (2018) 12:488. doi: 10.3389/fncel.2018.00488
104. Zhan Y, Paolicelli RC, Sforzini F, Weinhard L, Bolasco G, Pagani F, et al. Deficient Neuron-Microglia Signaling Results in Impaired Functional Brain Connectivity and Social Behavior. *Nat Neurosci* (2014) 17:400–6. doi: 10.1038/nn.3641
105. Jha MK, Jo M, Kim J-H, Suk K. Microglia-Astrocyte Crosstalk: An Intimate Molecular Conversation. *Neuroscientist* (2019) 25:227–40. doi: 10.1177/1073858418783959
106. Liddelow SA, Guttenplan KA, Clarke LE, Bennett FC, Bohlen CJ, Schirmer L, et al. Neurotoxic Reactive Astrocytes Are Induced by Activated Microglia. *Nature* (2017) 541:481–7. doi: 10.1038/nature21029
107. Rothhammer V, Borucki DM, Tjon EC, Takenaka MC, Chao C-C, Ardura-Fabregat A, et al. Microglial Control of Astrocytes in Response to Microbial Metabolites. *Nature* (2018) 557:724–8. doi: 10.1038/s41586-018-0119-x
108. Weisberg SP, McCann D, Desai M, Rosenbaum M, Leibel RL, Ferrante AW. Obesity Is Associated With Macrophage Accumulation in Adipose Tissue. *J Clin Invest* (2003) 112:1796–808. doi: 10.1172/JCI19246
109. Kratz M, Coats BR, Hisert KB, Hagman D, Mutskov V, Peris E, et al. Metabolic Dysfunction Drives a Mechanistically Distinct Proinflammatory Phenotype in Adipose Tissue Macrophages. *Cell Metab* (2014) 20:614–25. doi: 10.1016/j.cmet.2014.08.010
110. Jaitin DA, Adlung L, Thaiss CA, Weiner A, Li B, Descamps H, et al. Lipid-Associated Macrophages Control Metabolic Homeostasis in a Trem2-Dependent Manner. *Cell* (2019) 178:686–98. doi: 10.1016/j.cell.2019.05.054
111. De Souza CT, Araujo EP, Bordin S, Ashimine R, Zollner RL, Boschero AC, et al. Consumption of a Fat-Rich Diet Activates a Proinflammatory Response and Induces Insulin Resistance in the Hypothalamus. *Endocrinology* (2005) 146:4192–9. doi: 10.1210/en.2004-1520
112. Milanski M, Degasperi G, Coope A, Morari J, Denis R, Cintra DE, et al. Saturated Fatty Acids Produce an Inflammatory Response Predominantly Through the Activation of TLR4 Signaling in Hypothalamus: Implications for the Pathogenesis of Obesity. *J Neurosci* (2009) 29:359–70. doi: 10.1523/JNEUROSCI.2760-08.2009
113. Thaler JP, Yi C-X, Schur EA, Guyenet SJ, Hwang BH, Dietrich MO, et al. Obesity Is Associated With Hypothalamic Injury in Rodents and Humans. *J Clin Invest* (2012) 122:153–62. doi: 10.1172/JCI59660
114. Puig J, Blasco G, Daunis-I-Estadella J, Molina X, Xifra G, Ricart W, et al. Hypothalamic Damage Is Associated With Inflammatory Markers and Worse Cognitive Performance in Obese Subjects. *J Clin Endocrinol Metab* (2015) 100:E276–81. doi: 10.1210/jc.2014-2682
115. Schur EA, Melhorn SJ, Oh S-K, Lacy JM, Berkseth KE, Guyenet SJ, et al. Radiologic Evidence That Hypothalamic Gliosis Is Associated With Obesity and Insulin Resistance in Humans. *Obes (Silver Spring)* (2015) 23:2142–8. doi: 10.1002/oby.21248
116. Moraes JC, Coope A, Morari J, Cintra DE, Roman EA, Pauli JR, et al. High-Fat Diet Induces Apoptosis of Hypothalamic Neurons. *PLoS One* (2009) 4:e5045. doi: 10.1371/journal.pone.0005045
117. Zhang Y, Chen K, Sloan SA, Bennett ML, Scholze AR, O'Keefe S, et al. An RNA-Sequencing Transcriptome and Splicing Database of Glia, Neurons, and Vascular Cells of the Cerebral Cortex. *J Neurosci* (2014) 34:11929–47. doi: 10.1523/JNEUROSCI.1860-14.2014
118. Gimeno-Bayón J, López-López A, Rodríguez MJ, Mahy N. Glucose Pathways Adaptation Supports Acquisition of Activated Microglia Phenotype. *J Neurosci Res* (2014) 92:723–31. doi: 10.1002/jnr.23356
119. Voloboueva LA, Emery JF, Sun X, Giffard RG. Inflammatory Response of Microglial BV-2 Cells Includes a Glycolytic Shift and Is Modulated by Mitochondrial Glucose-Regulated Protein 75/Mortalin. *FEBS Lett* (2013) 587:756–62. doi: 10.1016/j.febslet.2013.01.067
120. Peruzzotti-Jametti L, Bernstock JD, Vicario N, Costa ASH, Kwok CK, Leonardi T, et al. Macrophage-Derived Extracellular Succinate Licenses Neural Stem Cells to Suppress Chronic Neuroinflammation. *Cell Stem Cell* (2018) 22:355–68.e13. doi: 10.1016/j.stem.2018.01.020
121. Nair S, Sobotka KS, Joshi P, Gressens P, Fleiss B, Thornton C, et al. Lipopolysaccharide-Induced Alteration of Mitochondrial Morphology Induces a Metabolic Shift in Microglia Modulating the Inflammatory Response In Vitro and In Vivo. *Glia* (2019) 67:1047–61. doi: 10.1002/glia.23587
122. Hu Y, Mai W, Chen L, Cao K, Zhang B, Zhang Z, et al. mTOR-mediated Metabolic Reprogramming Shapes Distinct Microglia Functions in Response to Lipopolysaccharide and ATP. *Glia* (2020) 68:1031–45. doi: 10.1002/glia.23760
123. Wang F, Zhang S, Jeon R, Vuckovic I, Jiang X, Lerman A, et al. Interferon Gamma Induces Reversible Metabolic Reprogramming of M1 Macrophages to Sustain Cell Viability and Pro-Inflammatory Activity. *EBioMedicine* (2018) 30:303–16. doi: 10.1016/j.ebiom.2018.02.009
124. Vats D, Mukundan L, Odegaard JI, Zhang L, Smith KL, Morel CR, et al. Oxidative Metabolism and PGC-1 $\beta$  Attenuate Macrophage-Mediated Inflammation. *Cell Metab* (2006) 4:13–24. doi: 10.1016/j.cmet.2006.05.011

125. Christ A, Günther P, Lauterbach MAR, Duewell P, Biswas D, Pelka K, et al. Western Diet Triggers NLRP3-Dependent Innate Immune Reprogramming. *Cell* (2018) 172:162–75.e14. doi: 10.1016/j.cell.2017.12.013
126. Na YR, Je S, Seok SH. Metabolic Features of Macrophages in Inflammatory Diseases and Cancer. *Cancer Lett* (2018) 413:46–58. doi: 10.1016/j.canlet.2017.10.044
127. Katoh M, Wu B, Nguyen HB, Thai TQ, Yamasaki R, Lu H, et al. Polymorphic Regulation of Mitochondrial Fission and Fusion Modifies Phenotypes of Microglia in Neuroinflammation. *Sci Rep* (2017) 7:4942. doi: 10.1038/s41598-017-05232-0
128. Kim JD, Yoon NA, Jin S, Diano S. Microglial UCP2 Mediates Inflammation and Obesity Induced by High-Fat Feeding. *Cell Metab* (2019) 30:952–62.e5. doi: 10.1016/j.cmet.2019.08.010
129. De Simone R, Ajmone-Cat MA, Pandolfi M, Bernardo A, De Nuccio C, Minghetti L, et al. The Mitochondrial Uncoupling Protein-2 Is a Master Regulator of Both M1 and M2 Microglial Responses. *J Neurochem* (2015) 135:147–56. doi: 10.1111/jnc.13244
130. Nègre-Salvayre A, Hirtz C, Carrera G, Cazenave R, Troly M, Salvayre R, et al. A Role for Uncoupling Protein-2 as a Regulator of Mitochondrial Hydrogen Peroxide Generation. *FASEB J* (1997) 11:809–15. doi: 10.1096/fasebj.11.10.9271366
131. Arsenijevic D, Onuma H, Pecqueur C, Raimbault S, Manning BS, Miroux B, et al. Disruption of the Uncoupling Protein-2 Gene in Mice Reveals a Role in Immunity and Reactive Oxygen Species Production. *Nat Genet* (2000) 26:435–9. doi: 10.1038/82565
132. Andrews ZB, Liu Z-W, Wallingford N, Erion DM, Borok E, Friedman JM, et al. UCP2 Mediates Ghrelin's Action on NPY/AgRP Neurons by Lowering Free Radicals. *Nature* (2008) 454:846–51. doi: 10.1038/nature07181
133. Palmer BF, Clegg DJ. The Sexual Dimorphism of Obesity. *Mol Cell Endocrinol* (2015) 402:113–9. doi: 10.1016/j.mce.2014.11.029
134. Griffin C, Lanzetta N, Eter L, Singer K. Sexually Dimorphic Myeloid Inflammatory and Metabolic Responses to Diet-Induced Obesity. *Am J Physiol Regul Integr Comp Physiol* (2016) 311:R211–6. doi: 10.1152/ajpregu.00136.2016
135. Morselli E, Fuente-Martin E, Finan B, Kim M, Frank A, Garcia-Caceres C, et al. Hypothalamic PGC-1 $\alpha$  Protects Against High-Fat Diet Exposure by Regulating *Erx*. *Cell Rep* (2014) 9:633–45. doi: 10.1016/j.celrep.2014.09.025
136. Kang S-C, Kim B-R, Lee S-Y, Park T-S. Sphingolipid Metabolism and Obesity-Induced Inflammation. *Front Endocrinol (Lausanne)* (2013) 4:67. doi: 10.3389/fendo.2013.00067
137. Villa A, Gelosa P, Castiglioni L, Cimino M, Rizzi N, Pepe G, et al. Sex-Specific Features of Microglia From Adult Mice. *Cell Rep* (2018) 23:3501–11. doi: 10.1016/j.celrep.2018.05.048
138. Thion MS, Low D, Silvin A, Chen J, Grisel P, Schulte-Schrepping J, et al. Microbiome Influences Prenatal and Adult Microglia in a Sex-Specific Manner. *Cell* (2018) 172:500–16.e16. doi: 10.1016/j.cell.2017.11.042
139. Dalile B, Van Oudenhove L, Vervliet B, Verbeke K. The Role of Short-Chain Fatty Acids in Microbiota-Gut-Brain Communication. *Nat Rev Gastroenterol Hepatol* (2019) 16:461–78. doi: 10.1038/s41575-019-0157-3
140. den Besten G, Bleeker A, Gerding A, van Eunen K, Havinga R, van Dijk TH, et al. Short-Chain Fatty Acids Protect Against High-Fat Diet-Induced Obesity Via a Ppar $\gamma$ -Dependent Switch From Lipogenesis to Fat Oxidation. *Diabetes* (2015) 64:2398–408. doi: 10.2337/db14-1213
141. Chambers ES, Viardot A, Psichas A, Morrison DJ, Murphy KG, Zaccarelli SEK, et al. Effects of Targeted Delivery of Propionate to the Human Colon on Appetite Regulation, Body Weight Maintenance and Adiposity in Overweight Adults. *Gut* (2015) 64:1744–54. doi: 10.1136/gutjnl-2014-307913
142. Erny D, Hrabě de Angelis AL, Jaitin D, Wieghofer P, Staszewski O, David E, et al. Host Microbiota Constantly Control Maturation and Function of Microglia in the CNS. *Nat Neurosci* (2015) 18:965–77. doi: 10.1038/nn.4030
143. den Brok MH, Raaijmakers TK, Collado-Camps E, Adema GJ. Lipid Droplets as Immune Modulators in Myeloid Cells. *Trends Immunol* (2018) 39:380–92. doi: 10.1016/j.it.2018.01.012
144. Maurer R, Walczak Y, Langmann T. Comprehensive mRNA Profiling of Lipid-Related Genes in Microglia and Macrophages Using Taqman Arrays. *Methods Mol Biol* (2009) 580:187–201. doi: 10.1007/978-1-60761-325-1\_10
145. Melo RCN, Weller PF. Lipid Droplets in Leukocytes: Organelles Linked to Inflammatory Responses. *Exp Cell Res* (2016) 340:193–7. doi: 10.1016/j.yexcr.2015.10.028
146. Maldonado-Ruiz R, Fuentes-Mera L, Camacho A. Central Modulation of Neuroinflammation by Neuropeptides and Energy-Sensing Hormones During Obesity. *BioMed Res Int* (2017) 2017:7949582. doi: 10.1155/2017/7949582
147. Lee JY, Yune TY. Ghrelin Inhibits Oligodendrocyte Cell Death by Attenuating Microglial Activation. *Endocrinol Metab (Seoul)* (2014) 29:371–8. doi: 10.3803/EnM.2014.29.3.371
148. Melo HM, Seixas da Silva G da S, Sant'Ana MR, Teixeira CVL, Clarke JR, Miya Coreixas VS, et al. Palmitate Is Increased in the Cerebrospinal Fluid of Humans With Obesity and Induces Memory Impairment in Mice Via Pro-inflammatory Tnf- $\alpha$ . *Cell Rep* (2020) 30:2180–94.e8. doi: 10.1016/j.celrep.2020.01.072
149. Gao Y, Bielohuby M, Fleming T, Grabner GF, Foppen E, Bernhard W, et al. Dietary Sugars, Not Lipids, Drive Hypothalamic Inflammation. *Mol Metab* (2017) 6:897–908. doi: 10.1016/j.molmet.2017.06.008
150. Hu S, Wang L, Yang D, Li L, Togo J, Wu Y, et al. Dietary Fat, But Not Protein or Carbohydrate, Regulates Energy Intake and Causes Adiposity in Mice. *Cell Metab* (2018) 28:415–31.e4. doi: 10.1016/j.cmet.2018.06.010
151. Cintra DE, Ropelle ER, Moraes JC, Pauli JR, Morari J, de SCT, et al. Unsaturated Fatty Acids Revert Diet-Induced Hypothalamic Inflammation in Obesity. *PLoS One* (2012) 7:e30571. doi: 10.1371/journal.pone.0030571
152. Zhao Y, Li G, Li Y, Wang Y, Liu Z. Knockdown of Tlr4 in the Arcuate Nucleus Improves Obesity Related Metabolic Disorders. *Sci Rep* (2017) 7:7441. doi: 10.1038/s41598-017-07858-6
153. Lancaster GI, Langley KG, Berglund NA, Kammoun HL, Reibe S, Estevez E, et al. Evidence That TLR4 Is Not a Receptor for Saturated Fatty Acids But Mediates Lipid-Induced Inflammation by Reprogramming Macrophage Metabolism. *Cell Metab* (2018) 27:1096–110.e5. doi: 10.1016/j.cmet.2018.03.014
154. Grajchen E, Wouters E, van de Haterd B, Haidar M, Hardonnière K, Dierckx T, et al. CD36-Mediated Uptake of Myelin Debris by Macrophages and Microglia Reduces Neuroinflammation. *J Neuroinflamm* (2020) 17:224. doi: 10.1186/s12974-020-01899-x
155. Moore KJ, El Khoury J, Medeiros LA, Terada K, Geula C, Luster AD, et al. A CD36-initiated Signaling Cascade Mediates Inflammatory Effects of Beta-Amyloid. *J Biol Chem* (2002) 277:47373–9. doi: 10.1074/jbc.M208788200
156. Bazinet RP, Layé S. Polyunsaturated Fatty Acids and Their Metabolites in Brain Function and Disease. *Nat Rev Neurosci* (2014) 15:771–85. doi: 10.1038/nrn3820
157. Madore C, Nadjar A, Delpech J-C, Sere A, Aubert A, Portal C, et al. Nutritional N-3 PUFAs Deficiency During Perinatal Periods Alters Brain Innate Immune System and Neuronal Plasticity-Associated Genes. *Brain Behav Immun* (2014) 41:22–31. doi: 10.1016/j.bbi.2014.03.021
158. Milligan G, Alvarez-Curto E, Hudson B, Prihandoko R, Tobin AB. FFA4/GPR120: Pharmacology and Therapeutic Opportunities. *Trends Pharmacol Sci* (2017) 38:809–21. doi: 10.1016/j.tips.2017.06.006
159. Dragano NRV, Solon C, Ramalho AF, de Moura RF, Razolli DS, Christiansen E, et al. Polyunsaturated Fatty Acid Receptors, GPR40 and GPR120, Are Expressed in the Hypothalamus and Control Energy Homeostasis and Inflammation. *J Neuroinflamm* (2017) 14:91. doi: 10.1186/s12974-017-0869-7
160. von Maydell D, Jorfi M. The Interplay Between Microglial States and Major Risk Factors in Alzheimer's Disease Through the Eyes of Single-Cell RNA-Sequencing: Beyond Black and White. *J Neurophysiol* (2019) 122:1291–6. doi: 10.1152/jn.00395.2019
161. Masuda T, Sankowski R, Staszewski O, Prinz M. Microglia Heterogeneity in the Single-Cell Era. *Cell Rep* (2020) 30:1271–81. doi: 10.1016/j.celrep.2020.01.010
162. Van Hove H, Martens L, Scheyltjens I, De Vlaminck K, Pombo Antunes AR, De Prijck S, et al. A Single-Cell Atlas of Mouse Brain Macrophages Reveals Unique Transcriptional Identities Shaped by Ontogeny and Tissue Environment. *Nat Neurosci* (2019) 22:1021–35. doi: 10.1038/s41593-019-0393-4
163. Keren-Shaul H, Spinrad A, Weiner A, Matcovitch-Natan O, Dvir-Szternfeld R, Ulland TK, et al. A Unique Microglia Type Associated With Restricting

- Development of Alzheimer's Disease. *Cell* (2017) 169:1276–90. doi: 10.1016/j.cell.2017.05.018
164. Hammond TR, Dufort C, Dissing-Olesen L, Giera S, Young A, Wysocki A, et al. Single-Cell RNA Sequencing of Microglia Throughout the Mouse Lifespan and in the Injured Brain Reveals Complex Cell-State Changes. *Immunity* (2019) 50:253–71. doi: 10.1016/j.immuni.2018.11.004
  165. van der Poel M, Ulas T, Mizze MR, Hsiao C-C, Miedema SSM, Adelia, et al. Transcriptional Profiling of Human Microglia Reveals Grey-White Matter Heterogeneity and Multiple Sclerosis-Associated Changes. *Nat Commun* (2019) 10:1139. doi: 10.1038/s41467-019-08976-7
  166. Sankowski R, Böttcher C, Masuda T, Geirsdottir L, Sagar, Sindram E, et al. Mapping Microglia States in the Human Brain Through the Integration of High-Dimensional Techniques. *Nat Neurosci* (2019) 22:2098–110. doi: 10.1038/s41593-019-0532-y
  167. Olah M, Amor S, Brouwer N, Vinet J, Eggen B, Biber K, et al. Identification of a Microglia Phenotype Supportive of Remyelination. *Glia* (2012) 60:306–21. doi: 10.1002/glia.21266
  168. Gao Y, Vidal-Itriago A, Kalsbeek MJ, Layritz C, García-Cáceres C, Tom RZ, et al. Lipoprotein Lipase Maintains Microglial Innate Immunity in Obesity. *Cell Rep* (2017) 20:3034–42. doi: 10.1016/j.celrep.2017.09.008
  169. Ren L, Ren X. Meta-Analyses of Four Polymorphisms of Lipoprotein Lipase Associated With the Risk of Alzheimer's Disease. *Neurosci Lett* (2016) 619:73–8. doi: 10.1016/j.neulet.2016.03.021
  170. Baum L, Wiebusch H, Pang CP. Roles for Lipoprotein Lipase in Alzheimer's Disease: An Association Study. *Microsc Res Tech* (2000) 50:291–6. doi: 10.1002/1097-0029(20000815)50:4<291::AID-JEMT8>3.0.CO;2-L
  171. Krasemann S, Madore C, Cialic R, Baufeld C, Calcagno N, El Fatimy R, et al. The TREM2-APOE Pathway Drives the Transcriptional Phenotype of Dysfunctional Microglia in Neurodegenerative Diseases. *Immunity* (2017) 47:566–581.e9. doi: 10.1016/j.immuni.2017.08.008
  172. Holtzman DM, Herz J, Bu G. Apolipoprotein E and Apolipoprotein E Receptors: Normal Biology and Roles in Alzheimer Disease. *Cold Spring Harb Perspect Med* (2012) 2:a006312. doi: 10.1101/cshperspect.a006312
  173. Mauch DH, Nägler K, Schumacher S, Göritz C, Müller EC, Otto A, et al. CNS Synaptogenesis Promoted by Glia-Derived Cholesterol. *Science* (2001) 294:1354–7. doi: 10.1126/science.294.5545.1354
  174. Rangaraju S, Dammer EB, Raza SA, Gao T, Xiao H, Betarbet R, et al. Quantitative Proteomics of Acutely-Isolated Mouse Microglia Identifies Novel Immune Alzheimer's Disease-Related Proteins. *Mol Neurodegener* (2018) 13:34. doi: 10.1186/s13024-018-0266-4
  175. Pocivavsek A, Mikhailenko I, Strickland DK, Rebeck GW. Microglial Low-Density Lipoprotein Receptor-Related Protein 1 Modulates C-Jun N-terminal Kinase Activation. *J Neuroimmunol* (2009) 214:25–32. doi: 10.1016/j.jneuroim.2009.06.010
  176. Lynch JR, Tang W, Wang H, Vitek MP, Bennett ER, Sullivan PM, et al. APOE Genotype and an ApoE-mimetic Peptide Modify the Systemic and Central Nervous System Inflammatory Response. *J Biol Chem* (2003) 278:48529–33. doi: 10.1074/jbc.M306923200
  177. Pocivavsek A, Rebeck GW. Inhibition of C-Jun N-terminal Kinase Increases ApoE Expression In Vitro and In Vivo. *Biochem Biophys Res Commun* (2009) 387:516–20. doi: 10.1016/j.bbrc.2009.07.048
  178. Ulland TK, Song WM, Huang SC-C, Ulrich JD, Sergushichev A, Beatty WL, et al. TREM2 Maintains Microglial Metabolic Fitness in Alzheimer's Disease. *Cell* (2017) 170:649–663.e13. doi: 10.1016/j.cell.2017.07.023
  179. Hardie DG. AMP-Activated Protein Kinase: An Energy Sensor That Regulates All Aspects of Cell Function. *Genes Dev* (2011) 25:1895–908. doi: 10.1101/gad.17420111
  180. Liu C, Li P, Li H, Wang S, Ding L, Wang H, et al. TREM2 Regulates Obesity-Induced Insulin Resistance Via Adipose Tissue Remodeling in Mice of High-Fat Feeding. *J Transl Med* (2019) 17:300. doi: 10.1186/s12967-019-2050-9
  181. Cochain C, Vafadarnejad E, Arampatzis P, Pelisek J, Winkels H, Ley K, et al. Single-Cell RNA-Seq Reveals the Transcriptional Landscape and Heterogeneity of Aortic Macrophages in Murine Atherosclerosis. *Circ Res* (2018) 122:1661–74. doi: 10.1161/CIRCRESAHA.117.312509
  182. Hamerman JA, Jarjoura JR, Humphrey MB, Nakamura MC, Seaman WE, Lanier LL. Cutting Edge: Inhibition of TLR and FcR Responses in Macrophages by Triggering Receptor Expressed on Myeloid Cells (TREM)-2 and DAP12. *J Immunol* (2006) 177:2051–5. doi: 10.4049/jimmunol.177.4.2051
  183. Gao X, Dong Y, Liu Z, Niu B. Silencing of Triggering Receptor Expressed on Myeloid Cells-2 Enhances the Inflammatory Responses of Alveolar Macrophages to Lipopolysaccharide. *Mol Med Rep* (2013) 7:921–6. doi: 10.3892/mmr.2013.1268
  184. Marschallinger J, Iram T, Zardeneta M, Lee SE, Lehallier B, Haney MS, et al. Lipid-Droplet-Accumulating Microglia Represent a Dysfunctional and Proinflammatory State in the Aging Brain. *Nat Neurosci* (2020) 23:194–208. doi: 10.1038/s41593-019-0566-1
  185. Miedema A, Wijering MHC, Eggen BJL, Kooistra SM. High-Resolution Transcriptomic and Proteomic Profiling of Heterogeneity of Brain-Derived Microglia in Multiple Sclerosis. *Front Mol Neurosci* (2020) 13:583811. doi: 10.3389/fnmol.2020.583811
  186. Lee CH, Kim HJ, Lee Y-S, Kang GM, Lim HS, Lee S-H, et al. Hypothalamic Macrophage Inducible Nitric Oxide Synthase Mediates Obesity-Associated Hypothalamic Inflammation. *Cell Rep* (2018) 25:934–46.e5. doi: 10.1016/j.celrep.2018.09.070

**Conflict of Interest:** The authors declare that the research was conducted in the absence of any commercial or financial relationships that could be construed as a potential conflict of interest.

Copyright © 2021 Folick, Koliwad and Valdearcos. This is an open-access article distributed under the terms of the Creative Commons Attribution License (CC BY). The use, distribution or reproduction in other forums is permitted, provided the original author(s) and the copyright owner(s) are credited and that the original publication in this journal is cited, in accordance with accepted academic practice. No use, distribution or reproduction is permitted which does not comply with these terms.



# Activity-Based Anorexia Induces Browning of Adipose Tissue Independent of Hypothalamic AMPK

Angela Fraga<sup>1,2,3</sup>, Eva Rial-Pensado<sup>1,2</sup>, Rubén Nogueiras<sup>1,2</sup>, Johan Fernø<sup>4</sup>, Carlos Diéguez<sup>1,2</sup>, Emilio Gutierrez<sup>3,5\*</sup> and Miguel López<sup>1,2\*</sup>

<sup>1</sup> Department of Physiology, Center for Research in Molecular Medicine and Chronic Diseases (CiMUS), University of Santiago de Compostela-Instituto de Investigación Sanitaria, Santiago de Compostela, Spain, <sup>2</sup> CIBER Fisiopatología de la Obesidad y Nutrición (CIBEROBN), Santiago de Compostela, Spain, <sup>3</sup> Department of Clinical Psychology and Psychobiology, School of Psychology, University of Santiago de Compostela-Instituto de Investigación Sanitaria, Santiago de Compostela, Spain, <sup>4</sup> Hormone Laboratory, Haukeland University Hospital, Bergen, Norway, <sup>5</sup> Unidad Venres Clínicos, School of Psychology, Universidad of Santiago de Compostela, Santiago de Compostela, Spain

## OPEN ACCESS

### Edited by:

Cristina García Cáceres,  
Ludwig Maximilian University of  
Munich, Germany

### Reviewed by:

Marc Claret,  
Institut de Recerca Biomèdica August  
Pi i Sunyer (IDIBAPS), Spain  
Kamal Rahmouni,  
The University of Iowa, United States

### \*Correspondence:

Emilio Gutierrez  
emilio.gutierrez@usc.es  
Miguel López  
m.lopez@usc.es

### Specialty section:

This article was submitted to  
Neuroendocrine Science,  
a section of the journal  
Frontiers in Endocrinology

**Received:** 19 February 2021

**Accepted:** 15 March 2021

**Published:** 02 June 2021

### Citation:

Fraga A, Rial-Pensado E, Nogueiras R,  
Fernø J, Diéguez C, Gutierrez E and  
López M (2021) Activity-Based  
Anorexia Induces Browning of  
Adipose Tissue Independent  
of Hypothalamic AMPK.  
Front. Endocrinol. 12:669980.  
doi: 10.3389/fendo.2021.669980

Anorexia nervosa (AN) is an eating disorder leading to malnutrition and, ultimately, to energy wasting and cachexia. Rodents develop activity-based anorexia (ABA) when simultaneously exposed to a restricted feeding schedule and allowed free access to running wheels. These conditions lead to a life-threatening reduction in body weight, resembling AN in human patients. Here, we investigate the effect of ABA on whole body energy homeostasis at different housing temperatures. Our data show that ABA rats develop hyperactivity and hypophagia, which account for a massive body weight loss and muscle cachexia, as well as reduced uncoupling protein 1 (UCP1) expression in brown adipose tissue (BAT), but increased browning of white adipose tissue (WAT). Increased housing temperature reverses not only the hyperactivity and weight loss of animals exposed to the ABA model, but also hypothermia and loss of body and muscle mass. Notably, despite the major metabolic impact of ABA, none of the changes observed are associated to changes in key hypothalamic pathways modulating energy metabolism, such as AMP-activated protein kinase (AMPK) or endoplasmic reticulum (ER) stress. Overall, this evidence indicates that although temperature control may account for an improvement of AN, key hypothalamic pathways regulating thermogenesis, such as AMPK and ER stress, are unlikely involved in later stages of the pathophysiology of this devastating disease.

**Keywords:** activity-based anorexia, temperature, cachexia, brown adipose tissue, white adipose tissue, hypothalamus, AMPK, ER stress

## INTRODUCTION

Anorexia nervosa (AN) is an eating disorder characterized by decreased food intake, severe weight loss and hyperactivity (1, 2). Due to chronic underfeeding, patients with AN present neuroendocrine changes, in an attempt to adapt to malnutrition, which in many cases are not completely reversed even with the recovery of body weight (3); this leads to several medical complications (4, 5).

Activity-Based Anorexia (ABA) is considered the best analogue animal model for AN (6), which is obtained by providing availability of food to rats 1-2 h/day and free access to a running wheel (7). Under these circumstances, rats develop an excessive running and reduced meal efficiency, eliciting massive weight loss and hypothermia, both mimicking the principal signs of AN disorder in humans. Notably, ABA also reproduces the metabolic and endocrine abnormalities observed in humans (8). AN-associated hyperactivity has been proposed as an adaptive behavioral response to compensate for hypothermia (9). Previous research has shown that exposure to a high ambient temperature (AT) prevents and reverses the hyperactivity and improves feeding patterns, allowing body weight recovery in both male and female rats under ABA conditions (10–15). These beneficial effects of temperature have been also found in the semi-starvation induced hyperactivity model (SIH) (16).

Due to the ability of the ABA model to reproduce many of the symptoms of the AN disorder in humans, as well as the identification of several genes involved in food intake regulation and energy balance as potential pathways that contribute to the etiology and maintenance of AN (17, 18), it would be interesting to examine the effect of high AT on energy sensors potentially involved in AN, as well as the possible clinical implications on the treatment of AN in humans. Here, we focused on AMP-activated protein kinase (AMPK) and endoplasmic reticulum (ER) stress, well-known mechanisms regulating both sides of the energy metabolism, namely feeding and thermogenesis (19–26).

## MATERIALS AND METHOD

### Animals

Male Sprague-Dawley rats (130–190 g) were acquired from the Animalario General USC, (Santiago de Compostela, Spain). They were kept with food and water *ad libitum* on a 12-hr light-dark cycle (LD, lights on from 08:00 to 20:00 hours). Ambient temperature set at  $21 \pm 1^\circ\text{C}$ . The Ethics Committee on the use and care of animals of Santiago de Compostela University approved all described procedures (project license 15004/17/002). All experiments were carried out in accordance with Royal Decree 53/2013 of February 1, Law 32/2007 of November 7, and European Communities Council Directive 2010/63/UE of September 22, on the protection of animals used for experimental and other scientific purposes.

### Running Wheels

Cages (48 x 31.5 x 47 cm) equipped with a Whatman-type activity wheel (1.12-m circumference 35.7 cm diameter, 10-cm-wide running surface of a 10-mm mesh bounded by clear Plexiglas and stainless-steel walls; *Panlab Harvard Apparatus*; Barcelona, Spain) were placed inside wooden incubators (60 x 60 x 60 cm) with polycarbonate roofs, provided with a 150 W heat wave lamp, connected to a thermostat and a probe positioned at the level of the animal, which allowed individual control of AT.

### ABA Procedure

One week prior to the start of the experiments body temperature and activity transmitters (*PTD 4000 E-Mitter*, *Respironics Mini Mitter Inc*; Bend, OR, US) were implanted under ketamine-xylazine anesthesia (50 mg/kg, intraperitoneal) and inserted in a subcutaneous pocket on the ventral surface created using blunt dissection. The rats were allowed seven days to recover. On the eighth day, rats were weighed and assigned to two weight matched groups: an active and restrictive-fed (AC) group and an inactive and restrictive-fed (IN) group. All the rats were transferred to running wheel cages, but only the rats assigned to the active condition had access to functional wheels. The rats assigned to the inactive condition remained with the activity wheel blocked during the whole experiment, avoiding any possibility of movement inside those devices. The ABA procedure started (day 0) with the removal of food at 12:30 h for restricted-fed groups. At the same time, the doors to the wheels were opened for the active group. From day 1 onward, all rats were given access to food according to a restricted feeding schedule from 11:00 to 12:30 h. The doors of the wheels were closed during this feeding period. Food intake was measured by weighing the food at the beginning and the end of every 1.5 h feeding period. Rats were also weighed daily at 10:30 h (as they were on day 0). This phase continued for each restricted-fed active rats until it reached a body weight loss criterion (BWLC) of 20% of their day 0 body weight. At this time, rats were assigned to one of two ambient temperature,  $21^\circ\text{C}$  or  $32^\circ\text{C}$ , as indicated in the two digits of the abbreviated group name (AC21 and AC32). These conditions were maintained until rats reached either the recovery criterion, which was defined as body weight on any particular day (day  $n$ ) greater than the weight of the animal 4 days before, (day  $n-4$ ), or the removal criterion which was defined as body weight under 75% of body weight on day 0 (7). The experiment was terminated after 15 days. The restricted-fed inactive rats were also assigned to two ambient temperature conditions,  $21^\circ\text{C}$  or  $32^\circ\text{C}$  (IN21 and IN32). For the rats maintained at  $21^\circ\text{C}$  the experiment lasted only six days (median of days that the restricted-fed active animals took to reach the BWLC). While rats assigned to  $21^\circ\text{C}$  AT remained in these conditions for three days more (median of days that de AC21 group took to reach the removal criterion), rats assigned to  $32^\circ\text{C}$  remained six days on experiment (median of days that the AC32 group took to reach the recovery criterion). At the end of the experiments rats were sacrificed by decapitation after the weighing routine; trunk blood, brain, brown adipose tissue (BAT), hind leg muscle and gonadal white adipose tissue (gWAT) were collected, frozen and stored at  $-80^\circ\text{C}$  until assay.

### Blood Biochemistry

Trunk blood was collected into specific tubes (*BD Vacutainer*; Plymouth, UK) and centrifuged at  $3,200\times g$  for 15 min at  $4^\circ\text{C}$  to separate the serum. Then serum was stored at  $-80^\circ\text{C}$ . Glucose free T3 and free T4 were measured using an automated chemistry analyzer (*ADVIA 2400 Chemistry System*, *Siemens Medical Solutions Inc*; Ann Arbor, MI US). Leptin, corticosterone (CORT), adrenaline and noradrenaline levels were measured

using ELISA kits (EZRL-83K; *Linco Research*; St. Charles, Missouri, US, for leptin; *ab108821*, *Abcam*, Cambridge, UK, for CORT; *EIA-3175*; *DRG Instruments GmbH*, Marburg, Germany, for adrenaline and noradrenaline).

## Hypothalamic Dissection

The brain was placed in an adult rat brain matrix (*Kent-Scientific Corporation*, #RBMA-300C; Torrington, CT, US) with the hypothalamus upward and dissected as previously described (23, 24, 26–28).

## Western Blotting

BAT, gWAT and the hypothalamic nuclei (arcuate, ARC, and ventromedial, VMH) were homogenized in lysis buffer containing protease inhibitor cocktail tablets (*Roche Diagnostics*; Indianapolis, IN, US) and the protein concentration was determined using the Bradford method (*Protein assay dye concentrate*, *Bio-Rad Laboratories*; Hercules, CA, US). The protein lysates were subjected to SDS-PAGE and electro-transferred to polyvinylidene difluoride membranes (PVDF; *Millipore*; Billerica, MA, US) with a semidry blotter. Membranes were blocked in TBS/Tween with 3% of BSA (Bovine serum albumin, *Sigma Aldrich*, St. Louis, US) and probed with the following antibodies against: pAMPK $\alpha$  (Thr172), glucose-regulated protein 78 (GRP78; *Cell Signaling*; Danvers, MA, US), UCP1 (uncoupling protein 1; *Abcam*; Cambridge, UK), C/EBP Homologous Protein (CHOP; *SCBT*; Dallas, Texas, USA),  $\alpha$ -tubulin and  $\beta$ -actin (*Sigma-Aldrich*; St. Louis, MO, US), as previously shown (23, 24, 26–29). Membranes were incubated with the corresponding secondary antibody: anti-rabbit, anti-mouse, or anti-goat (*DAKO*; Glostrup, Denmark). Detection of proteins was performed with Enhanced chemiluminescence (ECL) reagents (*Pierce ECL Western Blotting Substrate*, *Cultek*; Madrid, Spain) according to the manufacturer's instructions, exposed to x-ray films (*Fujifilm*; Tokyo, Japan), developed and fixed under appropriate dark room conditions. Autoradiographic films were scanned and the bands signal was quantified by densitometry using *ImageJ-1.33 software* (NIH; Bethesda, MD, US), as shown (23, 24, 26–29). Values were expressed in relation to  $\beta$ -actin (hypothalamus) or  $\alpha$ -tubulin (BAT). Representative images for all proteins are shown, all the bands for each picture always come from the same gel, although they may be spliced for clarity, as represented by vertical lines.

## Real-Time Quantitative RT-PCR

Real-time PCR (*TaqMan*<sup>®</sup>; *Applied Biosystems*; Foster City, CA, USA) was performed using specific primers and probes (**Supplementary Table 1**), as shown (27–30). Values were expressed in relation to hypoxanthine-guanine phosphoribosyl-transferase (*Hprt*) levels.

## Hematoxylin-Eosin Staining and UCP1 Immunohistochemistry

gWAT depots were fixed in 10% buffered formaldehyde and subsequently treated for histological study by dehydration (increasing alcohol concentrations), mounting in xylene and immersion in paraffin. The paraffin blocks were sliced into 3

mm sections that were processed, deparaffinized in xylene, rehydrated and rinsed in distilled water and then stained either for hematoxylin-eosin or UCP1 immunohistochemistry. For the hematoxylin-eosin processing, slices were first stained with hematoxylin for 5 min, washed and stained again with eosin for 1 min. For UCP1 immunohistochemistry, slices were incubated overnight with the primary antibody (UCP1; *Abcam*; Cambridge, UK), washed and incubated with the secondary antibody (*DAKO*; Glostrup, Denmark). Images were taken in an optical microscope with a digital camera *Olympus XC50* (*Olympus Corporation*; Tokyo, Japan) at 40X. Adipocyte area and UCP1 staining area were quantified using *ImageJ 1.33 software* (NIH, Bethesda, MD, US), as shown (25, 29, 31, 32).

## Statistical Analysis

Data are presented as mean  $\pm$  SEM. When two groups were compared, statistical significance was determined by two-sided Student's t-test; when more than groups were compared, statistical significance was determined by ANOVA followed by Bonferroni's test.  $P < 0.05$  was considered significant. Statistical analyses were performed using *SPSS 21.0 software* (IBM; Armonk, NY, US).

## RESULTS

### Increased Housing Temperature Reverses the Effect of ABA on Energy Balance and Activity

ABA rats exposed at a housing temperature of 32°C (AC32) ran six-fold less than rats housed at 21°C (AC21). During Phase II running activity of AC32 rats did not reach the activity level shown on the last day of Phase I, (day they met the body weight loss criterion of 20%, 20%BWLC), despite being an average of 4 more days being subjected to standard ABA conditions (restricted feeding plus wheel access) (**Figure 1A**). Active rats lose weight during Phase II while inactive rats keep it stable. Besides, the increase in room temperature to 32°C allowed for less weight loss in active rats and slightly increased weight in inactive rats, when compared to their counterparts at 21°C (**Figures 1B, C**). Both active and inactive rats exhibited higher body temperature when they were maintained at 32°C, as (**Figures 1D, E**). Rats kept at lower temperature of 21°C initially ate more than rats at 32°C although no significant differences were detected on the final day (**Figures 1F, G**).

### Increased Housing Temperature Reverses the Effects of ABA on Circulating Parameters

Next, we evaluated the effect of housing temperature on circulating parameters in the ABA model (**Table 1**). We first focused on leptin levels, since this hormone has been shown to have a controversial role in this model of disease (16, 33–39). Resembling the clinical evidence (34, 36, 37), our data showed that active rats had significantly lower circulating leptin levels than inactive ones, which were elevated after exposure of the rats

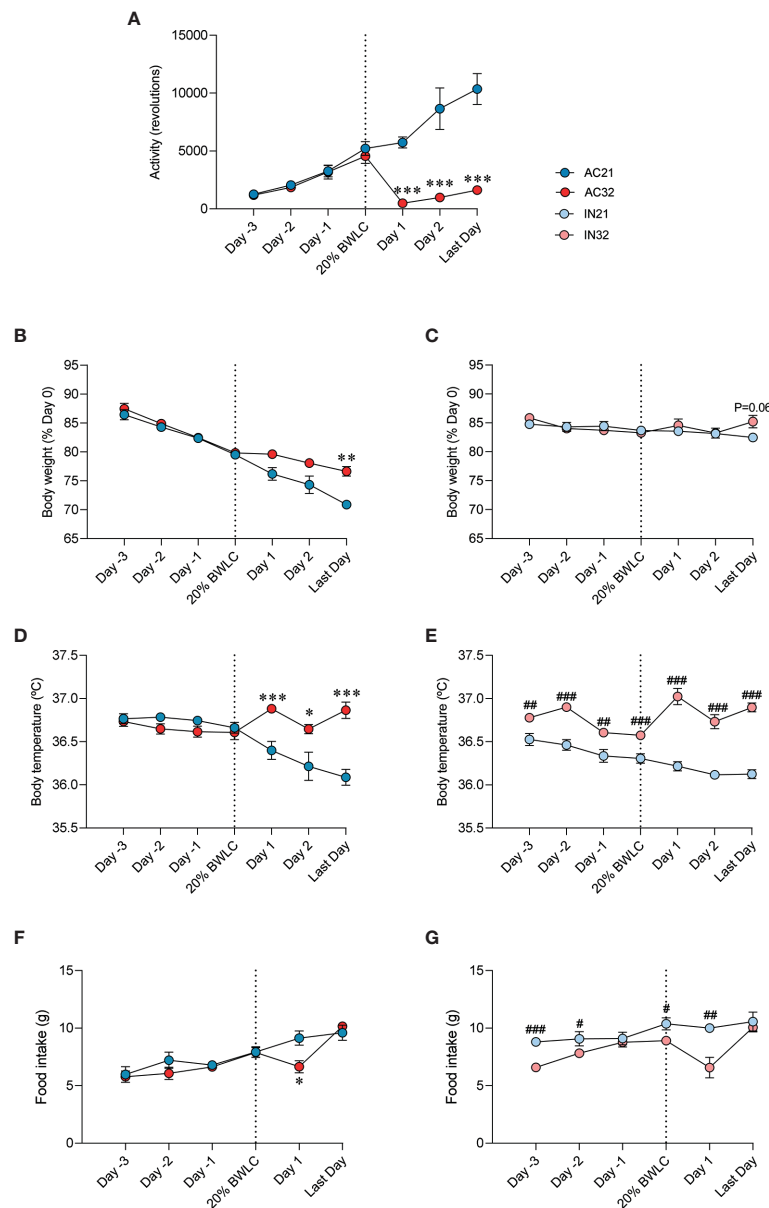


**FIGURE 1** | Effect of ABA and temperature on energy balance. **(A)** Activity ( $n = 9-12$  rats/group) **(B, C)** Body weight (% of day 0) ( $n = 8-12$  rats/group) **(D, E)** Body temperature ( $n = 7-10$  rats/group) **(F, G)** Food intake ( $n = 8-12$  rats/group) of active rats at 21°C and 32°C (AC21 and AC32) and inactive rats at 21°C and 32°C (IN21 and IN32) \* $P < 0.05$ , \*\* $P < 0.01$ , \*\*\* $P < 0.001$  vs. AC21; # $P < 0.05$ , ## $P < 0.01$ , ### $P < 0.001$  vs. IN21. Data expressed as mean  $\pm$  SEM. 20% BWLC, 20% body weight loss criterion.

to 32°C (Table 1). No major changes were detected in glycaemia. Regarding CORT, active rats housed at 21°C displayed the highest circulating levels of this hormone (Table 1), similarly to AN patients and other preclinical models (40–44), indicating greater stress. Notably, when maintained at 32°C, active rats normalized their circulating CORT, reaching even lower concentration than the inactive groups (Table 1). Thyroid hormones (T4 and T3) play a major role in the modulation of

temperature (45, 46), and we investigated how their circulating levels were affected in our setting. Inactive rats displayed the expected correlation between ambient temperature and thyroid status. Interestingly, that effect was not evident in active rats, which showed lower T4 and T3 when kept at 21°C as compared to 32°C (Table 1). Finally, active rats at 21°C also showed higher levels of noradrenaline, that were reduced when housed at 32°C (Table 1).

**TABLE 1 |** Serum parameters in the experimental groups.

	Active 21°C	Active 32°C	Inactive 21°C	Inactive 32°C
Leptin (ng/mL)	0.20 ± 0.002!!!	0.24 ± 0.005***	0.28 ± 0.02	0.29 ± 0.02
Glucose (mg/dL)	120.33 ± 8.29	137.75 ± 3.28*	129.86 ± 5.82	140.00 ± 3.49
Corticosterone (ng/mL)	1466.87 ± 125.28!!!	273.05 ± 43.77***	412.98 ± 63.40	435.91 ± 35.57
T4 (ng/dL)	0.98 ± 0.05!!!	1.54 ± 0.07***	1.89 ± 0.07	1.71 ± 0.04 <sup>#</sup>
T3 (pg/mL)	1.51 ± 0.09!!!	2.24 ± 0.05***	3.68 ± 0.05	3.07 ± 0.09 <sup>###</sup>
Adrenaline (ng/mL)	2.46 ± 0.50	2.16 ± 0.19	4.18 ± 1.21	3.43 ± 0.77
Noradrenaline (ng/mL)	2.64 ± 0.32	1.75 ± 0.17*	3.54 ± 0.58	3.58 ± 0.58

*n* = 9–11 animals/group.

\**P* < 0.05 and \*\*\**P* < 0.001 vs. AC21.

<sup>#</sup>*P* < 0.05, and <sup>###</sup>*P* < 0.001 vs. IN21.

!!!*P* < 0.001 IN21 vs. AC21.

## Increased Housing Temperature Reverses the Effects of ABA on WAT and Skeletal Muscle

AN is also characterized by a great loss of fat mass (38, 47, 48). Therefore, we decided to explore lipogenesis and lipolysis markers in the WAT of ABA rats. Active rats at 21°C had an extreme decrease in all examined lipogenic markers levels, such

as acetyl-CoA carboxylate  $\alpha$  (ACC $\alpha$ ), fatty acid synthase (FAS), sterol regulatory element-binding protein 1 (SREBP1), peroxisome proliferator-activated receptor- $\gamma$  (PPAR $\gamma$ ) and CCAAT/enhancer binding protein  $\alpha$  and  $\beta$  (C/EBP $\alpha$  and C/EBP $\beta$ ), compared to inactive rats. Active rats at 32°C showed a marked recovery in the expression of these factors (Figure 2A). Increased housing temperature did not impact on

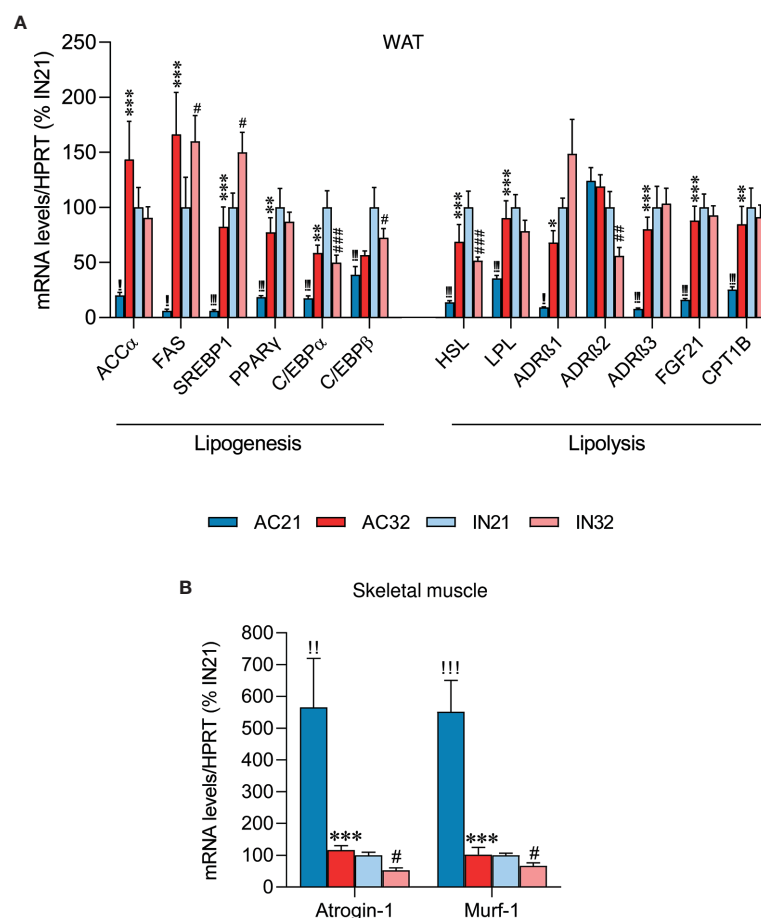


**FIGURE 2 |** Effect of ABA and temperature on WAT and muscle. mRNA levels of (A) lipogenesis and lipolysis markers in the WAT (*n* = 8–11 rats/group) and (B) cachexia markers in skeletal muscle (*n* = 8–11 rats/group) of active rats at 21°C and 32°C (AC21 and AC32) and inactive rats at 21°C and 32°C (IN21 and IN32). \**P* < 0.05, \*\**P* < 0.01, \*\*\**P* < 0.001 vs. AC21; <sup>#</sup>*P* < 0.05, <sup>##</sup>*P* < 0.01, <sup>###</sup>*P* < 0.001 vs. IN21; <sup>!!</sup>*P* < 0.01, <sup>!!!</sup>*P* < 0.001 IN21 vs. AC21. Data expressed as mean ± SEM.

gene expression levels in inactive rats, except for an increase in FAS and SREBP1 mRNA expression (**Figure 2A**). On the other hand, the levels of lipolysis markers, such as hormone-sensitive lipase (HSL), lipoprotein lipase (LPL), adrenergic receptor beta 1 (ADRB1) and adrenergic receptor beta 3 (ADRB3), but not beta 2 (ADRB2), fibroblast growth factor 21 (FGF21) and carnitine palmitoyltransferase 1B (CPT1B), were reduced in active rats at 21°C, likely due to the massive loss of adiposity of these animals, while heat reversed this expression (**Figure 2A**).

AN patients have a reduction in lean mass and wasting syndrome, leading to cachexia (3, 49, 50). Therefore, we explored two cachexia markers in skeletal muscle, namely Atrogin-1 and Murf-1. Our data showed that rats housed at 21°C exhibited a markedly increased expression of cachectic markers relative to rats housed at 32°C, evident both in the

inactive and the active cohort, possibly indicating muscle deteriorating (**Figure 2B**).

## ABA Reduces BAT UCP1 Levels But Increases the Browning of WAT

It is known that AN is associated with impaired thermogenesis (50). In fact, it has been reported that young women with AN exhibit reduced cold-activated BAT (50). Analysis of UCP1 expression in the BAT of our model showed decreased 21°C-induced UCP1 protein levels in AC rats (**Figures 3A, B**). As expected, increased environmental temperature decreased UCP1 expression in both active and inactive animals (**Figures 3A, B**).

Over the last years, accumulating evidence have demonstrated that activation of beige/brite (“brown in white”) adipocytes in the WAT, a process known as browning (51–53), is responsible for a

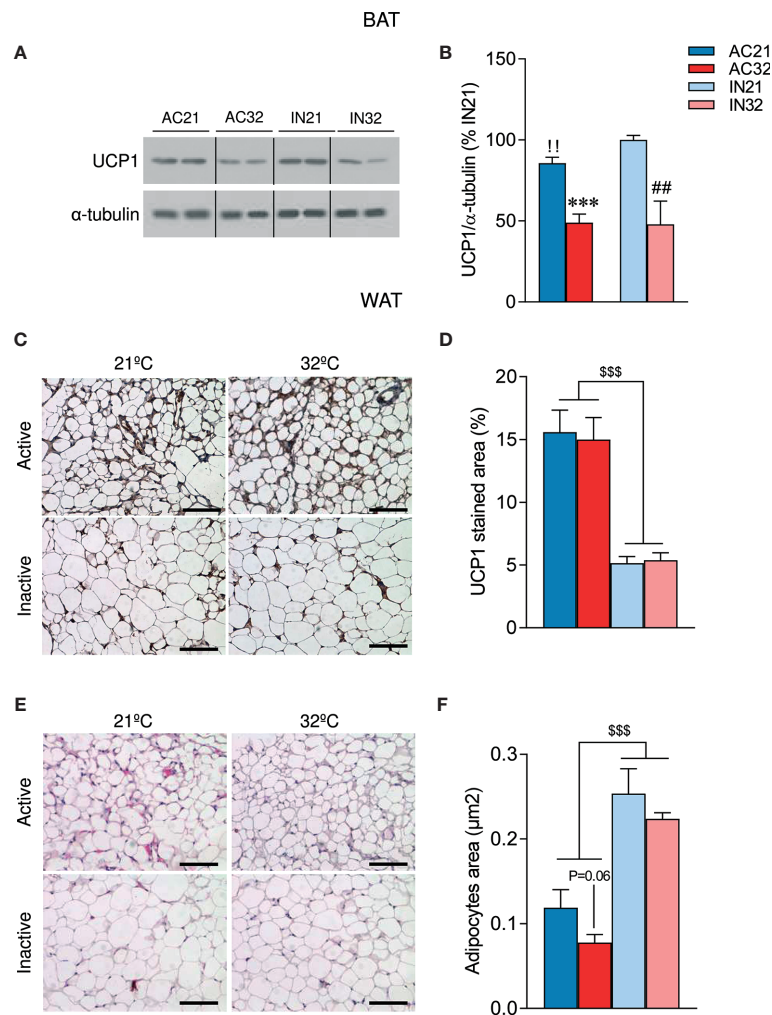


**FIGURE 3 |** Effect of ABA and temperature on BAT and WAT browning. (**A, B**) Protein levels of UCP1 in the BAT ( $n = 7$  rats/group) (**C, D**) UCP1 staining in WAT ( $n = 8-12$  rats/group) (**E, F**) Adipocyte are in WAT ( $n = 8-12$  rats/group) of active rats at 21°C and 32°C (AC21 and AC32) and inactive rats at 21°C and 32°C (IN21 and IN32). \*\*\* $P < 0.001$  vs. AC21; ### $P < 0.01$  vs. IN21; <sup>!!</sup> $P < 0.01$  IN21 vs. AC21; \$\$\$ $P < 0.001$  for simplification. Data expressed as mean  $\pm$  SEM. The bands in gels from panel (**A**) have been spliced from the same original gels. Scale bar: 100  $\mu$ m.

significant increase in total energy expenditure (54). Notably, recent studies have also linked the browning of WAT to other wasting syndromes, such as cancer-induced cachexia (55, 56); however, to date, no data have linked AN to browning of WAT. Our histological analysis of WAT showed that ABA rats exhibited a “brown-like” multilocular pattern, associated with increased UCP1 immunostaining (**Figures 3C, D**) and decreased adipocyte area (**Figures 3E, F**). Importantly, the induction of browning was not affected by housing temperature (**Figures 3C–F**). Overall, these data indicate that ABA rats, besides hypophagia, also displayed increased browning of WAT, that was compatible with the elevated catabolic state.

## ABA Does Not Impact Either AMPK or ER Stress in the Hypothalamus

Finally, we aimed to investigate if ABA might result in changes at the central level that could explain the catabolic state of this model. One of the principal regulators of energy balance at a central level is hypothalamic AMPK, an energy sensor that controls both sides of the energy balance equation: food intake and energy expenditure (20–22). Firstly, we investigated the effect of ABA and temperature on total hypothalamic extracts; our data did not show any significant impact of either ABA or temperature on the protein levels of the AMPK signaling pathway (**Supplementary Figure 1A**). Current data indicate that the effects of AMPK in the hypothalamus are nucleus-specific; thus while AMPK in the ARC is mainly involved in the regulation of feeding, AMPK in the VMH regulates BAT thermogenesis and browning of WAT (19–23, 32). Therefore, we performed further analysis of AMPK in ARC and VMH enriched protein lysates, which showed a non-significant tendency of phosphorylated AMPK (pAMPK) to be increased in the VMH of ABA rats, that might account for the decreased levels of BAT UCP1 protein levels observed in those animals (**Figures 4A, B**). No major effect of housing temperature was detected of pAMPK levels in the VMH (**Figures 4A, B**). Similar data were found when pAMPK was assayed in the ARC (**Figures 4C, D**). Overall, these results indicated that the impaired feeding and browning that characterized ABA model were unlikely associated to changes in AMPK signaling in these nuclei.

Finally, we investigated the effect of ABA on hypothalamic ER stress signaling, since recent data have linked this cellular response with the regulation of BAT thermogenesis and browning of WAT (24–26, 28). Our data did not show any major impact of either ABA or housing temperature on two key hypothalamic ER stress markers, namely GRP78 and CHOP (**Figures 4E, F**), excluding their association in the BAT and metabolic alterations of this model.

## DISCUSSION

Here, we show that the catabolic state that characterizes ABA is associated with major changes in BAT thermogenesis and WAT browning. Notably, those changes are not related to modification

in key central regulators of adipose tissue activity, namely hypothalamic AMPK and ER stress signaling.

AN is characterized by energy balance impairment as a result of decreased food intake and hyperactivity, leading to severe weight loss (1, 2). Different brain regions, such as reward-motivated learning or hippocampal structures, have been involved in the pathology of AN (1, 2, 8, 57). Here, we aimed to investigate whether the canonical hypothalamic (VMH)-AMPK-ER stress-SNS-BAT axis (21, 22) could be involved in the reduced feeding and the changes in BAT and WAT browning that characterize the ABA model in rats.

ABA is considered the best analogue animal model for AN (6). In addition, it is well-established that ABA-induced hyperactivity is an adaptive behavioral response to compensate for hypothermia (9). Our data are in line with previous studies reporting the beneficial effect of increased ambient temperature to 32°C on the recovery of rats subjected to the ABA model, even after 20% weight loss has occurred (10–13, 15, 58). Although our data confirm former evidence, the use of temperature recording by telemetry allows a constant monitoring of the body temperature throughout the experiment, which constitutes a big advantage when compared to previous reports. Food-restricted rats suffered hypothermia when given free access to a running wheel, as body temperature decreases over days. On the contrary, rats exposed to 32°C, both active and inactive, avoid hypothermia and their body temperature at the end of the experiment reached values higher than when meeting the weight loss criterion. These findings reinforce the hypothesis that hyperactivity is an adaptive response to compensate for the hypothermia derived from weight loss (9).

In mammals, the BAT is responsible for the adaptive thermogenesis which regulates body temperature when other mechanisms (i.e., heat conservation) are not enough to maintain homeothermy (59, 60). Food-restriction elicits reductions in energy expenditure through decreased BAT thermogenesis, as a strategy to save energy, although it leads to a hypothermic state (61–63). In ABA rats this response is exacerbated, entering in a vicious cycle situation that potentiates an overall catabolic state leading to wasting and cachexia. Notably, the increase in housing temperature reduced the expression of UCP1 in the BAT. That reduction in adaptive thermogenesis together with the reduction of hyperactivity would account for a better preservation of body mass (16) and the recovery of body weight of rats exposed to the ABA model. This is also demonstrated by an improved metabolic profile at the higher ambient temperature, exemplified by the reduction in the expression of cachectic markers in skeletal muscle and the increased WAT lipogenesis. Still, the recovery in body mass is not total, likely due to the maintained browning of WAT, which may account for a chronic increased energy expenditure (54), leading to a sustained basal catabolic state.

There are a huge amount of data linking hypothalamic AMPK and ER stress pathways in the hypothalamus, specifically in the VMH, with the regulation of thermogenesis in BAT, as well as the browning of WAT (19–26). This prompted us to investigate whether those hypothalamic molecular mediators could be associated to the BAT and WAT responses in the ABA model.

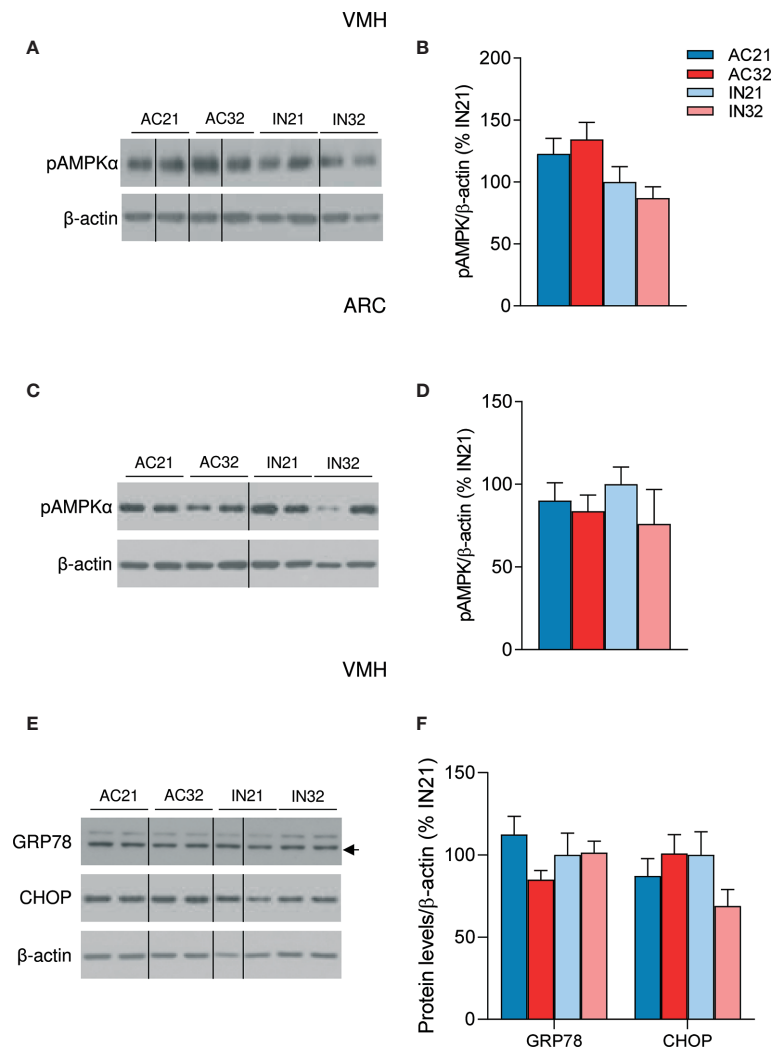


**FIGURE 4 |** Effect of ABA and temperature on AMPK and ER stress in the VMH and ARC. **(A, B)** Protein levels of pAMPKα in the VMH ( $n = 7-10$  rats/group) **(C, D)** Protein levels of pAMPKα in the ARC ( $n = 7$  rats/group) **(E, F)** Protein levels of GRP78 and CHOP in the VMH ( $n = 7$  rats/group) of active rats at 21°C and 32°C (AC21 and AC32) and inactive rats at 21°C and 32°C (IN21 and IN32). Data expressed as mean  $\pm$  SEM. The bands in gels from panel **(A, C, E)** have been spliced from the same original gels.

Our analysis did not find major expression differences in the levels of pAMPK (the active isoform), GRP78 and CHOP either in the VMH and/or the ARC of ABA rats. In fact, this result is opposite to a recent report where it has been described that hypothalamic pAMPK levels are reduced in ABA mice (64). These discrepancies could be likely explained by the different species (rats vs. mice), but also by the nuclei-specific analysis performed in our study, which is critical to understand AMPK and ER stress function in the hypothalamus (19–26) at the studied times. Moreover, timing could be also a factor, in this sense it is likely that at the final time point that we investigated, initial changes in hypothalamic AMPK and/or ER stress (maybe responsible for the BAT and browning changes observed) could

not be detected. Further work will be needed to address the exact role of these molecular mechanisms in the pathology of AN.

In summary, our study shows a general description of the metabolic state of rats exposed to the ABA model and of those rats treated with heat. The results are consistent with the hypothesis that body temperature is an important parameter in ABA. The application of heat reverses not only the hyperactivity and weight loss of animals exposed to the ABA model, but also hypothermia, hypoleptinemia and loss of muscle mass. However, none of the changes observed are associated to changes in key hypothalamic pathways modulating energy metabolism, such as AMPK or ER stress (19–26) at the studied times. Hence, hypothermia in AN should be given more attention in future

research to study the underlying brain mechanism involved in the warming effect and to explore new treatments.

## DATA AVAILABILITY STATEMENT

The raw data supporting the conclusions of this article will be made available by the authors, without undue reservation.

## ETHICS STATEMENT

The animal study was reviewed and approved by The Ethics Committee on the use and care of animals of Santiago de Compostela University approved all described procedures (project license 15004/17/002). All experiments were carried out in accordance with Royal Decree 53/2013 of February 1, Law 32/2007 of November 7, and European Communities Council Directive 2010/63/UE of September 22, on the protection of animals used for experimental and other scientific purposes.

## AUTHOR CONTRIBUTIONS

AF and ER-P performed the *in vivo* experiments, analytical methods and collected the data. AF, EG and ML designed the experiments and analyzed the data. AF, ER-P, RN, JF, CD, EG and ML interpreted and discussed the data. AF, EG and ML developed the hypothesis. AF and ML made the figures and

wrote the manuscript. ML is the senior author and lead contact, secured funding, coordinated, and led the project. All authors contributed to the article and approved the submitted version.

## FUNDING

The research leading to these results has received funding from the Xunta de Galicia (RN: 2016-PG057; ML: 2016-PG068); Ministerio de Economía y Competitividad (MINECO) co-funded by the FEDER Program of EU (RN: RTI2018-099413-B-I00; CD: BFU2017-87721-P; ML: RTI2018-101840-B-I00); Atresmedia Corporación (RN and ML); Fundación BBVA (RN); “la Caixa” Foundation (ID 100010434), under the agreements LCF/PR/HR19/52160016 (RN) and LCF/PR/HR19/52160022 (ML); European Foundation for the Study of Diabetes (RN), ERC Synergy Grant-2019-WATCH- 810331 (RN) and Western Norway Regional Health Authority (Helse Vest RHF) (JF). AF received a fellowship from Xunta de Galicia (Plan I2C-2014). The CiMUS is supported by the Xunta de Galicia (2016-2019, ED431G/05). CIBER de Fisiopatología de la Obesidad y Nutrición is an initiative of ISCIII. The funders had no role in study design, data collection and analysis, decision to publish, or preparation of the manuscript.

## SUPPLEMENTARY MATERIAL

The Supplementary Material for this article can be found online at: <https://www.frontiersin.org/articles/10.3389/fendo.2021.669980/full#supplementary-material>

## REFERENCES

- Treasure J, Zipfel S, Micali N, Wade T, Stice E, Claudino A, et al. Anorexia Nervosa. *Nat Rev Dis Primers* (2015) 1:15074. doi: 10.1038/nrdp.2015.74
- Frank GKW, Shott ME, DeGuzman MC. The Neurobiology of Eating Disorders. *Child Adolesc Psychiatr Clin N Am* (2019) 28(4):629–40. doi: 10.1016/j.chc.2019.05.007
- Singhal V, Misra M, Klibanski A. Endocrinology of Anorexia Nervosa in Young People: Recent Insights. *Curr Opin Endocrinol Diabetes Obes* (2014) 21(1):64–70. doi: 10.1097/MED.0000000000000026
- Gibson D, Workman C, Mehler PS. Medical Complications of Anorexia Nervosa and Bulimia Nervosa. *Psychiatr Clin North Am* (2019) 42(2):263–74. doi: 10.1016/j.psc.2019.01.009
- Schorr M, Miller KK. The Endocrine Manifestations of Anorexia Nervosa: Mechanisms and Management. *Nat Rev Endocrinol* (2017) 13(3):174–86. doi: 10.1038/nrendo.2016.175
- Gutierrez E. A Rat in the Labyrinth of Anorexia Nervosa: Contributions of the Activity-Based Anorexia Rodent Model to the Understanding of Anorexia Nervosa. *Int J Eat Disord* (2013) 46(4):289–301. doi: 10.1002/eat.22095
- Routtenberg A, Kuznesof AW. Self-Starvation of Rats Living in Activity Wheels on a Restricted Feeding Schedule. *J Comp Physiol Psychol* (1967) 64(3):414–21. doi: 10.1037/h0025205
- Schalla MA, Stengel A. Activity Based Anorexia as an Animal Model for Anorexia Nervosa—a Systematic Review. *Front Nutr* (2019) 6:69. doi: 10.3389/fnut.2019.00069
- Gutierrez E, Vazquez R, Boakes RA. Activity-Based Anorexia: Ambient Temperature Has Been a Neglected Factor. *Psychon Bull Rev* (2002) 9(2):239–49. doi: 10.3758/BF03196278
- Cerrato M, Carrera O, Vazquez R, Echevarria E, Gutierrez E. Heat Makes a Difference in Activity-Based Anorexia: A Translational Approach to Treatment Development in Anorexia Nervosa. *Int J Eat Disord* (2012) 45(1):26–35. doi: 10.1002/eat.20884
- Gutierrez E, Cerrato M, Carrera O, Vazquez R. Heat Reversal of Activity-Based Anorexia: Implications for the Treatment of Anorexia Nervosa. *Int J Eat Disord* (2008) 41(7):594–601. doi: 10.1002/eat.20535
- Gutierrez E, Churrua I, Zarate J, Carrera O, Portillo MP, Cerrato M, et al. High Ambient Temperature Reverses Hypothalamic MC4 Receptor Overexpression in an Animal Model of Anorexia Nervosa. *Psychoneuroendocrinology* (2009) 34(3):420–9. doi: 10.1016/j.psyneuen.2008.10.003
- Roura I, Fraga A, Gutierrez E. Differential Effects of Heat in the Phases of the Light-Dark Cycle in the Activity-Based Anorexia Model. *Int J Eat Disord* (2020) 53(11):1826–35. doi: 10.1002/eat.23363
- Hillebrand JJ, de Rijke CE, Brakkee JH, Kas MJ, Adan RA. Voluntary Access to a Warm Plate Reduces Hyperactivity in Activity-Based Anorexia. *Physiol Behav* (2005) 85(2):151–7. doi: 10.1016/j.physbeh.2005.03.017
- Carrera O, Gutierrez E. Hyperactivity in Anorexia Nervosa: to Warm or Not to Warm. That is the Question (a Translational Research One). *J Eat Disord* (2018) 6:4. doi: 10.1186/s40337-018-0190-6
- Fraga A, Carreira MC, Gonzalez-Izquierdo A, Dieguez C, Lopez M, Gutierrez E. Temperature But Not Leptin Prevents Semi-Starvation Induced Hyperactivity in Rats: Implications for Anorexia Nervosa Treatment. *Sci Rep* (2020) 10(1):5300. doi: 10.1038/s41598-020-62147-z
- Duncan L, Yilmaz Z, Gaspar H, Walters R, Goldstein J, Anttila V, et al. Significant Locus and Metabolic Genetic Correlations Revealed in Genome-Wide Association Study of Anorexia Nervosa. *Am J Psychiatry* (2017) 174(9):850–8. doi: 10.1176/appi.ajp.2017.16121402

18. Kim SF. Animal Models of Eating Disorders. *Neuroscience* (2012) 211:2–12. doi: 10.1016/j.neuroscience.2012.03.024
19. Claret M, Smith MA, Batterham RL, Selman C, Choudhury AI, Fryer LG, et al. AMPK is Essential for Energy Homeostasis Regulation and Glucose Sensing by POMC and AgRP Neurons. *J Clin Invest* (2007) 117(8):2325–36. doi: 10.1172/JCI31516
20. Schneeberger M, Claret M. Recent Insights Into the Role of Hypothalamic Ampk Signaling Cascade Upon Metabolic Control. *Front Neurosci* (2012) 6:185. doi: 10.3389/fnins.2012.00185
21. Lopez M, Nogueiras R, Tena-Sempere M, Dieguez C. Hypothalamic AMPK: A Canonical Regulator of Whole-Body Energy Balance. *Nat Rev Endocrinol* (2016) 12(7):421–32. doi: 10.1038/nrendo.2016.67
22. Lopez M. Ampk Wars: The VMH Strikes Back, Return of the PVH. *Trends Endocrinol Metab* (2018) 29(3):135–7. doi: 10.1016/j.tem.2018.01.004
23. Lopez M, Varela L, Vazquez MJ, Rodriguez-Cuenca S, Gonzalez CR, Velagapudi VR, et al. Hypothalamic AMPK and Fatty Acid Metabolism Mediate Thyroid Regulation of Energy Balance. *Nat Med* (2010) 16(9):1001–8. doi: 10.1038/nm.2207
24. Contreras C, Gonzalez-Garcia I, Martinez-Sanchez N, Seoane-Collazo P, Jacas J, Morgan DA, et al. Central Ceramide-Induced Hypothalamic Lipotoxicity and ER Stress Regulate Energy Balance. *Cell Rep* (2014) 9(1):366–77. doi: 10.1016/j.celrep.2014.08.057
25. Contreras C, Gonzalez-Garcia I, Seoane-Collazo P, Martinez-Sanchez N, Linares-Pose L, Rial-Pensado E, et al. Reduction of Hypothalamic Endoplasmic Reticulum Stress Activates Browning of White Fat and Ameliorates Obesity. *Diabetes* (2017) 66(1):87–99. doi: 10.2337/db15-1547
26. Gonzalez-Garcia I, Contreras C, Estevez-Salguero A, Ruiz-Pino F, Colsh B, Pensado I, et al. Estradiol Regulates Energy Balance by Ameliorating Hypothalamic Ceramide-Induced Er Stress. *Cell Rep* (2018) 25(2):413–23.e5. doi: 10.1016/j.celrep.2018.09.038
27. Martinez de Morentin PB, Gonzalez-Garcia I, Martins L, Lage R, Fernandez-Mallo D, Martinez-Sanchez N, et al. Estradiol Regulates Brown Adipose Tissue Thermogenesis Via Hypothalamic Ampk. *Cell Metab* (2014) 20(1):41–53. doi: 10.1016/j.cmet.2014.03.031
28. Martinez-Sanchez N, Seoane-Collazo P, Contreras C, Varela L, Villarroja J, Rial-Pensado E, et al. Hypothalamic AMPK-ER Stress-Jnk1 Axis Mediates the Central Actions of Thyroid Hormones on Energy Balance. *Cell Metab* (2017) 26(1):212–29.e12. doi: 10.1016/j.cmet.2017.06.014
29. Seoane-Collazo P, Linares-Pose L, Rial-Pensado E, Romero-Pico A, Moreno-Navarrete JM, Martinez-Sanchez N, et al. Central Nicotine Induces Browning Through Hypothalamic Kappa Opioid Receptor. *Nat Commun* (2019) 10(1):4037. doi: 10.1038/s41467-019-12004-z
30. Martins L, Seoane-Collazo P, Contreras C, Gonzalez-Garcia I, Martinez-Sanchez N, Gonzalez F, et al. A Functional Link Between AMPK and Orexin Mediates the Effect of BMP8B on Energy Balance. *Cell Rep* (2016) 16(8):2231–42. doi: 10.1016/j.celrep.2016.07.045
31. Seoane-Collazo P, Romero-Pico A, Rial-Pensado E, Linares-Pose L, Estevez-Salguero A, Ferno J, et al. Kappa-Opioid Signaling in the Lateral Hypothalamic Area Modulates Nicotine-Induced Negative Energy Balance. *Int J Mol Sci* (2021) 22(4):1515. doi: 10.3390/ijms22041515
32. Martinez-Sanchez N, Moreno-Navarrete JM, Contreras C, Rial-Pensado E, Ferno J, Nogueiras R, et al. Thyroid Hormones Induce Browning of White Fat. *J Endocrinol* (2017) 232(2):351–62. doi: 10.1530/JOE-16-0425
33. Haas V, Onur S, Paul T, Nutzinger DO, Bosy-Westphal A, Hauer M, et al. Leptin and Body Weight Regulation in Patients With Anorexia Nervosa Before and During Weight Recovery. *Am J Clin Nutr* (2005) 81(4):889–96. doi: 10.1093/ajcn/81.4.889
34. Focker M, Timmesfeld N, Scherag S, Buhren K, Langkamp M, Dempfle A, et al. Screening for Anorexia Nervosa Via Measurement of Serum Leptin Levels. *J Neural Transm (Vienna)* (2011) 118(4):571–8. doi: 10.1007/s00702-010-0551-z
35. Haas VK, Gaskin KJ, Kohn MR, Clarke SD, Muller MJ. Different Thermic Effects of Leptin in Adolescent Females With Varying Body Fat Content. *Clin Nutr* (2010) 29(5):639–45. doi: 10.1016/j.clnu.2010.03.013
36. Korek E, Krauss H, Gibas-Dorna M, Kupsz J, Piatek M, Piatek J. Fasting and Postprandial Levels of Ghrelin, Leptin and Insulin in Lean, Obese and Anorexic Subjects. *Prz Gastroenterol* (2013) 8(6):383–9. doi: 10.5114/pg.2013.39922
37. Misra M, Miller KK, Kuo K, Griffin K, Stewart V, Hunter E, et al. Secretory Dynamics of Leptin in Adolescent Girls With Anorexia Nervosa and Healthy Adolescents. *Am J Physiol Endocrinol Metab* (2005) 289(3):E373–81. doi: 10.1152/ajpendo.00041.2005
38. Grinspoon S, Gulick T, Askari H, Landt M, Lee K, Anderson E, et al. Serum Leptin Levels in Women With Anorexia Nervosa. *J Clin Endocrinol Metab* (1996) 81(11):3861–3. doi: 10.1210/jcem.81.11.8923829
39. Hebebrand J, Exner C, Hebebrand K, Holtkamp C, Casper RC, Remschmidt H, et al. Hyperactivity in Patients With Anorexia Nervosa and in Semistarved Rats: Evidence for a Pivotal Role of Hypoleptinemia. *Physiol Behav* (2003) 79(1):25–37. doi: 10.1016/S0031-9384(03)00102-1
40. Hotta M, Shibasaki T, Masuda A, Imaki T, Demura H, Ling N, et al. The Responses of Plasma Adrenocorticotropin and Cortisol to Corticotropin-Releasing Hormone (CRH) and Cerebrospinal Fluid Immunoreactive CRH in Anorexia Nervosa Patients. *J Clin Endocrinol Metab* (1986) 62(2):319–24. doi: 10.1210/jcem-62-2-319
41. Kaye WH, Gwirtsman HE, George DT, Ebert MH, Jimerson DC, Tomai TP, et al. Elevated Cerebrospinal Fluid Levels of Immunoreactive Corticotropin-Releasing Hormone in Anorexia Nervosa: Relation to State of Nutrition, Adrenal Function, and Intensity of Depression. *J Clin Endocrinol Metab* (1987) 64(2):203–8. doi: 10.1210/jcem-64-2-203
42. Lo Sauro C, Ravaldi C, Cabras PL, Faravelli C, Ricca V. Stress, Hypothalamic-Pituitary-Adrenal Axis and Eating Disorders. *Neuropsychobiology* (2008) 57(3):95–115. doi: 10.1159/000138912
43. de Rijke CE, Hillebrand JJ, Verhagen LA, Roeling TA, Adan RA. Hypothalamic Neuropeptide Expression Following Chronic Food Restriction in Sedentary and Wheel-Running Rats. *J Mol Endocrinol* (2005) 35(2):381–90. doi: 10.1677/jme.1.01808
44. Burden VR, White BD, Dean RG, Martin RJ. Activity of the Hypothalamic-Pituitary-Adrenal Axis is Elevated in Rats With Activity-Based Anorexia. *J Nutr* (1993) 123(7):1217–25. doi: 10.1093/jn/123.7.1217
45. Sents SC, Oelkrug R, Mittag J. Thyroid Hormones in the Regulation of Brown Adipose Tissue Thermogenesis. *Endocr Connect* (2021) 10(2):R106–15. doi: 10.1530/EC-20-0562
46. Lopez M, Alvarez CV, Nogueiras R, Dieguez C. Energy Balance Regulation by Thyroid Hormones At Central Level. *Trends Mol Med* (2013) 19(7):418–27. doi: 10.1016/j.molmed.2013.04.004
47. Bredella MA, Ghomi RH, Thomas BJ, Torriani M, Brick DJ, Gerweck AV, et al. Comparison of DXA and CT in the Assessment of Body Composition in Premenopausal Women With Obesity and Anorexia Nervosa. *Obes (Silver Spring)* (2010) 18(11):2227–33. doi: 10.1038/oby.2010.5
48. Misra M, Soyka LA, Miller KK, Grinspoon S, Levitsky LL, Klibanski A. Regional Body Composition in Adolescents With Anorexia Nervosa and Changes With Weight Recovery. *Am J Clin Nutr* (2003) 77(6):1361–7. doi: 10.1093/ajcn/77.6.1361
49. Grinspoon S, Thomas E, Pitts S, Gross E, Mickley D, Miller K, et al. Prevalence and Predictive Factors for Regional Osteopenia in Women With Anorexia Nervosa. *Ann Intern Med* (2000) 133(10):790–4. doi: 10.7326/0003-4819-133-10-200011210-00011
50. Bredella MA, Fazeli PK, Freedman LM, Calder G, Lee H, Rosen CJ, et al. Young Women With Cold-Activated Brown Adipose Tissue Have Higher Bone Mineral Density and Lower Pref-1 Than Women Without Brown Adipose Tissue: A Study in Women With Anorexia Nervosa, Women Recovered From Anorexia Nervosa, and Normal-Weight Women. *J Clin Endocrinol Metab* (2012) 97(4):E584–90. doi: 10.1210/jc.2011-2246
51. Nedergaard J, Cannon B. The Browning of White Adipose Tissue: Some Burning Issues. *Cell Metab* (2014) 20(3):396–407. doi: 10.1016/j.cmet.2014.07.005
52. Cereijo R, Giral M, Villarroya F. Thermogenic Brown and Beige/Brite Adipogenesis in Humans. *Ann Med* (2015) 47(2):169–77. doi: 10.3109/07853890.2014.952328
53. Villarroya F, Cereijo R, Villarroya J, Gavalda-Navarro A, Giral M. Toward an Understanding of How Immune Cells Control Brown and Beige Adipobiology. *Cell Metab* (2018) 27(5):954–61. doi: 10.1016/j.cmet.2018.04.006
54. Shabalina IG, Petrovic N, de Jong JM, Kalinovich AV, Cannon B, Nedergaard J. UCP1 in Brite/Beige Adipose Tissue Mitochondria is Functionally Thermogenic. *Cell Rep* (2013) 5(5):1196–203. doi: 10.1016/j.celrep.2013.10.044

55. Petruzzelli M, Schweiger M, Schreiber R, Campos-Olivas R, Tsoli M, Allen J, et al. A Switch From White to Brown Fat Increases Energy Expenditure in Cancer-Associated Cachexia. *Cell Metab* (2014) 20(3):433–47. doi: 10.1016/j.cmet.2014.06.011
56. Petruzzelli M, Wagner EF. Mechanisms of Metabolic Dysfunction in Cancer-Associated Cachexia. *Genes Dev* (2016) 30(5):489–501. doi: 10.1101/gad.276733.115
57. Lipsman N, Woodside DB, Lozano AM. Neurocircuitry of Limbic Dysfunction in Anorexia Nervosa. *Cortex* (2015) 62:109–18. doi: 10.1016/j.cortex.2014.02.020
58. Gutierrez E, Baysari MT, Carrera O, Whitford TJ, Boakes RA. High Ambient Temperature Reduces Rate of Body-Weight Loss Produced by Wheel Running. *Q J Exp Psychol (Hove)*. (2006) 59(7):1196–211. doi: 10.1080/17470210500417688
59. Cannon B, Nedergaard J. Brown Adipose Tissue: Function and Physiological Significance. *Physiol Rev* (2004) 84(1):277–359. doi: 10.1152/physrev.00015.2003
60. Oelkrug R, Mittag J. An Improved Method for the Precise Unravelment of non-Shivering Brown Fat Thermokinetics. *Sci Rep* (2021) 11(1):4799. doi: 10.1038/s41598-021-84200-1
61. Sakurada S, Shido O, Sugimoto N, Hiratsuka Y, Yoda T, Kanosue K. Autonomic and Behavioural Thermoregulation in Starved Rats. *J Physiol* (2000) 526(Pt 2):417–24. doi: 10.1111/j.1469-7793.2000.00417.x
62. Young JB, Saville E, Rothwell NJ, Stock MJ, Landsberg L. Effect of Diet and Cold Exposure on Norepinephrine Turnover in Brown Adipose Tissue of the Rat. *J Clin Invest* (1982) 69(5):1061–71. doi: 10.1172/JCI110541
63. Zhang LN, Mitchell SE, Hambly C, Morgan DG, Clapham JC, Speakman JR. Physiological and Behavioral Responses to Intermittent Starvation in C57BL/6J Mice. *Physiol Behav* (2012) 105(2):376–87. doi: 10.1016/j.physbeh.2011.08.035
64. Nobis S, Goichon A, Achamrah N, Guerin C, Azhar S, Chan P, et al. Alterations of Proteome, Mitochondrial Dynamic and Autophagy in the Hypothalamus During Activity-Based Anorexia. *Sci Rep* (2018) 8(1):7233. doi: 10.1038/s41598-018-25548-9

**Conflict of Interest:** The authors declare that the research was conducted in the absence of any commercial or financial relationships that could be construed as a potential conflict of interest.

Copyright © 2021 Fraga, Rial-Pensado, Nogueiras, Fernø, Diéguez, Gutierrez and López. This is an open-access article distributed under the terms of the Creative Commons Attribution License (CC BY). The use, distribution or reproduction in other forums is permitted, provided the original author(s) and the copyright owner(s) are credited and that the original publication in this journal is cited, in accordance with accepted academic practice. No use, distribution or reproduction is permitted which does not comply with these terms.



# Gray Matter Abnormalities in Type 1 and Type 2 Diabetes: A Dual Disorder ALE Quantification

Kevin K. K. Yu<sup>1,2†</sup>, Gladys L. Y. Cheing<sup>1,2†</sup>, Charlton Cheung<sup>3</sup>, Georg S. Kranz<sup>1,4,5\*</sup> and Alex Kwok-Kuen Cheung<sup>1</sup>

<sup>1</sup> Department of Rehabilitation Sciences, The Hong Kong Polytechnic University, Kowloon, Hong Kong, <sup>2</sup> University Research Facility in Behavioral and Systems Neuroscience (UBSN), The Hong Kong Polytechnic University, Kowloon, Hong Kong, <sup>3</sup> Department of Psychiatry, The University of Hong Kong, Pokfulam, Hong Kong, <sup>4</sup> The State Key Laboratory for Brain and Cognitive Sciences, The University of Hong Kong, Pokfulam, Hong Kong, <sup>5</sup> Department of Psychiatry and Psychotherapy, Medical University of Vienna, Vienna, Austria

## OPEN ACCESS

### Edited by:

Neil James MacLusky,  
University of Guelph, Canada

### Reviewed by:

Mikhail Votinov,  
Jülich Research Centre, Germany  
Alexandra Kautzky-Willer,  
Medical University of Vienna, Austria

### \*Correspondence:

Georg S. Kranz  
georg.kranz@polyu.edu.hk

<sup>†</sup>These authors share first authorship

### Specialty section:

This article was submitted to  
Neuroendocrine Science,  
a section of the journal  
Frontiers in Neuroscience

**Received:** 07 December 2020

**Accepted:** 07 May 2021

**Published:** 07 June 2021

### Citation:

Yu KKK, Cheing GLY, Cheung C, Kranz GS and Cheung AK-K (2021) Gray Matter Abnormalities in Type 1 and Type 2 Diabetes: A Dual Disorder ALE Quantification. *Front. Neurosci.* 15:638861. doi: 10.3389/fnins.2021.638861

**Aims/hypothesis:** Diabetes mellitus (DM) is associated with comorbid brain disorders. Neuroimaging studies in DM revealed neuronal degeneration in several cortical and subcortical brain regions. Previous studies indicate more pronounced brain alterations in type 2 diabetes mellitus (T2DM) than in type 1 diabetes mellitus (T1DM). However, a comparison of both types of DM in a single analysis has not been done so far. The aim of this meta-analysis was to conduct an unbiased objective investigation of neuroanatomical differences in DM by combining voxel-based morphometry (VBM) studies of T1DM and T2DM using dual disorder anatomical likelihood estimation (ALE) quantification.

**Methods:** PubMed, Web of Science and Medline were systematically searched for publications until June 15, 2020. VBM studies comparing gray matter volume (GMV) differences between DM patients and controls at the whole-brain level were included. Study coordinates were entered into the ALE meta-analysis to investigate the extent to which T1DM, T2DM, or both conditions contribute to gray matter volume differences compared to controls.

**Results:** Twenty studies (comprising of 1,175 patients matched with 1,013 controls) were included, with seven studies on GMV alterations in T1DM and 13 studies on GMV alterations in T2DM. ALE analysis revealed seven clusters of significantly lower GMV in T1DM and T2DM patients relative to controls across studies. Both DM subtypes showed GMV reductions in the left caudate, right superior temporal lobe, and left cuneus. Conversely, GMV reductions associated exclusively with T2DM (>99% contribution) were found in the left cingulate, right posterior lobe, right caudate and left occipital lobe. Meta-regression revealed no significant influence of study size, disease duration, and HbA1c values.

**Conclusions/interpretation:** Our findings suggest a more pronounced gray matter atrophy in T2DM compared to T1DM. The increased risk of microvascular or macrovascular complications, as well as the disease-specific pathology of T2DM may contribute to observed GMV reductions.

**Systematic Review Registration:** [PROSPERO], identifier [CRD42020142525].

**Keywords:** anatomical likelihood estimation, diabetes mellitus, voxel-based morphometry, meta-analysis, systematic review

## INTRODUCTION

Diabetes mellitus (DM) is a common disease affecting more than 451 million people worldwide, and its prevalence may increase to 693 million cases by 2,045 (Cho et al., 2018). DM is divided into two subtypes, type 1 diabetes (T1DM) and type 2 diabetes (T2DM). Both subtypes are associated with persistent hyperglycemia, but have distinct causes, a different age at onset and different pathophysiologies (Leslie et al., 2016). T1DM has an onset in childhood and young adulthood and is characterized by insulin deficiency due to an autoimmune attack of insulin producing pancreatic beta cells. Conversely, with its onset in adulthood, T2DM is a chronic condition characterized by the body's increasing inability to either respond to functional insulin effectively and/or produce sufficient insulin for normal glucose regulation. Because of impaired glucose metabolism, it is widely accepted that both types of DM share increased risk in similar clinical features and complications, primarily vascular disease such as retinopathy, neuropathy, nephropathy, and cardiovascular disease.

Growing attention has been paid to the effect of DM on central nervous system because proper glucose regulation is essential for optimal brain functioning. Cognitive decrement has been observed in neuropsychological tests among diabetic patients; in particular, information processing speed and psychomotor efficiency were more affected than other cognitive functioning domains by the disease (Ryan et al., 2003; Brands et al., 2006). Furthermore, DM has been found to be associated with increased risk of Alzheimer disease. Quantitative meta-analysis of longitudinal studies identified higher relative risk of Alzheimer disease of 1.5 (95% CI 1.2–1.8) and vascular dementia of 2.5 (95% CI 2.1–3.0) among diabetic patients when compared with their nondiabetic counterparts (Cheng et al., 2012). Collectively, both types of DM have been shown to be associated with reduced cognitive function. While several studies indicated more pronounced dysfunctions in T2DM compared to T1DM, direct comparisons showed no systematic differences in cognitive abilities such as abstract reasoning, memory, attention and executive function, visuoconstruction, and information processing speed (Brands et al., 2007).

Brain imaging such as magnetic resonance imaging (MRI) is an ideal means to explore the neural correlates of cognitive dysfunction in DM. Altered cerebral metabolism has been observed in T1DM and T2DM (Sarac et al., 2005; Sinha et al., 2014). In addition, structural neuroimaging revealed reduced

gray matter volume (GMV) in both types of DM. However, results were inconsistent, which may be attributed to numerous variables including differences in sample size, imaging devices and protocols used (Gold et al., 2007; Chen et al., 2012; Moran et al., 2013; Zhang et al., 2014). Direct comparisons of MRI ratings of white matter lesions and cortical atrophy by Brands et al. (2007) revealed more pronounced deep white matter lesions and cortical atrophy in T2DM compared to T1DM (Brands et al., 2007). A more recent study by Moulton et al. (2015) attempted to review neuroimaging research including voxel-based morphometry (VBM) data and volumetric data using meta-analysis (Moulton et al., 2015). The authors performed separate meta-analyses for T1DM and T2DM and found reduced bilateral thalamus in T1DM whereas reduced global brain volume and regional atrophy in the hippocampi, basal ganglia, and orbitofrontal and occipital lobes were seen in T2DM. However, a comparison of VBM data of both types of DM in a single analysis has not been done so far. Yet, such an analysis would be needed in order to investigate the distinctiveness or similarities of T1DM and T2DM directly in an unbiased objective comparison.

VBM is an automated whole-brain based analysis method that has several advantages over a region-of-interest (ROI)-based approach. VBM measures local volume or concentration of gray matter voxel-wise across the whole brain. Thus, in order to conduct an unbiased objective investigation of neuroanatomical differences in DM, the aim of this study was to conduct a meta-analysis combining VBM studies of T1DM and T2DM using the anatomical likelihood estimation (ALE) technique.

## METHODS

### Literature Search

Our meta-analysis was registered with PROSPERO (registration number CRD42020142525) and was conducted according to the Preferred Reporting Items for Systematic Reviews and Meta-Analyses (PRISMA) guidelines (Moher et al., 2009). The studies were selected from PubMed (<https://pubmed.ncbi.nlm.nih.gov/>), Web of Science (<https://www.webofknowledge.com/>) and Google Scholar (<https://scholar.google.com.hk/>) databases and were limited to publications before October 1, 2020. The keywords used were “diabetes” or “diabetes mellitus” or “DM” plus “VBM,” “voxel-based,” “voxel-wise,” “morphometry,” or “VBM.” In addition, review articles and reference lists of

identified articles were manually checked. Individual articles had to meet the following inclusion criteria:

- (1) Gray matter differences between patients with DM and non-DM controls were compared
- (2) Comparison was performed at the whole-brain level
- (3) The gray matter differences between patients and controls were reported in a stereotactic space in three coordinates (x, y, z), either in Montreal Neurological Institute (MNI) or Talairach space.
- (4) Coordinates were included as separate studies if they contained multiple independent patient samples.
- (5) Studies using ROI or seed voxel-based analysis were excluded.
- (6) For studies lacking the Talairach or MNI coordinates, study authors were contacted in order to minimize the possibility of a biased sample set.
- (7) Studies considered for inclusion had to be published in English in a peer-reviewed journal
- (8) Subjects included had to have formal diagnosis of either type 1 or type 2 diabetes. Moreover, voxel-based imaging methods and co-ordinates reported in 3D stereotactic space had to be used.

Studies restricted to males/females or children/adults were included. Studies presenting overlapping or identical samples were identified, and only the study presenting the largest number of subjects was retained. If there was possible overlapping but different results were presented, e.g., hippocampus presented in one study while frontal lobe in another, all data were included.

## Quality Assessment

A customized checklist was used to assess the quality of included studies, as done by others (Katon et al., 2010) (**Table 1**). The checklist contained 12 items, and was based on previous meta-analytic studies (Shepherd et al., 2012; Du et al., 2014) with additional parameters including the diagnostic procedures, the demographic and clinical characterization, the sample size, the MRI acquisition parameters, the analysis technique and the quality of the reported results. Due to the rapid changing of data-processing methods, we included a new item “included modern MRI processing methods of past 10 years” in the checklist (item 8). The checklist provided objective information about the quality of included studies. Each study was reviewed by two authors (K.K.K.Y., G.S.K.), and a completeness rating was independently determined. If ratings disagreements arose, the papers were discussed, after which a consensus score was obtained. Only studies with quality score of 8 or above were included in the analysis.

## ALE Procedure

ALE treats each foci reported in VBM as a probability distribution in order to test for agreement across studies (Turkeltaub et al., 2002; Laird et al., 2005; Ellison-Wright et al., 2008). Typically, ALE is applied on a single disorder to identify volumetric differences consistently reported across VBM studies. The result of this approach is an ALE map showing the same regions that are consistently reported across studies.

**TABLE 1 |** Customized checklist for study quality assessment (adopted from Du et al., 2014).

<b>Category 1: Subjects</b>	
1	Patients were evaluated prospectively, specific diagnostic criteria were applied, and demographic data was reported
2	Healthy comparison subjects were evaluated prospectively, psychiatric and medical illnesses were excluded and demographic data was reported
3	Important variables (e.g., age, gender, intelligence quotient, i.e., IQ, handedness, socio-economic status, height, or total brain measures) were checked, either by stratification or statistically
4	Sample size per group > 10
<b>Category 2: Methods for image acquisition and analysis</b>	
5	Magnet strength at least 1.5 T
6	MRI slice-thickness $\leq 3$ mm
7	Whole brain analysis was automated with no a priori regional selection
8	Modern MRI processing methods of past 10 years
9	The imaging technique used was clearly described so that it could be reproduced
10	Measurements were clearly described so that they could be reproduced
<b>Category 3: Results and conclusions</b>	
11	Statistical parameters for significant, and important non-significant, differences were provided
12	Conclusions were consistent with the results obtained and the limitations were discussed

In the present study, we adopted the “Dual Disorder ALE Quantification.” We have previously applied this method to study similarities across different disorders such as schizophrenia and bipolar disorder, and schizophrenia and autism (Cheung et al., 2010; Yu et al., 2010; McAlonan et al., 2011). In brief, a map of gray matter difference compared to controls was generated for each study. These “gray matter difference” maps were categorized based on their disorder type, and averaged into a mean map. As a result, a mean map of T1DM and a mean map of T2DM were created. The mean maps were combined to form a total gray matter difference map, after which whole brain permutation testing (Turkeltaub et al., 2002), and controlled false discovery rate (FDR) thresholding was conducted (Laird et al., 2005). These procedures were conducted using an ALE kernel (Leung et al., 2009) available from the open source software available at <http://csl.georgetown.edu/software/> (Turkeltaub et al., 2002). The intensity of the mean disorder maps and the intensity of the final ALE result were divided such that the intensity ratio for each resultant cluster was calculated (ALE kernel and customized scripts for Matlab and SPM12).

The first stage of ALE is to generate a Gaussian distribution surrounding the central coordinates for each significant focus reported in studies. The probability that any given voxel is linked to the disorder(s) in question can be quantitatively estimated from this whole brain likelihood map. ALE eliminates unlikely foci and only points to likely foci that are close in proximity, in effect outlining regions which were reported most often across studies, to generate resultant three-dimensional clusters. It is emphasized that the approach of this study was to combine datasets from both disorders into the same entry for a single

analysis. In order to do so, individual “likelihood” maps that reflect the probability of finding gray matter differences, were generated for each of the included studies. A study with no findings across subjects and controls were represented by an empty map. Each of the likelihood maps were grouped based on the type of DM (T1 or T2), and averaged together into a mean likelihood map of conditions. The purpose for generating the mean maps was to avoid bias toward the condition with more reported foci. The mean maps were summated together to a joint likelihood map and 10,000 permutations were used to sample the null distribution. The result was thresholded by FDR ( $p < 0.05$ ) and clusters smaller than  $100 \text{ mm}^3$  were filtered. The resultant ALE map then contained clusters consisting of foci from T1DM, or T2DM, or both conditions. The contribution of each disorder to every resultant cluster was calculable. Two separate ALE analyses were performed for reductions and elevated gray matter volumes.

Finally, for each of the included studies, a “gray matter difference” map was generated to determine how much each study contributes toward the resultant ALE clusters. This contribution score was then used for meta-regression to test whether demographics or clinical measures including the study size, disease duration, and % glycated hemoglobin (HbA1c) have any influences toward the ALE result.

## RESULTS

### Studies Demographics

**Figure 1** shows the detailed selection process of included studies. After screening through title and abstract and removal of duplicates, a total of 94 studies were checked for eligibility. Among which, 32 studies were excluded as the VBM method was not adopted, and 42 studies were not included because the coordinates representing gray matter differences were not reported. A total of 20 studies were included in this analysis, with seven studies and 13 studies describing gray matter alterations in T1DM and T2DM respectively (see **Table 2**). A total of 1,175 patients matched with 1,013 controls were included. The T1DM group was significantly younger than the T2DM group (with a mean age of 23.7 compared to 49.8 years, respectively). However, there were no significant differences in age and sex between patient groups and their respective control groups. A total of 509 patients in the T1DM group were matched with 351 controls, whereas a total of 666 patients constituted the T2DM group that was matched with 662 control participants. T1DM had diabetes for an average of 14.7 years which was double than the average 7.3 years of T2DM, although this difference did not reach significance given the considerable variance between studies (see **Table 2**). Both groups had comparable HbA1c levels (T1DM: 8.6; T2DM: 8.3).

### Results of Gray Matter Alterations From ALE

ALE analysis for GMV reductions revealed seven clusters of lower GMV in T1DM and T2DM patients relative to controls across studies (see **Table 3** and **Figure 2**). Both DM subtypes showed GMV reductions in the left caudate, right middle temporal lobe

and left cuneus (BA 19). Whereas reductions in left cuneus and right middle temporal lobe were more driven by T1DM, left caudate reductions were stronger in T2DM. Conversely, GMV reductions associated exclusively with T2DM ( $>99\%$  contribution) were found in the left cingulate (BA 31), right inferior temporal lobe, right caudate and left occipital lobe. GMV reductions associated mainly with T1DM were not present (for the exact % of contribution for each cluster, see **Table 2**). The ALE analysis for GMV increases revealed no significant clusters for any DM subtype.

Finally, a meta-regression to investigate the potential influence of study size (number of included participants), disease duration, and % glycated hemoglobin (HbA1c) revealed no significant influence of these covariates, neither when tested individually, nor when combined in one regression model.

## DISCUSSION

This ALE meta-analysis made use of 20 VBM studies including seven studies of T1DM patients and 13 studies of T2DM patients to reveal overlaps and differences in GMV alterations between both conditions. Our analysis showed only GMV reductions in diabetic patients compared to controls, but no GMV increases. At first glance, this is not surprising given that hyperglycemia leads to cellular damage, as seen in rodent studies (Sadeghi et al., 2016; Hamed, 2017). More specifically, our results can be explained by insulin resistance, the principal characteristics in DM, which lowers glucose metabolism in the brain, resulting in enhanced amount of plasma glucose in DM patients (Baker et al., 2011). Chronic hyperglycemia is a potential determinant for diabetes-induced problems in the brain, as it could cause metabolic and molecular alterations, leading to neuron dysfunction or death in the brain (Tomlinson and Gardiner, 2008). Similar to Alzheimer’s disease (AD), tau phosphorylation and activation of advanced glycation end products (AGE) have been known to contribute to multiple proinflammatory cytokine release that eventually leads to synapse reduction and neuronal loss in diabetic brain (Zhao et al., 2018). Consequently, the resulting neuronal loss and gray matter atrophy that accounted for the frequently observed cognitive dysfunctions in DM are observable by brain MRI as GMV reductions (Brands et al., 2005).

Our meta-analysis shows a preponderance of GMV reductions in T2DM compared to T1DM, although T2DM appears to be better as compared to that of T1DM from the perspective of disease duration of patients as well as the glycemic control. Our meta-regression analysis revealed no influence of study size, disease duration, or HbA1c values on GMV, further suggesting that the involvement of other contributing factors to the GMV reductions. It is, in fact, not entirely out of our expectation considering that the etiologies of the two types are quite different. A recent review from Tamarai et al. (2019) have indicated obvious differences in the known genetic variants associated with the two types of DM (Tamarai et al., 2019). T1DM is a result of insufficient insulin secreting  $\beta$ -cells, and the genetic variations associated with T1DM are mainly related to alterations in insulin synthesis. While T2DM demonstrates impaired mechanisms of

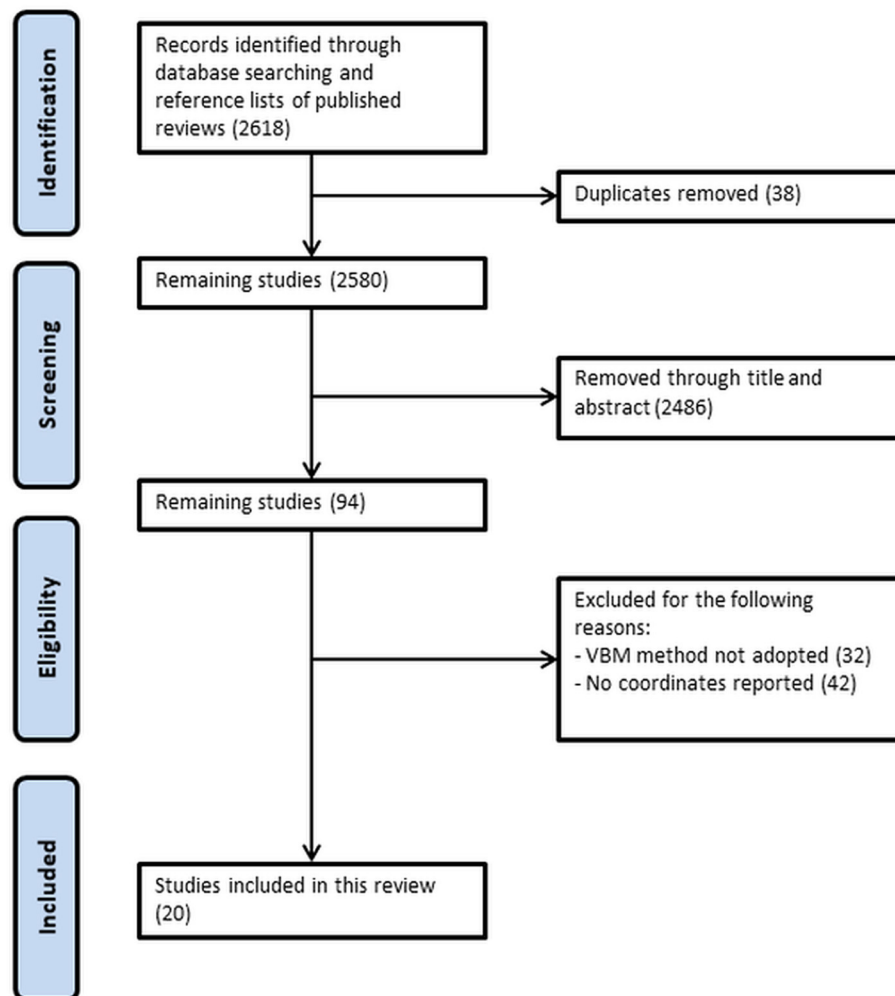


**FIGURE 1** | Preferred Reporting Items for Systematic Reviews and Meta-analyses (PRISMA) flow diagram of search strategy.

insulin release in response to hyperglycemia in addition to  $\beta$ -cells deficiency. The complexity of T2DM pathophysiology can be comprehended by interaction between multiple genes scattered all across the genome, as well as the interaction between genetic factors and environmental factors (e.g., life style; Tamarai et al., 2019).

Lower GMV in T2DM compared to T1DM is in accordance with a comparative study by Brands et al. (2007) who showed that MRI ratings of cortical atrophy are worse in T2DM compared to T1DM (Brands et al., 2007). Microvascular or macrovascular complications and comorbidities are more likely in T2DM than T1DM even when investigating youth-onset DM and adjusting for age (Luk et al., 2014; Dabelea et al., 2017). While it is possible that comorbid conditions, such as hypoglycaemia, hypercholesterolaemia, and hypertension may explain the difference, cognitive dysfunctions may also explain the differences in GMV reductions between DM types. Cognitive impairments seem to be stronger in T2DM compared to T1DM (Awad et al., 2004; Brands et al., 2005; Zilliox et al., 2016), but a

direct comparison of the two DM types revealed no significant differences in cognitive dysfunctions (Brands et al., 2007).

GMV reductions in our study were confined to seven clusters in specified brain regions including left and right caudate, temporal, occipital lobes, and cingulate cortex. GMV reductions in caudate, cingulate, inferior temporal, occipital lobe were exclusively driven by T2DM. These results partly concur with a volumetric meta-analysis by Moulton et al. (2015) who also observed occipital and caudate GMV reductions in T2DM (Moulton et al., 2015). The caudate exhibits a high insulin receptor density, so GMV in this region may be especially vulnerable to diabetes-associated atrophy (Schulinkamp et al., 2000). Interestingly, a recent transcriptomic analysis conducted with over 300 T2DM samples found that the T2DM-associated genes are expressed in the caudate significantly more than other brain regions (Zhou et al., 2019). Functional analysis revealed that these T2DM-associated genes affects synaptic functions and are related to other neurodegenerative diseases.

**TABLE 2 |** Papers included in the current meta-analysis.

References	Number of patients	Number of controls	Mean age of patients	Mean age of controls	Diabetes type	Diabetes duration (years)	HbA1c (%) <sup>#</sup>	Number receiving anti-diabetic therapy	MRI preprocessing methods	Quality score
Kaufmann et al. (2012)	30	19	14.3 ± 4.0	13 ± 3.2	T1DM	5.6 ± 3.8	8.4 ± 0.9	30	SPM	9.5
Liu et al. (2019)	21	21	9.3 ± 2.1	9.4 ± 1.1	T1DM	0.6 ± 0.1	11.2 ± 2.2	21	FSL	9
Marzelli et al. (2014)	142	68	7.0 ± 1.7	7 ± 1.8	T1DM	2.9 ± 2.0	7.9 ± 0.9	142	SPM	10
Musen et al. (2006)	82	36	32.6 ± 3.2	31.3 ± 5.1	T1DM	20.3 ± 3.6	7.8 ± 1.3	82	Analyze	10
Nunley et al. (2017)	95	135	49.1 ± 6.7	48.7 ± 7.3	T1DM	40.9 ± 6.2	n/a	95	FSL	10
Perantie et al. (2007)	108	51	12.6 ± 2.7	12.3 ± 2.7	T1DM	5.7 ± 2.9	8.4 ± 1.0	108	SPM	10
Wessels et al. (2006)	31	21	40.8 ± 5.9	36.3 ± 7.9	T1DM	26.8 ± 8.3	8.0 ± 1.1	31	SPM	10
	<b>509</b>	<b>351</b>	<b>23.7 ± 3.8</b>	<b>22.6 ± 4.2</b>		<b>14.7 ± 3.8</b>	<b>8.6 ± 1.2</b>	<b>509</b>		
Chen et al. (2012)	16	16	61.2 ± 7.8	59.6 ± 6.1	T2DM	13.2 ± 5.6	8.4 ± 1.7	n/a	SPM	10
Chen et al. (2017)	23	24	60.8 ± 8.3	57.0 ± 7.5	T2DM	9.0 ± 4.8	8.6 ± 2.2	12	SPM	10
Cui et al. (2017)	40	41	60.5 ± 6.9	57.9 ± 6.5	T2DM	8.9 ± 5.0	7.7 ± 1.6	8	SPM	9
Fang et al. (2019)	35	32	32.1 ± 5.3	34.1 ± 4.8	T2DM	1	10.4 ± 2.4	33	SPM	11
Ferreira et al. (2017)	24	27	58.6 ± 8.6	59.9 ± 5.9	T2DM	8.0 ± 7.9	10.0 ± 2.8	n/a	SPM	8.5
Garcia-Casares et al. (2014)	25	25	60.0 ± 4.6	57.8 ± 5.4	T2DM	11.25 ± 7.9	6.7 ± 0.8	25	SPM	10
Moran et al. (2013)	350	363	67.8 ± 6.9	72.1 ± 7.2	T2DM	7 (median)	7.2 ± 1.2	72	SPM	10
Nouwen et al. (2017)	14	19	16.1 ± 1.5	16.4 ± 1.7	T2DM	2.7 ± 2.5	8.1 ± 2.3	12	SPM	10
Redel et al. (2018)	20	20	16.7 ± 2.0	16.7 ± 2.6	T2DM	2.8 ± 2.1	7.9 ± 2.2	18	SPM	9
Wang et al. (2014)	23	23	53.1 ± 9.6	53.9 ± 9.2	T2DM	7	8.3 ± 1.4	n/a	SPM	9.5
Wang et al. (2017)	17	17	54.8 ± 8.3	54.4 ± 7.9	T2DM	n/a	n/a	n/a	SPM	12
Zhang et al. (2014)	53	29	54.2 ± 8.5	55.48	T2DM	7.3 ± 5.7	7.6 ± 1.5	n/a	SPM	10
Zhang et al. (2019)	26	26	51.9 ± 10.7	48.2 ± 6.7	T2DM	9.2 ± 7.1	n/a	21	SPM	10
	<b>666</b>	<b>662</b>	<b>49.8 ± 6.8**</b>	<b>49.5 ± 6.0**</b>		<b>7.3 ± 5.4<sup>ns</sup></b>	<b>8.3 ± 1.8<sup>ns</sup></b>	<b>201</b>		

Values represent mean ± SD if not stated otherwise.

Bold rows depict sum scores for number of patients, number of controls and number receiving anti-diabetic therapy, and average scores for mean age of patients and controls, diabetes duration and HbA1c values.

\*\*Indicates a significant difference ( $p < 0.01$ ) between T1DM and T2DM.

<sup>ns</sup>Indicates no significant difference between T1DM and T2DM (independent samples T-test).

T1DM, type-1 diabetes mellitus; T2DM, type-2 diabetes mellitus; HbA1c (%), Hemoglobin A1C (<sup>#</sup> provided for the DM group).

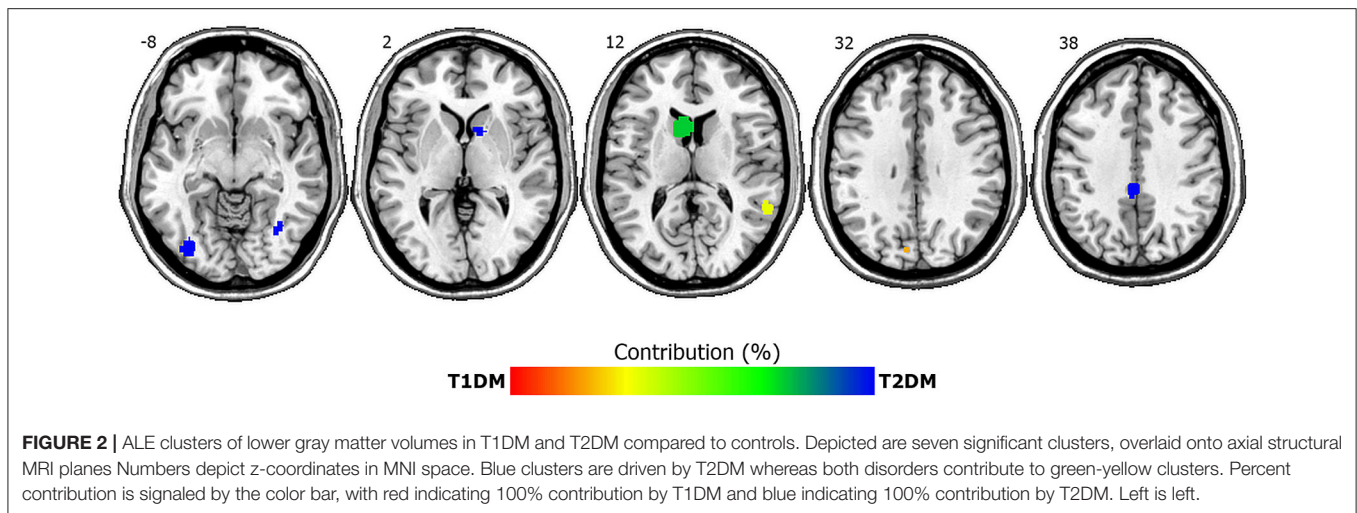
**TABLE 3 |** ALE clusters of lower gray matter volumes in T1DM and T2DM compared to controls.

Cluster	MNI coordinates	Location	T1DM %	T2DM %
1	(-1, -31, 41)	Left cingulate (BA 31)	0	100
2	(39, -67, -4)	Right inferior temporal lobe	0	100
3	(14, 12, -3)	Right caudate	0.01	99.99
4	(-37, -84, -3)	Left occipital lobe	0.02	99.98
5	(-7, 17, 9)	Left caudate	24.22	75.78
6	(64, -49, 15)	Right middle temporal lobe	64.76	35.24
7	(-6, -81, 42)	Left cuneus (BA 19)	78.41	21.59

Co-occurrence of DM and depression was observed previously (Katon et al., 2010; Balhara, 2011; Roy and Lloyd, 2012; Bădescu et al., 2016), and the prevalence of developing

depression is three times higher in T1DM patients and two times higher in T2DM patients as compared to general population (Roy and Lloyd, 2012). Moreover, those with depression are 60% more likely to develop T2DM (Mezuk et al., 2008). Consistent with our result, in structural and functional connectivity studies of depression disorder, it was reported that there is lower gray matter in the bilateral caudates (Shah et al., 2002; Kim et al., 2008; Ma et al., 2012) and right middle temporal gyrus (Peng et al., 2011; Ma et al., 2012; Kandilarova et al., 2019), and altered functional connectivity in the right caudate and right middle temporal gyrus (Ma et al., 2012). Deficits of these regions may suggest shared pathways that contribute to DM and depression.

GMV reductions in the cingulate cortex observed in our study were confined to a cluster in the posterior cingulate cortex (PCC). The PCC is considered as one of the “key hub” of the DMN, and is associated with functions such as memory retrieval



(Gusnard et al., 2001a) and regulating attention (Gusnard et al., 2001b). It has been reported that T2DM subjects have poorer memory and attention impairments as compared to matched controls (Gregg et al., 2000; Kanaya et al., 2004; van den Berg et al., 2010). Also, resting-states fMRI meta-analysis using ALE demonstrates that the PCC is affected in T2DM patients (Xia et al., 2017). Other quantitative fMRI studies using functional connectivity also show that resting-states is altered in the PCC (Cui et al., 2015; Ishibashi et al., 2018). These studies suggest that T2DM may have a disrupted DMN. Furthermore, Chen et al. found reduced functional activity in the PCC in T2DM patients when performing an encoding task related episodic memory, suggesting that DMN is affected in T2DM (Chen et al., 2016). It has also been observed that fractional anisotropy (FA) of the cingulum bundle are correlated to PCC and the medial frontal gyrus, which are important regions of the DMN (Hoogenboom et al., 2014). A previous meta-analysis speculated that gray matter volume differences in the DMN regions including PCC may be the reason why brain activation is affected in the DMN of T2DM patients, in terms of functional connectivity and activity, and ultimately leading to reduced cognitive performance (Liu et al., 2017).

DM (especially T2DM) and AD both shared some common neurocognitive functional deficits, one of which is the impaired memory (Karvani et al., 2019; Backström et al., 2021). Most research, especially using animal model, places hippocampus as the center of focus on memory loss. While hippocampal atrophy has been observed in T2DM, enlarged hippocampus was reported in T1DM (Hershey et al., 2010; Heyden et al., 2011), further indicating the mechanistic differences between T1DM and T2DM. Hippocampus, located deep within the temporal lobe, is not the only region responsible for memory function. Middle and Inferior temporal gyri, which are relatively superficial as compared to hippocampus, also play critical role in memory. Our data has revealed GMV reductions in right middle temporal gyrus and right inferior temporal gyrus. Middle and inferior temporal gyri (Musen et al., 2006; Chen et al., 2012; Wang et al., 2014; Redel et al., 2018; Zhang et al., 2019) have been

associated with semantic memory and semantic priming, in which semantically related stimuli resulted in faster or more effective activation. Early study has already shown a reduced cerebral blood flow in temporal lobe (Jimenez-Bonilla et al., 1996), which is believed to induce neuronal cell loss that resulted in temporal gyri atrophy that accounts for the reduced GMV of the respective regions.

Our data also indicated that left occipital lobe, and left cuneus which is also located in occipital lobe, demonstrated differential GMV in T2DM as compared to control. Occipital lobe is the center for visual processing, and it is possible that differential GMV could be a consequence of early sign of diabetic retinopathy. For example, glaucoma induced retinal damages has been shown to correlate with atrophy in occipital lobe, in particular the BA19 (Jiang et al., 2017). BA19 is located in parts of the cuneus and lingual gyrus. While lingual gyrus is associated with visual memory, cuneus is known to relate to inhibitory control (Haldane et al., 2008; Wang et al., 2018), the ability to inhibit or control impulsive responses by using attention and reasoning. Dysfunction in inhibition, although best known in people with attention deficits and hyperactivity disorder (ADHD), is also observed in T2DM (Cooke et al., 2020). In addition, strong correlation was observed between impaired cognitive performance in T2DM patients and reduced blood flow in cerebral regions, one of which was the occipital lobe (Cui et al., 2017). Therefore, GMV reduction in occipital lobe and cuneus may represent not only visual but also cognitive deficits.

Schizophrenia has long been found to link with increased risk of T2DM, as the prevalence of type 2 diabetes is 2–5-fold higher in patients with schizophrenia when compared with those without DM (Mamakou et al., 2018). While this may due to the impact of antipsychotic treatment and also the disease progression, the fact that drug naive patients of schizophrenia were still at 1.27–1.63-fold of risk of having T2DM than general population (Cohen and De Hert, 2011) may suggested that there is uniquely shared risk factor between the two diseases. A review of the genetic databases found 37 common susceptibility genes between schizophrenia and T2DM (Mamakou et al., 2018).

Association studies of the TCF7L2 gene in diabetes suggested increased risk of schizophrenia (Hansen et al., 2011; Alkelai et al., 2012).

Contrast to the suggested linkage between T2DM and schizophrenia, a large population study of over 800 k individuals in Finland suggested the reverse between T1DM and schizophrenia (Juvonen et al., 2007). The study found an incidence of 0.21/10,000 schizophrenia in type 1 diabetes, while it was 0.56 /1,000 schizophrenia in the general public, an over 60% reduction in risk of schizophrenia in type 1 diabetes. Our findings in predominantly larger contribution of T2DM in bilateral caudate deficit in gray matter echoes with the contradictory difference in linkage between T1DM and T2DM with schizophrenia. Bilateral caudate deficit was found in drug naïve patients of schizophrenia (Chua et al., 2007) but not with treated patients (Leung et al., 2009), suggesting caudate's role in the early stage and also in the treatment stage of schizophrenia.

In addition to focus given to the contribution of diabetes on cognitive dysfunction, association of antidiabetic treatment on cognitive performance on diabetic patients has also gained attention. A recent meta-analysis (Zhang et al., 2020) summarized 10 studies comprising 254,679 participants to determine the relationship between metformin therapy and cognitive function in T2DM patients, and compared metformin treatment with other antidiabetic drugs, including sulfonylureas, thiazolidinediones, and insulin. Despite all the treatments targeting T2DM, only metformin exhibited significant improvement in cognitive dysfunction, while insulin, suprisingly, aggravated cognitive dysfunction. Furthermore, such improvement was only significant in Americans and Europeans but not in Asian patients, indicating perhaps glycemic control alone might not be as effective in improving DM-induced cognitive dysfunction as expected. In addition to its primary antidiabetic action on reduction of glucose production in liver, metformin has also been shown to prevent neuronal cell death (El-Mir et al., 2008) and inhibited the molecular and pathological development of AD in cell culture model (Gupta et al., 2011). Metformin has been demonstrated to improve cognitive performance in AD patients (Cao et al., 2018) as well as in SAMP8 mice, one of the commonly used animal AD model, without altering blood glucose level (Farr et al., 2019), suggesting that this antidiabetic drug may improve cognitive function by acting on pathways other than glycemic control but the exact mechanism remained unclear. Although cognitive impairment in DM may arise from hyperglycemia, it is believed that a combinatorial effect of inflammation, oxidative stress, impaired cerebrovasculature, increase  $\beta$ -amyloid deposition, cerebral insulin resistance and formation of AGE all contribute to the progressive development of cognitive dysfunction in DM patients.

We acknowledge that there are a number of limitations to this study. First is the “file-drawer” problem which means that studies reporting null results are under-represented in the literature. This is a problem which all meta-analyses suffer. In this study, we tried to minimize this error by generating an empty

ALE map for studies that reported no gray matter differences between patient groups and controls. However, such studies demonstrating no differences are uncommon and not likely to be published. Second, MRI methodology is continually being improved, and the data extracted from various studies were pre-processed and analyzed in different ways. It is unfortunate that there were not enough studies to control for confounding factors including modulation and smoothing. To reduce the difference in methodologies affecting the outcome of our present study, we made use of a customized checklist to assess the quality of each study. The quality scores (mean: 9.9; s.d: 0.7) provide an overview of rigorous of each study. Without checking for quality scores, it is possible that lower quality studies (ex: outdated MRI acquisition or data processing methods, and low sample size) could influence the results. Lastly, while all T1DM patients were medicated, only about one third of T2DM patients received medication, hence we cannot rule out that our results could partly reflect an effect of medication.

## CONCLUSIONS

Our meta-analysis using the ALE methodology indicated GMV reductions in seven brain regions in T1DM and T2DM relative to controls. Clusters of lower GMV associated with both diabetes types were found in left caudate, right middle temporal lobe and left cuneus, whereas clusters exclusively found in T2DM were located in left cingulate, right inferior temporal lobe, right caudate and left occipital lobe. Our results indicate a more pronounced gray matter atrophy in T2DM compared to T1DM. We interpret this finding in terms of microvascular or macrovascular complications and disease-specific pathology of T2DM. To our knowledge, this study is the first meta-analysis of VBM studies in patients with DM which highlights overlapping and distinct brain atrophy found in T1DM and T2DM. The results of our study will aid understanding of the underlying neurodegenerative process in T1DM and T2DM.

## DATA AVAILABILITY STATEMENT

The original contributions presented in the study are included in the article/supplementary material, further inquiries can be directed to the corresponding author/s.

## AUTHOR CONTRIBUTIONS

GC, KY, and AC designed and conceptualized the study. KY and CC performed the data analysis. GK interpreted the data. KY, GK, CC, and AC contributed to discussion. GK and KY wrote the manuscript. All authors edited and reviewed the manuscript and agreed to its final version.

## FUNDING

This work was supported by the Hong Kong Polytechnic University (ZVP8 and ZVR4) and by a Grant from the Hong Kong Research Grants Council (25100219) to GK.

## REFERENCES

- Alkelai, A., Greenbaum, L., Lupoli, S., Kohn, Y., Sarnier-Kanyas, K., Ben-Asher, E. (2012). Association of the type 2 diabetes mellitus susceptibility gene TCF7L2 with schizophrenia in an Arab-Israeli family sample. *PLoS ONE* 7:e29228. doi: 10.1371/journal.pone.0029228
- Awad, N., Gagnon, M., and Messier, C. (2004). The relationship between impaired glucose tolerance, type 2 diabetes, and cognitive function. *J. Clin. Exp. Neuropsychol.* 26, 1044–1080. doi: 10.1080/13803390490514875
- Backström, A., Papadopoulos, K., Eriksson, S., Olsson, T., Andersson, M., Blennow, K., et al. (2021). Acute hyperglycaemia leads to altered frontal lobe brain activity and reduced working memory in type 2 diabetes. *PLoS ONE* 16:e0247753. doi: 10.1371/journal.pone.0247753
- Bădescu, S. V., Tătaru, C., Kobylinska, L., Georgescu, E. L., Zahiu, D. M., Zăgrean, A. M., et al. (2016). The association between Diabetes mellitus and Depression. *J. Med. Life* 9, 120–125.
- Baker, L. D., Cross, D. J., Minoshima, S., Belongia, D., Watson, G. S., and Craft, S. (2011). Insulin resistance and Alzheimer-like reductions in regional cerebral glucose metabolism for cognitively normal adults with prediabetes or early type 2 diabetes. *Arch. Neurol.* 68, 51–57. doi: 10.1001/archneurol.2010.225
- Balhara, Y. P. (2011). Diabetes and psychiatric disorders. *Indian J. Endocrinol. Metab.* 15, 274–283. doi: 10.4103/2230-8210.85579
- Brands, A. M., Biessels, G. J., de Haan, E. H., Kappelle, L. J., and Kessels, R. P. (2005). The effects of type 1 diabetes on cognitive performance: a meta-analysis. *Diabetes Care* 28, 726–735. doi: 10.2337/diacare.28.3.726
- Brands, A. M., Biessels, G. J., Kappelle, L. J., de Haan, E. H., de Valk, H. W., Algra, A., et al. (2007). Cognitive functioning and brain MRI in patients with type 1 and type 2 diabetes mellitus: a comparative study. *Dement. Geriatr. Cogn. Disord.* 23, 343–350. doi: 10.1159/000100980
- Brands, A. M., Kessels, R. P., Hoogma, R. P., Henselmans, J. M., van der Beek Boter, J. W., Kappelle, L. J., et al. (2006). Cognitive performance, psychological well-being, and brain magnetic resonance imaging in older patients with type 1 diabetes. *Diabetes* 55, 1800–1806. doi: 10.2337/db05-1226
- Cao, B., Rosenblat, J. D., Brietzke, E., Park, C., Lee, Y., Musial, N., et al. (2018). Comparative efficacy and acceptability of antidiabetic agents for Alzheimer's disease and mild cognitive impairment: a systematic review and network meta-analysis. *Diabetes Obes. Metab.* 20, 2467–2471. doi: 10.1111/dom.13373
- Chen, J., Zhang, J., Liu, X., Wang, X., Xu, X., Li, H., et al. (2017). Abnormal subcortical nuclei shapes in patients with type 2 diabetes mellitus. *Eur. Radiol.* 27, 4247–4256. doi: 10.1007/s00330-017-4790-3
- Chen, Y., Liu, Z., Wang, A., Zhang, J., Zhang, S., Qi, D., et al. (2016). Dysfunctional organization of default mode network before memory impairments in type 2 diabetes. *Psychoneuroendocrinology* 74, 141–148. doi: 10.1016/j.psyneuen.2016.08.012
- Chen, Z., Li, L., Sun, J., and Ma, L. (2012). Mapping the brain in type II diabetes: voxel-based morphometry using DARTEL. *Eur. J. Radiol.* 81, 1870–1876. doi: 10.1016/j.ejrad.2011.04.025
- Cheng, G., Huang, C., Deng, H., and Wang, H. (2012). Diabetes as a risk factor for dementia and mild cognitive impairment: a meta-analysis of longitudinal studies. *Intern. Med. J.* 42, 484–491. doi: 10.1111/j.1445-5994.2012.02758.x
- Cheung, C., Yu, K., Fung, G., Leung, M., Wong, C., Li, Q., et al. (2010). Autistic disorders and schizophrenia: related or remote? An anatomical likelihood estimation. *PLoS ONE* 5:e12233. doi: 10.1371/journal.pone.0012233
- Cho, N. H., Shaw, J. E., Karuranga, S., Huang, Y., da Rocha Fernandes, J. D., Ohlrogge, A. W., et al. (2018). IDF Diabetes Atlas: global estimates of diabetes prevalence for 2017 and projections for 2045. *Diabetes Res. Clin. Pract.* 138, 271–281. doi: 10.1016/j.diabres.2018.02.023
- Chua, S. E., Cheung, C., Cheung, V., Tsang, J. T., Chen, E. Y., Wong, J. C., et al. (2007). Cerebral grey, white matter and csf in never-medicated, first-episode schizophrenia. *Schizophr. Res.* 89, 12–21. doi: 10.1016/j.schres.2006.09.009
- Cohen, D., and De Hert, M. (2011). Endogenic and iatrogenic diabetes mellitus in drug-naïve schizophrenia: the role of olanzapine and its place in the psychopharmacological treatment algorithm. *Neuropsychopharmacology* 36, 2368–2369. doi: 10.1038/npp.2011.94
- Cooke, S., Pennington, K., Jones, A., Bridle, C., Smith, M. F., and Curtis, F. (2020). Effects of exercise, cognitive, and dual-task interventions on cognition in type 2 diabetes mellitus: a systematic review and meta-analysis. *PLoS ONE* 15:e0232958. doi: 10.1371/journal.pone.0232958
- Cui, Y., Jiao, Y., Chen, H. J., Ding, J., Luo, B., Peng, C. Y., et al. (2015). Aberrant functional connectivity of default-mode network in type 2 diabetes patients. *Eur. Radiol.* 25, 3238–3246. doi: 10.1007/s00330-015-3746-8
- Cui, Y., Liang, X., Gu, H., Hu, Y., Zhao, Z., Yang, X. Y., et al. (2017). Cerebral perfusion alterations in type 2 diabetes and its relation to insulin resistance and cognitive dysfunction. *Brain Imag. Behav.* 11, 1248–1257. doi: 10.1007/s11682-016-9583-9
- Dabelea, D., Stafford, J. M., Mayer-Davis, E. J., D'Agostino, R. Jr., Dolan, L., Imperatore, G., et al. (2017). Association of type 1 diabetes vs. type 2 diabetes diagnosed during childhood and adolescence with complications during teenage years and young adulthood. *JAMA* 317, 825–835. doi: 10.1001/jama.2017.0686
- Du, M., Liu, J., Chen, Z., Huang, X., Li, J., Kuang, W., et al. (2014). Brain grey matter volume alterations in late-life depression. *J. Psychiatry Neurosci.* 39, 397–406. doi: 10.1503/jpn.130275
- Ellison-Wright, I., Glahn, D. C., Laird, A. R., Thelen, S. M., and Bullmore, E. (2008). The anatomy of first-episode and chronic schizophrenia: an anatomical likelihood estimation meta-analysis. *Am. J. Psychiatry* 165, 1015–1023. doi: 10.1176/appi.ajp.2008.07101562
- El-Mir, M. Y., Detaillé, D., R-Villanueva, G., Delgado-Esteban, M., Guigas, B., Attia, S., et al. (2008). Neuroprotective role of antidiabetic drug metformin against apoptotic cell death in primary cortical neurons. *J. Mol. Neurosci.* 34, 77–87. doi: 10.1007/s12031-007-9002-1
- Fang, F., Lai, M. Y., Huang, J. J., Kang, M., Ma, M. M., Li, K. A., et al. (2019). Compensatory hippocampal connectivity in young adults with early-stage type 2 diabetes. *J. Clin. Endocrinol. Metab.* 104, 3025–3038. doi: 10.1210/je.2018-02319
- Farr, S. A., Roesler, E., Niehoff, M. L., Roby, D. A., McKee, A., Morley, J. E. (2019). Metformin improves learning and memory in the SAMP8 mouse model of Alzheimer's disease. *J. Alzheimers Dis.* 68, 1699–1710. doi: 10.3233/JAD-181240
- Ferreira, F. S., Pereira, J. M. S., Reis, A., Sanches, M., Duarte, J. V., Gomes, L., et al. (2017). Early visual cortical structural changes in diabetic patients without diabetic retinopathy. *Graefes. Arch. Clin. Exp. Ophthalmol.* 255, 2113–2118. doi: 10.1007/s00417-017-3752-4
- García-Casares, N., Berthier, M. L., Jorge, R. E., Gonzalez-Alegre, P., Gutiérrez Cardo, A., Rioja Villodres, J., et al. (2014). Structural and functional brain changes in middle-aged type 2 diabetic patients: a cross-sectional study. *J. Alzheimers Dis.* 40, 375–386. doi: 10.3233/JAD-131736
- Gold, S. M., Dziobek, I., Sweat, V., Tersi, A., Rogers, K., Bruehl, H., et al. (2007). Hippocampal damage and memory impairments as possible early brain complications of type 2 diabetes. *Diabetologia* 50, 711–719. doi: 10.1007/s00125-007-0602-7
- Gregg, E. W., Yaffe, K., Cauley, J. A., Rolka, D. B., Blackwell, T. L., Narayan, K. M., et al. (2000). Is diabetes associated with cognitive impairment and cognitive decline among older women? Study of Osteoporotic Fractures Research Group. *Arch. Intern. Med.* 160, 174–180. doi: 10.1001/archinte.160.2.174
- Gupta, A., Bisht, B., and Dey, C. S. (2011). Peripheral insulin-sensitizer drug metformin ameliorates neuronal insulin resistance and Alzheimer's-like changes. *Neuropharmacology* 60, 910–920. doi: 10.1016/j.neuropharm.2011.01.033
- Gusnard, D. A., Akbudak, E., Shulman, G. L., and Raichle, M. E. (2001a). Medial prefrontal cortex and self-referential mental activity: relation to a default mode of brain function. *Proc. Natl. Acad. Sci. U. S. A.* 98, 4259–4264. doi: 10.1073/pnas.071043098
- Gusnard, D. A., Raichle, M. E., and Raichle, M. E. (2001b). Searching for a baseline: functional imaging and the resting human brain. *Nat. Rev. Neurosci.* 2, 685–694. doi: 10.1038/35094500
- Haldane, M., Cunningham, G., Androustos, C., and Frangou, S. (2008). Structural brain correlates of response inhibition in Bipolar Disorder. *J. Psychopharmacol.* 22, 138–143. doi: 10.1177/0269881107082955
- Hamed, S. A. (2017). Brain injury with diabetes mellitus: evidence, mechanisms and treatment implications. *Expert. Rev. Clin. Pharmacol.* 10, 409–428. doi: 10.1080/17512433.2017.1293521
- Hansen, T., Ingason, A., Djurovic, S., Melle, I., Fenger, M., Gustafsson, O., et al. (2011). At-risk variant in TCF7L2 for type II diabetes increases risk of schizophrenia. *Biol. Psychiatry* 70, 59–63. doi: 10.1016/j.biopsych.2011.01.031

- Hershey, T., Perantie, D. C., Wu, J., Weaver, P. M., Black, K. J., and White, N. H. (2010). Hippocampal volumes in youth with type 1 diabetes. *Diabetes* 59, 236–241. doi: 10.2337/db09-1117
- Heyden, A., Ionescu, M. C., Romorini, S., Kracht, B., Ghiglieri, V., Calabresi, P., et al. (2011). Hippocampal enlargement in Basso-mutant mice is associated with enhanced neurogenesis, reduced apoptosis, and abnormal BDNF levels. *Cell Tissue Res.* 346, 11–26. doi: 10.1007/s00441-011-1233-3
- Hoogenboom, W. S., Marder, T. J., Flores, V. L., Huisman, S., Eaton, H. P., Schneiderman, J. S., et al. (2014). Cerebral white matter integrity and resting-state functional connectivity in middle-aged patients with type 2 diabetes. *Diabetes* 63, 728–738. doi: 10.2337/db13-1219
- Ishibashi, K., Sakurai, K., Shimoji, K., Tokumaru, A. M., and Ishii, K. (2018). Altered functional connectivity of the default mode network by glucose loading in young, healthy participants. *BMC Neurosci.* 19:33. doi: 10.1186/s12868-018-0433-0
- Jiang, M. M., Zhou, Q., Liu, X. Y., Shi, C. Z., Chen, J., and Huang, X. H. (2017). Structural and functional brain changes in early- and mid-stage primary open-angle glaucoma using voxel-based morphometry and functional magnetic resonance imaging. *Medicine* 96:e6139. doi: 10.1097/MD.00000000000006139
- Jimenez-Bonilla, J. F., Carril, J. M., Quirce, R., Gomez-Barquin, R., Amado, J. A., and Gutierrez-Mendiguchia, C. (1996). Assessment of cerebral blood flow in diabetic patients with no clinical history of neurological disease. *Nucl. Med. Commun.* 17, 790–794. doi: 10.1097/00006231-199609000-00009
- Juvonen, H., Reunanen, A., Haukka, J., Muhonen, M., Suvisaari, J., Arajärvi, R., et al. (2007). Incidence of schizophrenia in a nationwide cohort of patients with type 1 diabetes mellitus. *Arch. Gen. Psychiatry* 64, 894–899. doi: 10.1001/archpsyc.64.8.894
- Kanaya, A. M., Barrett-Connor, E., Gildengorin, G., and Yaffe, K. (2004). Change in cognitive function by glucose tolerance status in older adults: a 4-year prospective study of the Rancho Bernardo study cohort. *Arch. Intern. Med.* 164, 1327–1333. doi: 10.1001/archinte.164.12.1327
- Kandilarova, S., Stoyanov, D., Sirakov, N., Maes, M., and Specht, K. (2019). Reduced grey matter volume in frontal and temporal areas in depression: contributions from voxel-based morphometry study. *Acta Neuropsychiatr.* 31, 252–257. doi: 10.1017/neu.2019.20
- Karvani, M., Simos, P., Stavrakaki, S., and Kapoukranidou, D. (2019). Neurocognitive impairment in type 2 diabetes mellitus. *Hormones* 18, 523–534. doi: 10.1007/s42000-019-00128-2
- Katon, W. J., Lin, E. H., Williams, L. H., Ciechanowski, P., Heckbert, S. R., Ludman, E., et al. (2010). Comorbid depression is associated with an increased risk of dementia diagnosis in patients with diabetes: a prospective cohort study. *J. Gen. Intern. Med.* 25, 423–429. doi: 10.1007/s11606-009-1248-6
- Kaufmann, L., Pixner, S., Starke, M., Zotter, S., Köhle, J., Meraner, D., et al. (2012). Neurocognition and brain structure in pediatric patients with type 1 diabetes. *J. Pediatr. Neurol.* 1, 25–35. doi: 10.3233/PNR-2012-005
- Kim, M. J., Hamilton, J. P., and Gotlib, I. H. (2008). Reduced caudate gray matter volume in women with major depressive disorder. *Psychiatry Res.* 164, 114–122. doi: 10.1016/j.psychres.2007.12.020
- Laird, A. R., Fox, P. M., Price, C. J., Glahn, D. C., Uecker, A. M., Lancaster, J. L., et al. (2005). ALE meta-analysis: controlling the false discovery rate and performing statistical contrasts. *Hum. Brain Mapp.* 25, 155–164. doi: 10.1002/hbm.20136
- Leslie, R. D., Palmer, J., Schloot, N. C., and Lernmark, A. (2016). Diabetes at the crossroads: relevance of disease classification to pathophysiology and treatment. *Diabetologia* 59, 13–20. doi: 10.1007/s00125-015-3789-z
- Leung, M., Cheung, C., Yu, K., Yip, B., Sham, P., Li, Q., et al. (2009). Gray matter in first-episode schizophrenia before and after antipsychotic drug treatment. Anatomical likelihood estimation meta-analyses with sample size weighting. *Schizophr. Bull.* 2009:sbp099. doi: 10.1093/schbul/sbp099
- Liu, J., Liu, T., Wang, W., Ma, L., Ma, X., Shi, S., et al. (2017). Reduced gray matter volume in patients with type 2 diabetes mellitus. *Front. Aging Neurosci.* 9:161. doi: 10.3389/fnagi.2017.00161
- Liu, K., Huang, X., Cui, S., Ye, X., Zhou, Y., Song, J., et al. (2019). Voxel-based morphometry reveals regional reductions of gray matter volume in school-aged children with short-term type 1 diabetes mellitus. *Neuroreport* 30, 516–521. doi: 10.1097/WNR.0000000000001238
- Luk, A. O., Lau, E. S., So, W. Y., Ma, R. C., Kong, A. P., Ozaki, R., et al. (2014). Prospective study on the incidences of cardiovascular-renal complications in Chinese patients with young-onset type 1 and type 2 diabetes. *Diabetes Care* 37, 149–157. doi: 10.2337/dc13-1336
- Ma, C., Ding, J., Li, J., Guo, W., Long, Z., Liu, F., et al. (2012). Resting-state functional connectivity bias of middle temporal gyrus and caudate with altered gray matter volume in major depression. *PLoS ONE* 7:e45263. doi: 10.1371/journal.pone.0045263
- Mamakou, V., Thanopoulou, A., Gonidakis, F., Tentolouris, N., and Kontaxakis, V. (2018). Schizophrenia and type 2 diabetes mellitus. *Psychiatriki* 29, 64–73. doi: 10.22365/jpsych.2018.291.64
- Marzelli, M. J., Mazaika, P. K., Barnea-Goraly, N., Hershey, T., Tsalikian, E., Tamborlane, W., et al. (2014). Neuroanatomical correlates of dysglycemia in young children with type 1 diabetes. *Diabetes* 63, 343–353. doi: 10.2337/db13-0179
- McAlonan, G. M., Yu, K. K., Chan, R. C. K., Chua, S. E., and Cheung, C. (2011). Is there an anatomical endophenotype for neurodevelopmental disorders? A review of dual disorder anatomical likelihood estimation (ALE) meta-analyses of grey matter volumes. *Chin. Sci. Bull.* 56, 3376–3381. doi: 10.1007/s11434-011-4743-1
- Mezuk, B., Eaton, W. W., Albrecht, S., and Golden, S. H. (2008). Depression and type 2 diabetes over the lifespan: a meta-analysis. *Diabetes Care* 31, 2383–2390. doi: 10.2337/dc08-0985
- Moher, D., Liberati, A., Tetzlaff, J., Altman, D. G., and Group, P. (2009). Preferred reporting items for systematic reviews and meta-analyses: the PRISMA statement. *BMJ* 339:b2535. doi: 10.1136/bmj.b2535
- Moran, C., Phan, T. G., Chen, J., Blizzard, L., Beare, R., Venn, A., et al. (2013). Brain atrophy in type 2 diabetes: regional distribution and influence on cognition. *Diabetes Care* 36, 4036–4042. doi: 10.2337/dc13-0143
- Moulton, C. D., Costafreda, S. G., Horton, P., Ismail, K., and Fu, C. H. (2015). Meta-analyses of structural regional cerebral effects in type 1 and type 2 diabetes. *Brain Imag. Behav.* 9, 651–662. doi: 10.1007/s11682-014-9348-2
- Musen, G., Lyoo, I. K., Sparks, C. R., Weinger, K., Hwang, J., Ryan, C. M., et al. (2006). Effects of type 1 diabetes on gray matter density as measured by voxel-based morphometry. *Diabetes* 55, 326–333. doi: 10.2337/diabetes.55.02.06.db05-0520
- Nouwen, A., Chambers, A., Chechlacz, M., Higgs, S., Blissett, J., Barrett, T. G., et al. (2017). Microstructural abnormalities in white and gray matter in obese adolescents with and without type 2 diabetes. *Neuroimage Clin.* 16, 43–51. doi: 10.1016/j.nicl.2017.07.004
- Nunley, K. A., Ryan, C. M., Aizenstein, H. J., Jennings, J. R., MacCloud, R. L., Orchard, T. J., et al. (2017). Regional gray matter volumes as related to psychomotor slowing in adults with type 1 diabetes. *Psychosom. Med.* 79, 533–540. doi: 10.1097/PSY.0000000000000449
- Peng, J., Liu, J., Nie, B., Li, Y., Shan, B., Wang, G., et al. (2011). Cerebral and cerebellar gray matter reduction in first-episode patients with major depressive disorder: a voxel-based morphometry study. *Eur. J. Radiol.* 80, 395–399. doi: 10.1016/j.ejrad.2010.04.006
- Perantie, D. C., Wu, J., Koller, J. M., Lim, A., Warren, S. L., Black, K. J., et al. (2007). Regional brain volume differences associated with hyperglycemia and severe hypoglycemia in youth with type 1 diabetes. *Diabetes Care* 30, 2331–2337. doi: 10.2337/dc07-0351
- Redel, J. M., DiFrancesco, M., Vannest, J., Altaye, M., Beebe, D., Khoury, J., et al. (2018). Brain gray matter volume differences in obese youth with type 2 diabetes: a pilot study. *J. Pediatr. Endocrinol. Metab.* 31, 261–268. doi: 10.1515/jpem-2017-0349
- Roy, T., and Lloyd, C. E. (2012). Epidemiology of depression and diabetes: a systematic review. *J. Affect. Disord.* 142(Suppl.), S8–S21. doi: 10.1016/S0165-0327(12)70004-6
- Ryan, C. M., Geckle, M. O., and Orchard, T. J. (2003). Cognitive efficiency declines over time in adults with Type 1 diabetes: effects of micro- and macrovascular complications. *Diabetologia* 46, 940–948. doi: 10.1007/s00125-003-1128-2
- Sadeghi, A., Hani, J., Razavi, S., Esfandiary, E., and Hejazi, Z. (2016). The effect of diabetes mellitus on apoptosis in hippocampus: cellular and molecular aspects. *Int. J. Prev. Med.* 7:57. doi: 10.4103/2008-7802.178531
- Sarac, K., Akinci, A., Alkan, A., Aslan, M., Baysal, T., and Ozcan, C. (2005). Brain metabolite changes on proton magnetic resonance spectroscopy in children with poorly controlled type 1 diabetes mellitus. *Neuroradiology* 47, 562–565. doi: 10.1007/s00234-005-1387-3

- Schulinkamp, R. J., Pagano, T. C., Hung, D., and Raffa, R. B. (2000). Insulin receptors and insulin action in the brain: review and clinical implications. *Neurosci. Biobehav. Rev.* 24, 855–872. doi: 10.1016/S0149-7634(00)00040-3
- Shah, P. J., Glabus, M. F., Goodwin, G. M., and Ebmeier, K. P. (2002). Chronic, treatment-resistant depression and right fronto-striatal atrophy. *Br. J. Psychiatry*. 180, 434–440. doi: 10.1192/bjp.180.5.434
- Shepherd, A. M., Matheson, S. L., Laurens, K. R., Carr, V. J., and Green, M. J. (2012). Systematic meta-analysis of insula volume in schizophrenia. *Biol. Psychiatry* 72, 775–784. doi: 10.1016/j.biopsych.2012.04.020
- Sinha, S., Ekka, M., Sharma, U. P. R., Pandey, R. M., and Jagannathan, N. R. (2014). Assessment of changes in brain metabolites in Indian patients with type-2 diabetes mellitus using proton magnetic resonance spectroscopy. *BMC Res. Notes* 7:41. doi: 10.1186/1756-0500-7-41
- Tamarai, K., Bhatti, J. S., and Reddy, P. H. (2019). Molecular and cellular bases of diabetes: focus on type 2 diabetes mouse model-TallyHo. *Biochim. Biophys. Acta Mol. Basis Dis.* 1865, 2276–2284. doi: 10.1016/j.bbdis.2019.05.004
- Tomlinson, D. R., and Gardiner, N. J. (2008). Glucose neurotoxicity. *Nat. Rev. Neurosci.* 9, 36–45. doi: 10.1038/nrn2294
- Turkeltaub, P. E., Eden, G. F., Jones, K. M., and Zeffiro, T. A. (2002). Meta-analysis of the functional neuroanatomy of single-word reading: method and validation. *Neuroimage*. 16, 765–780. doi: 10.1006/nimg.2002.1131
- van den Berg, E., Reijmer, Y. D., de Bresser, J., Kessels, R. P., Kappelle, L. J., and Biessels, G. J. (2010). A 4 year follow-up study of cognitive functioning in patients with type 2 diabetes mellitus. *Diabetologia* 53, 58–65. doi: 10.1007/s00125-009-1571-9
- Wang, C., Fu, K., Liu, H., Xing, F., and Zhang, S. (2014). Brain structural changes and their correlation with vascular disease in type 2 diabetes mellitus patients: a voxel-based morphometric study. *Neural. Regen. Res.* 9, 1548–1556. doi: 10.4103/1673-5374.139482
- Wang, J., Fan, Y., Dong, Y., Ma, M., Dong, Y., Niu, Y., et al. (2018). Combining gray matter volume in the cuneus and the cuneus-prefrontal connectivity may predict early relapse in abstinent alcohol-dependent patients. *PLoS ONE* 13:e0196860. doi: 10.1371/journal.pone.0196860
- Wang, Y. F., Kong, X., Lu, G. M., and Zhang, L. J. (2017). Diabetes mellitus is associated with more severe brain spontaneous activity impairment and gray matter loss in patients with cirrhosis. *Sci. Rep.* 7:7775. doi: 10.1038/s41598-017-08075-x
- Wessels, A. M., Simsek, S., Remijnse, P. L., Veltman, D. J., Biessels, G. J., Barkhof, F., et al. (2006). Voxel-based morphometry demonstrates reduced grey matter density on brain MRI in patients with diabetic retinopathy. *Diabetologia* 49, 2474–2480. doi: 10.1007/s00125-006-0283-7
- Xia, W., Chen, Y. C., and Ma, J. (2017). Resting-state brain anomalies in type 2 diabetes: a meta-analysis. *Front. Aging Neurosci.* 9:14. doi: 10.3389/fnagi.2017.00014
- Yu, K., Cheung, C., Leung, M., Li, Q., Chua, S., and McAlonan, G. (2010). Are bipolar disorder and schizophrenia neuroanatomically distinct? An anatomical likelihood meta-analysis. *Front. Hum. Neurosci.* 2010:189. doi: 10.3389/fnhum.2010.00189
- Zhang, D., Shi, L., Song, X., Shi, C., Sun, P., Lou, W., et al. (2019). Neuroimaging endophenotypes of type 2 diabetes mellitus: a discordant sibling pair study. *Quant. Imag. Med. Surg.* 9, 1000–1013. doi: 10.21037/qims.2019.05.18
- Zhang, Q. Q., Li, W. S., Liu, Z., Zhang, H. L., Ba, Y. G., and Zhang, R. X. (2020). Metformin therapy and cognitive dysfunction in patients with type 2 diabetes: a meta-analysis and systematic review. *Medicine* 99:e19378. doi: 10.1097/MD.00000000000019378
- Zhang, Y., Zhang, X., Zhang, J., Liu, C., Yuan, Q., Yin, X., et al. (2014). Gray matter volume abnormalities in type 2 diabetes mellitus with and without mild cognitive impairment. *Neurosci. Lett.* 562, 1–6. doi: 10.1016/j.neulet.2014.01.006
- Zhao, Y., Luo, C., Chen, J., Sun, Y., Pu, D., Lv, A., et al. (2018). High glucose-induced complement component 3 up-regulation via RAGE-p38MAPK-NF-kappaB signalling in astrocytes: *in vivo* and *in vitro* studies. *J. Cell Mol. Med.* 22, 6087–6098. doi: 10.1111/jcmm.13884
- Zhou, Z., Zhu, Y., Liu, Y., and Yin, Y. (2019). Comprehensive transcriptomic analysis indicates brain regional specific alterations in type 2 diabetes. *Aging* 11, 6398–6421. doi: 10.18632/aging.102196
- Zilliox, L. A., Chadrasekaran, K., Kwan, J. Y., and Russell, J. W. (2016). Diabetes and cognitive impairment. *Curr. Diab. Rep.* 16:87. doi: 10.1007/s11892-016-0775-x

**Conflict of Interest:** The authors declare that the research was conducted in the absence of any commercial or financial relationships that could be construed as a potential conflict of interest.

Copyright © 2021 Yu, Cheing, Cheung, Kranz and Cheung. This is an open-access article distributed under the terms of the Creative Commons Attribution License (CC BY). The use, distribution or reproduction in other forums is permitted, provided the original author(s) and the copyright owner(s) are credited and that the original publication in this journal is cited, in accordance with accepted academic practice. No use, distribution or reproduction is permitted which does not comply with these terms.



# Retinal Neurovascular Impairment in Non-diabetic and Non-dialytic Chronic Kidney Disease Patients

## OPEN ACCESS

### Edited by:

Hubert Preissl,  
Institute for Diabetes Research  
and Metabolic Diseases (IDM),  
Germany

### Reviewed by:

Davide Viggiano,  
University of Campania Luigi Vanvitelli,  
Italy  
Haoyu Chen,  
Shantou University and the Chinese  
University of Hong Kong, China  
Haotian Lin,  
Sun Yat-sen University, China

### \*Correspondence:

Zhiming Ye  
yezhiming@gdph.org.cn  
Xiaohong Yang  
syyangxh@scut.edu.cn  
Honghua Yu  
yuhonghua@gdph.org.cn

<sup>†</sup>These authors have contributed  
equally to this work and share first  
authorship

### Specialty section:

This article was submitted to  
Neuroendocrine Science,  
a section of the journal  
Frontiers in Neuroscience

**Received:** 21 June 2021

**Accepted:** 11 October 2021

**Published:** 18 November 2021

### Citation:

Zeng X, Hu Y, Chen Y, Lin Z,  
Liang Y, Liu B, Zhong P, Xiao Y, Li C,  
Wu G, Kong H, Du Z, Ren Y, Fang Y,  
Ye Z, Yang X and Yu H (2021) Retinal  
Neurovascular Impairment  
in Non-diabetic and Non-dialytic  
Chronic Kidney Disease Patients.  
Front. Neurosci. 15:703898.  
doi: 10.3389/fnins.2021.703898

Xiaomin Zeng<sup>1,2†</sup>, Yijun Hu<sup>3,4†</sup>, Yuanhan Chen<sup>5†</sup>, Zhanjie Lin<sup>1,6</sup>, Yingying Liang<sup>1,2</sup>,  
Baoyi Liu<sup>1,2</sup>, Pingting Zhong<sup>1,6</sup>, Yu Xiao<sup>1,2</sup>, Cong Li<sup>1,7</sup>, Guanrong Wu<sup>1,7</sup>, Huiqian Kong<sup>1,2</sup>,  
Zijing Du<sup>1,2</sup>, Yun Ren<sup>1,6</sup>, Ying Fang<sup>1</sup>, Zhiming Ye<sup>5\*</sup>, Xiaohong Yang<sup>1,2\*</sup> and Honghua Yu<sup>1,2\*</sup>

<sup>1</sup> Guangdong Eye Institute, Department of Ophthalmology, Guangdong Provincial People's Hospital, Guangdong Academy of Medical Sciences, Guangzhou, China, <sup>2</sup> The Second School of Clinical Medicine, Southern Medical University, Guangzhou, China, <sup>3</sup> Aier Institute of Refractive Surgery, Refractive Surgery Center, Guangzhou Aier Eye Hospital, Guangzhou, China, <sup>4</sup> Aier School of Ophthalmology, Central South University, Changsha, China, <sup>5</sup> Division of Nephrology, Guangdong Provincial People's Hospital, Guangdong Academy of Medical Sciences, Guangzhou, China, <sup>6</sup> Shantou University Medical College, Shantou, China, <sup>7</sup> School of Medicine, South China University of Technology, Guangzhou, China

**Background:** Widespread neural and microvascular injuries are common in chronic kidney disease (CKD), increasing risks of neurovascular complications and mortality. Early detection of such changes helps assess the risks of neurovascular complications for CKD patients. As an extension of central nervous system, the retina provides a characteristic window to observe neurovascular alterations in CKD. This study aimed to determine the presence of retinal neurovascular impairment in different stages of CKD.

**Methods:** One hundred fifteen non-diabetic and non-dialytic CKD patients of all stages and a control group of 35 healthy subjects were included. Retinal neural and microvascular parameters were obtained by optical coherence tomography angiography (OCTA) examination.

**Results:** CKD 1–2 group (versus control group) had greater odds of having decreased retinal ganglion cell-inner plexiform layer thickness (GC-IPLt) (odds ratio [OR]: 0.92; 95% confidence interval [CI]: 0.86–0.98), increased ganglion cell complex-focal loss volume (GCC-FLV) (OR: 3.51; 95% CI: 1.27–9.67), and GCC-global loss volume (GCC-GLV) (OR: 2.48; 95% CI: 1.27–4.82). The presence of advanced stages of CKD (CKD 3–5 group versus CKD 1–2 group) had greater odds of having decreased retinal vessel density in superficial vascular plexus (SVP)-WholeImage (OR: 0.77, 95% CI: 0.63–0.92), SVP-ParaFovea (OR: 0.83, 95% CI: 0.71–0.97), SVP-ParaFovea (OR: 0.76, 95% CI: 0.63–0.91), deep vascular plexus (DVP)-WholeImage (OR: 0.89, 95% CI: 0.81–0.98), DVP-ParaFovea (OR: 0.88, 95% CI: 0.78–0.99), and DVP-PeriFovea (OR: 0.90, 95% CI: 0.83–0.98). Besides, stepwise multivariate linear regression among CKD patients showed that  $\beta$ 2-microglobulin was negatively associated with GC-IPLt ( $\beta$ : -0.294; 95% CI: -0.469 ~ -0.118), and parathyroid hormone was positively associated with increased GCC-FLV ( $\beta$ : 0.004; 95% CI: 0.002~0.006) and GCC-GLV ( $\beta$ : 0.007; 95% CI: 0.004~0.01). Urine protein to creatinine ratio was positively associated with

increased GCC-FLV ( $\beta$ : 0.003; 95% CI: 0.001~0.004) and GCC-GLV ( $\beta$ : 0.003; 95% CI: 0.001~0.006).

**Conclusion:** Retinal neuronal impairment is present in early stages of CKD (stages 1–2), and it is associated with accumulation of uremic toxins and higher UACR, while retinal microvascular hypoperfusion, which is associated with worse eGFR, was only observed in relatively advanced stages of CKD (stages 3–5). The results highlight the importance of monitoring retinal neurovascular impairment in different stages of CKD.

**Keywords:** retinal imaging, neuronal impairment, microvascular hypoperfusion, optical coherence tomography angiography (OCTA), chronic kidney disease

## INTRODUCTION

As an emerging public health issue, chronic kidney disease (CKD) is predicted to be the fifth most common cause of death worldwide by 2040 (Foreman et al., 2018). Uremia exposure, endocrine failure, and impaired vascular homeostasis result in widespread neural and microvascular injury (Futrakul et al., 2008). In general, neurovascular complications, especially those of the central nervous system (CNS), such as cognitive deterioration (Kurella et al., 2005), cerebrovascular stroke (Smogorzewski, 2001), and encephalopathy (Raskin and Fishman, 1976), are commonly and largely contribute to morbidity and mortality in CKD patients (Wanner et al., 2016). Therefore, there has been an urgent need for early identifying neurovascular impairment in CKD patients (Houben et al., 2017).

As an extension of the brain and sharing the same embryological origin with the CNS. Chua et al. (2020), Kashani et al. (2021), the retina is widely regarded as an accessible source for studying neurodegenerative and vascular injury processes occurring in the CNS (Hart et al., 2016; Mutlu et al., 2018). Consistently, there has also been intense interest in using retinal imaging technology to understand, diagnose, and monitor neurological diseases (Kashani et al., 2021). Recent advancements in optical coherence tomography angiography (OCTA) technologies have allowed for non-invasive and quantitative assessment of the neurovascular structure on different retinal layers (Pujari et al., 2020; Hormel et al., 2021). In some studies, OCTA has been used to monitor retinal neural and microvascular alterations in degenerative neural diseases such as Alzheimer's disease (O'bryhim et al., 2018; Den Haan et al., 2019) and Parkinson's disease (Kashani et al., 2021; Robbins et al., 2021).

Previous investigations have shown that both retinal neural impairment and microvascular hypoperfusion can be detected in CKD patients (stages 3–5) using OCTA (Vadala et al., 2019; Yeung et al., 2019; Zhuang et al., 2020). However, those studies failed to included CKD patients at the early stages (stages 1–2), so it still reminds unknown whether retinal neurovascular impairment occurs in earlier stages of CKD and what are the related factors for such damage. Furthermore, the inclusion of diabetes mellitus (DM) patients and dialysis population in prior studies challenge the direct comparison between CKD patients and normal subjects (Yeung et al., 2019; Wu et al., 2020), as both DM (Zeng et al., 2019; Zhuang et al., 2020) and dialysis (Wu

et al., 2020) can deteriorate neurovascular system independent of declining renal function.

Therefore, we conducted this cross-sectional study in CKD patients of all stages without a history of DM or dialysis, aiming to investigate the changes of retinal neurovascular parameters detected by OCTA in patients of different CKD stages and further analyze the association between neurovascular alterations and CKD-related risk factors.

## MATERIALS AND METHODS

### Design and Population of the Study

This cross-sectional study included a total of 150 eyes from 115 CKD patients and 35 healthy subjects. The study was conducted in the Department of Ophthalmology and the Department of Nephrology, Guangdong Provincial People's Hospital from August 2019 to December 2020. The procedures followed the ethical standards of the Research Ethics Committee of Guangdong Provincial People's Hospital [registration number: GDREC2020069(R1)] and the Helsinki Declaration. This study followed the Strengthening the Reporting of Observational Studies in Epidemiology (STROBE) reporting guideline. Informed consent was obtained from all participants.

The inclusion criteria were patients with CKD and aged  $\geq 18$  years. The definition of CKD was based on the presence of kidney damage (i.e., albuminuria or urinary albumin to creatinine ratio) or decreased kidney function [i.e., estimated glomerular filtration rate (eGFR)  $< 60$  ml/min/1.73 m<sup>2</sup> for 3 months or more] (Levey and Coresh, 2012). The eGFR value was calculated from serum creatinine (Scr) using the CKD-EPI creatinine equation (Levey et al., 2009). Severity of CKD was categorized based on the eGFR values: more than 90 ml/min/1.73 m<sup>2</sup> (stage 1), 60~89 ml/min/1.73 m<sup>2</sup> (stage 2), 30~59 ml/min/1.73 m<sup>2</sup> (stage 3), 15~29 ml/min/1.73 m<sup>2</sup> (stage 4), and less than 15 ml/min/1.73 m<sup>2</sup> (stage 5) (Levey and Coresh, 2012). The CKD 1–2 group were CKD patients in stages 1–2, and the CKD 3–5 group were CKD patients in stages 3–5. The control group was healthy subjects without major systemic diseases or ocular diseases.

The exclusion criteria were patients with (1) any type of DM; (2) HbA<sub>1c</sub>  $> 6.5\%$ ; (3) history of dialysis (hemodialysis or peritoneal dialysis); (4) any ocular issue that may impair ocular

circulation (e.g., glaucoma, eye trauma, retinal vascular occlusion, choroidal neovascularization, endophthalmitis, or refractive error  $> \pm 6$  diopters); (5) inadequate quality of OCTA image (quality score  $< 6$  or the presence of significant artifact); (6) any severe systemic diseases (e.g., cerebral infarction, myocardial infarction, heart failure, or connective tissue disorder); (7) women who were pregnant.

## Ophthalmic Examinations

All participants underwent comprehensive ophthalmic examinations including best-corrected visual acuity (BCVA) (measured on a decimal chart and presented as logMAR), autorefraction, intraocular pressure, slit-lamp examination, and color fundus photography. Retinal microvasculature and neural parameters were measured with Optical Coherence Tomography Angiography (OCTA).

Optical Coherence Tomography Angiography with RTVue-XR Avanti (Optovue, Fremont, CA, United States, version 2018) is a device combining structural and functional imaging by analyzing the changing variance in light speckle created by erythrocyte flow over multiple scans (Spaide et al., 2018). The OCTA machine generates a contract-free angiogram down to the capillary level and surrogate indices of perfusion. The OCTA platform has been integrated with split-spectrum amplitude-decorrelation angiography (SSADA) algorithm that automatically segments OCT images alongside angiographic data to report global and regional vessel density (VD) of each retinal layer (Hormel et al., 2021).

The detailed procedures of the OCTA examination were shown in **Supplementary Figure S1**. The OCTA examination was performed in a darkroom. Before examination, participants' pupils were dilated with Tropicamide Phenylephrine Eye Drops. An internal fixation light was used as the center the scanning area. The OCT signal position and quality were optimized using the Auto All function, aiming to find the best position, focus, and polarization match for obtaining the retina OCT image (Toto et al., 2016). Besides, considering that media opacity made an effect of on the measurement of retinal neurovascular parameters (Zhang et al., 2020, 2021), the OCTA system generated a signal strength index (SSI) to help determine whether the scan quality is acceptable. The signal strength intensity (SSI; ranged from 0 to 100) is based on the intensity or brightness of the reflected light during scanning. The higher the intensity, the higher the SSI.

Retinal vascular retinal layers were visualized as follows: a set of high definition (HD) Angio Retina Scan (6\*6mm) was captured to evaluate the VD of the macular, which contained superficial retinal plexus and deep retinal plexus. The boundaries of each layer were segmented as follows: a slab extending from 3 to 15  $\mu\text{m}$  from the internal limiting membrane (ILM) was generated to detect the superficial vascular plexus (SVP), and a slab extending from 15 to 70  $\mu\text{m}$  below ILM to detect the deep vascular plexus (DVP) (Zhuang et al., 2020). Besides, HD Angio Disk Scan (4.5\*4.5 mm) was imaged to visualize the radial peripapillary capillary, which was defined as the vessel on the layer between the outer limit of the retinal nerve fiber layer (RNFL) and ILM in the peripapillary region. The

segmentations of these three retinal vascular plexuses were shown in **Supplementary Figure S2** (Wu et al., 2020).

As for the retinal neural parameters, a ganglion cell complex (GCC) scan was used to measure retinal ganglion cell-inner plexiform layer thickness (GC-IPLt), which was defined as the layer between the retinal nerve fiber layer (RNFL) and IPL within a 6-mm circle. An optic nerve head (ONH) scan was obtained for the measurement of RNFL thickness (RNFLT). The average RNFLT was measured over a 3.45-mm-diameter circle centered on the ONH.

All the retinal VD and layer thickness retinal VD and layer thickness were calculated automatically and quantitatively using the AngioVue SSADA software (Peng et al., 2020; Wu et al., 2020). Both eyes of the participants were examined by OCTA, but only the data of the right eye was included for analysis. If the scan of the right eye was uninterpretable, data of the left eye were utilized. Only images with quality index  $\geq 6$  and SSI  $\geq 60$  were retained.

## Systemic Data Collection

Medical history and laboratory data in the last 3 months were collected. Demographic and blood test data were extracted from the electronic medical record system by a trained researcher (YF) and double-checked by an ophthalmologist (XZ). The basic information included age, sex, body mass index (BMI), systolic blood pressure (SBP), diastolic blood pressure (DBP), duration of CKD, and the history of smoking, hypertension, and cardiovascular disease (CVD). Laboratory tests included glycated hemoglobin (HbA<sub>1c</sub>), Scr, blood urea nitrogen (BUN), hemoglobin (HGB), cholesterol (CHOL), low-density lipoprotein (LDL), urine albumin to creatinine ratio (UACR), urine protein to creatinine ratio (UPCR), parathyroid hormone (PTH), albumin (ALB), and  $\beta 2$ -microglobulin ( $\beta 2$ -M).

## Statistical Analysis

SPSS version 25.0 (SPSS, Inc., Chicago, IL, United States) was used to perform statistical analyses. A two-sided  $p$ -value of less than 0.05 was considered significant. Mean and standard deviation (SD) were used for presenting quantitative variables for normal distribution, medians and interquartile range (IQR) for abnormal distribution, and numbers (percentages) were used for categorical variables. In the comparison of basic characteristics among three groups, one-way ANOVA was used for normally distributed continuous data and the Kruskal–Wallis  $H$  test was used for non-normally distributed continuous data, and Bonferroni's correction was used for *post hoc* analysis.  $\chi^2$  tests were utilized to compare categorical variables. Mann–Whitney test was applied to compare the duration of CKD between the CKD 1–2 group and the CKD 3–5 group. Crude logistic regression models were used to compare the OCTA parameters (dependent variables) between different groups (independent variables, 1<sup>a</sup>: CKD 1–2 versus control, 2<sup>a</sup>: CKD 1–2 versus CKD 3–5) without adjusting confounders. We also used adjusted logistic regression models (1<sup>b</sup>: CKD 1–2 versus control, 2<sup>b</sup>: CKD 3–5 versus CKD 1–2) to adjust the confounders, including age, sex, BMI, SBP, DBP, history of smoking, history of CVD, Hb1Ac, CHOL, and LDL. Partial correlation analysis was used

to determine risk factors associated with the OCTA parameters in the CKD patients after controlling for age, sex, BMI, history of smoking, history of CVD, RE, and IOP. Besides, stepwise multivariate regression was performed to figure out the independent risk factors for the retinal neurovascular alterations in the CKD patients. Age, sex, BMI, history of hypertension, history of smoking, history of CVD, eGFR, BUN, PTH, UACR, HGB, CKD duration, Hb1Ac,  $\beta$ 2-M, and LDL were independent variables entered into the model. Finally, Spearman correlation analysis was used to determine the relationship between BCVA and OCTA parameters in all subjects.

## RESULTS

### Basic Characteristics Among the Three Groups

The basic characteristics of the participants were summarized in **Table 1**. The etiology of the CKD patients was shown in **Supplementary Table S1**. There were significantly higher results of DBP, BUN, and HGB in the CKD 1–2 group compared to the control group (all  $p < 0.05$ ). The CKD 3–5 group showed significantly higher results of SBP, DBP, Hb1Ac, Scr, BUN, BCVA (logMAR), as well as decreased eGFR and HGB compared to the CKD 1–2 group and the control group (all  $p < 0.05$ ). Besides, the CKD 3–5 group also showed significantly higher results of age, BMI, PTH,  $\beta$ 2-M, history of hypertension, and CVD compared to the CKD 1–2 group (all  $p < 0.05$ ). No significant difference was found in sex, history of smoking, CHOL, SER, and IOP among the three groups. Duration of CKD, UACR, UPCr, and ALB and the etiology of CKD were comparable between the CKD 1–2 group and the CKD 3–5 group. Besides, the signal strength index of the macular, disk, GGG, and ONH areas and the overall quality index of the macular and disk areas are comparable among the three groups (**Supplementary Table S2**).

### Comparisons of Optical Coherence Tomography Angiography Parameters Among the Three Groups

Comparisons of OCTA parameters among the three groups were shown in **Table 2** and **Figure 1**. Significantly reduced GC-IPLt and increased GCC-FLV and GCC-GLV were detected in the CKD 1–2 group and the CKD 3–5 group compared to the control group (all  $p < 0.05$ ). Also, significantly reduced GCCt and increased GCC-GLV were found in the CKD 3–5 group compared to the CKD 1–2 group. A representative picture showing the changes in GC-IPLt, GCC-FLV, and GCC-GLV in CKD groups and control group was shown in **Supplementary Figure S3**. No significant difference was found in RNFL parameters among the three groups. For retinal microvascular parameters, significantly reduced VD in all SVP regions and DVP regions were found in the CKD 3–5 group compared to the CKD 1–2 group and control group (all  $p < 0.001$ ). No significant difference was found in all microvascular parameters between the CKD 1–2 group and the control group. No significant difference was found in VD in all RPC regions among the three groups.

### Independent Associations Between Optical Coherence Tomography Angiography Parameters and Severity of Chronic Kidney Disease

**Table 3** shows the results of logistic regression models investigating associations of OCTA parameters and the incidence and progression of CKD. After adjusting for confounders including age, sex, BMI, SBP, DBP, history of smoking, history of CVD, Hb1Ac, CHOL, and LDL, the model 1<sup>b</sup> showed that the presence of early stages of CKD (CKD1–2 group versus control group) was significantly associated with decreased GC-IPLt (odds ratio [OR]: 0.92; 95% confidence interval [CI]: 0.86–0.98), meaning one-micrometer increase of GC-IPLt is associated with 0.92-fold risk of CKD after adjusting for the confounding factors. Meanwhile, the presence of early stages of CKD (CKD1–2 group versus control group) was significantly associated with increased GCC-FLV (OR: 3.51; 95% CI: 1.27–9.67) and GCC-GLV (OR: 2.48; 95% CI: 1.27–4.82). Further investigation in the crude model 2<sup>b</sup> showed that the presence of advanced stages of CKD (CKD 3–5 group versus CKD 1–2 group) had greater odds of having decreased VD in SVP-WholeImage (OR: 0.77; 95% CI: 0.63–0.92), SVP-ParaFovea (OR: 0.83; 95% CI: 0.71–0.97), SVP-PeriFovea (OR: 0.76; 95% CI: 0.63–0.91), DVP-WholeImage (OR: 0.89; 95% CI: 0.81–0.98), DVP-ParaFovea (OR: 0.88; 95% CI: 0.78–0.99), DVP-PeriFovea (OR: 0.90; 95% CI: 0.83–0.98), and increased GCC-GLV (OR: 1.35; 95% CI: 1.05–1.73).

### Partial Correlation Between Optical Coherence Tomography Angiography Parameters and Chronic Kidney Disease-Related Parameters

The results of partial correlation analyses of OCTA parameters and CKD-related parameters among all 115 CKD patients were shown in **Table 4**. The results showed that all retinal microvascular parameters as well as GC-IPLt were positively correlated with eGFR and HGB ( $r = 0.199 \sim 0.355$ , all  $p < 0.05$ ) and negatively with  $\beta$ 2-M, BUN, and PTH ( $r = -0.185 \sim -0.354$ , all  $p < 0.05$ ). Furthermore, GCC-FLV and GCC-GLV were positively correlated with  $\beta$ 2-M, BUN, UPCr, UACr, and PTH ( $r = 0.193 \sim 0.344$ , all  $p < 0.05$ ) and negatively with eGFR ( $r = -0.200 \sim -0.276$ , all  $p < 0.05$ ). Partial correlation of GCC variables and eGFR were shown in **Supplementary Figure S4**.

### Stepwise Multivariate Linear Regression Between Optical Coherence Tomography Angiography Parameters and Chronic Kidney Disease-Related Parameters

The result of stepwise multivariate linear regression between OCTA parameters and clinical data among all 115 CKD patients was presented in **Table 5**.  $\beta$ 2-M was associated with thinner GC-IPLt ( $\beta$ : -0.294; 95% CI: -0.469~ -0.118), where PTH was associated with higher GCC-FLV ( $\beta$ : 0.004; 95% CI: 0.002~0.006) and GCC-GLV ( $\beta$ : 0.007; 95% CI: 0.004~0.01) among CKD

**TABLE 1** | Comparison of basic characteristics among the three groups.

	Control (n = 35)	CKD 1–2 (n = 50)	CKD 3–5 (n = 65)	p	p <sup>a</sup>	p <sup>b</sup>	p <sup>c</sup>
<b>Basic characteristics</b>							
Age, year	45.06 ± 11.28	40.24 ± 13.40	47.58 ± 12.76	<b>0.010<sup>δ</sup></b>	0.259	1.000	<b>0.007</b>
Sex, male, n (%)	15 (42.90)	20 (40.00)	38 (58.50)	0.107 <sup>†</sup>	–	–	–
BMI, kg/m <sup>2</sup>	22.18 ± 2.11	22.36 ± 3.65	23.88 ± 3.09	<b>0.009<sup>δ</sup></b>	0.989	0.059	<b>0.005</b>
SBP, mmHg	118 ± 11.43	124.32 ± 13.12	141.98 ± 21.3	<b>&lt;0.001<sup>δ</sup></b>	0.061	<b>&lt;0.001</b>	<b>&lt;0.001</b>
DBP, mmHg	73 ± 6.06	80.02 ± 11.27	85.88 ± 12.89	<b>&lt;0.001<sup>δ</sup></b>	<b>0.001</b>	<b>&lt;0.001</b>	<b>0.032</b>
History of smoking, n (%)	4 (11.40)	6 (12.00)	11 (16.90)	0.664 <sup>†</sup>	–	–	–
History of hypertensive, n (%)	–	10 (20.00)	46 (70.80)	<b>&lt;0.001<sup>†</sup></b>	–	–	–
History of CVD, n (%)	–	2 (4.00)	12 (18.50)	<b>0.019<sup>†</sup></b>	–	–	–
Duration of CKD, month	–	12 (16.25)	12 (27.00)	0.132 <sup>‡</sup>	–	–	–
<b>Laboratory test</b>							
Scr, μmol/L	70.36 ± 14.61	73.2 ± 22.69	358.44 ± 316.13	<b>&lt;0.001<sup>δ</sup></b>	0.862	<b>&lt;0.001</b>	<b>&lt;0.001</b>
eGFR, ml/min/1.73 m <sup>2</sup>	100.7 ± 20.88	99.02 ± 25.25	27.26 ± 17.60	<b>&lt;0.001<sup>δ</sup></b>	0.976	<b>&lt;0.001</b>	<b>&lt;0.001</b>
BUN, mmol/L	5.29 (2.15)	5.78 (2.55)	11.82 (11.09)	<b>&lt;0.001<sup>ε</sup></b>	<b>0.005</b>	<b>&lt;0.001</b>	<b>&lt;0.001</b>
HbA1c, (%)	5.18 ± 0.41	5.36 ± 0.53	5.60 ± 0.48	<b>&lt;0.001<sup>δ</sup></b>	0.281	<b>&lt;0.001</b>	<b>0.020</b>
HGB, 10 <sup>9</sup> /L	137.33 ± 15.10	124.66 ± 19.74	104.94 ± 23.65	<b>&lt;0.001<sup>δ</sup></b>	<b>0.004</b>	<b>&lt;0.001</b>	<b>&lt;0.001</b>
CHOL, mmol/L	4.89 ± 0.68	5.71 ± 2.60	5.59 ± 1.83	0.133 <sup>δ</sup>	0.174	0.270	1.000
LDL, mmol/L	3.10 ± 0.85	3.72 ± 1.75	3.86 ± 1.27	<b>0.030<sup>δ</sup></b>	0.124	<b>0.029</b>	1.000
UACR, mg/g	–	794.20 (1414.13)	1274.06 (1966.94)	0.163 <sup>‡</sup>	–	–	–
UPCR, mg/g	–	1150.50 (2499.47)	2249.44 (2856.25)	0.052 <sup>‡</sup>	–	–	–
PTH, pg/ml	–	35.38(12.93)	92.78(113.20)	<b>&lt;0.001<sup>‡</sup></b>	–	–	–
ALB, g/L	–	35.21(11.50)	37.02(12.88)	0.197 <sup>‡</sup>	–	–	–
β2-M, μg/ml	–	2.30(1.39)	8.85(10.79)	<b>&lt;0.001<sup>‡</sup></b>	–	–	–
<b>Ocular characteristics</b>							
BCVA, LogMAR	−0.0146 ± 0.0671	−0.0087 ± 0.0841	0.0283 ± 0.1208	<b>&lt;0.001<sup>δ</sup></b>	0.997	<b>&lt;0.001</b>	<b>&lt;0.001</b>
RE, diopters	−0.99 ± 2.18	−1.27 ± 3.58	−0.55 ± 2.28	0.371 <sup>δ</sup>	1.000	1.000	0.496
IOP, mmHg	14.15 ± 2.20	14.16 ± 3.83	13.31 ± 3.30	0.291 <sup>δ</sup>	1.000	0.655	0.505

CKD, chronic kidney disease; BMI, body mass index; SBP, systolic blood pressure; DBP, diastolic blood pressure; CVD, cardiovascular disease; Scr, serum creatinine; eGFR, estimated glomerular filtration rate; BUN, blood urea nitrogen; HbA1c, glycated hemoglobin; HGB, hemoglobin; CHOL, cholesterol; LDL, low-density lipoprotein; UACR, urine albumin to creatinine ratio; UPCR, urine protein to creatinine ratio; PTH, parathyroid hormone; ALB, albumin; β2-M, β2-microglobulin; BCVA, best-corrected visual acuity; RE, refraction error; IOP, intraocular pressure.

Results are presented as mean ± standard deviation, medians (IQR), or as numbers (percentages).

A, p (One-Way ANOVA and  $\chi^2$  Kruskal–Wallis H test) for the comparison among three groups. p ( $\chi^2$  test and  $\pm$  Mann–Whitney Test) for the comparison between the CKD 1–2 group and the CKD 3–5 group.

B, p<sup>a</sup> for the comparison between the control group and the CKD 1–2 group using post hoc analysis.

C, p<sup>b</sup> for the comparison between the control group and the CKD 3–5 group using post hoc analysis.

D, p<sup>c</sup> for the comparison between the CKD 1–2 group and the CKD 3–5 group using post hoc analysis.

The bold values indicated statistically significant (p value < 0.05).

patients. UACR was also found associated with higher GCC-FLV ( $\beta$ : 0.003; 95% CI: 0.001~0.004) and GCC-GLV ( $\beta$ : 0.003; 95% CI: 0.001~0.006). Besides, the results showed that the eGFR was positively associated with VD in SVP-WholeImage ( $\beta$ : 0.029; 95% CI: 0.017~0.041), SVP-ParaFovea ( $\beta$ : 0.021; 95% CI: 0.002~0.040), SVP-PeriFovea ( $\beta$ : 0.029; 95% CI: 0.016~0.041), DVP-WholeImage ( $\beta$ : 0.033; 95% CI: 0.007~0.058), DVP-ParaFovea ( $\beta$ : 0.044; 95% CI: 0.024~0.065), and DVP-PeriFovea ( $\beta$ : 0.037; 95% CI: 0.008~0.066).

## Correlation Between Best-Corrected Visual Acuity and Optical Coherence Tomography Angiography Parameters

The results of correlation analyses of BCVA and OCTA parameters among all subjects were shown in Table 6. BCVA

(LogMAR) was negatively correlated with VD in SVP and DVP ( $r = -0.399 \sim -0.514$ , all  $p < 0.05$ ), while positively with GCC-GLV ( $r = 0.201$ ,  $p = 0.014$ ).

## DISCUSSION

Two crucial findings were observed in this cross-sectional study. Firstly, our study revealed that retinal ganglion cell complex impairment occurs in the early stages (CKD stages 1–2) without detectable retinal microvascular rarefaction and RNFL damage in non-diabetic and non-dialytic CKD patients. Secondly, among CKD patients, the accumulation of uremic toxins of β2-M and PTH, and higher UACR was independently associated with retinal ganglion cell complex impairment, while reduced eGFR was associated with deceased retinal microvascular perfusion.

**TABLE 2 |** Comparison of OCTA parameters among the three groups.

	Control (n = 35)	CKD 1–2 (n = 50)	CKD 3–5 (n = 65)	p	p <sup>a</sup>	p <sup>b</sup>	p <sup>c</sup>
<b>Retinal microvascular parameters</b>							
SVP-WholeImage, %	52.22 ± 1.98	52.06 ± 2.44	49.53 ± 2.92	<b>&lt;0.001</b>	1.000	<b>&lt;0.001</b>	<b>&lt;0.001</b>
SVP-ParaFovea, %	54.90 ± 1.95	54.46 ± 2.81	51.28 ± 4.19	<b>&lt;0.001</b>	1.000	<b>&lt;0.001</b>	<b>&lt;0.001</b>
SVP-PeriFovea, %	53.15 ± 2.00	53.01 ± 2.44	50.43 ± 2.94	<b>&lt;0.001</b>	1.000	<b>&lt;0.001</b>	<b>&lt;0.001</b>
DVP-WholeImage, %	55.12 ± 4.30	54.60 ± 5.15	50.15 ± 5.36	<b>&lt;0.001</b>	1.000	<b>&lt;0.001</b>	<b>&lt;0.001</b>
DVP-ParaFovea, %	57.83 ± 2.98	57.51 ± 4.09	53.35 ± 4.76	<b>&lt;0.001</b>	1.000	<b>&lt;0.001</b>	<b>&lt;0.001</b>
DVP-PeriFovea, %	56.77 ± 4.62	56.28 ± 5.69	51.13 ± 6.03	<b>&lt;0.001</b>	1.000	<b>&lt;0.001</b>	<b>&lt;0.001</b>
RPC-WholeImage, %	57.28 ± 1.85	57.53 ± 2.40	56.44 ± 3.70	0.124	1.000	0.538	0.156
RPC-WholeImage-Capillary, %	50.28 ± 1.85	50.64 ± 2.36	50.19 ± 3.50	0.686	1.000	1.000	1.000
<b>Retinal neural parameters</b>							
RNFLt-Average, $\mu\text{m}$	108.63 ± 8.04	108.28 ± 8.26	106.74 ± 9.65	0.506	1.000	0.929	1.000
RNFLt-Superior, $\mu\text{m}$	112.06 ± 8.45	111.25 ± 9.62	108.36 ± 12.7	0.188	1.000	0.317	0.473
RNFLt-Inferior, $\mu\text{m}$	106.80 ± 8.35	105.24 ± 8.07	102.45 ± 11.25	0.143	1.000	0.099	0.378
GC-IPLt, $\mu\text{m}$	105.60 ± 8.77	100.98 ± 7.79	97.27 ± 7.89	<b>0.004</b>	<b>0.042</b>	<b>&lt;0.001</b>	<b>0.040</b>
GCC-FLV, %	0.78 ± 0.44	1.34 ± 1.19	1.94 ± 2.26	<b>&lt;0.001</b>	<b>0.009</b>	<b>&lt;0.001</b>	0.204
GCC-GLV, %	1.14 ± 0.98	1.98 ± 1.29	3.32 ± 3.09	<b>&lt;0.001</b>	<b>0.003</b>	<b>&lt;0.001</b>	<b>0.007</b>

OCTA, optical coherence tomography angiography; CKD, chronic kidney disease; SVP, superficial vascular plexus; DVP, deep vascular plexus; RPC, retinal peripapillary capillary; RNFLT, retinal nerve fiber layer thickness; GC-IPLt, ganglion cell-inner plexiform layer thickness; GCC, ganglion cell complex; GLV, global loss volume; FLV, focal loss volume.

A, p for the comparison among the three groups using One-Way ANOVA.

B, p<sup>a</sup> for the comparison between the control group and the CKD 1~2 group using post hoc analysis.

C, p<sup>b</sup> for the comparison between the control group and the CKD 3~5 group using post hoc analysis.

D, p<sup>c</sup> for the comparison between the CKD 1~2 group and the CKD 3~5 group using post hoc analysis.

The bold values indicated statistically significant (p value < 0.05).

The major finding of this study is that increased GCC-FLV and GCC-GLV, and thinner GC-IPL could be detected in earlier CKD stages (stages 1–2), while no significant difference was found in all retinal microvascular parameters and RNFLT in the CKD 1–2 group compared to the control group, suggesting that retinal neuronal impairment has already existed in early CKD stages even in the absence of histologically assessed microvascular rarefaction and retinal axon damage. In fact, neurological complications, such as cognitive deterioration, cerebrovascular stroke, and cranial neuropathy, are common in CKD patients (Hamed, 2019). Recent population-based studies have documented an association between early stages of CKD and impaired cognition (Elias et al., 2009; Tsai et al., 2010). Given that the GC-IPL layer is where the retinal ganglion cell bodies are located, we postulated that it could serve as a window to observe CKD-related neuronal cell body loss in the CNS, particularly in the early stages of CKD. A recent population-based study consisting of 4464 non-glaucoma, multi-ethnic Asian participants showed that the presence of CKD is significantly associated with thinner GC-IPL (Tham et al., 2020). Furthermore, a prior study (Wu et al., 2020) also confirmed that macular thinning (GC-IPL and RNFLT) is a characteristic of retinal neural impairment in patients with CKD and such impairment is strongly associated with decreased eGFR. However, the definition of CKD applied in the aforementioned studies was based on an eGFR of <60 ml/min/1.73 m<sup>2</sup> (CKD stages 3–5) and failed to include earlier stages CKD patients with an eGFR of > 60 ml/min/1.73 m<sup>2</sup> (namely, CKD stages 1–2) using parameters such as proteinuria or UACR to detect early renal damage and declining renal function. Our study evaluated retinal

neural parameters in non-diabetic CKD patients of stages 1–2 (versus health subjects) and revealed that retinal neuronal impairment, which might even precede microvascular rarefaction and retinal axon damage, could be detected in earlier CKD stages than those reported in prior studies (Jung et al., 2020; Wu et al., 2020).

On the other hand, significantly decreased RNFLT was observed in CKD patients according to previous studies (Demir et al., 2009; Jung et al., 2020; Wu et al., 2020). However, our study failed to detect significantly decreased RNFLT in either the CKD 1–2 group or the CKD 3–5 group compared to the control group. Two possible reasons may suffice to explain this conflicting result: firstly, significant reduced RNFLT were detected in end-stage renal disease patients which have been treated with dialysis in previous studies (Demir et al., 2009; Jung et al., 2020). But in our study, patients undergoing dialysis were excluded because dialysis itself might exert a significant impact on the neurovascular system. Thus, our results suggested that RNFL thickness is not reduced in non-dialysis CKD patients. Second, exclusion of DM patients may also play an important role. A previous study (Wu et al., 2020) reported significantly reduced RNFLT in CKD patients in stages 3–5. However, diabetic patients accounted for 42% of the CKD group in their study. It is reported that RNFLT could be significantly reduced even in preclinical DR stages (Zeng et al., 2019), suggesting that RNFL is highly susceptible to hyperglycemic injury. Diabetic patients were excluded from our study to avoid its strong impact on retinal neurovascular structures. Taken together, it could be speculated that RNFL damage

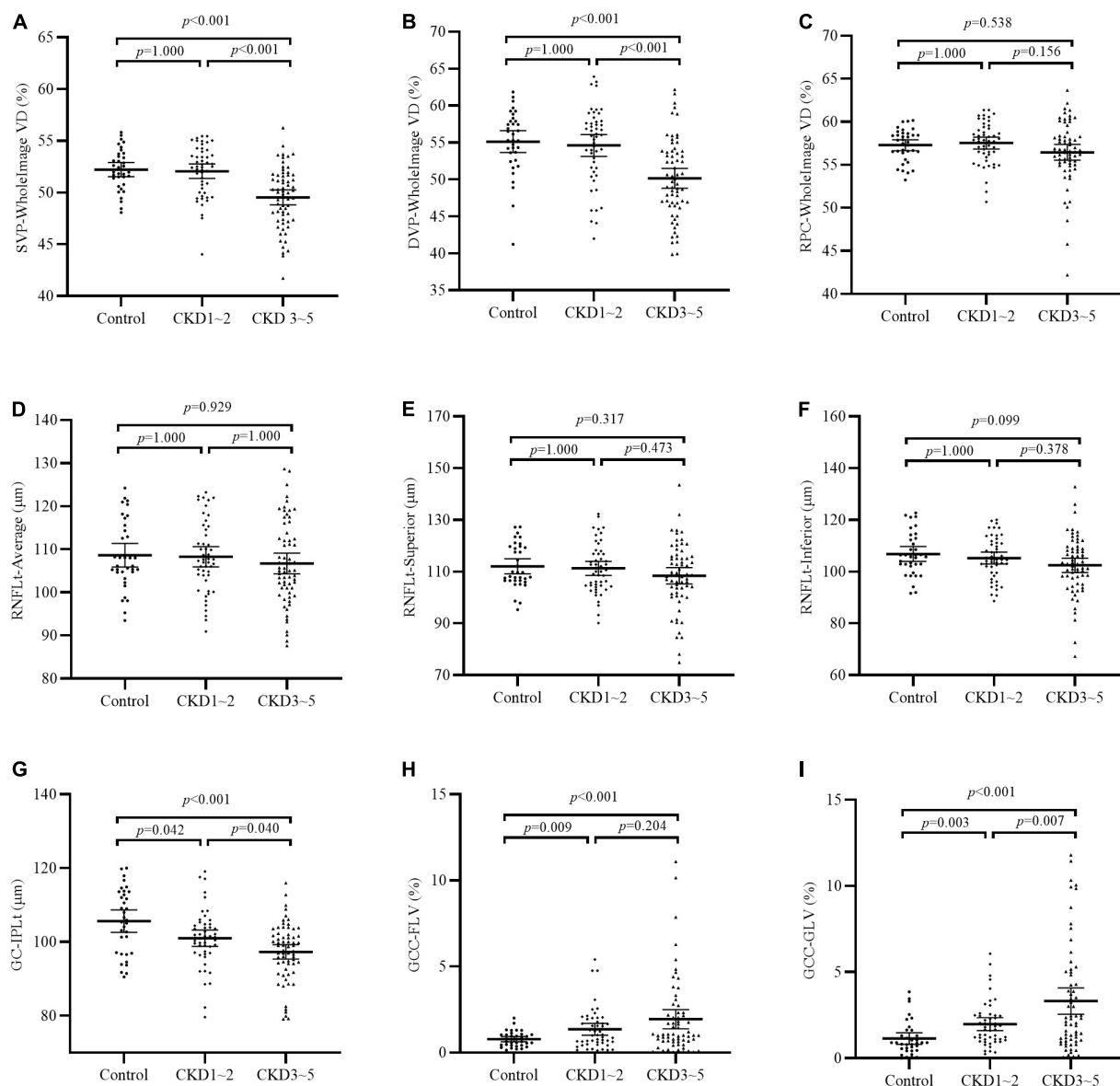


**FIGURE 1 |** Comparison of OCTA parameters among the three groups. (A–C) VD of SVP-WholeImage, DVP-WholeImage, and RPC-WholeImage among three groups; (D–F) Thickness of RNFLT-Average, RNFLT-superior, and RNFLT-inferior among three groups; (G) Thickness of GC-IPLt among three groups; (H) Focal loss volume of GCC among three groups; (I) Global loss volume of GCC among three groups. CKD, chronic kidney disease; VD, vessel density; SVP, superficial vascular plexus; DVP, deep vascular plexus; RPC, retinal peripapillary capillary; RNFLT, retinal nerve fiber layer thickness; GC-IPLt, ganglion cell-inner plexiform layer thickness; GCC, ganglion cell complex; GLV, global loss volume; FLV, focal loss volume.

might not be present in non-diabetic and non-dialytic CKD patients. With the progression of CKD, the RNFLT might reduce independently or secondary to GCC loss and retinal capillary rarefaction.

Stepwise multivariate linear regression was used to figure out independent risk factors associated with neurovascular alterations in the CKD patients of our study. It was shown that higher  $\beta 2$ -M was associated with thinner GG-IPLt, and excessive PTH was associated with increased GCC-FLV and GCC-GLV, indicating the underlying pathophysiology of

retinal neurodegeneration in CKD patients was related to the neurotoxic effects exerted by uremic toxins. In fact, as CKD progresses, there is the accumulation of organic toxic products which is considered highly associated with the incidence and progression of neurological complications (Hamed, 2019). Our results showed that GC-IPLt was independently associated with  $\beta 2$ -M, after adjusting other confounding factors. The plasmatic level of  $\beta 2$ -M increases as the kidney function gets impaired. The present study found that neuronal cell impairment in the retina

**TABLE 3 |** Association between OCTA parameters and severity of CKD.

	Model 1 (CKD 1–2 group vs. control group)				Model 2 (CKD 1–2 group vs. CKD 3–5 group)			
	Crude model 1 <sup>a</sup>		Model 1 <sup>b</sup>		Crude model 2 <sup>a</sup>		Model 2 <sup>b</sup>	
	OR (95% CI)	p	OR (95% CI)	p	OR (95% CI)	p	OR (95% CI)	p
SVP-WholeImage	0.97 (0.80–1.18)	0.742	0.97 (0.77–1.23)	0.788	0.70 (0.59–0.83)	<b>&lt;0.001</b>	0.77 (0.63–0.92)	<b>0.005</b>
SVP-ParaFovea	0.93 (0.77–1.11)	0.418	0.93 (0.73–1.17)	0.526	0.75 (0.65–0.87)	<b>&lt;0.001</b>	0.83 (0.71–0.97)	<b>0.022</b>
SVP-PeriFovea	0.97 (0.80–1.18)	0.777	0.94 (0.75–1.19)	0.632	0.70 (0.59–0.83)	<b>&lt;0.001</b>	0.76 (0.63–0.91)	<b>0.003</b>
DVP-WholeImage	0.98 (0.89–1.07)	0.621	0.98 (0.87–1.11)	0.758	0.85 (0.73–0.89)	<b>&lt;0.001</b>	0.89 (0.81–0.98)	<b>0.019</b>
DVP-ParaFovea	0.98 (0.87–1.10)	0.688	0.98 (0.82–1.18)	0.865	0.81 (0.77–0.93)	<b>&lt;0.001</b>	0.88 (0.78–0.99)	<b>0.037</b>
DVP-PeriFovea	0.98 (0.90–1.07)	0.669	0.99 (0.89–1.11)	0.856	0.86 (0.80–0.93)	<b>&lt;0.001</b>	0.90 (0.83–0.98)	<b>0.017</b>
RPC-WholeImage	1.05 (0.86–1.29)	0.599	1.01 (0.79–1.31)	0.908	0.89 (0.78–1.01)	0.080	0.95 (0.81–1.12)	0.519
RPC-WholeImage-Capillary	1.08 (0.88–1.33)	0.439	1.02 (0.78–1.33)	0.876	0.95 (0.84–1.08)	0.435	0.97 (0.82–1.15)	0.736
RNFLt-Average	0.99 (0.94–1.05)	0.845	0.95 (0.89–1.02)	0.189	0.98 (0.94–1.02)	0.366	0.98 (0.93–1.03)	0.432
RNFLt-Superior	0.99 (0.94–1.04)	0.687	0.96 (0.90–1.02)	0.186	0.98 (0.95–1.01)	0.183	0.97 (0.93–1.01)	0.172
RNFLt-Inferior	0.98 (0.93–1.03)	0.385	0.94 (0.88–1.02)	0.122	0.98 (0.94–1.01)	0.223	0.98 (0.94–1.02)	0.360
GC-IPLt	0.92 (0.88–0.99)	<b>0.016</b>	0.92 (0.86–0.98)	<b>0.015</b>	0.94 (0.89–0.99)	<b>0.017</b>	0.94 (0.88–1.00)	0.061
GCC-FLV	2.43 (1.19–4.97)	<b>0.015</b>	3.51 (1.27–9.67)	<b>0.015</b>	1.22 (0.96–1.54)	0.109	1.21 (0.91–1.60)	0.185
GCC-GLV	2.07 (1.26–3.42)	<b>0.004</b>	2.48 (1.27–4.82)	<b>0.007</b>	1.30 (1.07–1.58)	<b>0.009</b>	1.35 (1.05–1.73)	<b>0.018</b>

OCTA, optical coherence tomography angiography; CKD, chronic kidney disease; OR, odds ratio; CI, confidence interval; SVP, superficial vascular plexus; DVP, deep vascular plexus; RPC, retinal peripapillary capillary; RNFLT, retinal nerve fiber layer thickness; GC-IPLt, ganglion cell-inner plexiform layer thickness; GCC, ganglion cell complex; GLV, global loss volume; FLV, focal loss volume.

Model 1: Binary logistics regression model with enter method in the control group and the CKD 1~2 group.

Model 2: Binary logistics regression model with enter method in the CKD 1~2 group and the CKD 3~5 group.

Model 1<sup>b</sup> and Model 2<sup>b</sup> were adjusted for age, sex, body mass index, systolic blood pressure, diastolic blood pressure, history of smoking, history of cardiovascular disease, glycated hemoglobin, cholesterol, and low-density lipoprotein.

The bold values indicated statistically significant (*p* value < 0.05).

**TABLE 4 |** Partial correlation between OCTA parameters and CKD-related data (115 CKD patients).

	eGFR	β2-M	BUN	UPCR	UACR	PTH	HGB
SVP-WholeImage	<b>(0.283, 0.003)</b>	<b>(−0.222, 0.022)</b>	<b>(−0.325, 0.001)</b>	(−0.066, 0.504)	(−0.058, 0.557)	<b>(−0.349, &lt;0.001)</b>	<b>(0.212, 0.029)</b>
SVP-ParaFovea	<b>(0.322, 0.001)</b>	<b>(−0.188, 0.046)</b>	<b>(−0.354, &lt;0.001)</b>	(−0.014, 0.885)	(0.008, 0.935)	<b>(−0.271, 0.005)</b>	<b>(0.206, 0.034)</b>
SVP-PeriFovea	<b>(0.314, 0.001)</b>	<b>(−0.196, 0.044)</b>	<b>(−0.348, &lt;0.001)</b>	(−0.055, 0.577)	(−0.035, 0.719)	<b>(−0.252, 0.009)</b>	<b>(0.199, 0.04)</b>
DVP-WholeImage	<b>(0.294, 0.002)</b>	<b>(−0.222, 0.022)</b>	<b>(−0.189, 0.041)</b>	(−0.002, 0.984)	(0.027, 0.787)	<b>(−0.185, 0.049)</b>	<b>(0.295, 0.002)</b>
DVP-ParaFovea	<b>(0.355, &lt;0.001)</b>	<b>(−0.275, 0.004)</b>	<b>(−0.280, 0.004)</b>	(−0.025, 0.795)	(0.004, 0.965)	<b>(−0.267, 0.006)</b>	<b>(0.283, 0.003)</b>
DVP-PeriFovea	<b>(0.297, 0.002)</b>	<b>(−0.233, 0.016)</b>	<b>(−0.191, 0.050)</b>	(−0.005, 0.956)	(0.019, 0.846)	<b>(−0.200, 0.04)</b>	<b>(0.295, 0.002)</b>
GCI-IPLt	<b>(0.222, 0.022)</b>	<b>(−0.314, 0.001)</b>	<b>(−0.285, 0.003)</b>	(0.016, 0.869)	(0.037, 0.708)	<b>(−0.221, 0.023)</b>	<b>(0.249, 0.01)</b>
GCC-FLV	<b>(−0.200, 0.040)</b>	<b>(0.252, 0.009)</b>	<b>(0.214, 0.027)</b>	<b>(0.264, 0.006)</b>	<b>(0.255, 0.008)</b>	<b>(0.254, 0.009)</b>	(−0.119, 0.226)
GCC-GLV	<b>(−0.276, 0.004)</b>	<b>(0.344, &lt;0.001)</b>	<b>(0.262, 0.007)</b>	<b>(0.232, 0.017)</b>	<b>(0.193, 0.047)</b>	<b>(0.319, 0.001)</b>	(−0.181, 0.063)

OCTA, optical coherence tomography angiography; CKD, chronic kidney disease; eGFR, estimated glomerular filtration rate; β2-M, β2-microglobulin; BUN, blood urea nitrogen; UACR, urine albumin to creatinine ratio; UPCR, urine protein to creatinine ratio; PTH, parathyroid hormone; HGB, hemoglobin; SVP, superficial vascular plexus; DVP, deep vascular plexus; GC-IPLt, ganglion cell-inner plexiform layer thickness; GCC, ganglion cell complex; GLV, global loss volume; FLV, focal loss volume.

Partial correlation adjusted for age, sex, body mass index, history of smoking, history of cardiovascular disease, refraction error, and intraocular pressure.

The bold values indicated statistically significant (*p* value < 0.05).

was associated with the β2-M, which is supported by a previous study confirming the cytotoxic activity of β2-M on neuronal cell lines (Giorgetti et al., 2009). Excessive PTH can increase the influx of calcium into the brain which interferes with neurotransmission in the CNS and induces neurotoxicity (Cogan et al., 1978); therefore, it is considered to be neurotoxic and associated with cognitive dysfunction in CKD patients (Craver et al., 2007). Therefore, it is possible that GCC loss could be used as a biomarker to indicate or even predict CNS neuronal loss in CKD patients.

Another interesting finding is that higher UACR was independently associated with increased GCC-FLV and GCC-GLV. Previous studies have documented that albuminuria was independently associated with POAG (Kim et al., 2016), an ocular disease characterized by loss of the retinal ganglion cells in the retina (Shin et al., 2018), suggesting that albuminuria might be associated with retinal ganglion cell loss. In this regard, albuminuria (as indicated by higher UACR) might be a potential biomarker suggestive of neuronal damage in the retina. However, no association was found between UACR and decreased VD in SVP and

**TABLE 5 |** Stepwise multivariate linear regression between OCTA parameters and CKD-related parameters (115 CKD patients).

	eGFR		$\beta$ 2-M		UACR		PTH	
	$\beta$ and 95% CI	<i>p</i>	$\beta$ and 95% CI	<i>p</i>	$\beta$ and 95% CI	<i>p</i>	$\beta$ and 95% CI	<i>p</i>
SVP-WholeImage	0.029 (0.017~0.041)	<b>&lt;0.001</b>	—	—	—	—	—	—
SVP-ParaFovea	0.021 (0.002~0.040)	<b>0.032</b>	—	—	—	—	—	—
SVP-PeriFovea	0.029 (0.016~0.041)	<b>&lt;0.001</b>	—	—	—	—	—	—
DVP-WholeImage	0.033 (0.007~0.058)	<b>0.014</b>	—	—	—	—	—	—
DVP-ParaFovea	0.044 (0.024~0.065)	<b>&lt;0.001</b>	—	—	—	—	—	—
DVP-PeriFovea	0.037 (0.008~0.066)	<b>0.013</b>	—	—	—	—	—	—
GC-IPLt	—	—	-0.294 (-0.469~-0.118)	<b>0.001</b>	—	—	—	—
GCC-FLV	—	—	—	—	0.003 (0.001~0.004)	<b>0.006</b>	0.004 (0.002~0.006)	<b>0.001</b>
GCC-GLV	—	—	—	—	0.003 (0.001~0.006)	<b>0.012</b>	0.007 (0.004~0.010)	<b>&lt;0.001</b>

OCTA, optical coherence tomography angiography; CKD, chronic kidney disease; eGFR, estimated glomerular filtration rate;  $\beta$ 2-M,  $\beta$ 2-microglobulin; UACR, urine albumin to creatinine ratio; PTH, parathyroid hormone; CI, confidence interval; SVP, superficial vascular plexus; DVP, deep vascular plexus; GC-IPLt, ganglion cell-inner plexiform layer thickness; GCC, ganglion cell complex; FLV, focal loss volume; GLV, global loss volume.

Sex, age, BMI, history of hypertension, history of smoking, history of cardiovascular disease, eGFR, PTH, UACR, HGB, CKD duration, Hb1Ac,  $\beta$ 2-M, and LDL were independent variables entered into the model.

The bold values indicated statistically significant (*p* value < 0.05).

**TABLE 6 |** Correlations of retinal neurovascular parameters and BCVA (LogMAR).

Microvascular parameters	BCVA (LogMAR)		Neural parameters	BCVA (LogMAR)	
	<i>r</i>	<i>P</i>		<i>r</i>	<i>p</i>
SVP-WholeImage	-0.406	<b>&lt;0.001</b>	GC-IPLt	-0.07	0.395
SVP-ParaFovea	-0.422	<b>&lt;0.001</b>	GCC-FLV	0.114	0.166
SVP-PeriFovea	-0.399	<b>&lt;0.001</b>	GCC-GLV	0.201	<b>0.014</b>
DVP-WholeImage	-0.488	<b>&lt;0.001</b>	RNFLt-Average	-0.14	0.089
DVP-ParaFovea	-0.514	<b>&lt;0.001</b>	RNFLt-Superior	-0.117	0.155
DVP-PeriFovea	-0.418	<b>&lt;0.001</b>	RNFLt-Inferior	-0.072	0.384
RPC-WholeImage	-0.118	0.151			
RPC-WholeImage-Capillary	-0.008	0.919			

BCVA, best-corrected visual acuity; SVP, superficial vascular plexus; DVP, deep vascular plexus; RPC, retinal peripapillary capillary; RNFLT, retinal nerve fiber layer thickness; GC-IPLt, ganglion cell-inner plexiform layer thickness; GCC, ganglion cell complex; GLV, global loss volume; FLV, focal loss volume.

The bold values indicated statistically significant (*p* value < 0.05).

DVP regions in CKD patients. In fact, the associations between albuminuria and retinal VD are controversial. A prior study reported that higher UACR was inversely related to SCP VD in non-diabetic hypertensive CKD patients (Vadala et al., 2019), while another research (Zhuang et al., 2020) showed that increased UACR was not associated with the VD in both SVP and DVP regions. Future studies are required to confirm the association between albuminuria and retinal VD alterations.

In addition, we also found that retinal VD decrease was detected in more advanced CKD stages (stages 3–5) and was associated with declined eGFR. This is consistent with the fact that microangiopathy and cardiovascular complications of CKD are also more prevalent in these patients (Houben et al., 2017). Thus, the retinal VD could serve as a biomarker to monitor the condition of systemic microvasculature in CKD patients and alert the risks of cardiovascular complications (Farrah et al., 2020). In fact, as the eGFR declining, the combination of uremia exposure (Zoccali et al., 2017), renal anemia (Chen et al., 2019), and impaired endothelial dysfunction compromise the

structure and function of the systemic microcirculation (Ooi et al., 2011), which is considered a crucial pathway in the development and progression of cardiovascular complications of CKD (Houben et al., 2017). Our study also suggests that non-invasive imaging of the retinal vessels may reflect these systemic microvascular alterations, providing valuable information for identifying patients at risk of developing CKD-related cardiovascular complications.

There are two major implications of our findings. Firstly, strict control of uremia and close monitoring of neuronal impairment should be started in CKD patients at early stages (eGFR of > 60 ml/min/1.73m<sup>2</sup>), and parameters of the retinal ganglion cell complex layer can be used as indicators of early neuronal damage in these patients. Secondly, once retinal neuronal damage (such as GCC loss) is detected, the eGFR should be closely monitored to reduce CKD-related microangiopathy and other adverse cardiovascular complications.

There are two main strengths of our study. Firstly, by including patients with stages 1–2 CKD without diabetes and dialysis history, we were able to detect retinal neuronal

impairment in early stages of CKD. Secondly, we also determine systemic risk factors associated with retinal neuronal damage and retinal capillary rarefaction in CKD patients. However, there are limitations in our study. Firstly, the cross-sectional design of our study prevented determining temporality and causal association between retinal neuronal impairment and microvascular hypoperfusion in CKD patients at different stages. The temporal sequence of the reported associations is needed to be validated in prospective cohort studies. Also, in patients with advanced stages of CKD, retinal microvasculature disease may be present even after kidney transplant (Ooi et al., 2015); it is important to explore more details about retinal neurovascular changes after renal replacement therapy. Secondly, the present study was also limited by its relatively limited sample size and further studies with larger sample sizes are required to confirm the findings in our future researches. Thirdly, some of the baseline variations, such as age and BMI, were not comparable among the three groups. Therefore, we adjusted them using binary logistic regression analysis to minimize the bias and made the results more reliable during the statistical analysis. Fourthly, we did not test the retinal function of CKD patients except visual acuity. In further investigations, we are going to evaluate retinal functions using multifocal electroretinogram (mfERG) in CKD patients to clarify the relationships between retinal neurovascular damages and retinal functions.

## CONCLUSION

Retinal neuronal impairment is present in early stages of CKD (stages 1–2) and it is associated with accumulation of uremic toxins and higher UACR, while retinal microvascular hypoperfusion, which is associated with worse eGFR, was only observed in relatively advanced stages of CKD (stages 3–5). The results highlight the importance of monitoring retinal neurovascular impairment in different stages of CKD.

## DATA AVAILABILITY STATEMENT

The raw data supporting the conclusions of this article will be made available by the authors, upon request to HY, yuhonghua@gadph.org.cn.

## ETHICS STATEMENT

The studies involving human participants were reviewed and approved by the Research Ethics Committee of

Guangdong Provincial People's Hospital [registration number: GDREC2020069(R1)]. The patients/participants provided their written informed consent to participate in this study.

## AUTHOR CONTRIBUTIONS

HY, XY, ZY, XZ, YH, and YC: conception and design. XZ, YL, BL, PZ, YX, CL, GW, HK, ZL, ZD, YR, and YF: analysis and interpretation of data. XZ, YH, YC, and ZL: drafting the manuscript and revising it. HY, XY, ZY, XZ, YH, and YC: providing intellectual content of critical importance to the work described. All authors approved the final version to be published.

## FUNDING

This study was supported by the National Natural Science Foundation of China (Grant 81870663 of HY), the Science and Technology Program of Guangzhou (Grant 202002030074 of HY and Grant 202002020049 of XY), the Outstanding Young Talent Trainee Program of Guangdong Provincial People's Hospital (Grant KJ012019087 of HY), the GDPH Scientific Research Funds for Leading Medical Talents and Distinguished Young Scholars in Guangdong Province (Grant KJ012019457 of HY), the talent introduction fund of Guangdong Provincial People's Hospital (Grant Y012018145 of HY), the Technology Innovation Guidance Program of Hunan Province (Grant 2018SK50106 of YH), and the Science Research Foundation of Aier Eye Hospital Group (Grant AR1909D2, AM1909D2 of YH). The funders had no role in the conduct of the surgery; collection, analysis, and interpretation of the data; preparation, review, or approval of the manuscript; and decision to submit the manuscript for publication.

## ACKNOWLEDGMENTS

We would like to thank the staff of the Nephrology Department of Guangdong Provincial People's Hospital for their assistance with the recruitment of the participants.

## SUPPLEMENTARY MATERIAL

The Supplementary Material for this article can be found online at: <https://www.frontiersin.org/articles/10.3389/fnins.2021.703898/full#supplementary-material>

## REFERENCES

- Chen, Z., Mo, Y., Ouyang, P., Shen, H., Li, D., and Zhao, R. (2019). Retinal vessel optical coherence tomography images for anemia screening. *Med. Biol. Eng. Comput.* 57, 953–966. doi: 10.1007/s11517-018-1927-8
- Chua, S. Y. L., Lascaratos, G., Atan, D., Zhang, B., Reisman, C., Khaw, P. T., et al. (2020). Relationships between retinal layer thickness and brain volumes in the UK Biobank cohort. *Eur. J. Neurol.* 28, 1490–1498. doi: 10.1111/ene.14706
- Cogan, M. G., Covey, C. M., Arieff, A. I., Wisniewski, A., Clark, O. H., Lazarowitz, V., et al. (1978). Central nervous system manifestations of hyperparathyroidism. *Am. J. Med.* 65, 963–970.
- Craver, L., Marco, M. P., Martinez, I., Rue, M., Borrás, M., Martin, M. L., et al. (2007). Mineral metabolism parameters throughout chronic kidney disease

- stages 1–5—achievement of K/DOQI target ranges. *Nephrol. Dial. Transplant.* 22, 1171–1176. doi: 10.1093/ndt/gfl718
- Demir, M. N., Eksioglu, U., Altay, M., Tok, O., Yilmaz, F. G., Acar, M. A., et al. (2009). Retinal nerve fiber layer thickness in chronic renal failure without diabetes mellitus. *Eur. J. Ophthalmol.* 19, 1034–1038. doi: 10.1177/112067210901900621
- Den Haan, J., Csinscik, L., Parker, T., Paterson, R. W., Slattery, C. F., Foulkes, A., et al. (2019). Retinal thickness as potential biomarker in posterior cortical atrophy and typical Alzheimer's disease. *Alzheimers Res. Ther.* 11:62. doi: 10.1186/s13195-019-0516-x
- Elias, M. F., Elias, P. K., Seliger, S. L., Narsipur, S. S., Dore, G. A., and Robbins, M. A. (2009). Chronic kidney disease, creatinine and cognitive functioning. *Nephrol. Dial. Transplant.* 24, 2446–2452.
- Farrah, T., Dhillon, B., Keane, P., Webb, D., and Dhaun, N. (2020). The eye, the kidney, and cardiovascular disease: old concepts, better tools, and new horizons. *Kidney Int.* 98, 323–342. doi: 10.1016/j.kint.2020.01.039
- Foreman, K., Marquez, N., Dolgert, A., Fukutaki, K., Fullman, N., McGaughey, M., et al. (2018). Forecasting life expectancy, years of life lost, and all-cause and cause-specific mortality for 250 causes of death: reference and alternative scenarios for 2016–40 for 195 countries and territories. *Lancet* 392, 2052–2090. doi: 10.1016/S0140-6736(18)31694-5
- Futrakul, N., Butthep, P., and Futrakul, P. (2008). Altered vascular homeostasis in chronic kidney disease. *Clin. Hemorheol. Microcirc.* 38, 201–207.
- Giorgetti, S., Raimondi, S., Cassinelli, S., Bucciantini, M., Stefani, M., Gregorini, G., et al. (2009). beta2-Microglobulin is potentially neurotoxic, but the blood brain barrier is likely to protect the brain from its toxicity. *Nephrol. Dial. Transplant.* 24, 1176–1181. doi: 10.1093/ndt/gfn623
- Hamed, S. A. (2019). Neurologic conditions and disorders of uremic syndrome of chronic kidney disease: presentations, causes, and treatment strategies. *Expert Rev. Clin. Pharmacol.* 12, 61–90. doi: 10.1080/17512433.2019.1555468
- Hart, N. J., Koronyo, Y., Black, K. L., and Koronyo-Hamaoui, M. (2016). Ocular indicators of Alzheimer's: exploring disease in the retina. *Acta Neuropathol.* 132, 767–787. doi: 10.1007/s00401-016-1613-6
- Hormel, T. T., Jia, Y., Jian, Y., Hwang, T. S., Bailey, S. T., Pennesi, M. E., et al. (2021). Plexus-specific retinal vascular anatomy and pathologies as seen by projection-resolved optical coherence tomographic angiography. *Prog. Retin. Eye Res.* 80:100878. doi: 10.1016/j.preteyeres.2020.100878
- Houben, A., Martens, R. J. H., and Stehouwer, C. D. A. (2017). Assessing microvascular function in humans from a chronic disease perspective. *J. Am. Soc. Nephrol.* 28, 3461–3472. doi: 10.1681/asn.201702.0157
- Jung, S., Bosch, A., Ott, C., Kannenkeril, D., Dienemann, T., Harazny, J. M., et al. (2020). Retinal neurodegeneration in patients with end-stage renal disease assessed by spectral-domain optical coherence tomography. *Sci. Rep.* 10:5255. doi: 10.1038/s41598-020-61308-4
- Kashani, A. H., Asanad, S., Chan, J. W., Singer, M. B., Zhang, J., Sharifi, M., et al. (2021). Past, present and future role of retinal imaging in neurodegenerative disease. *Prog. Retin. Eye Res.* 83:100938. doi: 10.1016/j.preteyeres.2020.100938
- Kim, G. A., Park, S. H., Ko, J., Lee, S. H., Bae, H. W., Seong, G. J., et al. (2016). Albuminuria is associated with open-angle glaucoma in nondiabetic Korean subjects: a cross-sectional study. *PLoS One* 11:e0168682. doi: 10.1371/journal.pone.0168682
- Kurella, M., Yaffe, K., Shlipak, M. G., Wenger, N. K., and Chertow, G. M. (2005). Chronic kidney disease and cognitive impairment in menopausal women. *Am. J. Kidney Dis.* 45, 66–76.
- Levey, A., and Coresh, J. (2012). Chronic kidney disease. *Lancet* 379, 165–180.
- Levey, A., Stevens, L., Schmid, C., Zhang, Y., Castro, A., Feldman, H., et al. (2009). A new equation to estimate glomerular filtration rate. *Ann. Intern. Med.* 150, 604–612.
- Mutlu, U., Colijn, J. M., Ikram, M. A., Bonnemaier, P. W. M., Licher, S., Wolters, F. J., et al. (2018). Association of retinal neurodegeneration on optical coherence tomography with dementia: a population-based study. *JAMA Neurol.* 75, 1256–1263. doi: 10.1001/jamaneurol.2018.1563
- O'bryhim, B. E., Apte, R. S., Kung, N., Coble, D., and Van Stavern, G. P. (2018). Association of preclinical Alzheimer disease with optical coherence tomographic angiography findings. *JAMA Ophthalmol.* 136, 1242–1248.
- Ooi, Q. L., Tow, F. K., Deva, R., Alias, M. A., Kawasaki, R., Wong, T. Y., et al. (2011). The microvasculature in chronic kidney disease. *Clin. J. Am. Soc. Nephrol.* 6, 1872–1878.
- Ooi, Q. L., Tow, F. K., Deva, R., Kawasaki, R., Wong, T. Y., Colville, D., et al. (2015). Microvascular disease after renal transplantation. *Kidney Blood Press. Res.* 40, 575–583.
- Peng, Q., Hu, Y., Huang, M., Wu, Y., Zhong, P., Dong, X., et al. (2020). Retinal neurovascular impairment in patients with essential hypertension: an optical coherence tomography angiography study. *Invest. Ophthalmol. Vis. Sci.* 61:42. doi: 10.1167/iovs.61.8.42
- Pujari, A., Bhaskaran, K., Sharma, P., Singh, P., Phuljhele, S., Saxena, R., et al. (2020). Optical coherence tomography angiography in neuro-ophthalmology: current clinical role and future perspectives. *Surv. Ophthalmol.* 66, 471–481. doi: 10.1016/j.survophthal.2020.10.009
- Raskin, N. H., and Fishman, R. A. (1976). Neurologic disorders in renal failure (second of two parts). *N. Engl. J. Med.* 294, 204–210.
- Robbins, C. B., Thompson, A. C., Bhullar, P. K., Koo, H. Y., Agrawal, R., Soundararajan, S., et al. (2021). Characterization of retinal microvascular and choroidal structural changes in parkinson disease. *JAMA Ophthalmol.* 139, 182–188. doi: 10.1001/jamaophthalmol.2020.5730
- Shin, J. W., Sung, K. R., and Park, S. W. (2018). Patterns of progressive ganglion cell-inner plexiform layer thinning in glaucoma detected by OCT. *Ophthalmology* 125, 1515–1525. doi: 10.1016/j.ophtha.2018.03.052
- Smogorzewski, M. J. (2001). Central nervous dysfunction in uremia. *Am. J. Kidney Dis.* 38, S122–S128.
- Spaide, R., Fujimoto, J., Waheed, N., Sadda, S., and Staurengi, G. (2018). Optical coherence tomography angiography. *Prog. Retin. Eye Res.* 64, 1–55.
- Tham, Y. C., Chee, M. L., Dai, W., Lim, Z. W., Majithia, S., Siantar, R., et al. (2020). Profiles of Ganglion Cell-Inner Plexiform layer thickness in a multi-ethnic Asian population: the Singapore epidemiology of eye diseases study. *Ophthalmology* 127, 1064–1076. doi: 10.1016/j.ophtha.2020.01.055
- Toto, L., Borrelli, E., Mastropasqua, R., Senatore, A., Di Antonio, L., Di Nicola, M., et al. (2016). Macular features in retinitis pigmentosa: correlations among ganglion cell complex thickness, capillary density, and macular function. *Invest. Ophthalmol. Vis. Sci.* 57, 6360–6366. doi: 10.1167/iovs.16-20544
- Tsai, C. F., Wang, S. J., and Fuh, J. L. (2010). Moderate chronic kidney disease is associated with reduced cognitive performance in midlife women. *Kidney Int.* 78, 605–610. doi: 10.1038/ki.2010.185
- Vadala, M., Castellucci, M., Guarrasi, G., Terrasi, M., La Blasca, T., and Mule, G. (2019). Retinal and choroidal vasculature changes associated with chronic kidney disease. *Graefes Arch. Clin. Exp. Ophthalmol.* 257, 1687–1698. doi: 10.1007/s00417-019-04358-3
- Wanner, C., Amann, K., and Shoji, T. (2016). The heart and vascular system in dialysis. *Lancet* 388, 276–284. doi: 10.1016/s0140-6736(16)30508-6
- Wu, I. W., Sun, C. C., Lee, C. C., Liu, C. F., Wong, T. Y., Chen, S. Y., et al. (2020). Retinal neurovascular changes in chronic kidney disease. *Acta Ophthalmol.* 98, e848–e855.
- Yeung, L., Wu, I. W., Sun, C. C., Liu, C. F., Chen, S. Y., Tseng, C. H., et al. (2019). Early retinal microvascular abnormalities in patients with chronic kidney disease. *Microcirculation* 26:e12555.
- Zeng, Y., Cao, D., Yu, H., Yang, D., Zhuang, X., Hu, Y., et al. (2019). Early retinal neurovascular impairment in patients with diabetes without clinically detectable retinopathy. *Br. J. Ophthalmol.* 103, 1747–1752.
- Zhang, J., Tang, F. Y., Cheung, C., Chen, X., and Chen, H. (2021). Different effect of media opacity on automated and manual measurement of foveal avascular zone of optical coherence tomography angiographies. *Br. J. Ophthalmol.* 105, 812–818. doi: 10.1136/bjophthalmol-2019-315780
- Zhang, J., Tang, F. Y., Cheung, C. Y., and Chen, H. (2020). Different effect of media opacity on vessel density measured by different optical coherence tomography angiography algorithms. *Trans. Vis. Sci. Technol.* 9:19. doi: 10.1167/tvst.9.8.19
- Zhuang, X., Cao, D., Zeng, Y., Yang, D., Yao, J., Kuang, J., et al. (2020). Associations between retinal microvasculature/microstructure and renal function in type 2 diabetes patients with early chronic kidney disease. *Diabetes Res. Clin. Pract.* 168:108373. doi: 10.1016/j.diabres.2020.108373

Zoccali, C., Vanholder, R., Massy, Z. A., Ortiz, A., Sarafidis, P., Dekker, F. W., et al. (2017). The systemic nature of CKD. *Nat. Rev. Nephrol.* 13, 344–358. doi: 10.1038/nrneph.2017.52

**Conflict of Interest:** The authors declare that the research was conducted in the absence of any commercial or financial relationships that could be construed as a potential conflict of interest.

**Publisher's Note:** All claims expressed in this article are solely those of the authors and do not necessarily represent those of their affiliated organizations, or those of the publisher, the editors and the reviewers. Any product that may be evaluated in

this article, or claim that may be made by its manufacturer, is not guaranteed or endorsed by the publisher.

Copyright © 2021 Zeng, Hu, Chen, Lin, Liang, Liu, Zhong, Xiao, Li, Wu, Kong, Du, Ren, Fang, Ye, Yang and Yu. This is an open-access article distributed under the terms of the Creative Commons Attribution License (CC BY). The use, distribution or reproduction in other forums is permitted, provided the original author(s) and the copyright owner(s) are credited and that the original publication in this journal is cited, in accordance with accepted academic practice. No use, distribution or reproduction is permitted which does not comply with these terms.



# Altered Cortisol Metabolism Increases Nocturnal Cortisol Bioavailability in Prepubertal Children With Type 1 Diabetes Mellitus

Julie Brossaud<sup>1,2</sup>, Jean-Benoît Corcuff<sup>1,2</sup>, Vanessa Vautier<sup>3</sup>, Aude Bergeron<sup>3</sup>, Aurelie Valade<sup>4</sup>, Anne Lienhardt<sup>5</sup>, Marie-Pierre Moisan<sup>2</sup> and Pascal Barat<sup>2,3\*</sup>

<sup>1</sup> Nuclear Medicine, Hospital of Bordeaux, Pessac, France, <sup>2</sup> Université de Bordeaux, INRAE, Bordeaux INP, NutriNeuro, Bordeaux, France, <sup>3</sup> Pediatric Endocrinology and DiaBEA Unit, Hôpital des Enfants, Hospital of Bordeaux, Bordeaux, France, <sup>4</sup> Paediatric Unit, Hospital of Bayonne, Bayonne, France, <sup>5</sup> Paediatric Unit, Hospital of Limoges, Limoges, France

## OPEN ACCESS

### Edited by:

Rachel Nicole Lippert,  
German Institute of Human Nutrition  
Potsdam-Rehbruecke (DIfE), Germany

### Reviewed by:

Hershel Raff,  
Medical College of Wisconsin,  
United States  
Qingchun Tong,  
University of Texas Health Science  
Center at Houston, United States

### \*Correspondence:

Pascal Barat  
pascal.barat@chu-bordeaux.fr

### Specialty section:

This article was submitted to  
Neuroendocrine Science,  
a section of the journal  
Frontiers in Endocrinology

**Received:** 16 July 2021

**Accepted:** 22 November 2021

**Published:** 14 December 2021

### Citation:

Brossaud J, Corcuff J-B, Vautier V,  
Bergeron A, Valade A, Lienhardt A,  
Moisan M-P and Barat P (2021)  
Altered Cortisol Metabolism  
Increases Nocturnal Cortisol  
Bioavailability in Prepubertal Children  
With Type 1 Diabetes Mellitus.  
Front. Endocrinol. 12:742669.  
doi: 10.3389/fendo.2021.742669

**Objective:** Disturbances in the activity of the hypothalamus-pituitary-adrenal axis could lead to functional alterations in the brain of diabetes patients. In a later perspective of investigating the link between the activity of the hypothalamus-pituitary-adrenal axis and the developing brain in children with diabetes, we assessed here nocturnal cortisol metabolism in prepubertal children with type 1 diabetes mellitus (T1DM).

**Methods:** Prepubertal patients (aged 6–12 years) diagnosed with T1DM at least 1 year previously were recruited, along with matched controls. Nocturnal urine samples were collected, with saliva samples taken at awakening and 30 minutes after awakening. All samples were collected at home over 5 consecutive days with no detectable nocturnal hypoglycaemia. The State-Trait Anxiety Inventory (trait scale only) and Child Depression Inventory were also completed. Glucocorticoid metabolites in the urine, salivary cortisol (sF) and cortisone (sE) were measured by liquid chromatography–tandem mass spectrometry. Metabolic data were analysed by logistic regression, adjusting for sex, age, BMI and trait anxiety score.

**Results:** Urine glucocorticoid metabolites were significantly lower in T1DM patients compared to controls. 11 $\beta$ -hydroxysteroid dehydrogenase type 1 activity was significantly higher, while 11 $\beta$ -hydroxysteroid dehydrogenase type 2, 5( $\alpha$ + $\beta$ )-reductase and 5 $\alpha$ -reductase levels were all lower, in T1DM patients compared to controls. There was a significant group difference in delta sE level but not in delta sF level between the time of awakening and 30 minutes thereafter.

**Conclusions:** Our findings suggest that altered nocturnal cortisol metabolism and morning HPA axis hyperactivity in children with T1DM leads to greater cortisol bioavailability and lower cortisol production as a compensatory effect. This altered nocturnal glucocorticoid metabolism when cortisol production is physiologically reduced and this HPA axis hyperactivity question their impact on brain functioning.

**Keywords:** 5 $\alpha$ -Reductase, 11 $\beta$ -hydroxy steroid dehydrogenase-1, glucocorticoids, children, type 1 diabetes

## INTRODUCTION

It is well established that type 1 diabetes mellitus (T1DM) in children can have a significant impact on the developing brain, as reflected in high prevalence of depression (1) and poor performance on certain cognitive tasks (2) along with structural and functional changes (3). The mechanisms underlying depression and cognitive dysfunction in diabetic patients are complex and include factors directly related to diabetes itself, but also to diabetes-related cardiovascular disease and microvascular dysfunction (4). In children with diabetes, sustained dysregulation of blood glucose is currently considered the cause of cognitive dysfunction. However, the extent to which acute hypoglycaemia, chronic hyperglycaemia and/or blood sugar variations directly and indirectly affect brain function has yet to be clarified (2). In addition to chronic hyperglycaemia and relative insulin insufficiency, disturbances in the activity of the hypothalamus-pituitary-adrenal (HPA) axis, often implicated in autoimmune or pharmacological models of diabetes mellitus, could also participate in brain alterations (5, 6). Indeed, dysregulated glucocorticoids are well known to lead to depression (7) or mnemonic dysfunctions (8).

The effect of glucocorticoids on brain function in diabetes is not only dependent on secretion but also bioavailability, which is linked with 11 $\beta$ -hydroxysteroid dehydrogenase (11 $\beta$ -HSD) cellular activity. Indeed, 11 $\beta$ -HSD is an important factor in peripheral cortisol metabolism. 11 $\beta$ -HSD is an intracellular enzyme that regulates the tissue response to cortisol at an intracellular pre-receptor step by catalyzing the interconversion of biologically active cortisol to biologically inactive cortisone. 11 $\beta$ -HSD type 1 (11 $\beta$ -HSD1) converts cortisone to cortisol predominantly in the liver and hippocampus, whereas 11 $\beta$ -HSD type 2 (11 $\beta$ -HSD2) inactivates cortisol to cortisone, mainly in the kidney, thus protecting the mineralocorticoid receptor from inappropriate stimulation by cortisol (9, 10). In animal studies, we showed that glucocorticoid levels and 11 $\beta$ -HSD1 activity were elevated in diabetic rats not treated with insulin. Subcutaneous administration of insulin partially prevented glucocorticoid dysregulation by decreasing 11 $\beta$ -HSD1 activity in the liver (11). We also showed that insulin treatment partially rescued several hippocampus-dependent behavioural and structural changes in early onset insulin-deficient diabetic rats, as well as 11 $\beta$ -HSD1 activity in the hippocampus (12) indicating that the elevated bioavailability of glucocorticoids may be involved in the diabetes cognitive dysfunctions.

In humans, 11 $\beta$ -HSD1 can be estimated from urine samples as the ratio of (alpha + beta) tetrahydrocortisol (THF) to tetrahydrocortisone (THE) (13). In a previous pilot study, we showed elevated 11 $\beta$ -HSD1 level in nocturnal urine samples of diabetic children (14).

The present study aims at evaluating cortisol metabolism in prepubertal children with T1DM to 1) validate these previous results, 2) widen the scope of the investigation into cortisol metabolism and 3) justify a study that will examine the association between HPA disturbances and diabetes alterations in the developing brain of T1DM children. This investigation benefitted from including diabetes patients free from micro- and

macrovascular comorbidities, which may also contribute to brain alterations (15). Glucocorticoid metabolites were analysed in prepubertal children under strict conditions, focusing on repeated nocturnal excretion of glucocorticoids while also taking anxiety levels into account. Examination of nocturnal excretion of glucocorticoids, when glucocorticoid production is at its lowest due to the physiological nychthemeral cycle, should allow for the detection of subtle changes in cortisol metabolism.

## MATERIALS AND METHODS

### Clinical Protocol

Prepubertal patients (aged 6–12 years) diagnosed with T1DM at least 1 year previously were routinely followed up in three different pediatric units in France (Bordeaux, Limoges and Bayonne), and enrolled in the present study. Forty percent of patients were treated by insulin pump and 60% by insulin injection. The prepubertal children in the control group were siblings of diabetic patients followed up in the 3 units. The exclusion criteria included any clinical signs of puberty onset, use of oral or inhaled corticoids during the month prior to inclusion in the study, the presence of acute infectious disease in the week prior to inclusion in the study, and any other chronic diseases apart from T1DM, including psychiatric disorders (and psychiatric treatment).

At the time of inclusion, the clinical characteristics of all participants were recorded and biological analyses were performed to confirm the absence of diabetes in the control group. Then, the State-Trait Anxiety Inventory (STAI) Trait scale and Child Depression Inventory (CDI) were completed. Only the trait scale of the STAI was used, as a measure of stable feelings of anxiety. The glucocorticoid metabolite to creatinine ratio was calculated based on nocturnal urine samples, which were taken in addition to morning salivary cortisol (sF) and cortisone (sE) samples at home over 5 consecutive days. No nocturnal hypoglycaemia (defined as glucose < 60 mg/dL) was detected at the time of awakening. Nocturnal urine samples were taken in the morning (first morning void after awakening). If hypoglycaemia occurred during the night-time or at the time of awakening, urine and saliva sampling was postponed by 24 hours. The children were asked to collect a sample of saliva to determine sF and sE using a Salivette<sup>®</sup> kit (Sarstedt, Nümbrecht, Germany) upon awakening and 30 minutes thereafter. Samples were kept frozen at home until the next visit to the hospital.

The study protocol was approved by the local medical ethics committee and written informed consent was obtained from both the parents and children.

### Laboratory Measurements

Urine Glucocorticoid metabolites were measured by liquid chromatography–tandem mass spectrometry (LC-MS/MS) (ACQUITY UPLC System and TQD detector with electrospray ionization, Waters Ltd., Elstree, Hertfordshire, UK). Briefly, 6 $\alpha$ -pharmethylprednisolone was used as an internal standard, and

hydrolysis with  $\beta$ -glucuronidase was performed before dichloromethane extraction. The ratio of each analyte to creatinine (analyte/cr) was determined.

Total glucocorticoid metabolites were calculated as  $(\alpha+\beta)$ -THF + THE +  $(\alpha+\beta)$ -cortisol +  $(\alpha+\beta)$ -cortisone. Active metabolites included all metabolites derived from cortisol i.e. F+  $(\alpha+\beta)$ -THF +  $(\alpha+\beta)$ -cortisol. The  $(\alpha+\beta)$ -THF/THE ratio was considered a proxy for 11 $\beta$ -HSD1 activity. The cortisone/cortisol ratio (E/F) was considered a proxy for 11 $\beta$ -HSD2 activity.  $(\alpha+\beta)$ -THF/F and  $\alpha$ -THF/F were considered as proxies for 5 $(\alpha+\beta)$ -reductase and 5 $\alpha$ -reductase activity, respectively (**Figure 1**).

sF and sE was measured by LC-MS/MS (Prominence liquid chromatography system; Shimadzu, Nakagyo, Japan; and 5500 Qtrap detector, Sciex, Framingham, MA, USA). A liquefying agent (Sputasol; Thermo Fisher Scientific, Waltham, MA, USA) was added to 400  $\mu$ L of saliva sample, which was then incubated for 30 minutes at 37°C. Next, solid-phase extraction with a hydrophilic lipophilic balance (Waters) was performed before injecting the extract into the LC-MS/MS system. The cortisol and cortisone concentrations were determined based on the peak area ratio of the cortisol and cortisone transitions and the Internal Standard (deuterated cortisol) transition.

## Statistical Analysis

Analyses and graphs were performed using SAS (ver. 9.4; SAS Institute, Cary, NC, USA), R (R Development Core Team, Vienna, Austria), STATISTICA 6 (TIBCO Software, Palo Alto, CA, USA) and GraphPad Prism software.

Unless otherwise stated, all values are presented as the mean  $\pm$  standard deviation and  $p < 0.05$  was considered significant. The significance of the differences in qualitative variables between T1DM patients and controls was tested using a logistic regression model. The correlation within diabetic and non-diabetic “pairs” (siblings of the subjects) has been taken into account by a pair-related random effect.

Dispersion was estimated by the coefficient of variation. The homogeneity of variance was assessed using Levene’s test; the variance in the data for all metabolites did not differ between controls and T1DM patients (**Figures 1A–E**). The intraday variability was also similar between the groups for all metabolites; thus, results are reported as the mean of five samples for all of the children.

Group differences in metabolic data were evaluated using a logistic regression model adjusted for sex, age, BMI and STAI score. Mean and 95% confidential intervals are provided. Pearson correlation analyses were conducted to identify associations among age, BMI, insulin dose, HbA1c and metabolic data.

## RESULTS

### Description of the Study Population

The baseline characteristics of the T1DM ( $n = 49$ ) and control ( $n = 26$ ) groups are presented in **Table 1**. No significant differences in age, sex, education level or clinical characteristics such as weight, height, BMI, waist circumference, systolic or diastolic blood

pressure or Tanner score were observed between the groups. All children were pre-pubertal. However, the STAI Trait scale score tended to be higher in the control group ( $p = 0.07$ ). No difference was observed between the two groups in CDI score.

### Urine Glucocorticoid Metabolites in T1DM Children

No differences were observed between males and females in levels of urine glucocorticoid metabolites. The data for each group before and after adjustment for the STAI Trait scale score and urine cortisol and cortisone metabolites, as well as 11 $\beta$ -HSD1, 11 $\beta$ -HSD2, 5 $(\alpha+\beta)$ -reductase and 5 $\alpha$ -reductase enzymatic activity, are shown in **Table 2**.

Due to the lower THE/cr ratio, the total glucocorticoid metabolite level was significantly lower in T1DM patients compared to controls. The 11 $\beta$ -HSD1 activity was significantly higher, while 11 $\beta$ -HSD2, 5 $(\alpha+\beta)$ -reductase and 5 $\alpha$ -reductase activities were significantly lower, in T1DM patients compared to controls (**Figures 2A–E**). These differences remained after adjusting the regression analyses for STAI trait anxiety score.

### Salivary Cortisol and Cortisone on Awakening

No difference was observed between males and females in sF and sE levels. There was also no significant difference between the T1DM patients and controls in sF and sE level on awakening (sF T0 or sE T0) or 30 minutes thereafter (sF T30 or sE T30) neither in sE/sF ratio level, including after adjusting the analyses for STAI trait anxiety score. However, we found a significant difference in delta sE levels between the time of awakening and 30 minutes thereafter (sE Delta T30-T0) (**Table 2** and **Figure 2F**).

### Correlation Between Metabolic Data and Clinical Characteristics

No significant correlation was found between 11 $\beta$ -HSD1 or 5 $\alpha$ -reductase activity and clinical characteristics: neither 11 $\beta$ -HSD1 nor 5 $\alpha$ -reductase activity was significantly correlated with BMI in the T1DM or control group, or with HbA1c or insulin levels in the T1DM group.

## DISCUSSION

Our analysis of the nocturnal urine samples of prepubertal children, obtained over a 5-day period in the home setting, revealed altered nocturnal cortisol metabolism (higher 11 $\beta$ -HSD1 and lower 11 $\beta$ -HSD2 activity) in those with T1DM, in addition to lower glucocorticoid metabolite excretion and 5 $\alpha$ -reductase activity. The results remained significant after adjusting for STAI trait scale score. In addition to these changes in nocturnal glucocorticoid metabolism, the morning reactivity of the HPA axis, as indexed by sE Delta T30-T0 levels upon awakening, was significantly higher in the T1DM group than in the control group.

To later assess brain alterations in T1DM patients, we specifically targeted prepubertal children due to the absence of micro- and macro-vascular comorbidities in that population.

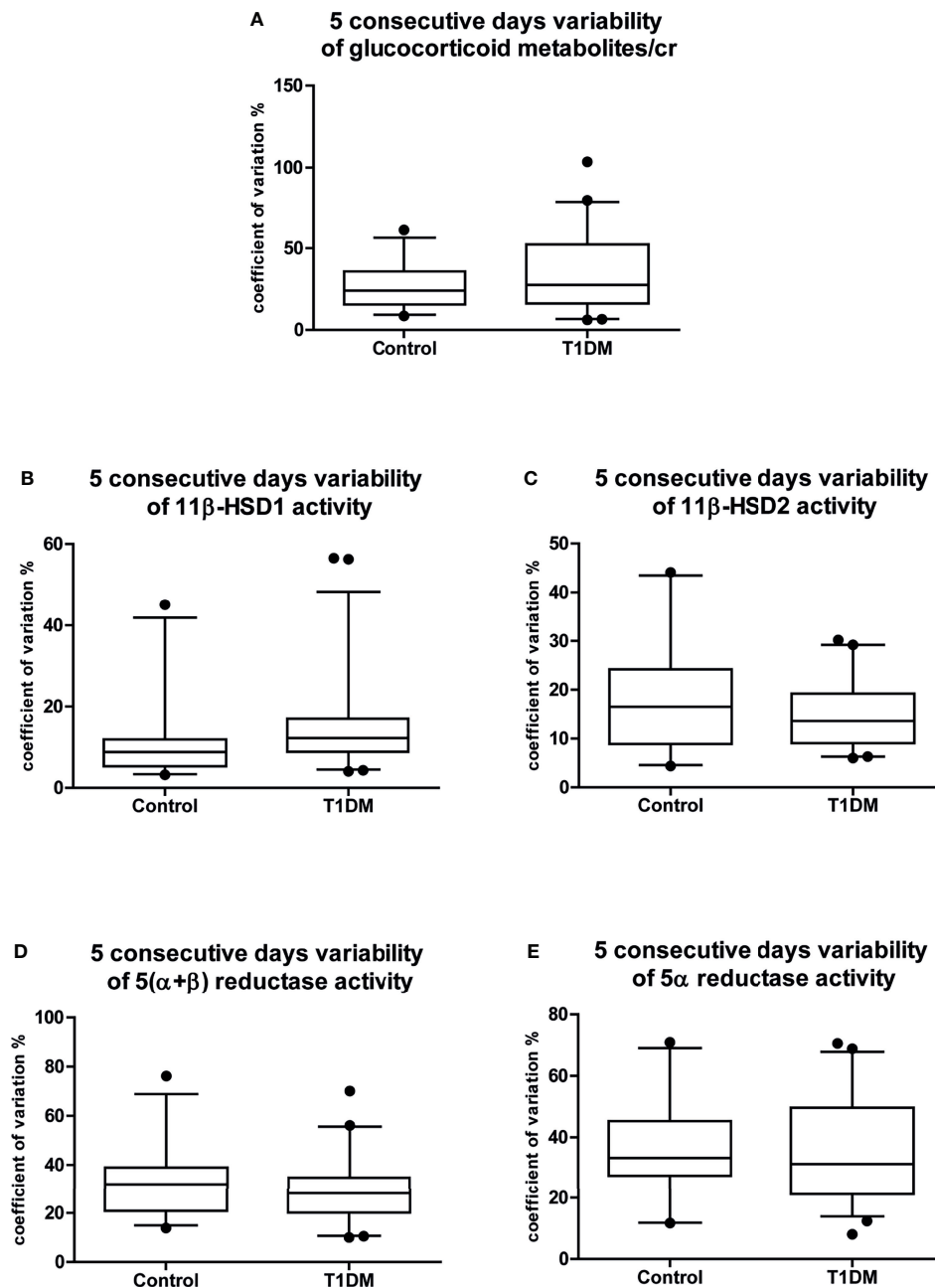


**FIGURE 1** | Five consecutive days variability of the main cortisol metabolism results. Coefficients of variation of the 5 consecutive days variability of **(A)** glucocorticoid metabolites/cr; **(B)** 11β-HSD1 activity; **(C)** 11β-HSD2 activity; **(D)** 5(α+β) reductase activity; **(E)** 5α reductase activity. Data are expressed as median [25-75% percentile; plot; 5-95% percentile: whiskers]. Points below and above the whiskers are drawn as individual points. T1DM, type 1 diabetes mellitus; cr, to creatinine.

Our results call into question sexual dimorphism in cortisol metabolism in this age group. Finken et al. described sexual dimorphism in cortisol metabolism in association with 5α-reductase, but not 11β-HSD1, activity in healthy young adults (16). In healthy children, the 24-hour excretion rate of glucocorticoid metabolites rose markedly between the ages of 4 and 14 years in both boys and girls, in association with the body

fat percentage and BMI (17). No sex difference in glucocorticoid metabolite excretion, or 11β-HSD1 and 11β-HSD2 activities, was seen in healthy prepubertal children, unlike pubertal children (17). Similarly, the present study found no sex difference in the glucocorticoid metabolite excretion rate or enzymatic activity, in either the T1DM or control group, from which individuals with any signs of pubertal onset were excluded.

**TABLE 1** | Characteristics of the study population at enrolment.

	<b>Controls (n = 26)</b>	<b>T1DM (n = 49)</b>	<b>p</b>
<b>Age (years)</b>	9.0 (1.7)	9.3 (1.4)	0.41
<b>Sex (male/female)</b>	12/14	27/22	0.46
<b>Education level relative to children of the same age (%)</b>	100	95.9	0.29
<b>Onset of diabetes (years)</b>		3.7 (2.2)	
<b>Height (cm)</b>	133.5 (9.3)	132.4 (10.9)	0.66
<b>Weight (kg)</b>	28.8 (6.3)	28.9 (5.7)	0.94
<b>BMI (kg/m<sup>2</sup>)</b>	16.0 (1.7)	16.3 (1.3)	0.39
<b>Systolic blood pressure (mmHg)</b>	107.0 (9.3)	104.0 (9.0)	0.17
<b>Diastolic blood pressure (mmHg)</b>	64.9 (7.1)	62.0 (6.5)	0.07
<b>Tanner stage</b>			0.94
<b>B1 or G1 (%)</b>	100	100	
<b>P1 (%)</b>	96.2	95.9	
<b>P2 (%)</b>	3.8	4.1	
<b>Insulin dose (U/day)</b>		23.5 (9.5)	
<b>Glycaemia (g/l)</b>	0.8 (0.1)		
<b>HbA1c (%)</b>	5.3 (0.3)	7.6 (0.7)	< 0.0001
<b>Child Depression Inventory score</b>	9.0 (6.3)	6.9 (6.0)	0.16
<b>STAI score</b>	33.0 (7.8)	29.7 (6.6)	0.057

Results are expressed as mean (SD). CDI, Child Depression Inventory; STAI, State-Trait Anxiety Inventory (trait scale only).

In a previous study, 11 $\beta$ -HSD2 and 11 $\beta$ -HSD1 activities measured in 24 hour urine samples were similarly elevated in children aged below 10 years diagnosed with T1DM (18) while others found a decrease of 11 $\beta$ -HSD1 activity but in adults (19). In our study, we confirmed our previous finding of elevated 11 $\beta$ -HSD1 level in children with T1DM, with urine samples collected over the course of a single night (14). However, we also found that 11 $\beta$ -HSD2 activity was lower during the night. Our results underline the importance of measuring subtle nocturnal changes in glucocorticoid metabolism. The circadian rhythm of cortisol secretion dictates that the rate of production of cortisol metabolites at night is low. Changes in nocturnal 11 $\beta$ -HSD type 1 and 2 activity suggest an abnormal increase in cortisol bioavailability due to upregulated conversion of cortisone to cortisol.

5 $\alpha$ -reductase is responsible for the irreversible reduction of cortisol to 5 $\alpha$ -THF, which mainly occurs in the liver and contributes to the clearance of cortisol. Decreased production and metabolic clearance of cortisol, as determined by 24-hour urine collection, has previously been described in normotensive type 1 diabetic males with adequate glycaemic control and without severe complications (9), as well as in children aged below 10 years with T1DM. In our study, reductase activity was decreased, mainly due to a lower level of 5 $\alpha$ -reductase activity. Furthermore, we confirmed diminished glucocorticoid production, based on the total urinary glucocorticoid metabolite excretion. The impaired production and metabolic clearance of cortisol are hypothesized to be due to lower 5 $\alpha$ -reductase activity, which could result in reduced metabolic clearance of cortisol. Due to the comparatively longer half-life of cortisol, this could in turn lead to a decrease in cortisol production *via* a negative feedback loop (9).

Children with T1DM show relative insulin insufficiency in the liver on subcutaneous delivery of insulin and, as a consequence, the absence of a first hepatic pass. Higher 11 $\beta$ -HSD1 activity and lower 5 $\alpha$ -reductase activity could result from this insulin insufficiency.

Regarding 11 $\beta$ -HSD1 activity, this hypothesis (proposed by Kerstens et al.) was rejected because 11 $\beta$ -HSD1 activity increased in healthy adults submitted to a hyperinsulinaemic euglycaemic clamp (20). However, in a rodent model of insulin-deficient diabetes, we showed that intraperitoneal insulin led to a decrease in 11 $\beta$ -HSD1 activity in the liver, whereas subcutaneous insulin did not (11). At the cellular level, results are contradictory regarding whether glucose control (via insulin administration) has a direct (21) or indirect inhibitory effect (22) on 11 $\beta$ -HSD1 transcription or activity.

The activity of 5 $\alpha$ -reductase was shown to be increased in association with hyperinsulinemia in patients with polycystic ovary syndrome (23), as well as in those with type 2 diabetes (24) or impaired glucose tolerance (25). Furthermore, Kayampilly et al. reported dose-dependent stimulation of 5 $\alpha$ -reductase activity by insulin in a human granulosa cell line (26). In the normal-weight children dependent on subcutaneous insulin treatment included in our study, we speculate that relative insulin deficiency was responsible for the observed increase in 11 $\beta$ -HSD1 activity and decrease in 5 $\alpha$ -reductase activity, which both contribute to greater cortisol bioavailability and suppression of cortisol production as a compensatory effect.

Hyperactivity of the HPA axis has been well described in adults with insulin-dependent diabetes (27, 28). In the present study, we investigated HPA activity *via* repeated saliva sampling in the home setting. We found a significant difference between the T1DM and control groups in levels of sE Delta T30-T0, thus indicating an increase in HPA axis reactivity. Indeed as 11 $\beta$ -HSD2 is very active in saliva, cortisol is immediately converted in cortisone which thus reflects HPA axis reactivity when cortisol production is at its highest level (i.e. during the nycthemeral cycle). High intragroup variability was seen in the sF and sE data; we speculate that this was due to the difficulty that the children had in following the instructions as they pertained to taking repeated measurements (where the samples must be obtained on

**TABLE 2 |** Metabolites of cortisol and cortisone of the T1DM and control groups.

Metabolite	Group	Group effect	Group effect adjusted for STAI score
<b>F/cr</b> (μg/mmol)	Control	4.5 [3.8;5.3]	4.7 [3.8;5.7]
	T1DM	5.2 [4.6;5.8]	5.3 [4.6;6.1]
<b>E/cr</b> (μg/mmol)	Control	11.1 [9.5;12.6]	11.0 [9.1;12.8]
	T1DM	11.2 [10.0;12.3]	11.3 [9.9;12.7]
<b>β-THF/cr</b> (μg/mmol)	Control	111 [98;127]	107 [89;125]
	T1DM	95 [84;107]	91 [78;105]
<b>α-THF/cr</b> (μg/mmol)	Control	30.4 [25.9;34.8]	30.3 [25.2;35.4]
	T1DM	25.3 [22.0;28.7]	24.2 [20.3;28.1]
<b>THE/cr</b> (μg/mmol)	Control	355 [317;392]***	338 [293;383]***
	T1DM	256 [227;284]	261 [227;296]
<b>α-cortol/cr</b> (μg/mmol)	Control	9.22 [7.41;11.03]	9.26 [7.76;10.76]*
	T1DM	11.3 [9.98;12.71]	10.8 [9.71;11.99]
<b>β-cortol/cr</b> (μg/mmol)	Control	24.6 [20.7;28.5]**	23.0 [18.7;27.4]**
	T1DM	25.6 [22.6;28.5]	25.7 [22.4;29.0]
<b>α-cortolone/cr</b> (μg/mmol)	Control	79.7 [70.1;89.4]	75.9 [65.2;86.5]
	T1DM	78.8 [71.5;86.1]	81.2 [73.1;89.3]
<b>β-cortolone/cr</b> (μg/mmol)	Control	58.8 [52.1;65.5]	54.5 [47.0;62.0]
	T1DM	45.9 [40.8;50.9]	47.9 [42.2;53.6]
<b>Total cortisol metabolites/cr</b> (μg/mmol)	Control	173 [146;200]	175 [152;198]
	T1DM	146 [127;166]	157 [140;175]
<b>Total glucocorticoid metabolites/cr</b> (μg/mmol)	Control	676 [606;745]*	655 [576;734]*
	T1DM	564 [513;616]	560 [500;620]
<b>(α+β)-THF/THE</b>	Control	0.42 [0.38;0.46]*	0.42 [0.37;0.47]*
	T1DM	0.48 [0.45;0.51]	0.47 [0.43;0.50]
<b>Reflecting 11β-HSD1 activity</b>	Control	2.53 [2.26;2.89]*	2.38 [2.08;2.77]*
	T1DM	2.17 [2.01;2.35]	2.07 [1.89;2.28]
<b>(α+β)-THF/F</b>	Control	37.4 [32.7;42.1]**	34.5 [29.4;39.7]**
	T1DM	28.2 [24.7;31.8]	26.3 [22.4;30.2]
<b>Reflecting 5(α+β) reductase activity</b>	Control	8.11 [6.95;9.27]***	7.62 [6.43;8.81]**
	T1DM	5.62 [4.76;6.47]	5.32 [4.42;6.22]
<b>α-THF/F</b>	Control	3.65 [3.02;4.28]	3.61 [3.02;4.37]
	T1DM	3.51 [3.03;3.98]	3.59 [2.81;4.21]
<b>sF T30</b> (nmol/l)	Control	4.16 [3.38;4.94]	4.36 [3.43;5.28]
	T1DM	4.49 [3.92;5.05]	4.58 [3.88;5.28]
<b>sF Delta T30-T0</b> (nmol/l)	Control	0.30 [-0.54;1.13]	0.71 [0.34;1.66]
	T1DM	1.14 [0.52;1.76]	1.00 [-0.15;1.57]
<b>sE T0</b> (nmol/l)	Control	15.3 [13.5;17.0]	15.0 [14.7;15.3]
	T1DM	13.9 [12.5;16.0]	13.9 [13.7;14.2]
<b>sE T30</b> (nmol/l)	Control	16.0 [14.4;19.1]	16.7 [16.4;17.1]
	T1DM	17.8 [16.0;19.5]	17.4 [17.1;17.7]
<b>sE Delta T30-T0</b> (nmol/l)	Control	1.42 [-0.66;3.50]*	1.63 [1.30;1.96]*
	T1DM	4.42 [2.82;6.07]	4.21 [3.93;4.48]
<b>sE/sF T0 ratio</b>	Control	5.23 [4.34;6.13]	5.05 [4.91;5.18]
	T1DM	4.68 [4.17;5.19]	4.73 [4.64;4.82]
<b>sE/sF T30 ratio</b>	Control	4.99 [4.19;5.79]	4.88 [4.76;5.00]
	T1DM	4.50 [4.03;4.96]	4.58 [4.50;4.67]

Group differences in metabolic data were evaluated with a logistic regression model, adjusted for the STAI trait scale score. Data are expressed as mean [95% confidential interval]. T1DM, type 1 diabetes mellitus; F, cortisol; E, cortisone; THF, tetrahydrocortisol; THE, tetrahydrocortisone; sF, salivary cortisol; sE, salivary cortisone; cr, to creatinine; STAI, State-Trait Anxiety Inventory (trait scale only). \* $p < 0.05$ ; \*\* $p < 0.01$ ; \*\*\* $p < 0.001$ .

awakening and exactly 30 minutes thereafter). Furthermore, when interpreting our data suggesting reactivity of the HPA axis, changes in 5α-reductase activity should be taken account. Indeed, due to the longer half-life of corticosterone, mice deficient in 5α-reductase type 1 show an impaired adrenal response to adrenocorticotrophic hormone (ACTH) (29).

For ethical and practical reasons, we used the siblings of diabetic children as the control subjects. Previous studies have shown a reassuring psychosocial effect (30) and no adverse psychiatric disorders (31) in siblings of children with T1DM. Because HPA axis activity could be associated with chronic stress, anxiety or depression we measured these traits in our

cohort. Unexpectedly, the control group tended to show higher STAI trait scale scores than the T1DM patients, but there was no significant group difference in depression. Although we focused on trait rather than state anxiety, it is possible that exposing the siblings of the diabetic children to a hospital environment, to which they are not accustomed, may have influenced our findings. Finally, adjusting the analysis for STAI trait score had little impact on the urinary metabolite data, but was useful in confirming the absence of any differences between the two groups in terms of the activity and reactivity of the HPA axis.

One limitation of this study was that nocturnal hypoglycaemia was not detected using a glucose sensor.

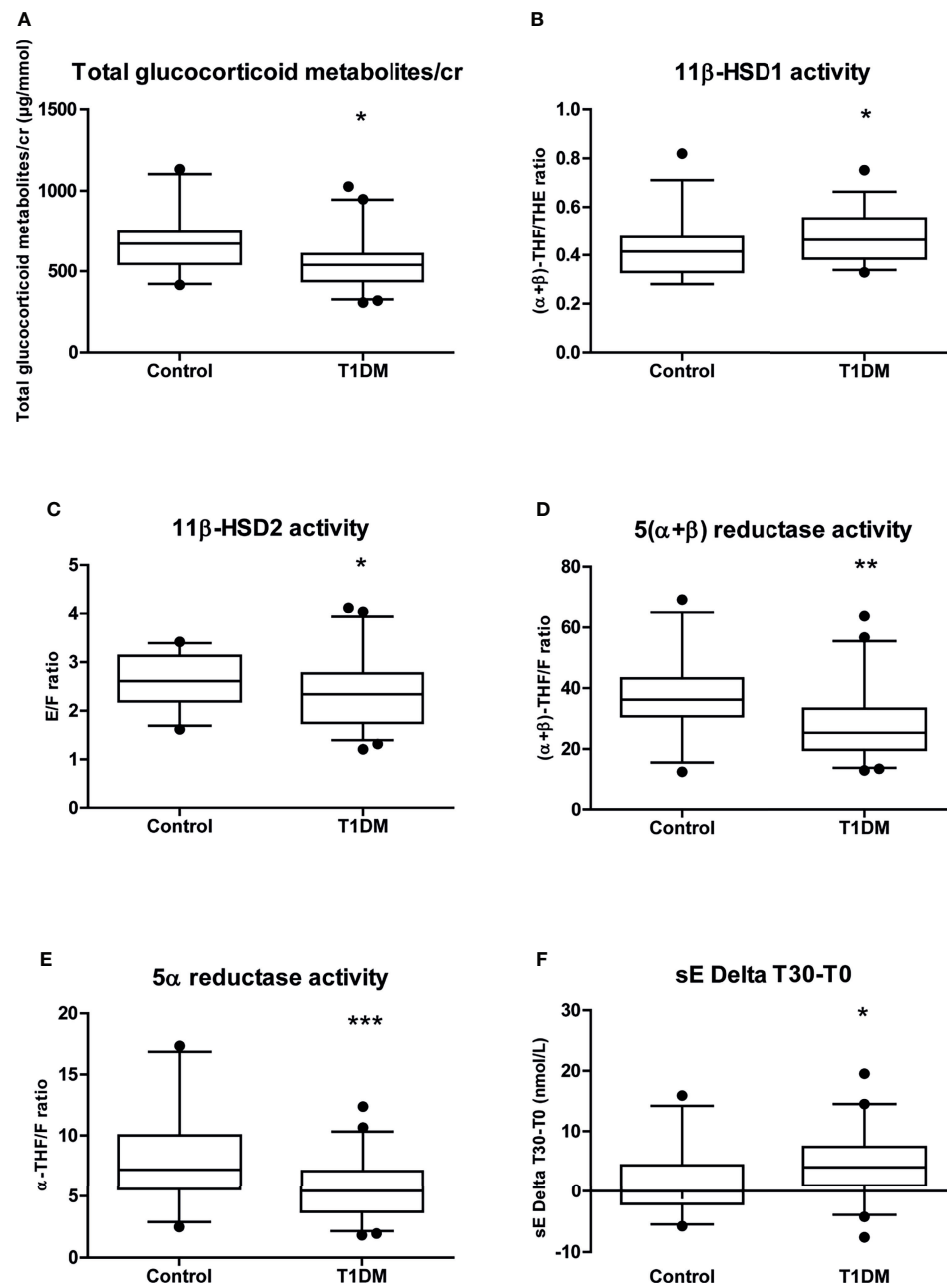


**FIGURE 2** | Whisker plots representation of the main cortisol metabolism results from the data in **Table 2**. Whisker plots of **(A)** glucocorticoid metabolites/cr; **(B)** 11β-HSD1 activity; **(C)** 11β-HSD2 activity; **(D)** 5(α+β) reductase activity; **(E)** 5α reductase activity; **(F)** sE Delta T30-T0. Data are expressed as median [25-75% percentile; plot; 5-95% percentile; whiskers]. Points below and above the whiskers are drawn as individual points. T1DM, type 1 diabetes mellitus; F, cortisol; E, cortisone; THF, tetrahydrocortisol; THE, tetrahydrocortisone; sF, salivary cortisol; sE, salivary cortisone/cr, to creatinine. \* $p < 0.05$ ; \*\* $p < 0.01$ ; \*\*\* $p < 0.001$ .

However, the parents were asked not to take urine samples during periods of nocturnal or waking hypoglycaemia. Samples were obtained over a 5-day period in all children, and differences in the variability of metabolic data were not apparent between the two groups; therefore, we used the mean values of these consecutively obtained samples in the analysis. Furthermore, our results suggested lower nocturnal production of cortisol in

children with T1DM. For these reasons, it is unlikely that clinically significant nocturnal hypoglycaemia can explain our findings. Another limitation of this study is that only morning sF and sE have been sampled. Nocturnal sF and sE at bedtime would be interesting measurements to underline changes in cortisol negative feedback (32), even though bedtime is variable between children.

In conclusion, our findings suggested that altered nocturnal cortisol metabolism in children with T1DM leads to greater cortisol bioavailability due to an abnormal increase in the conversion of cortisone to cortisol, which ultimately lowers cortisol production as a compensatory effect. Moreover, we objectified an increase of the morning HPA axis reactivity. Overall, this greater availability of cortisol when cortisol production is physiologically reduced due to the circadian rhythm of cortisol and this higher HPA axis reactivity prompt many questions regarding its impact on the brain. It is well known that the activity of the HPA axis and glucocorticoid production have an impact on brain structures involved in cognition and mental health (33), specifically in the context of diabetes (34). Furthermore, our results call into question the route of insulin administration, and its ability to prevent altered glucocorticoid metabolism in T1DM patients. A recent rat study of early onset insulin-deficient diabetes supported this hypothesis, by showing that subcutaneous insulin treatment cannot completely prevent several of the hippocampal-dependent behavioural and structural alterations linked with an increase in local 11 $\beta$ -HSD1 activity (12). It also suggested that an increase in peripheral glucocorticoid bioavailability may be associated with a local increase in these hormones within the hippocampus, which has central consequences. Thus, our findings suggest that elevated 11 $\beta$ -HSD1 activity and lower 5 $\alpha$ -reductase activity should be considered as a potential factor for cortisol-dependent brain alterations in diabetic patients.

## AUTHOR'S NOTE

The English in this document has been checked by at least two professional editors, both native speakers of English. For a

certificate, please see: (<http://www.textcheck.com/certificate/qiFziq>).

## DATA AVAILABILITY STATEMENT

The raw data supporting the conclusions of this article will be made available by the authors, without undue reservation.

## ETHICS STATEMENT

The studies involving human participants were reviewed and approved by Le comité de protection des personnes (CPP). Written informed consent to participate in this study was provided by the participants' legal guardian/next of kin.

## AUTHOR CONTRIBUTIONS

JB, J-BC, VV, AB, AV, AL, and PB performed the research. JB, J-BC, M-PM, and PB designed the research study. JB, J-BC, and M-PM contributed essential reagents or tools. JB, J-BC, M-PM, and PB analyzed the data. JB, J-BC, M-PM, and PB wrote the paper. All authors contributed to the article and approved the submitted version.

## FUNDING

This work was supported by the "Programme Hospitalier de Recherche Clinique" CHUBX 2011/24 of Bordeaux' Hospital.

## REFERENCES

- Zanoveli JM, Moraes H, Dias IC, Schreiber AK, Souza CP, Cunha JM. Depression Associated With Diabetes: From Pathophysiology to Treatment. *Curr Diabetes Rev* (2016) 12(3):165–78. doi: 10.2174/1573399811666150515125349
- Litmanovitch E, Geva R, Rachmiel M. Short and Long Term Neuro-Behavioral Alterations in Type 1 Diabetes Mellitus Pediatric Population. *World J Diabetes* (2015) 6(2):259–70. doi: 10.4239/wjd.v6.i2.259
- Biessels GJ, Reijmer YD. Brain Changes Underlying Cognitive Dysfunction in Diabetes: What can We Learn From MRI? *Diabetes* (2014) 63(7):2244–52. doi: 10.2337/db14-0348
- Shalimova A, Graff B, Gasecki D, Wolf J, Sabisz A, Szurowska E, et al. Cognitive Dysfunction in Type 1 Diabetes Mellitus. *J Clin Endocrinol Metab* (2019) 104(6):2239–49. doi: 10.1210/je.2018-01315
- Beauquis J, Homo-Delarche F, Reysin Y, De Nicola AF, Saravia F. Brain Alterations in Autoimmune and Pharmacological Models of Diabetes Mellitus: Focus on Hypothalamic-Pituitary-Adrenocortical Axis Disturbances. *Neuroimmunomodulation* (2008) 15(1):61–7. doi: 10.1159/000135625
- MacLulich AM, Seckl JR. Diabetes and Cognitive Decline: Are Steroids the Missing Link? *Cell Metab* (2008) 7(4):286–7. doi: 10.1016/j.cmet.2008.03.012
- Menke A. Is the HPA Axis as Target for Depression Outdated, or Is There a New Hope? *Front Psychiatry* (2019) 10:101. doi: 10.3389/fpsy.2019.00101
- de Quervain D, Schwabe L, Roozendaal B. Stress, Glucocorticoids and Memory: Implications for Treating Fear-Related Disorders. *Nat Rev Neurosci* (2017) 18(1):7–19. doi: 10.1038/nrn.2016.155
- Kerstens MN, Luik PT, van der Kleij FG, Boonstra AH, Breukelman H, Sluiter WJ, et al. Decreased Cortisol Production in Male Type 1 Diabetic Patients. *Eur J Clin Invest* (2003) 33(7):589–94. doi: 10.1046/j.1365-2362.2003.01171.x
- Chapman K, Holmes M, Seckl J. 11beta-Hydroxysteroid Dehydrogenases: Intracellular Gate-Keepers of Tissue Glucocorticoid Action. *Physiol Rev* (2013) 93(3):1139–206. doi: 10.1152/physrev.00020.2012
- Rougeon V, Moisan MP, Barthe N, Beauvieux MC, Helbling JC, Pallet V, et al. Diabetes and Insulin Injection Modalities: Effects on Hepatic and Hippocampal Expression of 11beta-Hydroxysteroid Dehydrogenase Type 1 in Juvenile Diabetic Male Rats. *Front Endocrinol (Lausanne)* (2017) 8:81. doi: 10.3389/fendo.2017.00081
- Marissal-Arvy N, Campas MN, Semont A, Ducroix-Crepy C, Beauvieux MC, Brossaud J, et al. Insulin Treatment Partially Prevents Cognitive and Hippocampal Alterations as Well as Glucocorticoid Dysregulation in Early-Onset Insulin-Deficient Diabetic Rats. *Psychoneuroendocrinology* (2018) 93:72–81. doi: 10.1016/j.psyneuen.2018.04.016
- Walker BR, Andrew R. Tissue Production of Cortisol by 11beta-Hydroxysteroid Dehydrogenase Type 1 and Metabolic Disease. *Ann N Y Acad Sci* (2006) 1083:165–84. doi: 10.1196/annals.1367.012
- Barat P, Brossaud J, Lacoste A, Vautier V, Nacka F, Moisan MP, et al. Nocturnal Activity of 11beta-Hydroxy Steroid Dehydrogenase Type 1 Is Increased in Type 1 Diabetic Children. *Diabetes Metab* (2013) 39(2):163–8. doi: 10.1016/j.diabet.2012.10.001
- Biessels GJ, Deary IJ, Ryan CM. Cognition and Diabetes: A Lifespan Perspective. *Lancet Neurol* (2008) 7(2):184–90. doi: 10.1016/S1474-4422(08)70021-8

16. Finken MJ, Andrews RC, Andrew R, Walker BR. Cortisol Metabolism in Healthy Young Adults: Sexual Dimorphism in Activities of A-Ring Reductases, But Not 11 $\beta$ -Hydroxysteroid Dehydrogenases. *J Clin Endocrinol Metab* (1999) 84(9):3316–21.
17. Dimitriou T, Maser-Gluth C, Remer T. Adrenocortical Activity in Healthy Children Is Associated With Fat Mass. *Am J Clin Nutr* (2003) 77(3):731–6. doi: 10.1093/ajcn/77.3.731
18. Remer T, Maser-Gluth C, Boye KR, Hartmann MF, Heinze E, Wudy SA. Exaggerated Adrenarche and Altered Cortisol Metabolism in Type 1 Diabetic Children. *Steroids* (2006) 71(7):591–8. doi: 10.1016/j.steroids.2006.02.005
19. Dullaart RP, Ubels FL, Hoogenberg K, Smit AJ, Pratt JJ, Muntinga JH, et al. Alterations in Cortisol Metabolism in Insulin-Dependent Diabetes Mellitus: Relationship With Metabolic Control and Estimated Blood Volume and Effect of Angiotensin-Converting Enzyme Inhibition. *J Clin Endocrinol Metab* (1995) 80(10):3002–8. doi: 10.1210/jcem.80.10.7559888
20. Kerstens MN, Riemens SC, Sluiter WJ, Pratt JJ, Wolthers BG, Dullaart RP. Lack of Relationship Between 11 $\beta$ -Hydroxysteroid Dehydrogenase Setpoint and Insulin Sensitivity in the Basal State and After 24h of Insulin Infusion in Healthy Subjects and Type 2 Diabetic Patients. *Clin Endocrinol (Oxf)* (2000) 52(4):403–11. doi: 10.1046/j.1365-2265.2000.00975.x
21. Voice MW, Seckl JR, Edwards CR, Chapman KE. 11  $\beta$ -Hydroxysteroid Dehydrogenase Type 1 Expression in 2S FAZA Hepatoma Cells Is Hormonally Regulated: A Model System for the Study of Hepatic Glucocorticoid Metabolism. *Biochem J* (1996) 317(Pt 2):621–5.
22. Fan Z, Du H, Zhang M, Meng Z, Chen L, Liu Y. Direct Regulation of Glucose and Not Insulin on Hepatic Hexose-6-Phosphate Dehydrogenase and 11 $\beta$ -Hydroxysteroid Dehydrogenase Type 1. *Mol Cell Endocrinol* (2011) 333(1):62–9. doi: 10.1016/j.mce.2010.12.010
23. Tsilchorozidou T, Honour JW, Conway GS. Altered Cortisol Metabolism in Polycystic Ovary Syndrome: Insulin Enhances 5 $\alpha$ -Reduction But Not the Elevated Adrenal Steroid Production Rates. *J Clin Endocrinol Metab* (2003) 88(12):5907–13. doi: 10.1210/jc.2003-030240
24. Andrews RC, Herlihy O, Livingstone DE, Andrew R, Walker BR. Abnormal Cortisol Metabolism and Tissue Sensitivity to Cortisol in Patients With Glucose Intolerance. *J Clin Endocrinol Metab* (2002) 87(12):5587–93. doi: 10.1210/jc.2002-020048
25. Tomlinson JW, Finney J, Gay C, Hughes BA, Hughes SV, Stewart PM. Impaired Glucose Tolerance and Insulin Resistance Are Associated With Increased Adipose 11 $\beta$ -Hydroxysteroid Dehydrogenase Type 1 Expression and Elevated Hepatic 5 $\alpha$ -Reductase Activity. *Diabetes* (2008) 57(10):2652–60. doi: 10.2337/db08-0495
26. Kayampilly PP, Wanamaker BL, Stewart JA, Wagner CL, Menon KM. Stimulatory Effect of Insulin on 5 $\alpha$ -Reductase Type 1 (SRD5A1) Expression Through an Akt-Dependent Pathway in Ovarian Granulosa Cells. *Endocrinology* (2010) 151(10):5030–7. doi: 10.1210/en.2010-0444
27. Roy M, Collier B, Roy A. Hypothalamic-Pituitary-Adrenal Axis Dysregulation Among Diabetic Outpatients. *Psychiatry Res* (1990) 31(1):31–7. doi: 10.1016/0165-1781(90)90106-F
28. Roy MS, Roy A, Gallucci WT, Collier B, Young K, Kamilaris TC, et al. The Ovine Corticotropin-Releasing Hormone-Stimulation Test in Type I Diabetic Patients and Controls: Suggestion of Mild Chronic Hypercortisolism. *Metabolism* (1993) 42(6):696–700. doi: 10.1016/0026-0495(93)90235-G
29. Livingstone DE, Di Rollo EM, Yang C, Codrington LE, Mathews JA, Kara M, et al. Relative Adrenal Insufficiency in Mice Deficient in 5 $\alpha$ -Reductase 1. *J Endocrinol* (2014) 222(2):257–66. doi: 10.1530/JOE-13-0563
30. Jackson C, Richer J, Edge JA. Sibling Psychological Adjustment to Type 1 Diabetes Mellitus. *Pediatr Diabetes* (2008) 9(4 Pt 1):308–11. doi: 10.1111/j.1399-5448.2008.00385.x
31. Butwicka A, Frisen L, Almqvist C, Zethelius B, Lichtenstein P. Risks of Psychiatric Disorders and Suicide Attempts in Children and Adolescents With Type 1 Diabetes: A Population-Based Cohort Study. *Diabetes Care* (2015) 38(3):453–9. doi: 10.2337/dc14-0262
32. Raff H, Phillips JM. Bedtime Salivary Cortisol and Cortisone by LC-MS/MS in Healthy Adult Subjects: Evaluation of Sampling Time. *J Endocr Soc* (2019) 3(8):1631–40. doi: 10.1210/js.2019-00186
33. Lupien SJ, McEwen BS, Gunnar MR, Heim C. Effects of Stress Throughout the Lifespan on the Brain, Behaviour and Cognition. *Nat Rev Neurosci* (2009) 10(6):434–45. doi: 10.1038/nrn2639
34. Stranahan AM, Arumugam TV, Cutler RG, Lee K, Egan JM, Mattson MP. Diabetes Impairs Hippocampal Function Through Glucocorticoid-Mediated Effects on New and Mature Neurons. *Nat Neurosci* (2008) 11(3):309–17. doi: 10.1038/nn2055

**Conflict of Interest:** The authors declare that the research was conducted in the absence of any commercial or financial relationships that could be construed as a potential conflict of interest.

**Publisher's Note:** All claims expressed in this article are solely those of the authors and do not necessarily represent those of their affiliated organizations, or those of the publisher, the editors and the reviewers. Any product that may be evaluated in this article, or claim that may be made by its manufacturer, is not guaranteed or endorsed by the publisher.

Copyright © 2021 Brossaud, Corcuff, Vautier, Bergeron, Valade, Lienhardt, Moisan and Barat. This is an open-access article distributed under the terms of the Creative Commons Attribution License (CC BY). The use, distribution or reproduction in other forums is permitted, provided the original author(s) and the copyright owner(s) are credited and that the original publication in this journal is cited, in accordance with accepted academic practice. No use, distribution or reproduction is permitted which does not comply with these terms.

# Advantages of publishing in Frontiers



## OPEN ACCESS

Articles are free to read  
for greatest visibility  
and readership



## FAST PUBLICATION

Around 90 days  
from submission  
to decision



## HIGH QUALITY PEER-REVIEW

Rigorous, collaborative,  
and constructive  
peer-review



## TRANSPARENT PEER-REVIEW

Editors and reviewers  
acknowledged by name  
on published articles

## Frontiers

Avenue du Tribunal-Fédéral 34  
1005 Lausanne | Switzerland

**Visit us:** [www.frontiersin.org](http://www.frontiersin.org)

**Contact us:** [frontiersin.org/about/contact](http://frontiersin.org/about/contact)



## REPRODUCIBILITY OF RESEARCH

Support open data  
and methods to enhance  
research reproducibility



## DIGITAL PUBLISHING

Articles designed  
for optimal readership  
across devices



## FOLLOW US

@frontiersin



## IMPACT METRICS

Advanced article metrics  
track visibility across  
digital media



## EXTENSIVE PROMOTION

Marketing  
and promotion  
of impactful research



## LOOP RESEARCH NETWORK

Our network  
increases your  
article's readership